



Neutrino interactions on nuclei at MINERvA

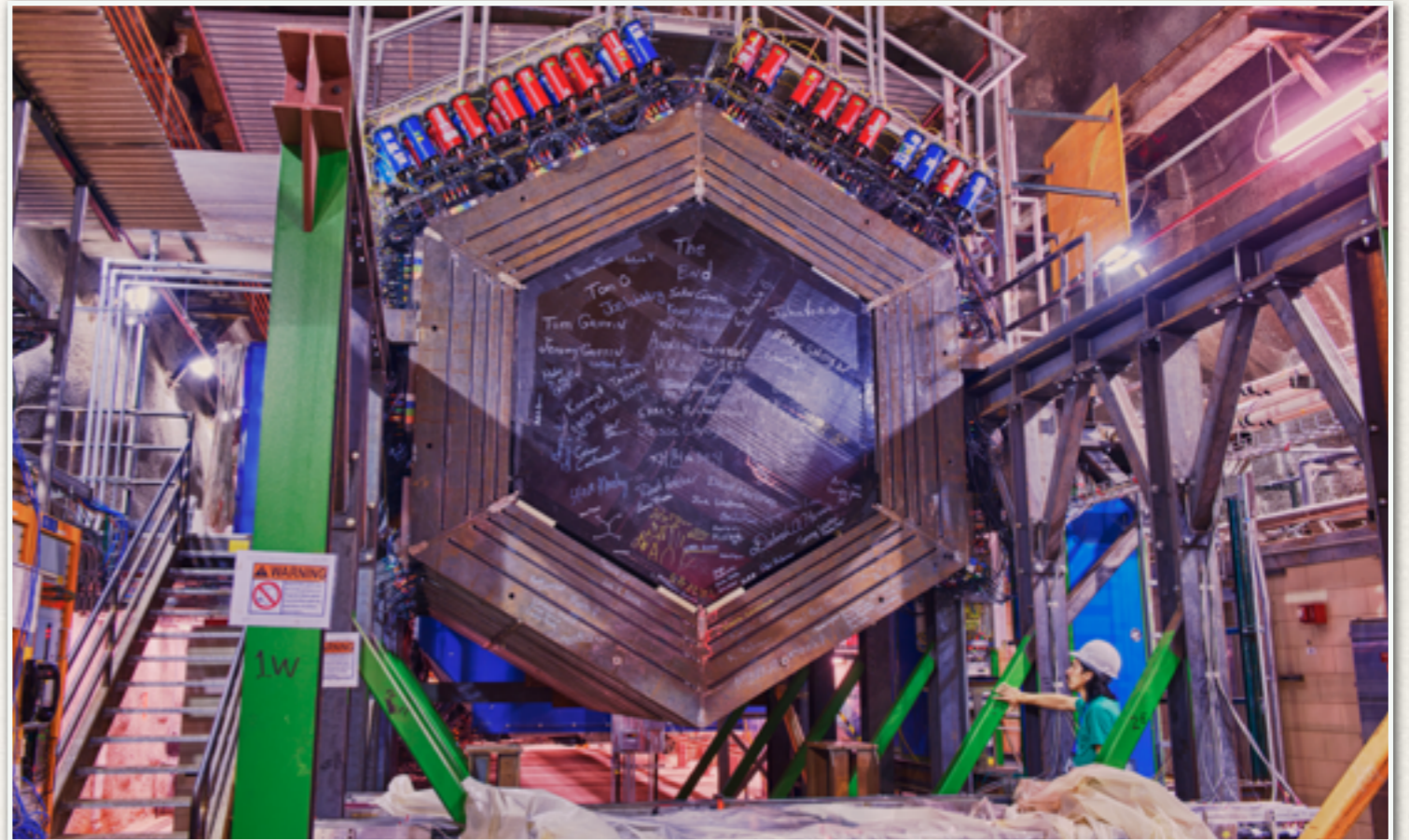
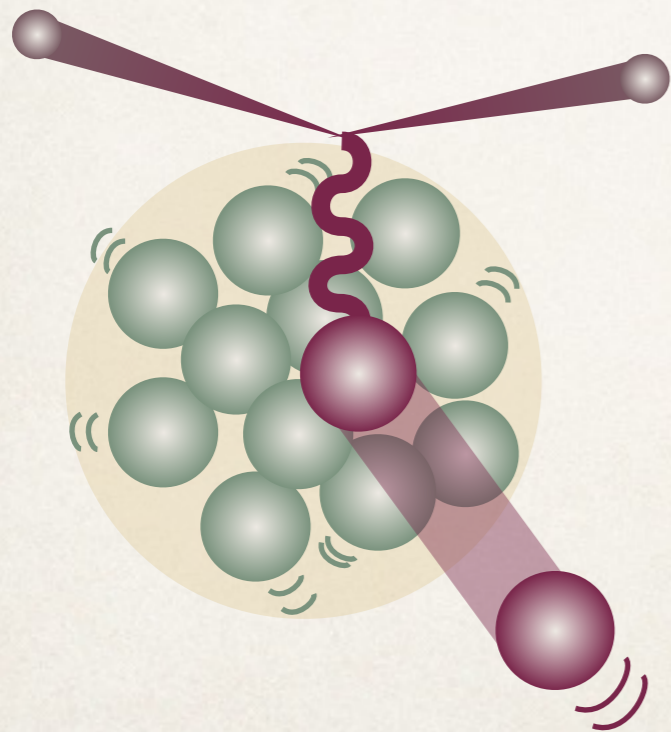
Cheryl Patrick, Northwestern University, USA

Seminar, University College London, 10 April, 2015

About MINERvA

MINERvA is a dedicated neutrino-nucleus cross section experiment, situated in Fermilab's NuMI beam along with MINOS and NOvA along with MINOS and NOvA

It is able to make high-precision cross-section measurements for many different materials, in the 1-20 GeV range



Photograph: Reidar Hahn, Fermilab visual media services

- * MINERvA is excellent for probing the **structure of the nucleus**, and its effects on neutrino scattering cross sections
- * Its measurements can also provide vital information to **oscillation experiments**

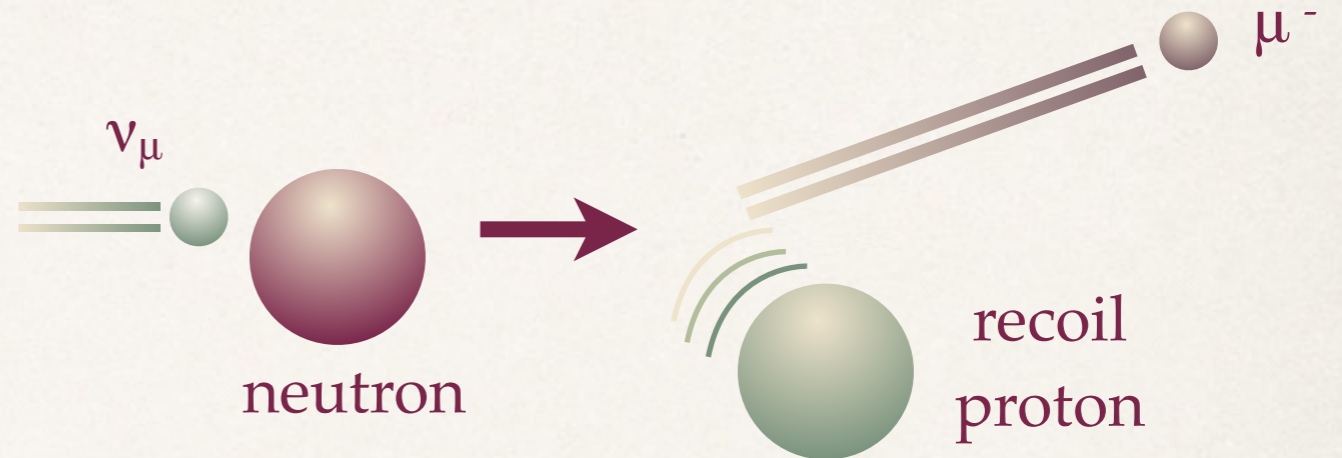


Motivation: oscillation experiments

Who can make use of our results?

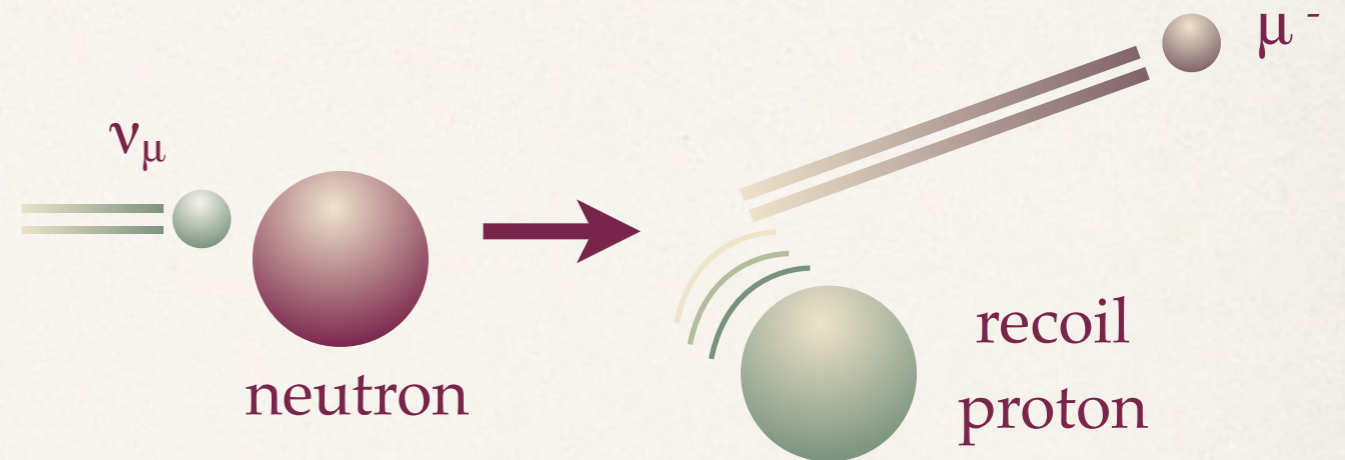
The story of neutrino oscillations

- ❖ Our detectors can only see **charged** particles i.e. **not neutrinos**
- ❖ When a neutrino interacts, we infer what flavor it was (ν_e, ν_μ, ν_τ) from the partner lepton it produces (e, μ or τ)
- ❖ But while it's not interacting, we don't know what it is

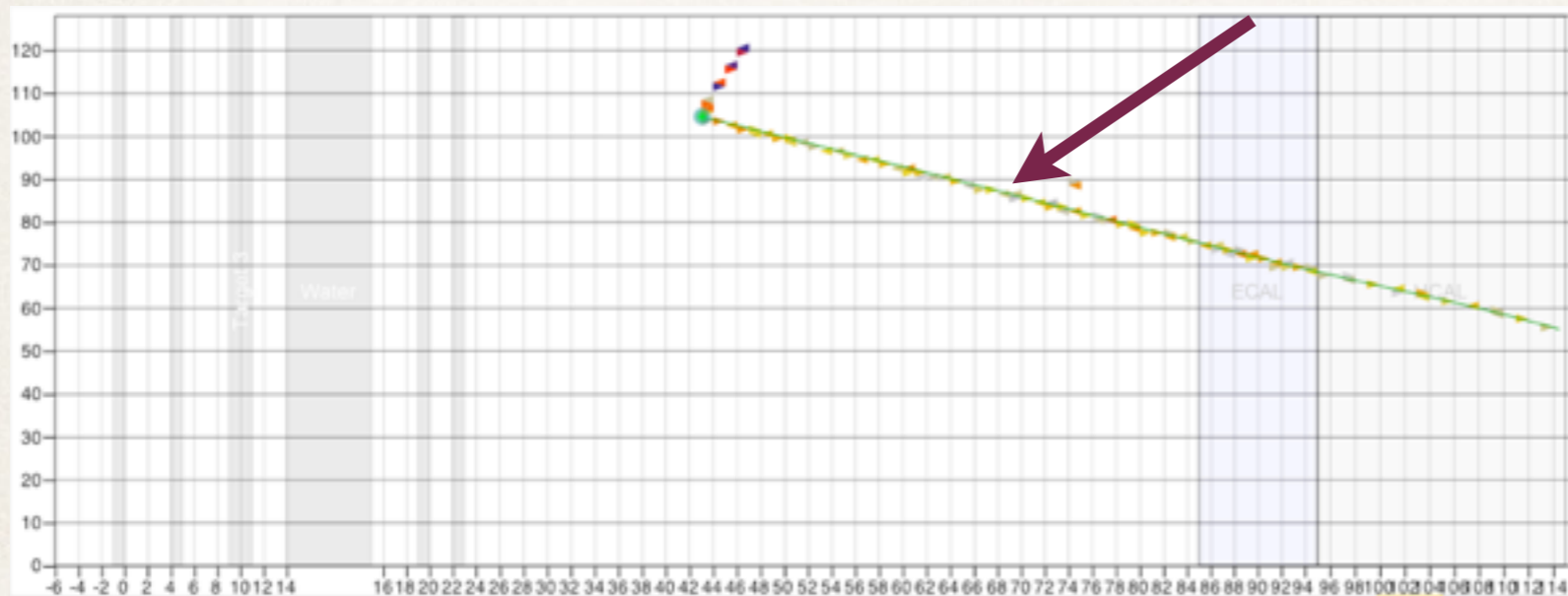


The story of neutrino oscillations

- ❖ Our detectors can only see **charged** particles i.e. **not neutrinos**
- ❖ When a neutrino interacts, we infer what flavor it was (ν_e, ν_μ, ν_τ) from the partner lepton it produces (e, μ or τ)
- ❖ But while it's not interacting, we don't know what it is

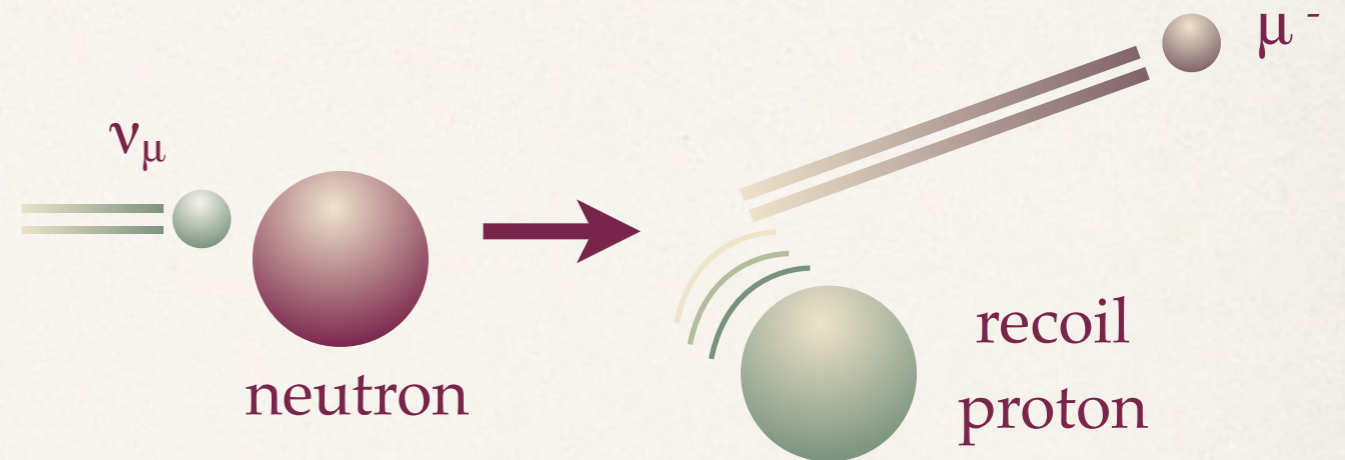


This is a muon

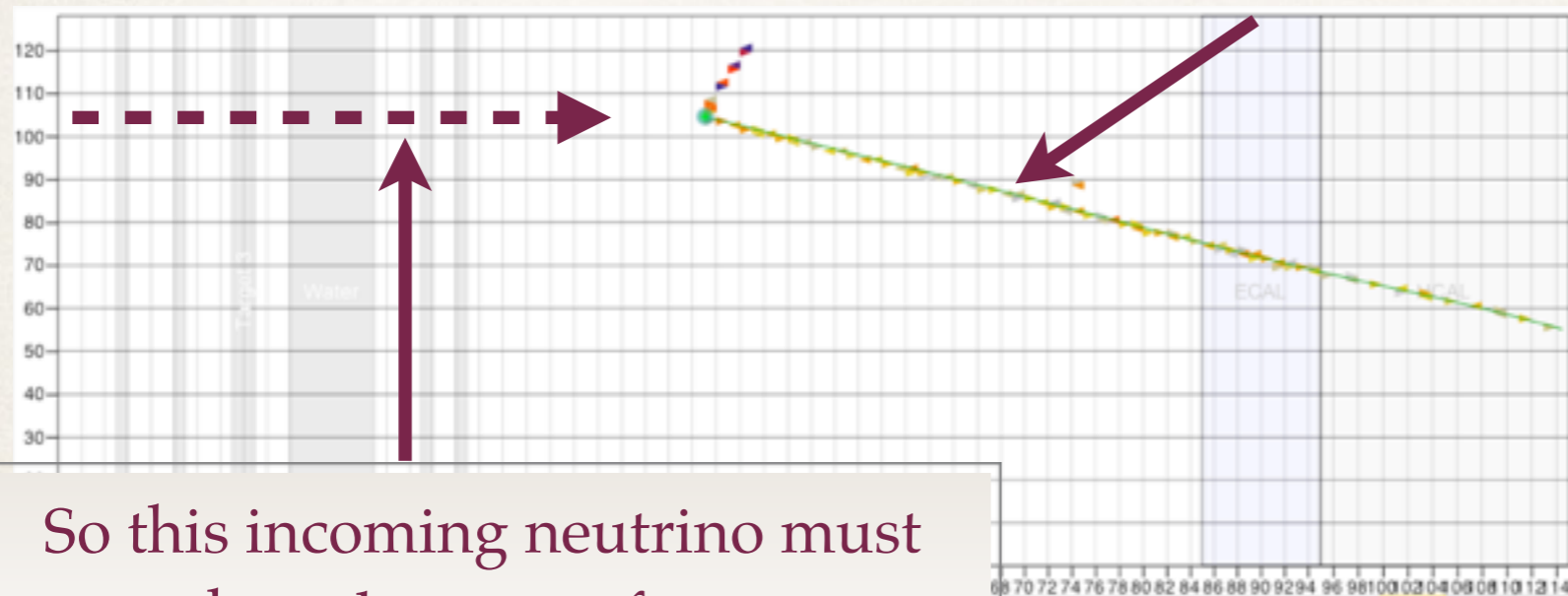


The story of neutrino oscillations

- ❖ Our detectors can only see **charged** particles i.e. **not neutrinos**
- ❖ When a neutrino interacts, we infer what flavor it was (ν_e, ν_μ, ν_τ) from the partner lepton it produces (e, μ or τ)
- ❖ But while it's not interacting, we don't know what it is



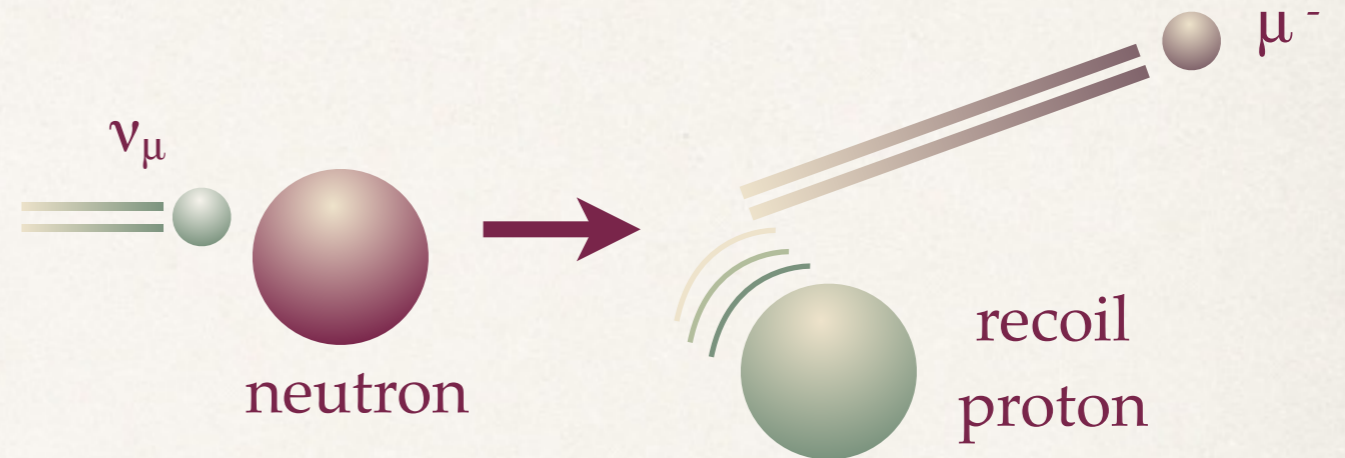
This is a muon



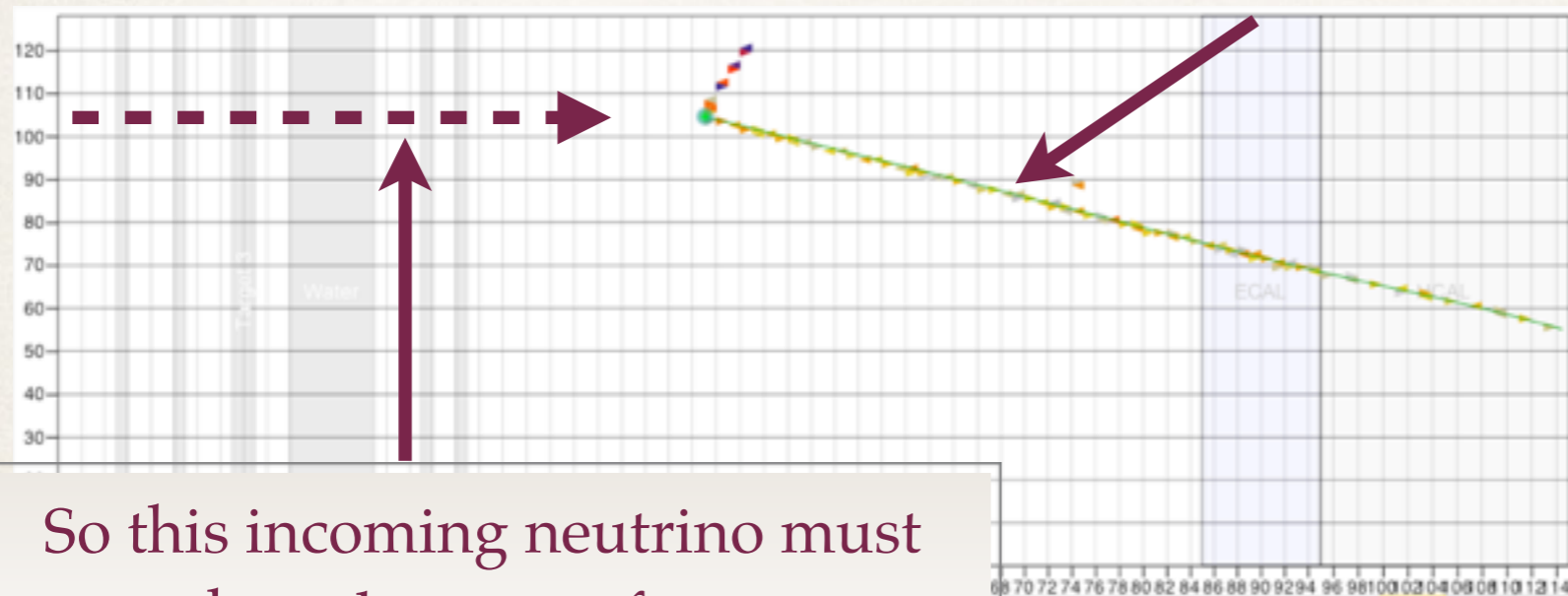
So this incoming neutrino must have been a ν_μ from our ν_μ beam

The story of neutrino oscillations

- ❖ Our detectors can only see **charged** particles i.e. **not neutrinos**
- ❖ When a neutrino interacts, we infer what flavor it was (ν_e, ν_μ, ν_τ) from the partner lepton it produces (e, μ or τ)
- ❖ But while it's not interacting, we don't know what it is



This is a muon

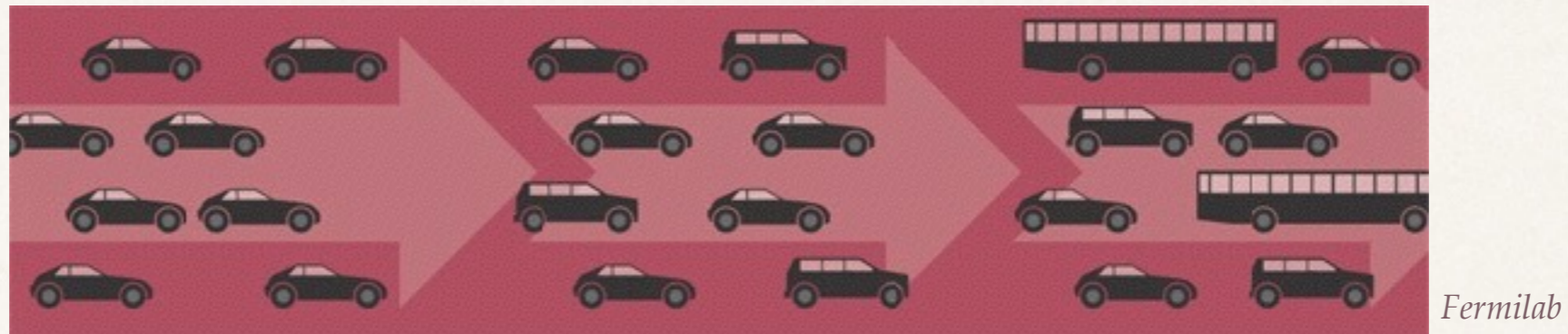


So this incoming neutrino must have been a ν_μ from our ν_μ beam

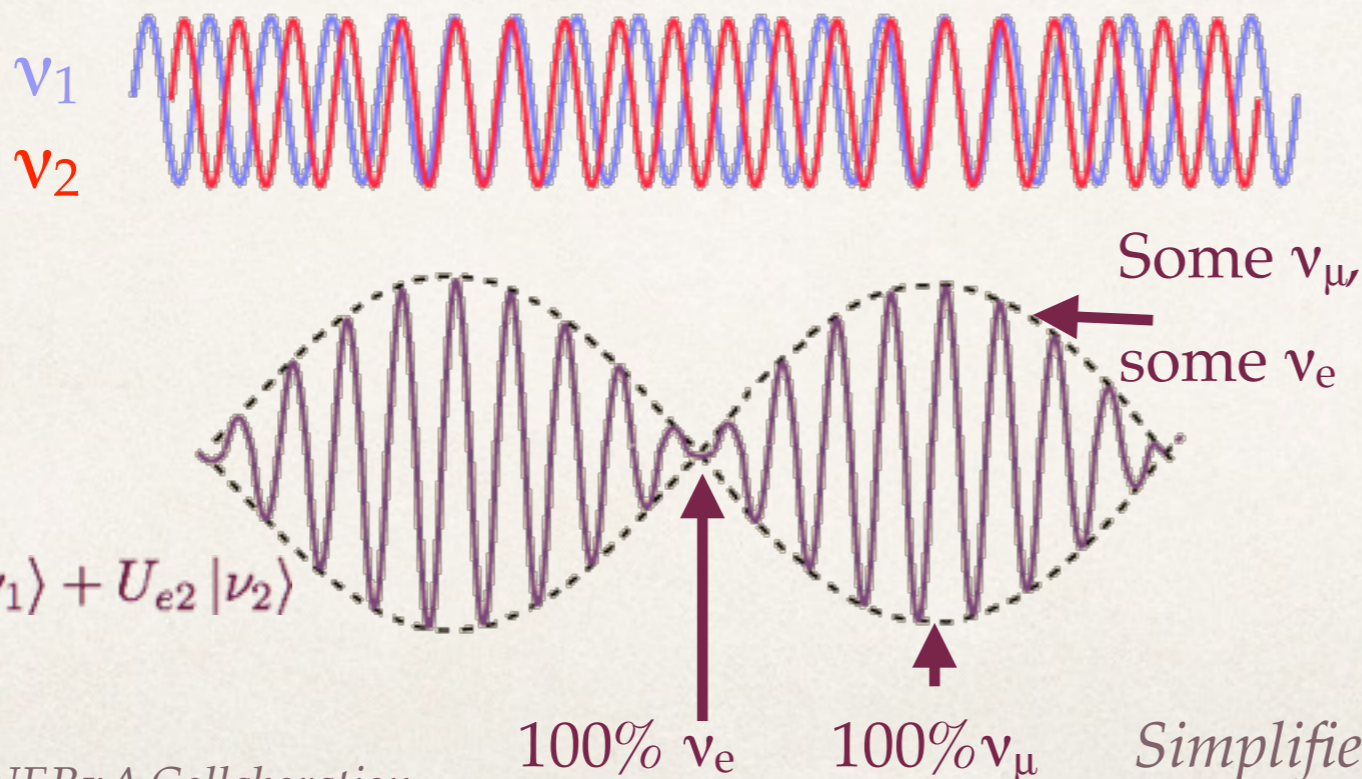
But what if we saw an electron instead? Where would THAT have come from?

Neutrinos oscillate between flavors

- ❖ As a beam of, say, ν_e travels, some start to turn into ν_μ and ν_τ



- ❖ This can be explained only if **neutrinos have mass**, and there are multiple mass states
- ❖ For a given energy, states of different mass will have **different wavelengths**
- ❖ Each mass state is a **superposition** of the flavor states, and vice versa

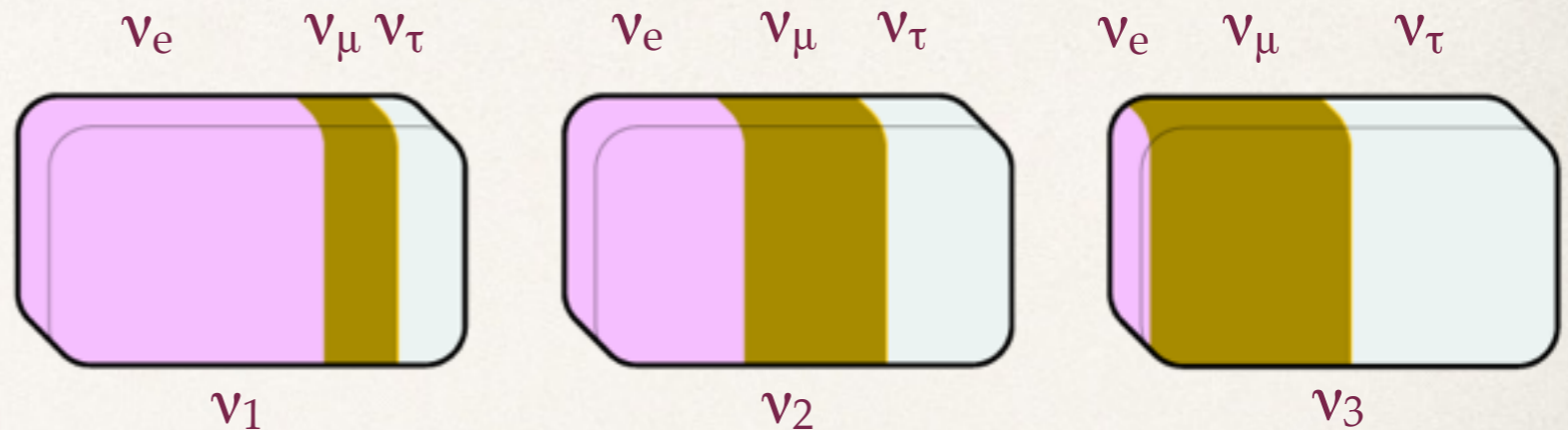


- ❖ “Beats” between the states determine the probability of seeing each flavor
- ❖ With 3 states, this gets complicated!
- ❖ And there’s more we still don’t know...

We don't know: mixing angles

- ❖ To what extent do the flavors **mix**?
- ❖ In other words, what's the flavor composition of the mass states?

$$\begin{bmatrix} \nu_e \\ \nu_\mu \\ \nu_\tau \end{bmatrix} = \begin{bmatrix} U_{e1} & U_{e2} & U_{e3} \\ U_{\mu1} & U_{\mu2} & U_{\mu3} \\ U_{\tau1} & U_{\tau2} & U_{\tau3} \end{bmatrix} \begin{bmatrix} \nu_1 \\ \nu_2 \\ \nu_3 \end{bmatrix}.$$

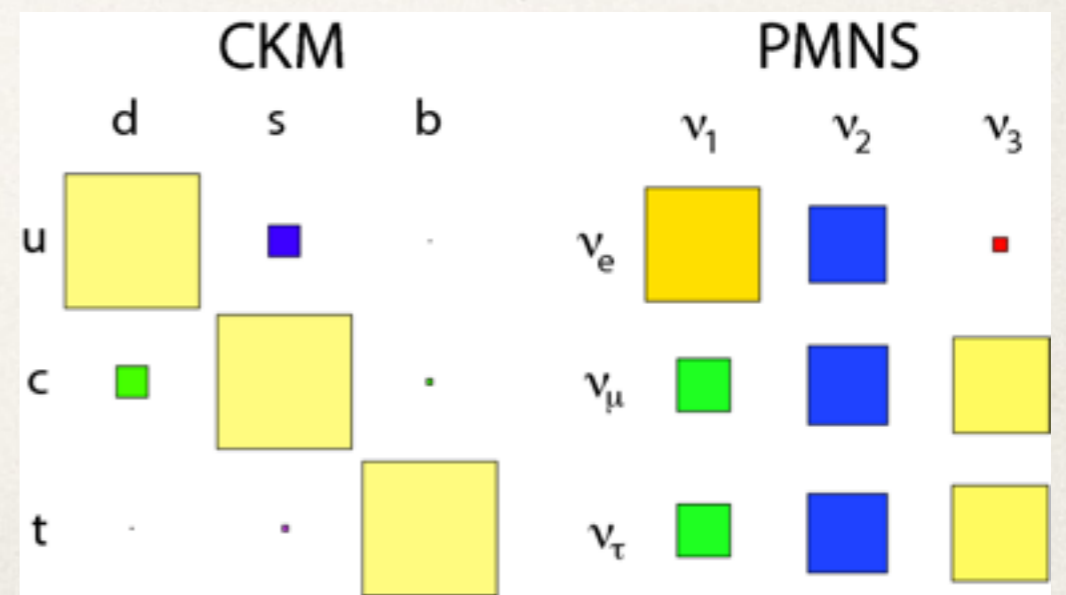


Quantum diaries



- ❖ And could there be **more than 3** flavors?
- ❖ Only 3 weakly interact, but some experiments saw hints of a 4th "sterile" neutrino

- ❖ Quark flavors also mix - but why is the CKM matrix (for quarks) so different from the PMNS matrix (for neutrinos)?
- ❖ Is there a theory that can explain both?



We don't know: masses

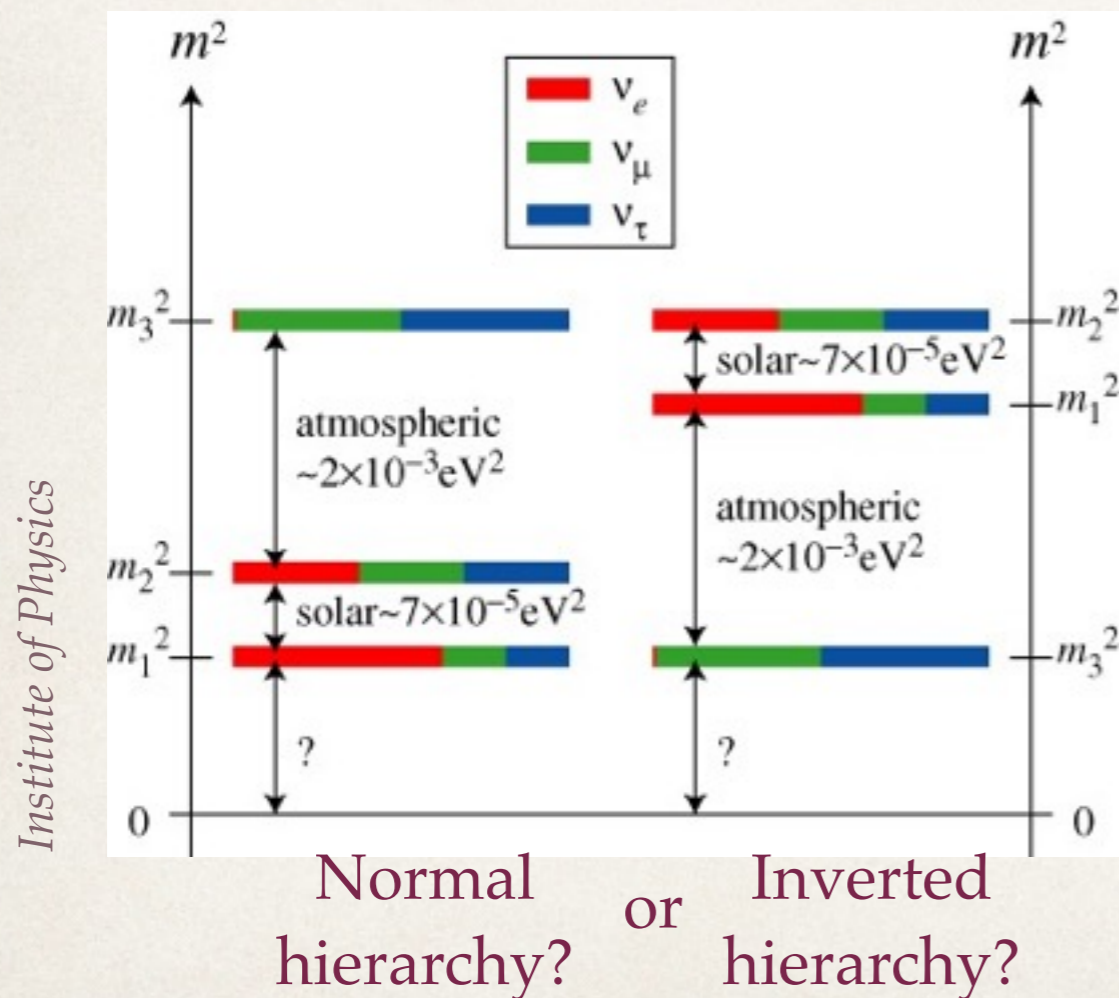
It's easier to measure squared mass differences between the states than absolute masses.

$$P(\nu_{l_a} \rightarrow \nu_{l_b}, x) = \sin^2 2\theta \sin^2 \left(1.27 \frac{\Delta M^2 (eV^2) x (\text{km})}{p_\nu (\text{GeV})} \right)$$

Mixing angle \nearrow ΔM^2 \nwarrow
(Two-flavor approximation)



Fermilab

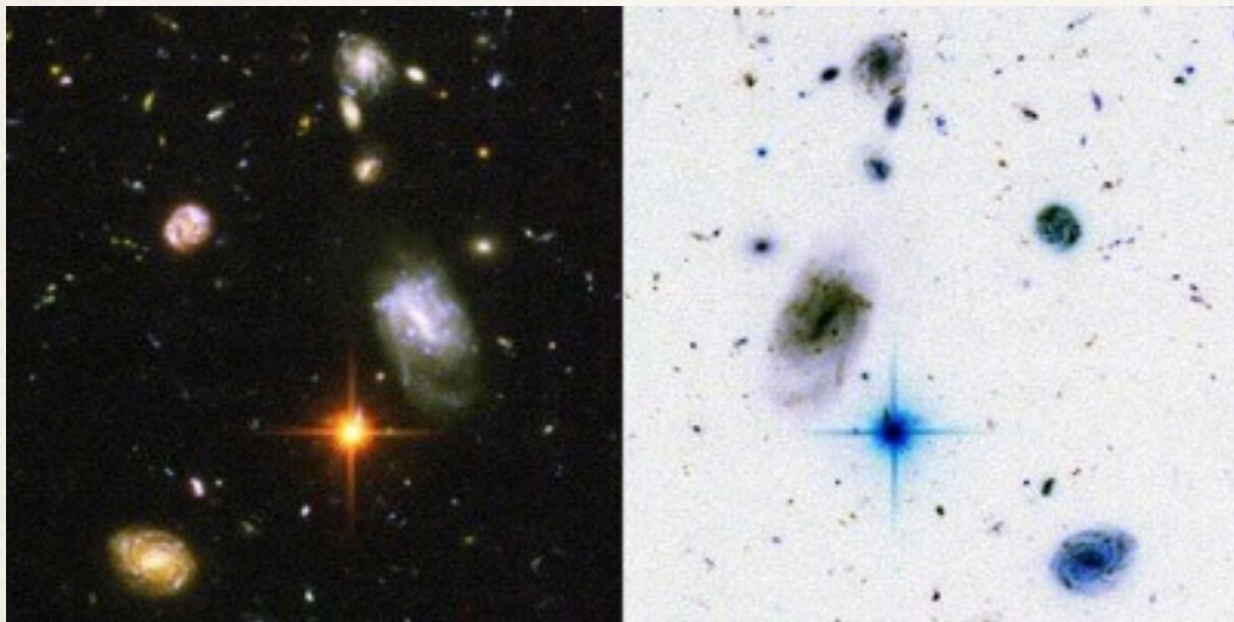


- * Which mass state is heaviest?
- * Which is lightest?
- * And could the lightest neutrino be massless?
- * We call this the **mass hierarchy**

We don't know:

Universe

Anti-universe



Fermilab

CP violation?

- ❖ Do neutrinos and antineutrinos oscillate and interact differently?
- ❖ In other words, do they break charge-parity symmetry (**CP violation**)?
- ❖ If the Big Bang made equal amounts of matter and antimatter, could this explain why **the universe is only made of matter**?

Majorana neutrinos?

- ❖ If neutrinos are “Majorana” particles, they are their own antiparticles
- ❖ Or they could be Dirac fermions like the other leptons and quarks



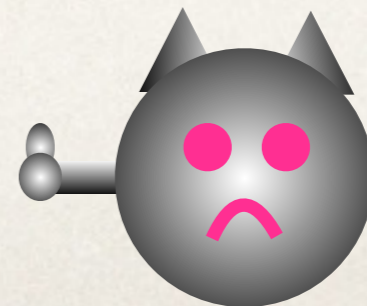
ν



$\bar{\nu}$

Majorana?

or



Dirac?

Oscillations lead to answers

The 3-flavor mixing (PMNS) matrix looks daunting, but here's what to notice:

$$\begin{aligned}
 U &= \begin{bmatrix} U_{e1} & U_{e2} & U_{e3} \\ U_{\mu1} & U_{\mu2} & U_{\mu3} \\ U_{\tau1} & U_{\tau2} & U_{\tau3} \end{bmatrix} \\
 &= \begin{bmatrix} 1 & 0 & 0 \\ 0 & c_{23} & s_{23} \\ 0 & -s_{23} & c_{23} \end{bmatrix} \begin{bmatrix} c_{13} & 0 & s_{13}e^{-i\delta} \\ 0 & 1 & 0 \\ -s_{13}e^{i\delta} & 0 & c_{13} \end{bmatrix} \begin{bmatrix} c_{12} & s_{12} & 0 \\ -s_{12} & c_{12} & 0 \\ 0 & 0 & 1 \end{bmatrix} \begin{bmatrix} 1 & 0 & 0 \\ 0 & e^{i\alpha_1/2} & 0 \\ 0 & 0 & e^{i\alpha_2/2} \end{bmatrix} \\
 &= \begin{bmatrix} c_{12}c_{13} & s_{12}c_{13} & s_{13}e^{-i\delta} \\ -s_{12}c_{23} - c_{12}s_{23}s_{13}e^{i\delta} & c_{12}c_{23} - s_{12}s_{23}s_{13}e^{i\delta} & s_{23}c_{13} \\ s_{12}s_{23} - c_{12}c_{23}s_{13}e^{i\delta} & -c_{12}s_{23} - s_{12}c_{23}s_{13}e^{i\delta} & c_{23}c_{13} \end{bmatrix} \begin{bmatrix} 1 & 0 & 0 \\ 0 & e^{i\alpha_1/2} & 0 \\ 0 & 0 & e^{i\alpha_2/2} \end{bmatrix}
 \end{aligned}$$

Oscillation experiments such as T2K, NOvA, MINOS, and Daya Bay have already measured some of these values, and are working on the rest

Oscillations lead to answers

The 3-flavor mixing (PMNS) matrix looks daunting, but here's what to notice:

$$\begin{aligned}
 U &= \begin{bmatrix} U_{e1} & U_{e2} & U_{e3} \\ U_{\mu1} & U_{\mu2} & U_{\mu3} \\ U_{\tau1} & U_{\tau2} & U_{\tau3} \end{bmatrix} \\
 &= \begin{bmatrix} 1 & 0 & 0 \\ 0 & c_{23} & s_{23} \\ 0 & -s_{23} & c_{23} \end{bmatrix} \begin{bmatrix} c_{13} & 0 & s_{13}e^{-i\delta} \\ 0 & 1 & 0 \\ -s_{13}e^{i\delta} & 0 & c_{13} \end{bmatrix} \begin{bmatrix} c_{12} & s_{12} & 0 \\ -s_{12} & c_{12} & 0 \\ 0 & 0 & 1 \end{bmatrix} \begin{bmatrix} 1 & 0 & 0 \\ 0 & e^{i\alpha_1/2} & 0 \\ 0 & 0 & e^{i\alpha_2/2} \end{bmatrix} \\
 &= \begin{bmatrix} c_{12}c_{13} & s_{12}c_{13} & s_{13}e^{-i\delta} \\ -s_{12}c_{23} - c_{12}s_{23}s_{13}e^{i\delta} & c_{12}c_{23} - s_{12}s_{23}s_{13}e^{i\delta} & s_{23}c_{13} \\ s_{12}s_{23} - c_{12}c_{23}s_{13}e^{i\delta} & -c_{12}s_{23} - s_{12}c_{23}s_{13}e^{i\delta} & c_{23}c_{13} \end{bmatrix} \begin{bmatrix} 1 & 0 & 0 \\ 0 & e^{i\alpha_1/2} & 0 \\ 0 & 0 & e^{i\alpha_2/2} \end{bmatrix}
 \end{aligned}$$

Three "mixing angles" define how much ν_μ , ν_e and ν_τ contribute to each mass state

Oscillation experiments such as T2K, NOvA, MINOS, and Daya Bay have already measured some of these values, and are working on the rest

Oscillations lead to answers

The 3-flavor mixing (PMNS) matrix looks daunting, but here's what to notice:

$$\begin{aligned}
 U &= \begin{bmatrix} U_{e1} & U_{e2} & U_{e3} \\ U_{\mu1} & U_{\mu2} & U_{\mu3} \\ U_{\tau1} & U_{\tau2} & U_{\tau3} \end{bmatrix} \\
 &= \begin{bmatrix} 1 & 0 & 0 \\ 0 & c_{23} & s_{23} \\ 0 & -s_{23} & c_{23} \end{bmatrix} \begin{bmatrix} c_{13} & 0 & s_{13}e^{-i\delta} \\ 0 & 1 & 0 \\ -s_{13}e^{i\delta} & 0 & c_{13} \end{bmatrix} \begin{bmatrix} c_{12} & s_{12} & 0 \\ -s_{12} & c_{12} & 0 \\ 0 & 0 & 1 \end{bmatrix} \begin{bmatrix} 1 & 0 & 0 \\ 0 & e^{i\alpha_1/2} & 0 \\ 0 & 0 & e^{i\alpha_2/2} \end{bmatrix} \\
 &= \begin{bmatrix} c_{12}c_{13} & s_{12}c_{13} & s_{13}e^{-i\delta} \\ -s_{12}c_{23} - c_{12}s_{23}s_{13}e^{i\delta} & c_{12}c_{23} - s_{12}s_{23}s_{13}e^{i\delta} & s_{23}c_{13} \\ s_{12}s_{23} - c_{12}c_{23}s_{13}e^{i\delta} & -c_{12}s_{23} - s_{12}c_{23}s_{13}e^{i\delta} & c_{23}c_{13} \end{bmatrix} \begin{bmatrix} 1 & 0 & 0 \\ 0 & e^{i\alpha_1/2} & 0 \\ 0 & 0 & e^{i\alpha_2/2} \end{bmatrix}
 \end{aligned}$$

A non-zero δ
means CP-
violation

Three "mixing angles" define how much ν_μ , ν_e
and ν_τ contribute to each mass state

Oscillation experiments such as T2K, NOvA, MINOS, and Daya Bay have already measured some of these values, and are working on the rest

Oscillations lead to answers

The 3-flavor mixing (PMNS) matrix looks daunting, but here's what to notice:

$$\begin{aligned}
 U &= \begin{bmatrix} U_{e1} & U_{e2} & U_{e3} \\ U_{\mu1} & U_{\mu2} & U_{\mu3} \\ U_{\tau1} & U_{\tau2} & U_{\tau3} \end{bmatrix} \\
 &= \begin{bmatrix} 1 & 0 & 0 \\ 0 & c_{23} & s_{23} \\ 0 & -s_{23} & c_{23} \end{bmatrix} \begin{bmatrix} c_{13} & 0 & s_{13}e^{-i\delta} \\ 0 & 1 & 0 \\ -s_{13}e^{i\delta} & 0 & c_{13} \end{bmatrix} \begin{bmatrix} c_{12} & s_{12} & 0 \\ -s_{12} & c_{12} & 0 \\ 0 & 0 & 1 \end{bmatrix} \begin{bmatrix} 1 & 0 & 0 \\ 0 & e^{i\alpha_1/2} & 0 \\ 0 & 0 & e^{i\alpha_2/2} \end{bmatrix} \\
 &= \begin{bmatrix} c_{12}c_{13} & s_{12}c_{13} & s_{13}e^{-i\delta} \\ -s_{12}c_{23} - c_{12}s_{23}s_{13}e^{i\delta} & c_{12}c_{23} - s_{12}s_{23}s_{13}e^{i\delta} & s_{23}c_{13} \\ s_{12}s_{23} - c_{12}c_{23}s_{13}e^{i\delta} & -c_{12}s_{23} - s_{12}c_{23}s_{13}e^{i\delta} & c_{23}c_{13} \end{bmatrix} \begin{bmatrix} 1 & 0 & 0 \\ 0 & e^{i\alpha_1/2} & 0 \\ 0 & 0 & e^{i\alpha_2/2} \end{bmatrix}
 \end{aligned}$$

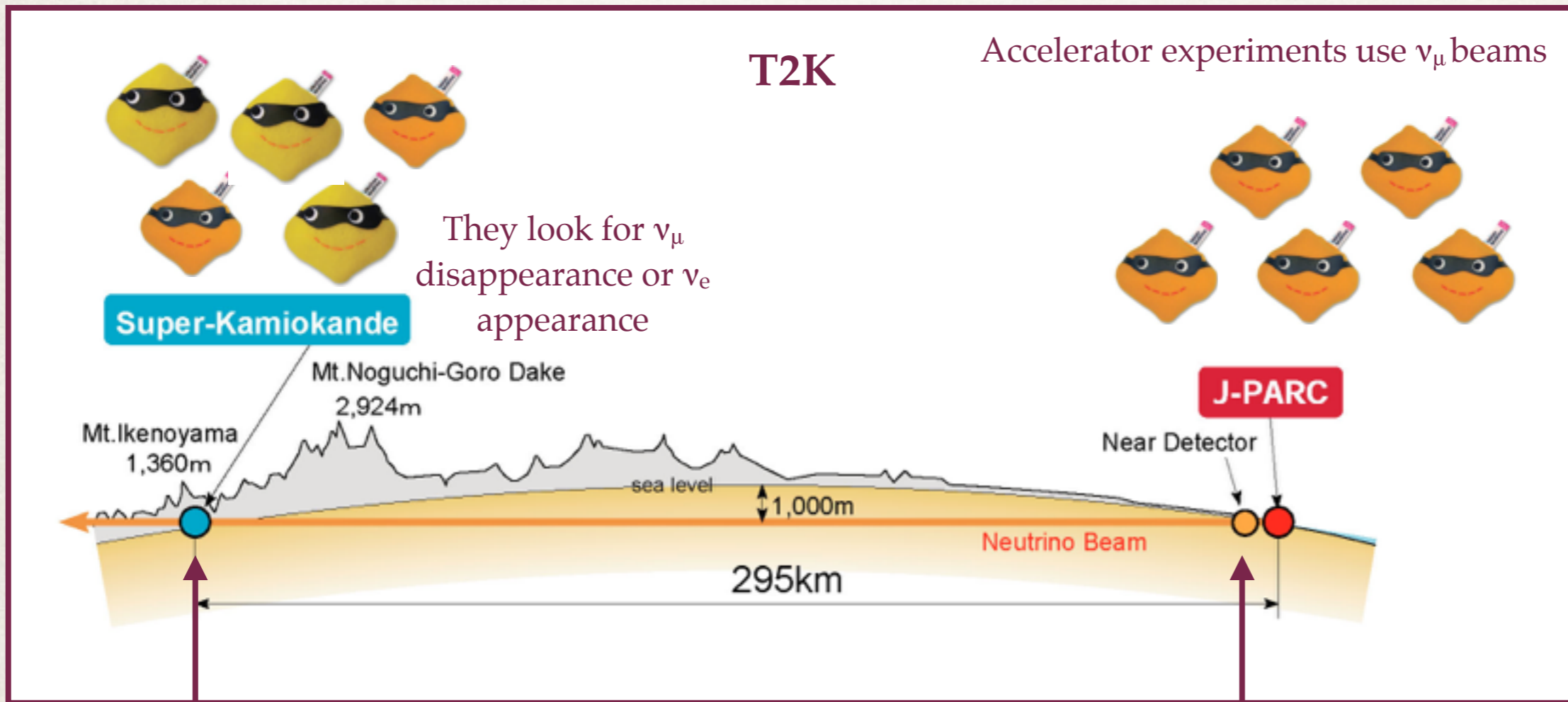
A non-zero δ
means CP-
violation

The α phases only
apply to Majorana
neutrinos

Three "mixing angles" define how much ν_μ , ν_e
and ν_τ contribute to each mass state

Oscillation experiments such as T2K, NOvA, MINOS, and Daya Bay have already measured some of these values, and are working on the rest

How to make an oscillation experiment



<http://www.t2k.org>

Then see if they disappeared here (or if another flavor appeared)...

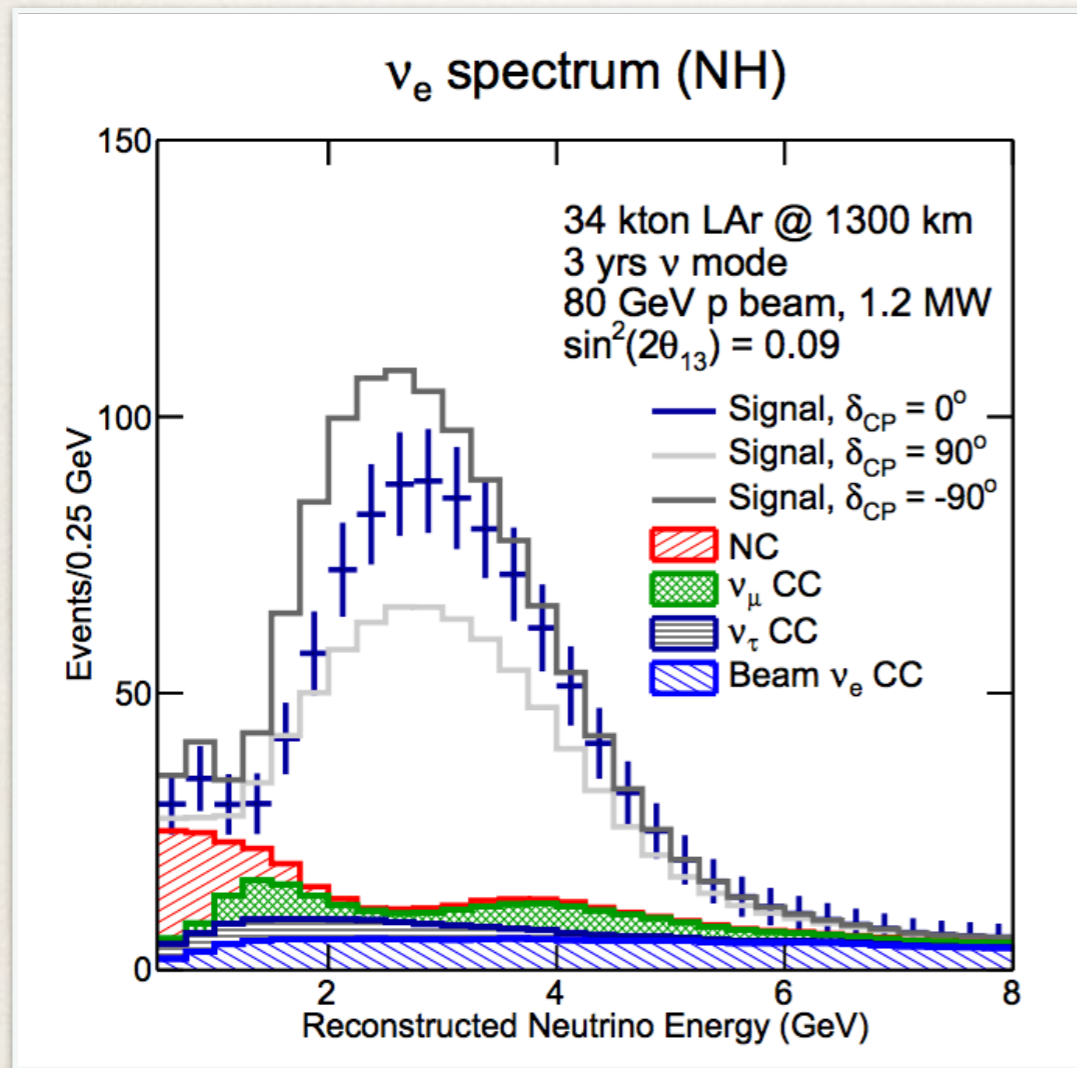
But to know whether you see as many as you expected, you need to know the probability that a neutrino will produce a signal in your detector...

... in other words - you need to know the cross section

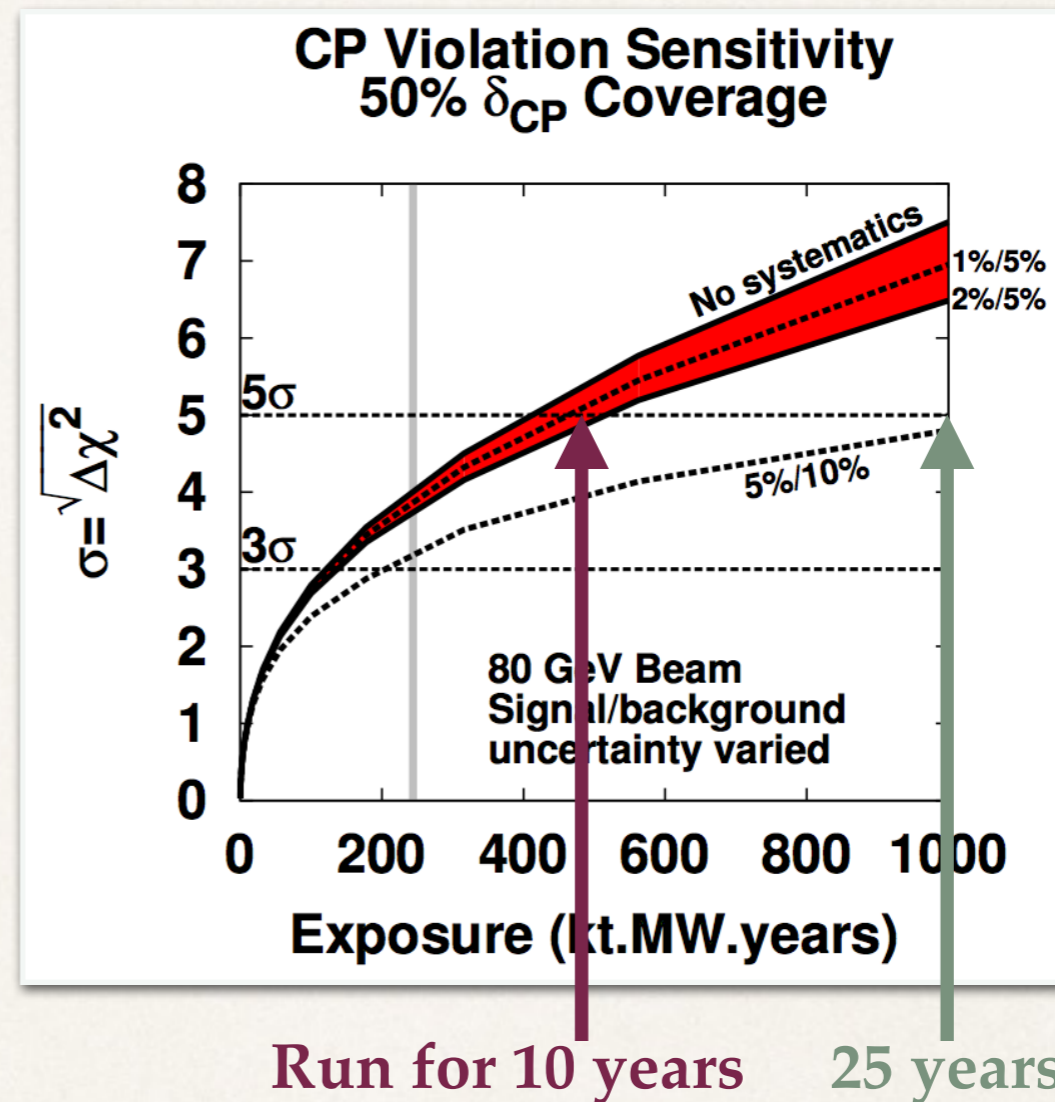
The importance of cross sections

Oscillation experiments compare event rates with predictions to determine parameters such as δ_{CP}

DUNE δ_{CP} sensitivity for different systematic uncertainties



DUNE signal predictions
arXiv 1307.7335



M. Bass,
NuInt 2014

To distinguish these parameters, they must reduce systematics. The **cross section model** is one of the largest contributors to the uncertainty.

MINERvA can reduce the uncertainties!



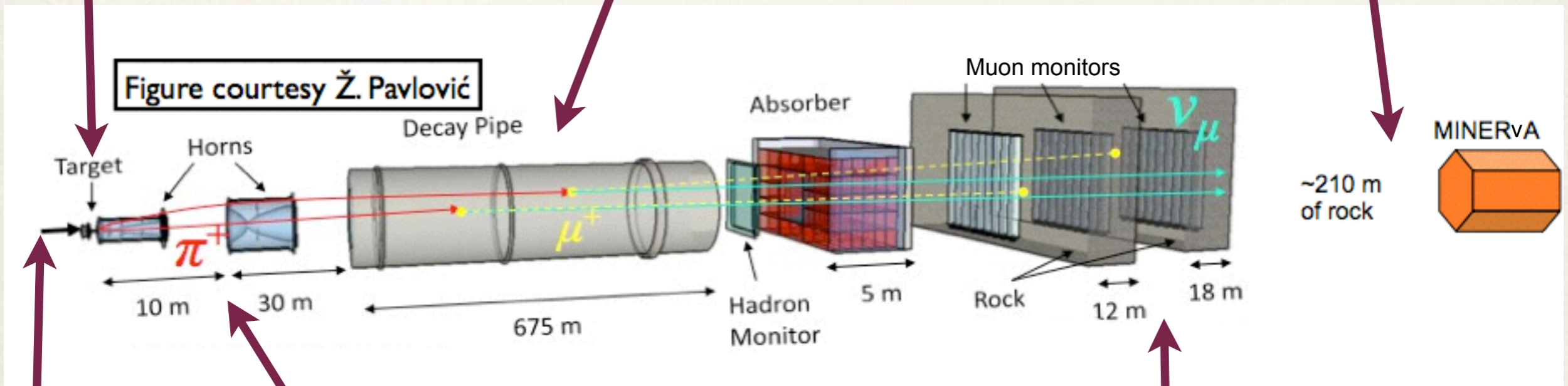
The MINERvA experiment

NUMI beamline

Protons hit graphite target, produce mesons (mostly pions, some kaons)



Neutrinos!

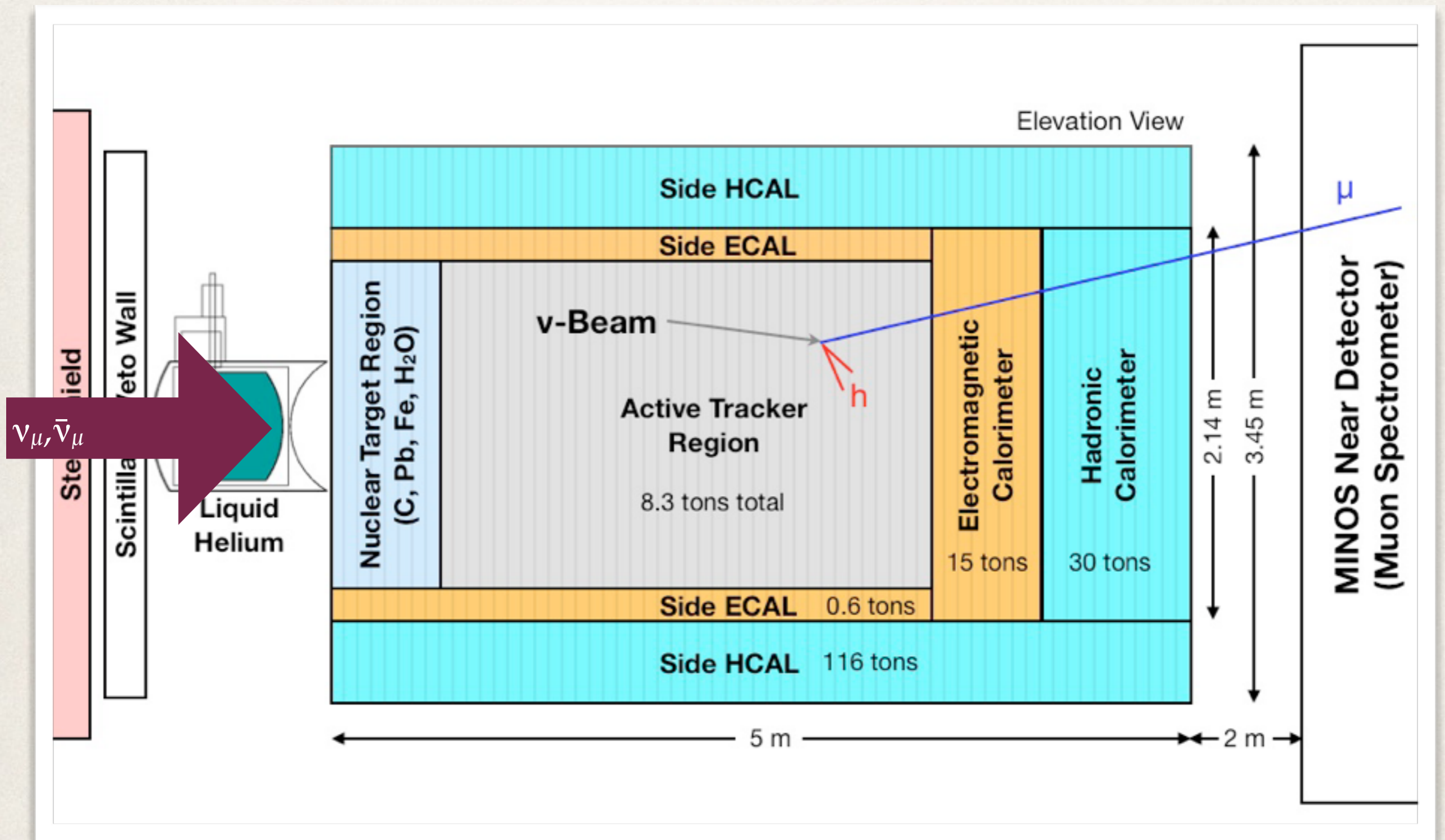


120 GeV protons

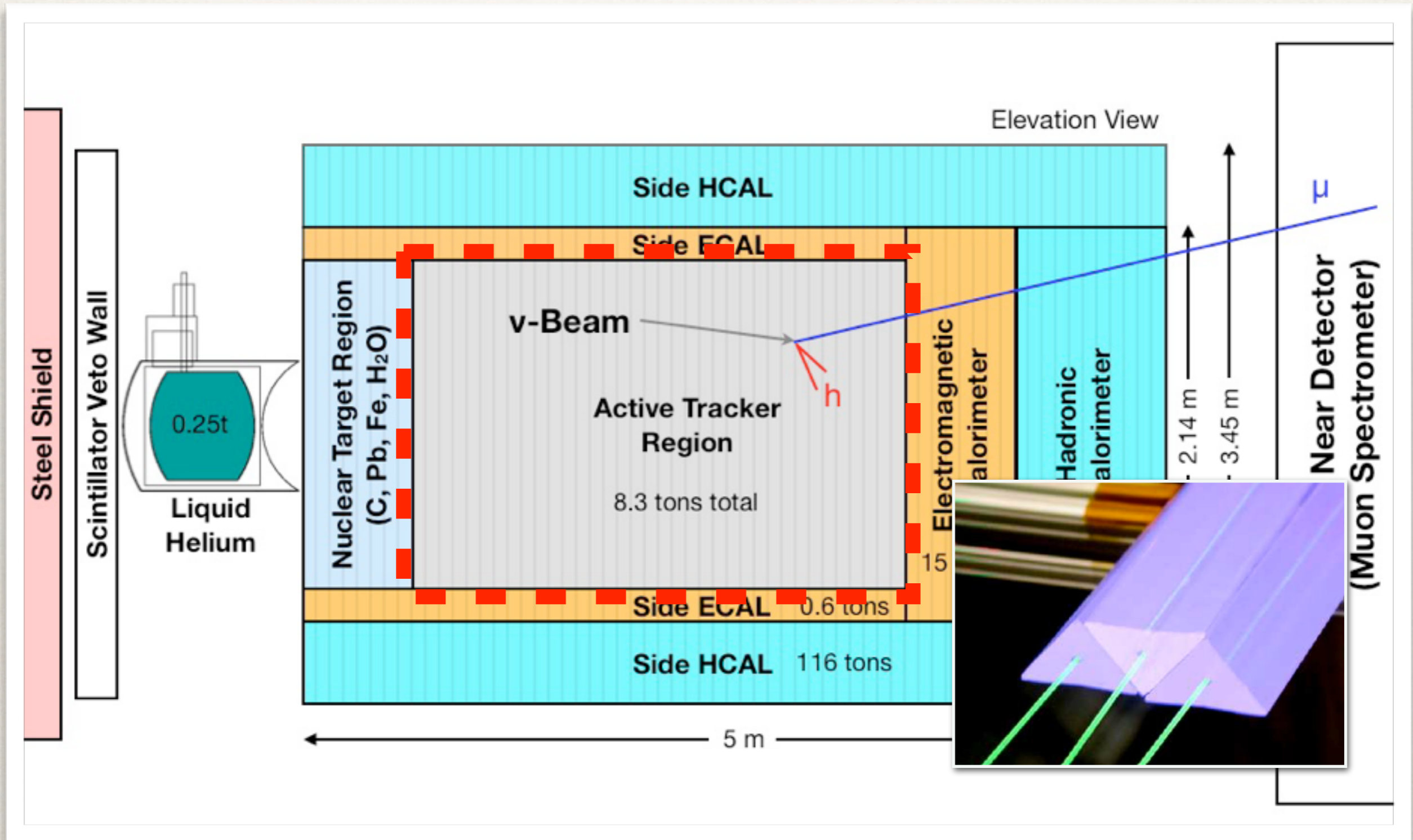
Horns focus one charge of meson and defocus the other, leading to neutrinos or antineutrinos

Rocks remove muons from beam

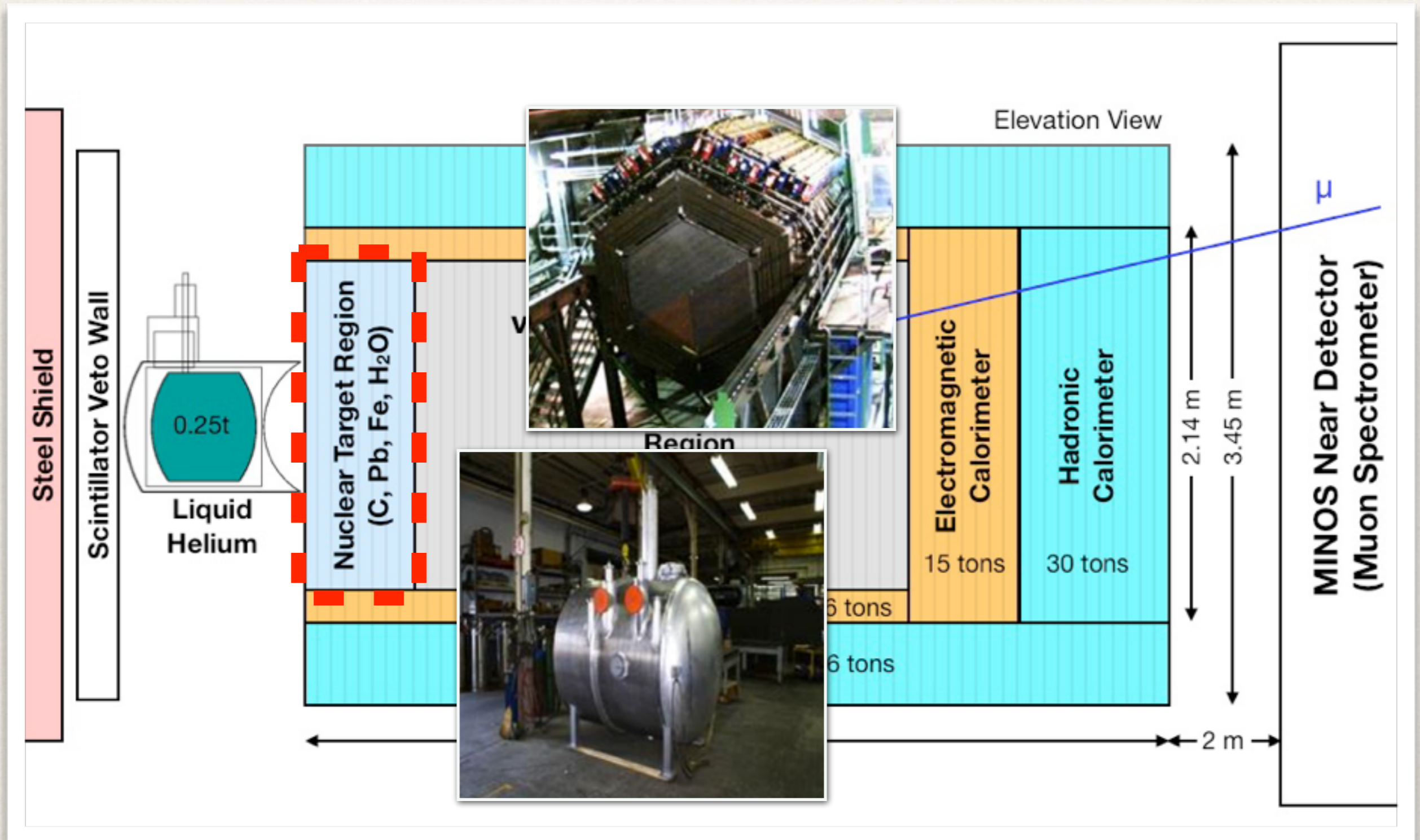
MINERvA detector



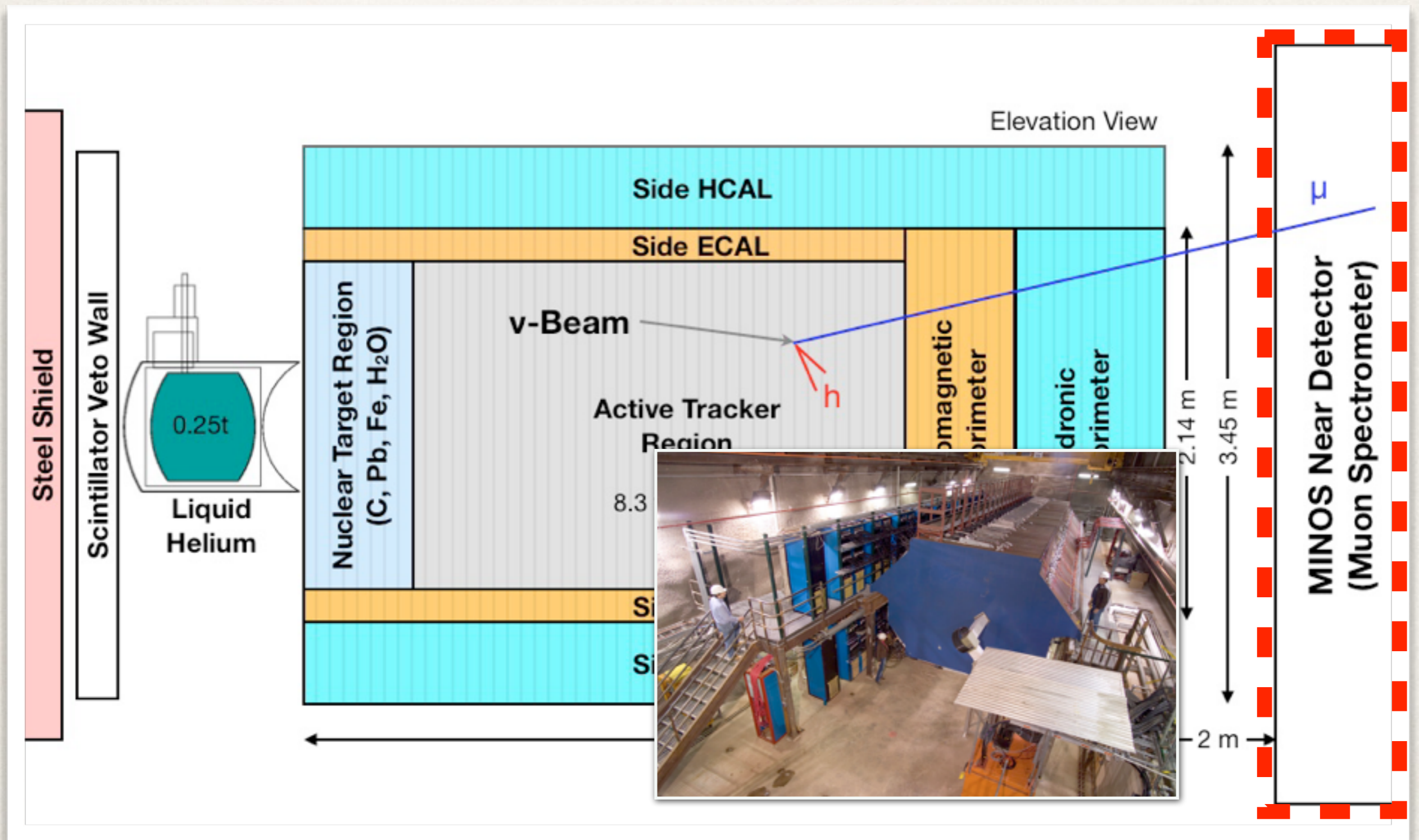
MINERvA detector



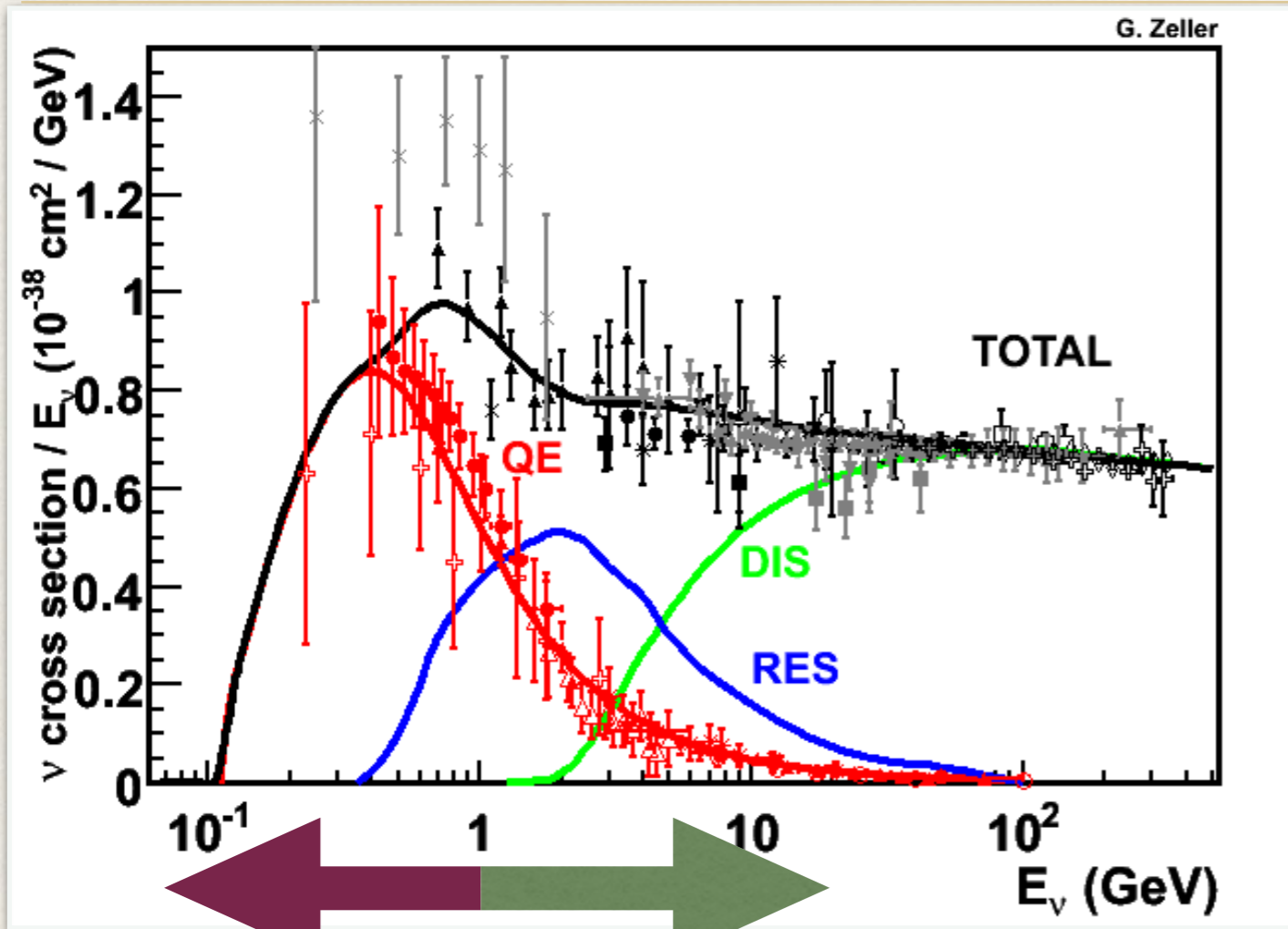
MINERvA detector



MINERvA detector



The MINERvA energy range



J.A. Formaggio and G.P. Zeller,
Rev. Mod. Phys. 84, 1307-1341,
 2012

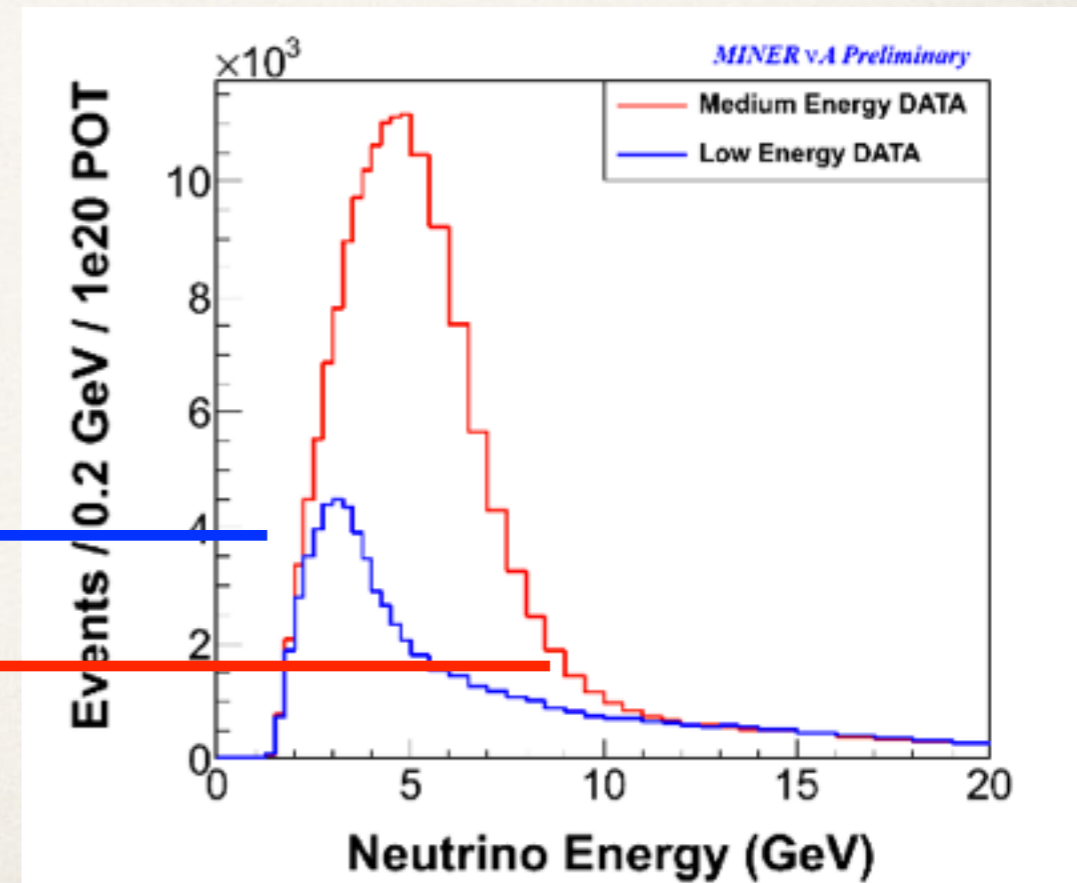
BooNE experiments, MINERvA, DUNE, NOvA, MINOS

T2K

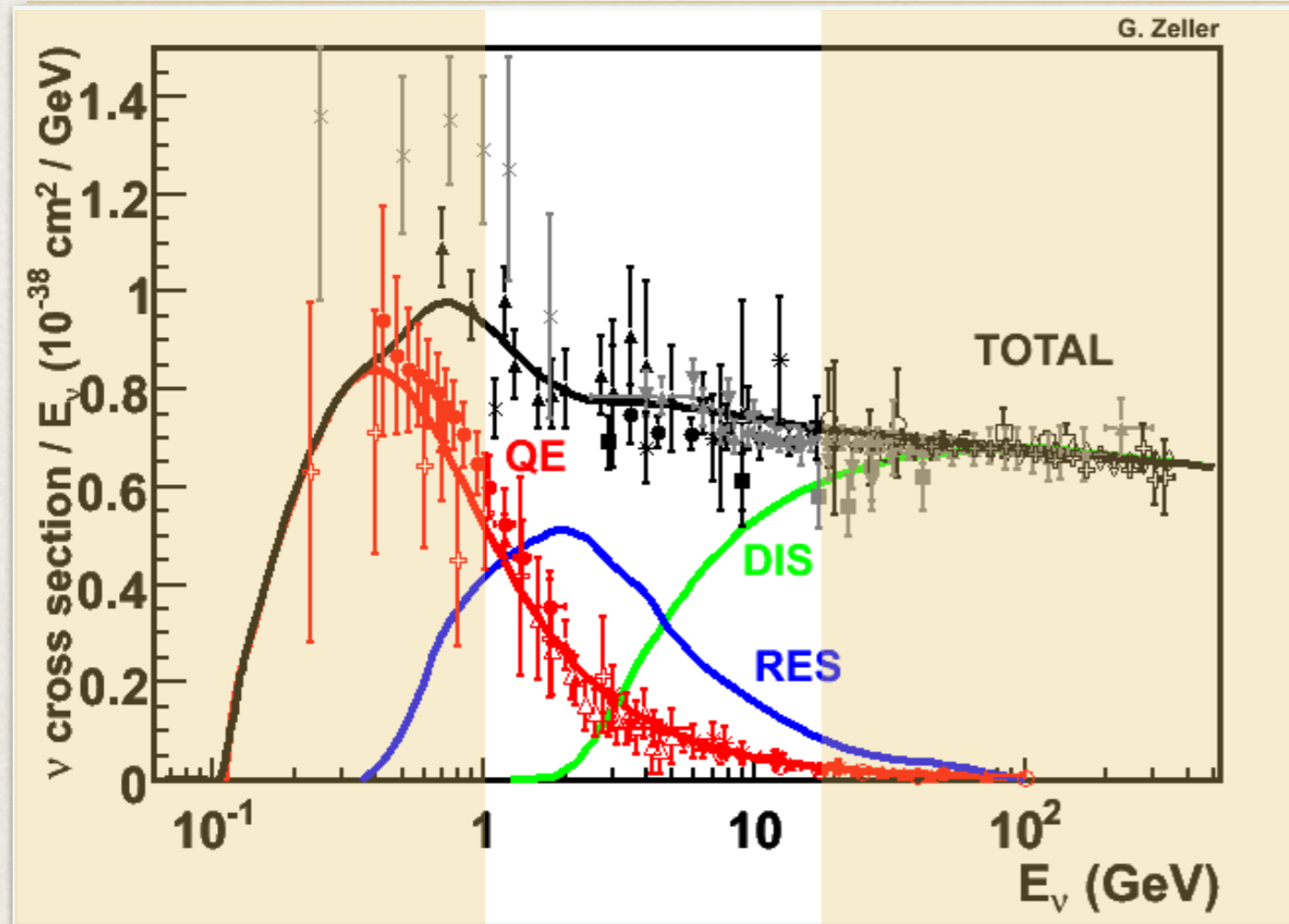
Low-energy run,
 2010-2012

3.98×10^{20} POT (ν)
 1.7×10^{20} POT ($\bar{\nu}$)

Medium-energy run, 2013-
 Already exceeded low-
 energy POT in ν mode

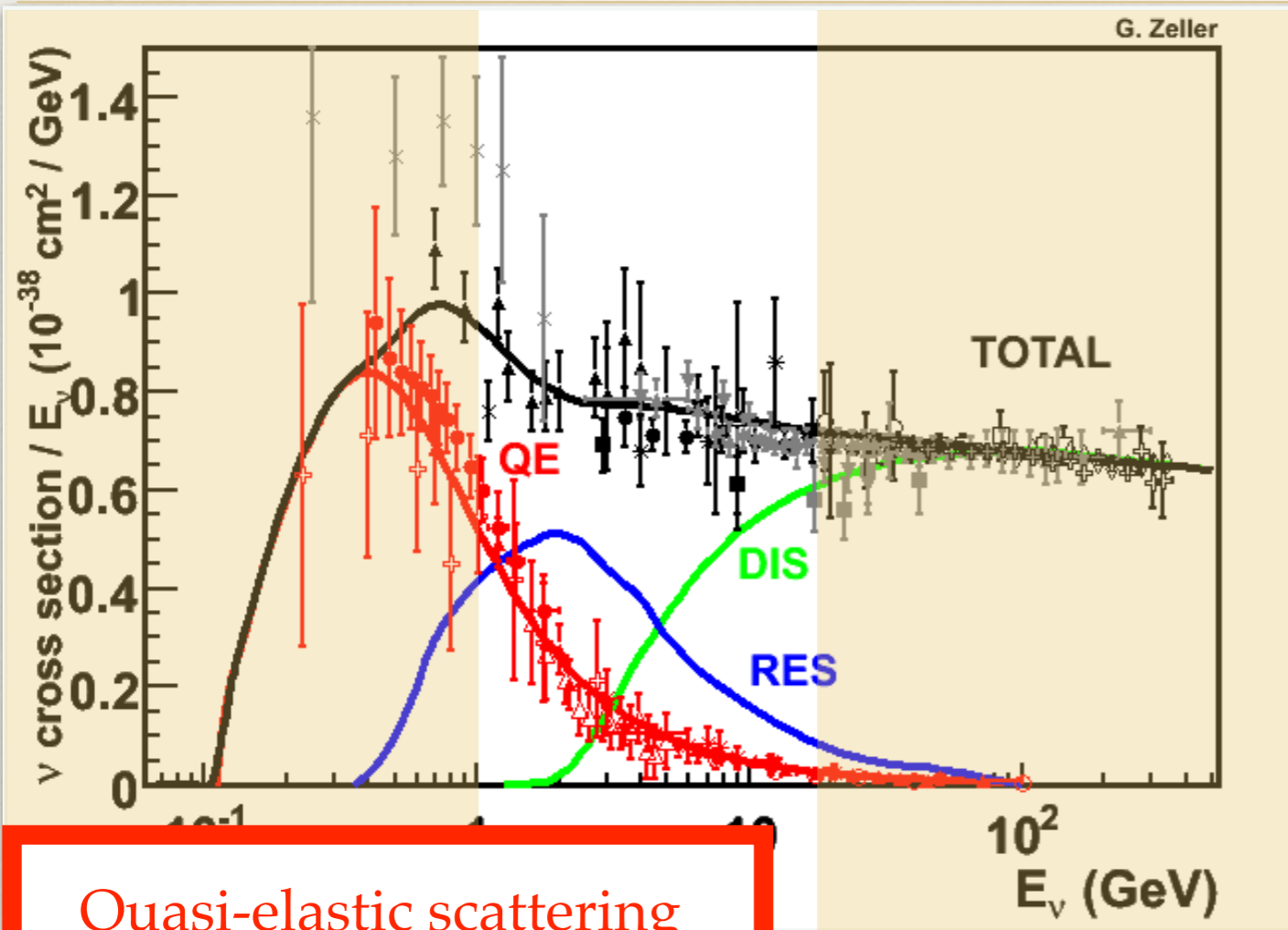


The MINERvA energy range



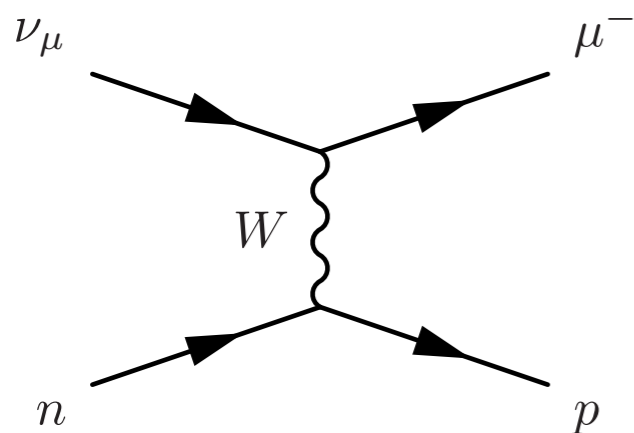
*J.A. Formaggio and G.P. Zeller,
Rev. Mod. Phys. 84, 1307-1341,
2012*

The MINERvA energy range

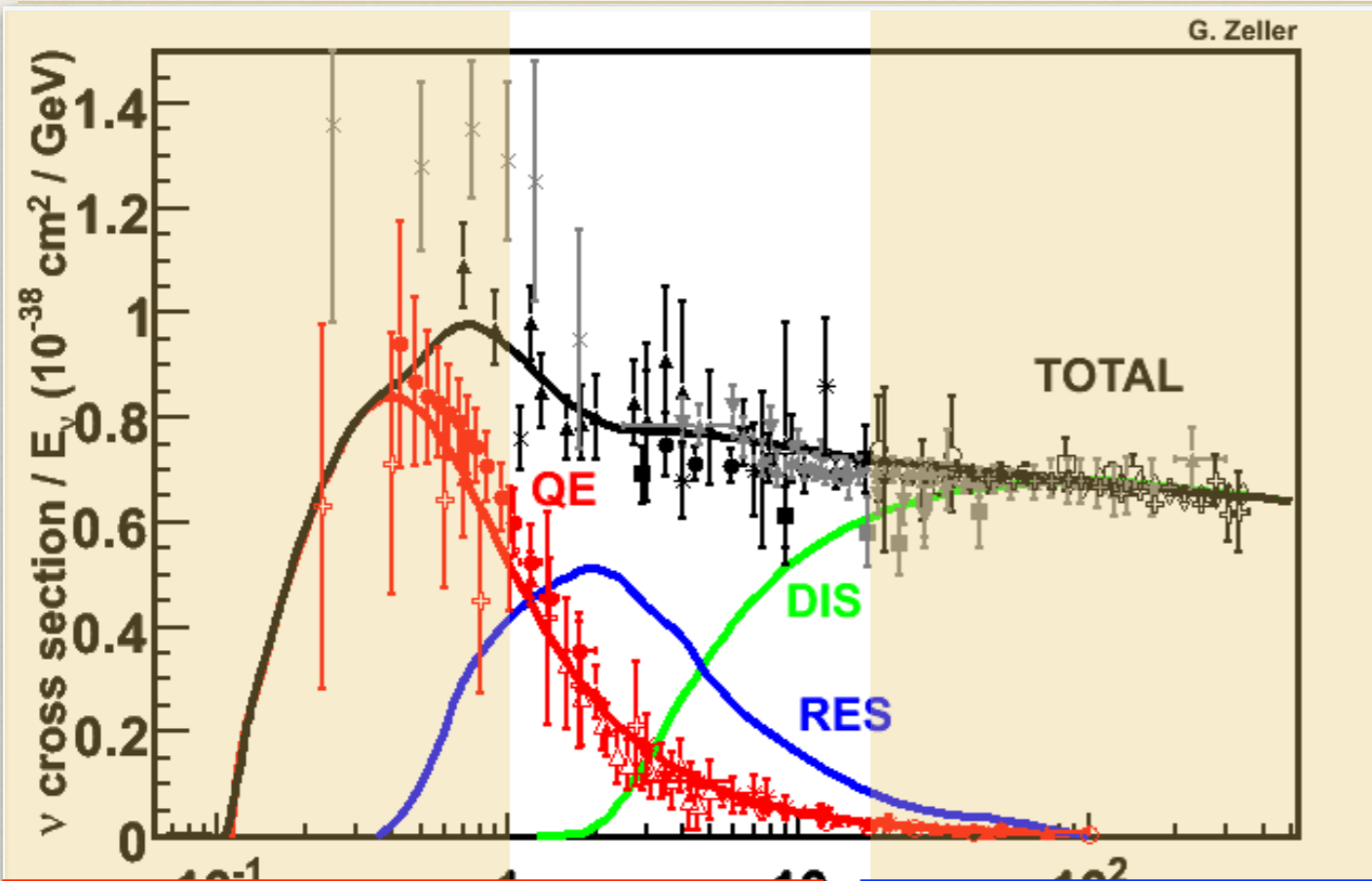


*J.A. Formaggio and G.P. Zeller,
Rev. Mod. Phys. 84, 1307-1341,
2012*

Quasi-elastic scattering

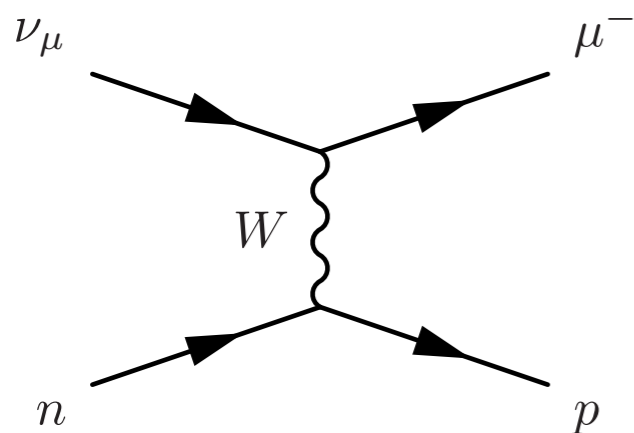


The MINERvA energy range

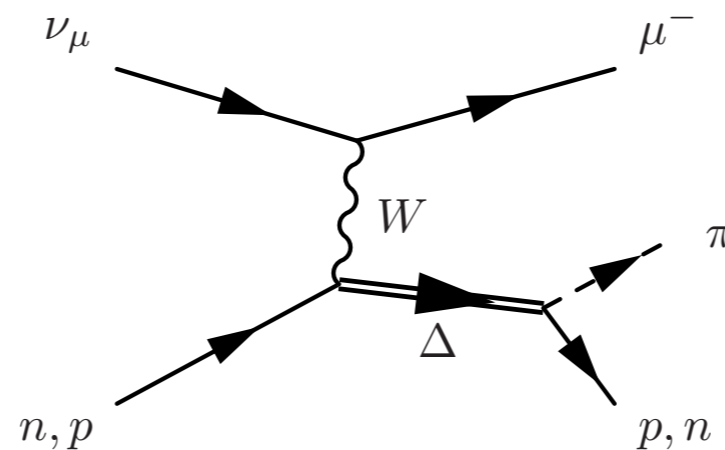


*J.A. Formaggio and G.P. Zeller,
Rev. Mod. Phys. 84, 1307-1341,
2012*

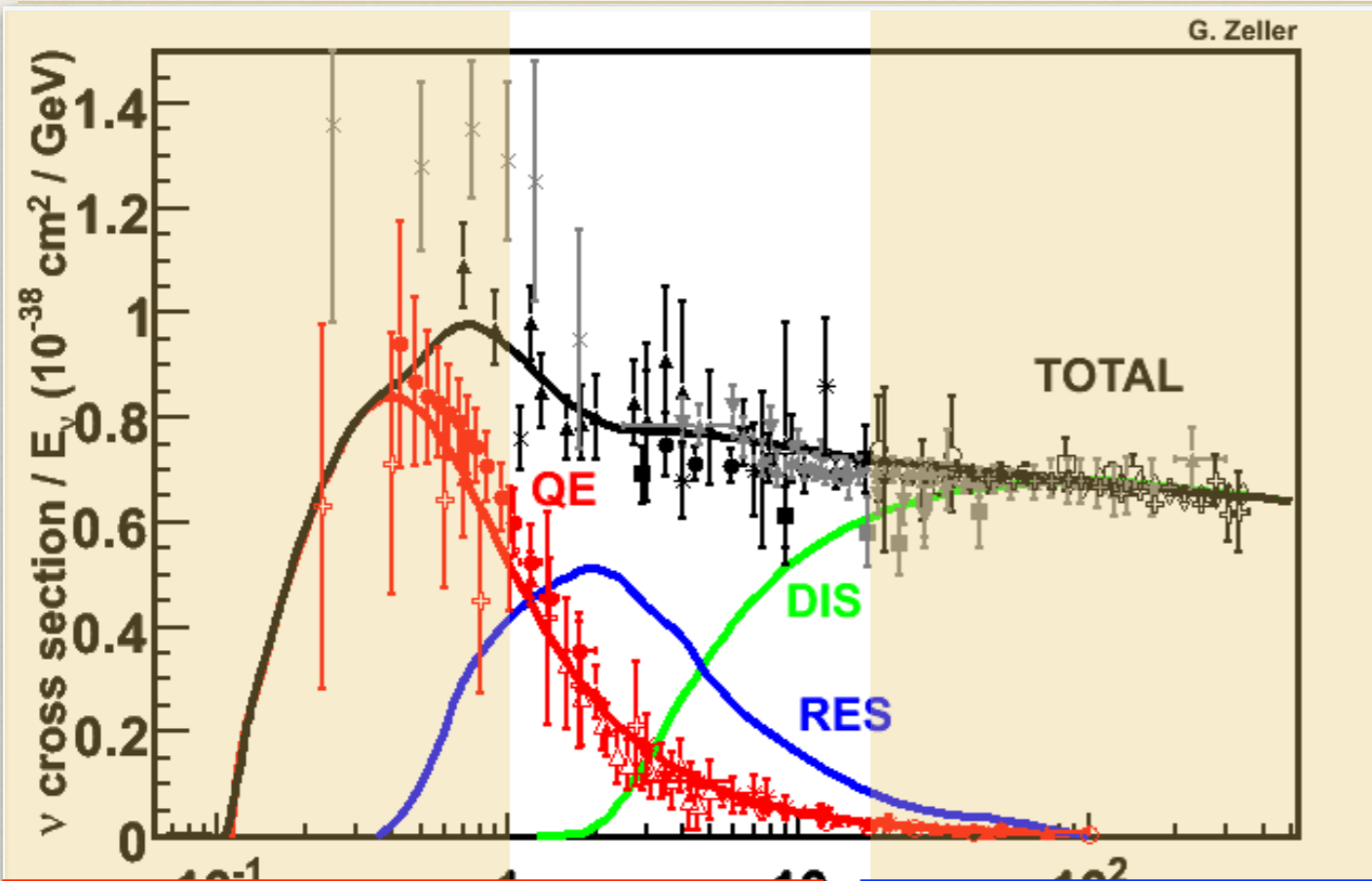
Quasi-elastic scattering



Resonant pion production

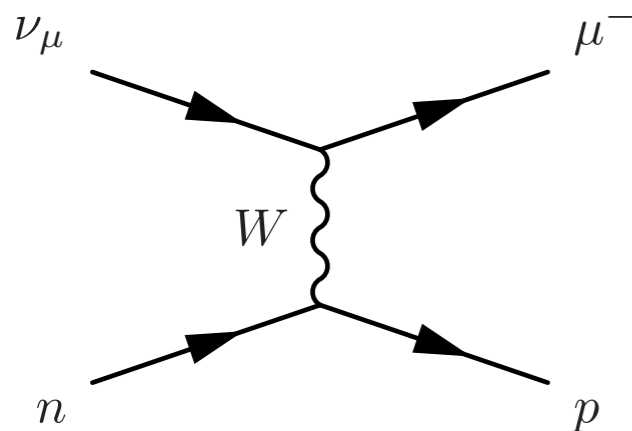


The MINERvA energy range

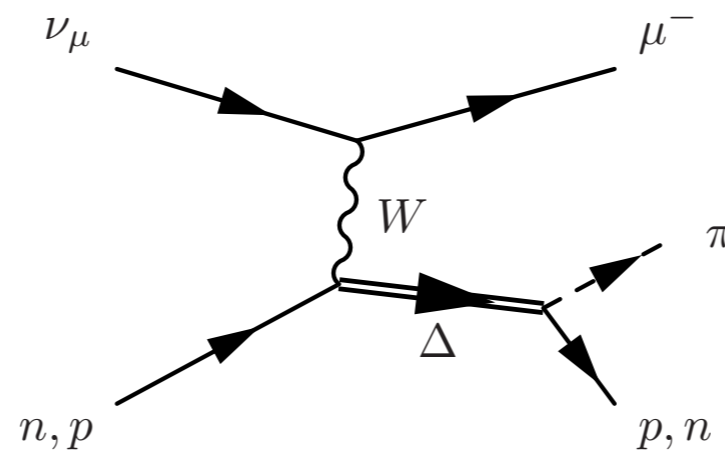


*J.A. Formaggio and G.P. Zeller,
Rev. Mod. Phys. 84, 1307-1341,
2012*

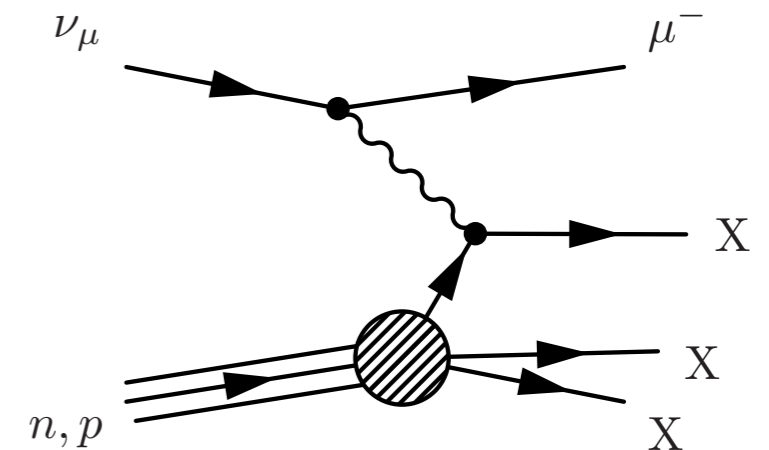
Quasi-elastic scattering



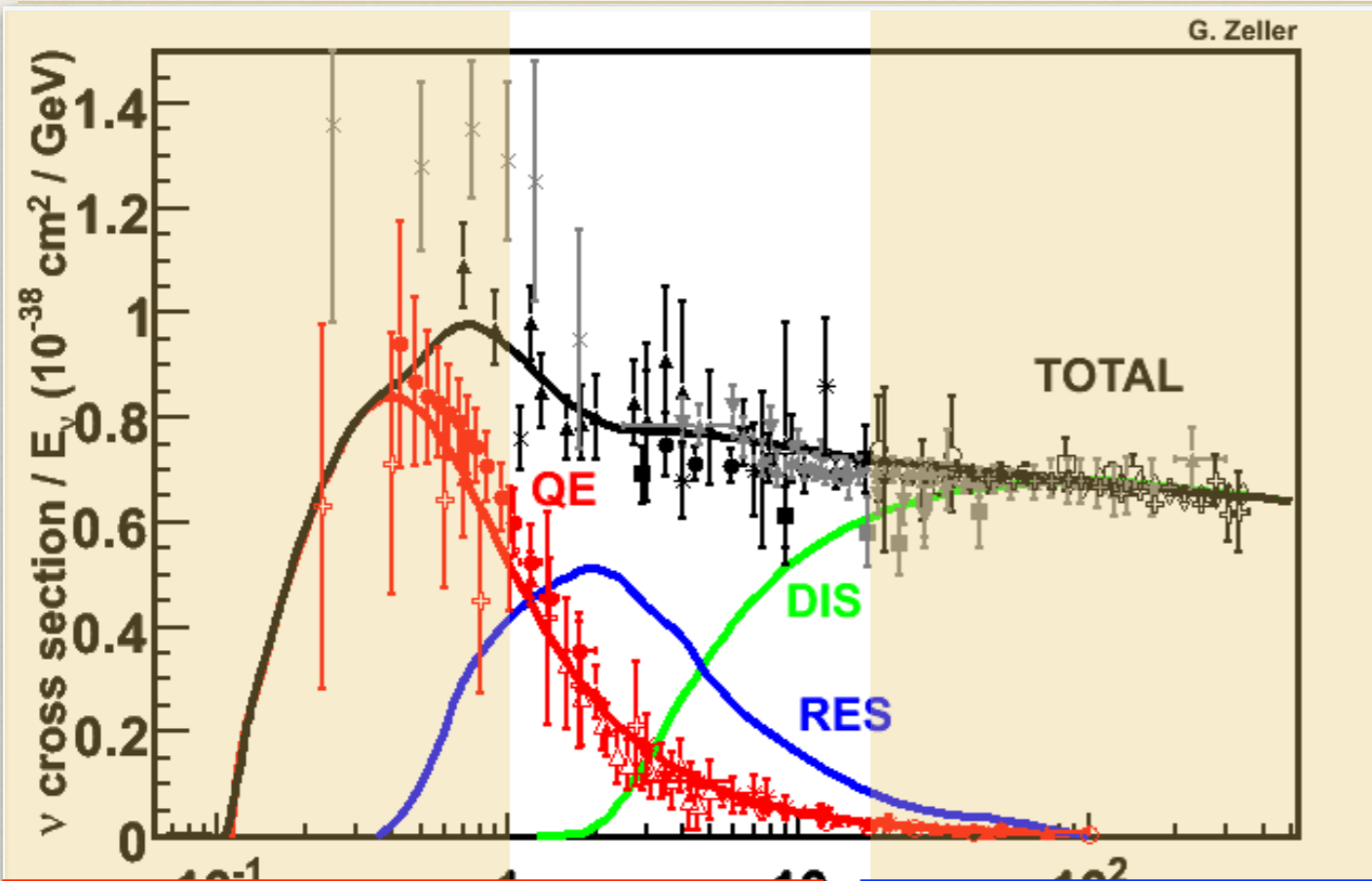
Resonant pion production



Deep inelastic scattering



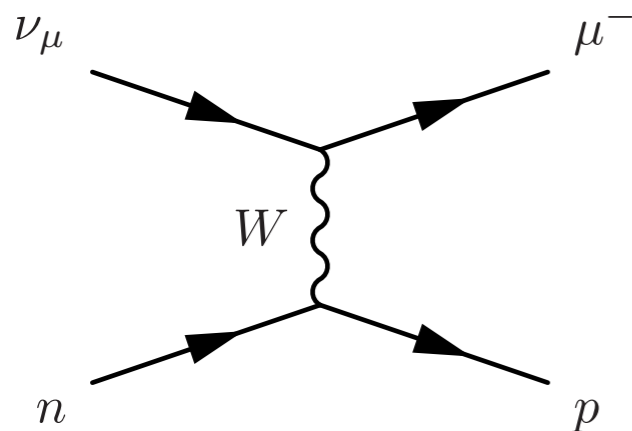
The MINERvA energy range



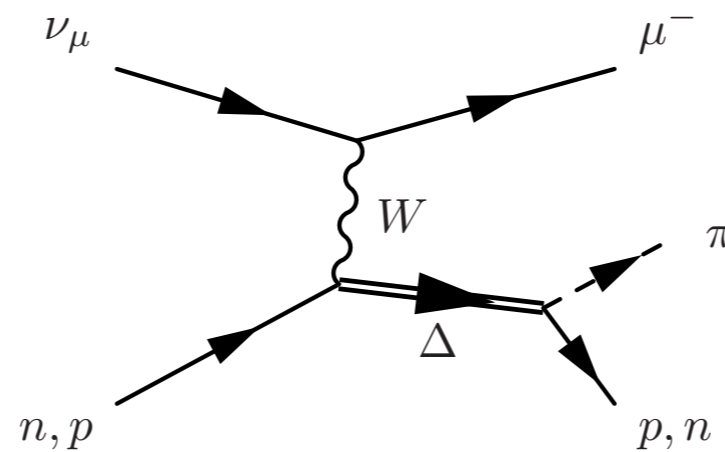
*J.A. Formaggio and G.P. Zeller,
Rev. Mod. Phys. 84, 1307-1341,
2012*

To see how we calculate cross sections, let's look at quasi-elastic scattering in detail

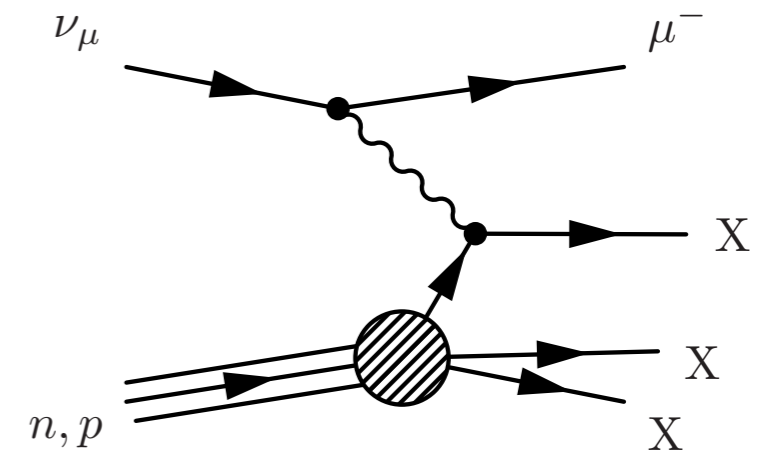
Quasi-elastic scattering

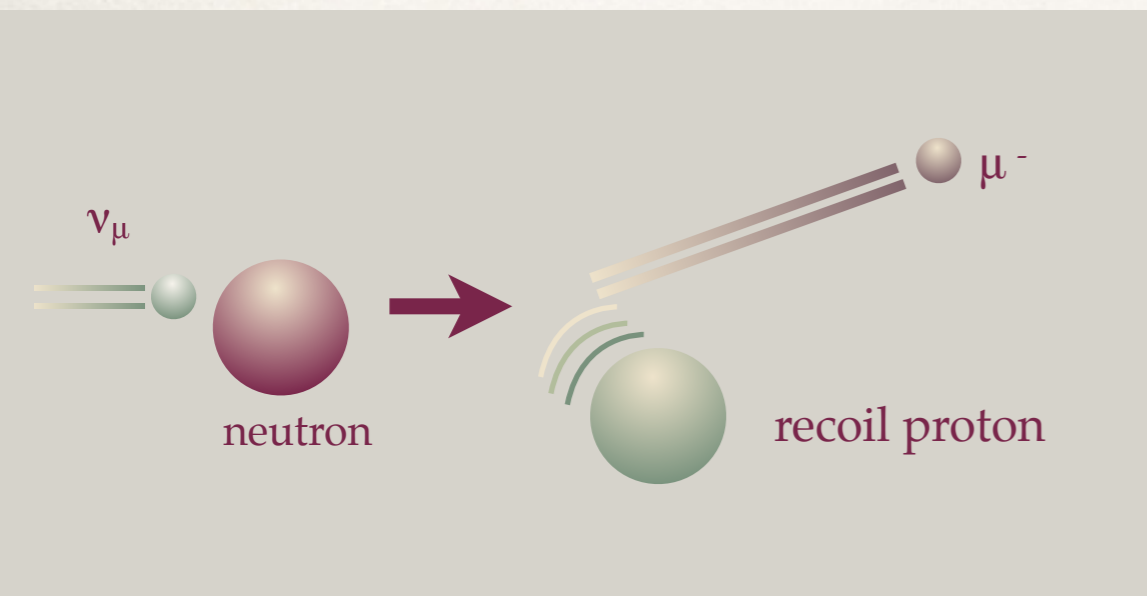


Resonant pion production



Deep inelastic scattering





Quasi-elastic scattering

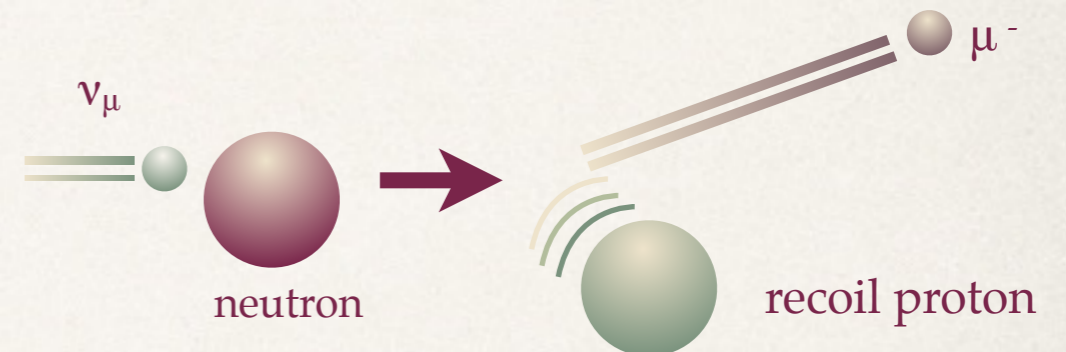
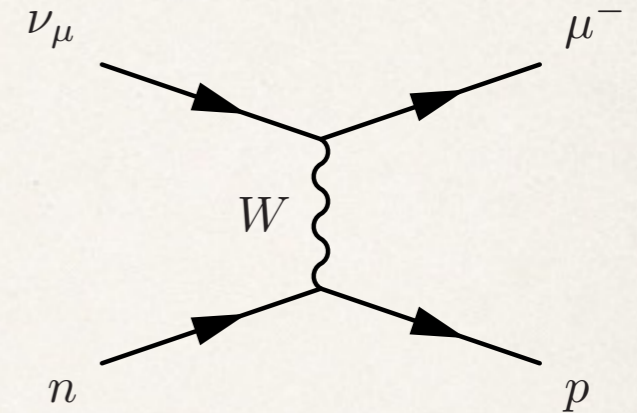
...a little bit of theory

Quasi-elastic scattering (CCQE)

- * A relatively “simple” interaction process
- * There is a **single charged muon** in the final state, plus the **recoil nucleon** (no pions etc)
- * We can **reconstruct the neutrino energy and 4-momentum transfer Q^2** from just the **muon kinematics**

$$Q_{QE}^2 = 2E_\nu^{QE} (E_\mu - p_\mu \cos \theta_\mu) - m_\mu^2$$

$$E_\nu^{QE} = \frac{m_n^2 - (m_p - E_b)^2 - m_\mu^2 + 2(m_p - E_b)E_\mu}{2(m_p - E_b - E_\mu + p_\mu \cos \theta_\mu)}$$



- * But this assumes scattering from a stationary nucleon
- * Once we know Q^2 , the cross-section model is well-proven on hydrogen/deuterium

Llewellyn-Smith formula

$$\frac{d\sigma}{dQ^2}{}_{QE} \left(\begin{array}{l} \nu_l n \rightarrow l^- p \\ \bar{\nu}_l p \rightarrow l^+ n \end{array} \right) = \frac{M^2 G_F^2 \cos^2 \theta_C}{8\pi E_\nu^2} \left\{ A(Q^2) \mp B(Q^2) \frac{s-u}{M^2} + C(Q^2) \frac{(s-u)^2}{M^4} \right\}$$

$$A(Q^2) = \frac{m_l^2 + Q^2}{M^2} \left\{ \left(1 + \frac{Q^2}{4M^2}\right) |F_A|^2 - \left(1 - \frac{Q^2}{4M^2}\right) F_1^2 \right. \\ \left. + \frac{Q^2}{4M^2} \left(1 - \frac{Q^2}{4M^2}\right) (\xi F_2)^2 + \frac{Q^2}{M^2} \text{Re}(F_1^* \xi F_2) - \frac{Q^2}{M^2} \left(1 + \frac{Q^2}{4M^2}\right) (F_A^3)^2 \right. \\ \left. - \frac{m_\mu^2}{4M^2} \left[|F_1 + \xi F_2|^2 + |F_A + 2F_P|^2 - 4 \left(1 + \frac{Q^2}{4M^2}\right) ((F_V^3)^2 + F_P^2) \right] \right\}$$

$$B(Q^2) = \frac{Q^2}{M^2} \text{Re} [F_A^* (F_1 + \xi F_2)] - \frac{m_l^2}{M^2} \text{Re} \left[(F_1 - \tau \xi F_2) F_V^{3*} - \left(F_A^* - \frac{Q^2}{2M^2} F_P\right) F_A^3 \right]$$

$$C(Q^2) = \frac{1}{4} \left\{ F_A^2 + F_1^2 + \tau (\xi F_2)^2 + \frac{Q^2}{M^2} (F_A^3)^2 \right\}$$

C.H. Llewellyn Smith, Phys. Rept. 3C, 261 (1972)



Llewellyn-Smith formula

$$\frac{d\sigma}{dQ^2} \Big|_{QE} \left(\begin{array}{l} \nu_l n \rightarrow l^- p \\ \bar{\nu}_l p \rightarrow l^+ n \end{array} \right) = \frac{M^2 G_F^2 \cos^2 \theta_C}{8\pi E_\nu^2} \left\{ A(Q^2) \mp B(Q^2) \frac{s-u}{M^2} + C(Q^2) \frac{(s-u)^2}{M^4} \right\}$$

$$A(Q^2) = \frac{m_l^2 + Q^2}{M^2} \left\{ \left(1 + \frac{Q^2}{4M^2} \right) |F_A|^2 - \left(1 - \frac{Q^2}{4M^2} \right) F_1^2 \right. \\ \left. + \frac{Q^2}{4M^2} \left(1 - \frac{Q^2}{4M^2} \right) \xi F_2^2 + \frac{Q^2}{M^2} \text{Re} [F_1^* \xi F_2] - \frac{Q^2}{M^2} \left(1 + \frac{Q^2}{4M^2} \right) (F_A^3)^2 \right. \\ \left. - \frac{m_\mu^2}{4M^2} \left[|F_1 + \xi F_2|^2 + |F_A + 2F_P|^2 - 4 \left(1 + \frac{Q^2}{4M^2} \right) ((F_V^3)^2 + F_P^2) \right] \right\}$$

$$B(Q^2) = \frac{Q^2}{M^2} \text{Re} [F_A^* (F_1 + \xi F_2)] - \frac{m_l^2}{M^2} \text{Re} \left[(F_1 - \tau \xi F_2) F_V^{3*} - \left(F_A^* - \frac{Q^2}{2M^2} F_P \right) F_A^3 \right]$$

$$C(Q^2) = \frac{1}{4} \left\{ F_A^2 + F_1^2 + \tau (\xi F_2)^2 + \frac{Q^2}{M^2} (F_A^3)^2 \right\}$$

C.H. Llewellyn Smith, Phys. Rept. 3C, 261 (1972)

- * F_1, F_2 are vector (electromagnetic) form-factors, based on the electric and magnetic form factors of the nucleons

$$F_1(Q^2) = \frac{G_E + \tau G_M}{1 + \tau} \quad \xi F_2(Q^2) = \frac{G_M - G_E}{1 + \tau}$$

$$\tau = \frac{Q^2}{4M^2}$$

Llewellyn-Smith formula

$$\frac{d\sigma}{dQ^2} \Big|_{QE} \left(\begin{array}{l} \nu_l n \rightarrow l^- p \\ \bar{\nu}_l p \rightarrow l^+ n \end{array} \right) = \frac{M^2 G_F^2 \cos^2 \theta_C}{8\pi E_\nu^2} \left\{ A(Q^2) \mp B(Q^2) \frac{s-u}{M^2} + C(Q^2) \frac{(s-u)^2}{M^4} \right\}$$

$$A(Q^2) = \frac{m_l^2 + Q^2}{M^2} \left\{ \left(1 + \frac{Q^2}{4M^2}\right) |F_A|^2 - \left(1 - \frac{Q^2}{4M^2}\right) F_1^2 \right. \\ \left. + \frac{Q^2}{4M^2} \left(1 - \frac{Q^2}{4M^2}\right) (\xi F_2)^2 + \frac{Q^2}{M^2} \text{Re}(F_1^* \xi F_2) - \frac{Q^2}{M^2} \left(1 + \frac{Q^2}{4M^2}\right) (F_A^3)^2 \right. \\ \left. - \frac{m_\mu^2}{4M^2} \left[|F_1 + \xi F_2|^2 + |F_A + 2F_P|^2 - 4\left(1 + \frac{Q^2}{4M^2}\right) (F_V^3)^2 + F_P^2 \right] \right\}$$

$$B(Q^2) = \frac{Q^2}{M^2} \text{Re} [F_A^* (F_1 + \xi F_2)] - \frac{m_l^2}{M^2} \text{Re} \left[(F_1 - \tau \xi F_2) F_V^{3*} - \left(F_A^* - \frac{Q^2}{2M^2} F_P\right) F_A^3 \right]$$

$$C(Q^2) = \frac{1}{4} \left\{ F_A^2 + F_1^2 + \tau (\xi F_2)^2 + \frac{Q^2}{M^2} (F_A^3)^2 \right\}$$

C.H. Llewellyn Smith, Phys. Rept. 3C, 261 (1972)

- * F_P corresponds to non-tree-level corrections involving pions, and can be related to F_A using PCAC
- * F_3 terms are second-class currents and can be taken to be zero

Llewellyn-Smith formula

$$\frac{d\sigma}{dQ^2} \Big|_{QE} \left(\begin{array}{l} \nu_l n \rightarrow l^- p \\ \bar{\nu}_l p \rightarrow l^+ n \end{array} \right) = \frac{M^2 G_F^2 \cos^2 \theta_C}{8\pi E_\nu^2} \left\{ A(Q^2) \mp B(Q^2) \frac{s-u}{M^2} + C(Q^2) \frac{(s-u)^2}{M^4} \right\}$$

$$A(Q^2) = \frac{m_l^2 + Q^2}{M^2} \left\{ \left(1 + \frac{Q^2}{4M^2}\right) |F_A|^2 - \left(1 - \frac{Q^2}{4M^2}\right) F_1^2 \right. \\ \left. + \frac{Q^2}{4M^2} \left(1 - \frac{Q^2}{4M^2}\right) (\xi F_2)^2 + \frac{Q^2}{M^2} \text{Re}(F_1^* \xi F_2) - \frac{Q^2}{M^2} \left(1 + \frac{Q^2}{4M^2}\right) (F_A^3)^2 \right. \\ \left. - \frac{m_\mu^2}{4M^2} \left[|F_1 + \xi F_2|^2 + |F_A + 2F_P|^2 - 4\left(1 + \frac{Q^2}{4M^2}\right) ((F_V^3)^2 + F_P^2) \right] \right\}$$

$$B(Q^2) = \frac{Q^2}{M^2} \text{Re} [F_A^* (F_1 + \xi F_2)] - \frac{m_l^2}{M^2} \text{Re} \left[(F_1 - \tau \xi F_2) F_V^{3*} - \left(F_A^* - \frac{Q^2}{2M^2} F_P\right) F_A^3 \right]$$

$$C(Q^2) = \frac{1}{4} \left\{ F_A^2 + F_1^2 + \tau (\xi F_2)^2 + \frac{Q^2}{M^2} (F_A^3)^2 \right\}$$

C.H. Llewellyn Smith, *Phys. Rept.* 3C, 261 (1972)

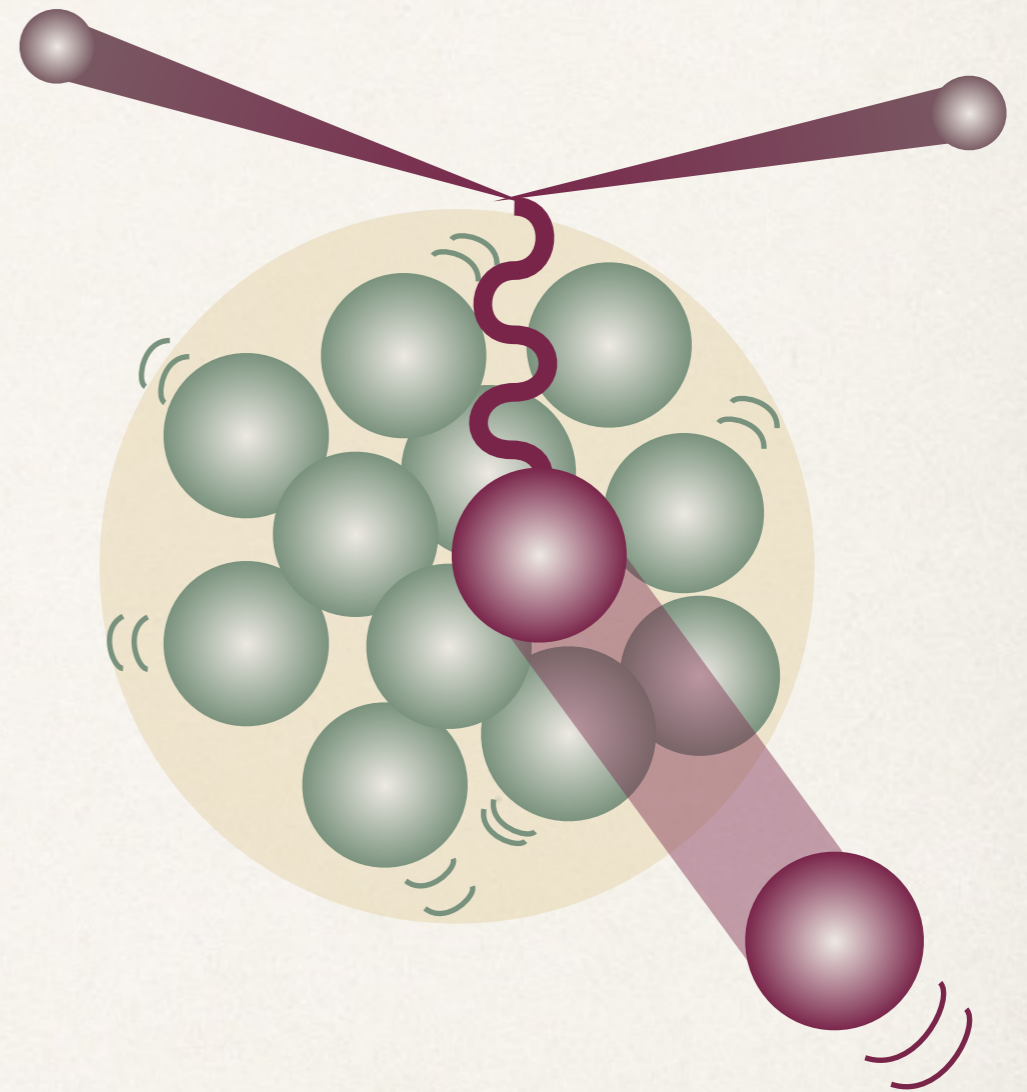
- * F_A , the axial form factor, cannot be measured in electromagnetic electron scattering (a vector process). We typically model the axial form factor as a dipole:

$$F_A(Q^2) = - \frac{g_A}{\left(1 + \frac{Q^2}{M_A^2}\right)^2}$$

Axial mass, M_A , is the only free parameter

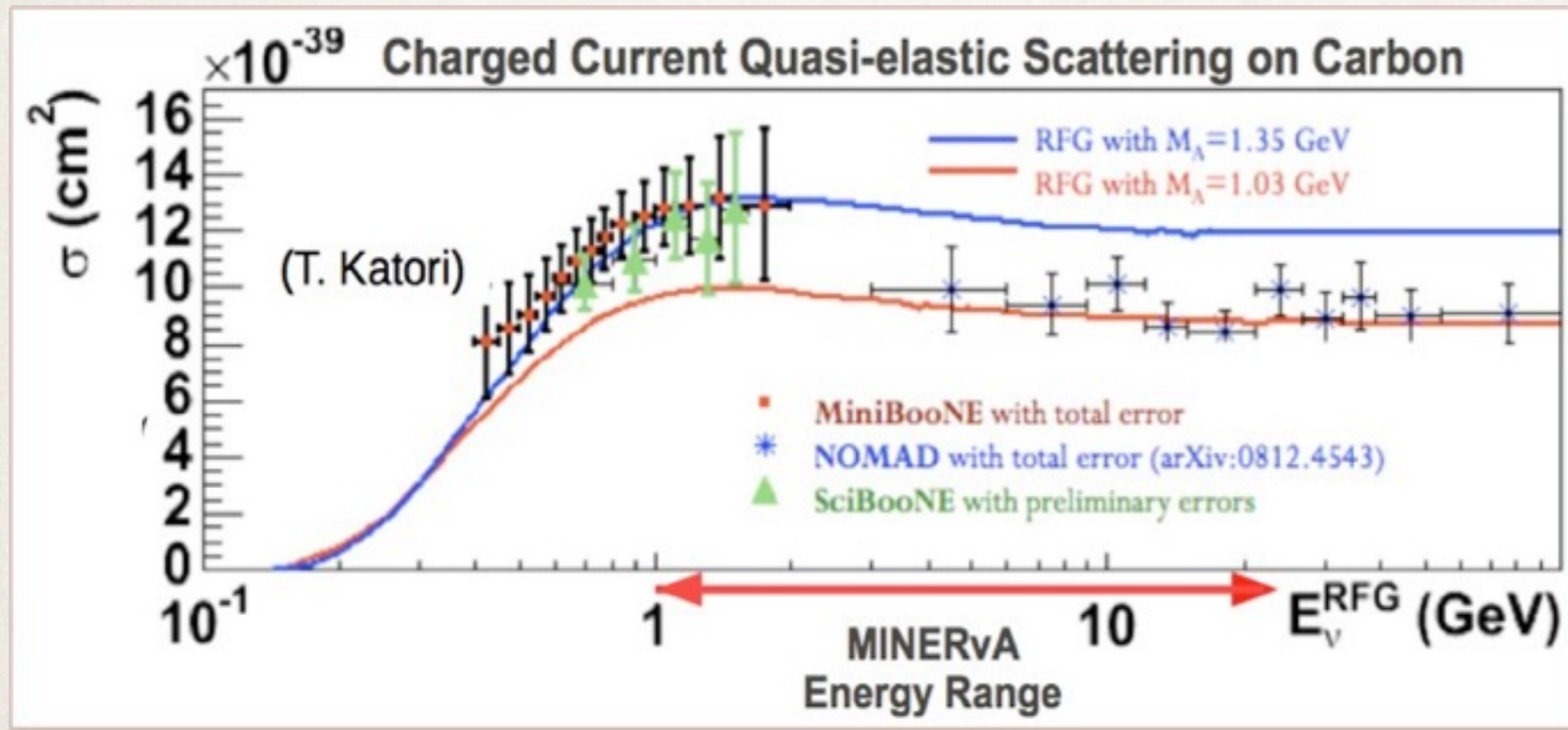
Nucleons in the nucleus

- ❖ In a heavy nucleus, nucleons are **not stationary**
- ❖ They interact with the other nucleons
- ❖ A commonly-used simulation of this is the Relativistic Fermi Gas model
 - ❖ Treat nucleons as independent particles, but in a **mean field** generated by the rest of the nucleus
 - ❖ Initial-state momenta are **Fermi distributed**
 - ❖ Pauli blocking
- ❖ Cross-sections can be modeled by a multiplier to the Llewellyn Smith cross-section



R. Smith and E. Moniz, Nucl.Phys. B43, 605 (1972); Bodek, S. Avvakumov, R. Bradford, and H. S. Budd, J.Phys.Conf.Ser. 110, 082004 (2008);

Limitations of RFG model

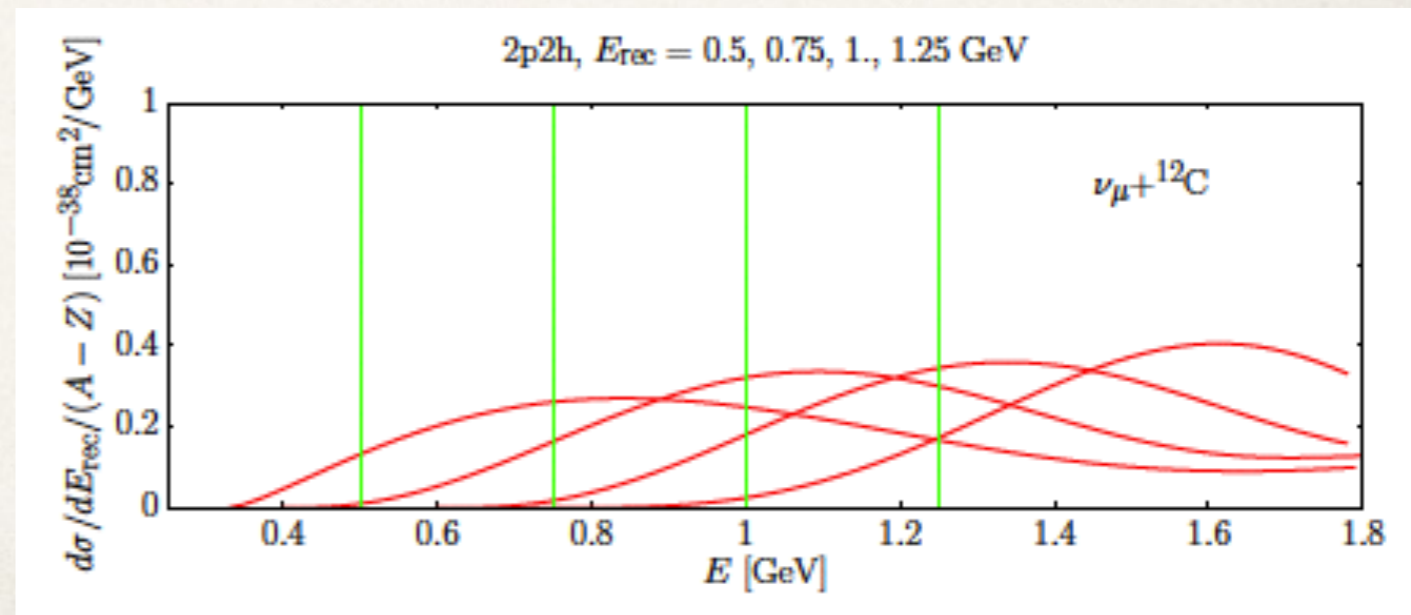


Best fits of **MiniBooNE**, **SciBooNE** and **NOMAD** cross-sections to RFG

A.A. Aguilar-Arevalo et al.
[MiniBooNE Collaboration],
Phys. Rev. D 81, 092005 (2010)

Lower-energy experiments predict $M_A=1.35$ GeV, NOMAD predicts $M_A=1.03$ GeV

- * We could be seeing additional **nuclear effects beyond the RFG model**
- * **Correlated nucleon pairs** have been observed in electron scattering (JLab)
- * These can affect **energy reconstruction**, and can cause **extra nucleons** to be emitted



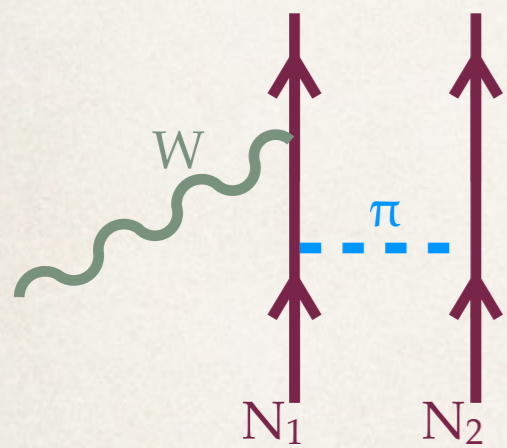
Energy resolution with correlated pairs

Modeling nuclear effects

Relativistic Fermi Gas (RFG) extensions

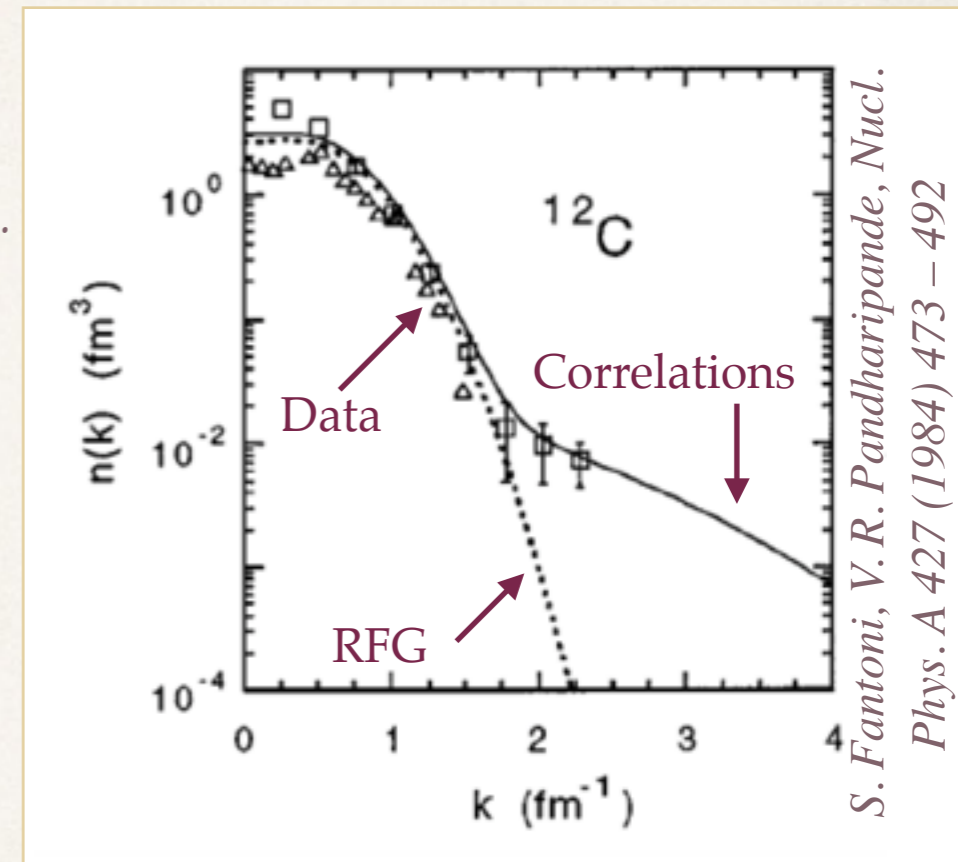
- ❖ Bodek and Ritchie model short-range correlations to give **high-energy tail** *A. Bodek, and J. L. Ritchie, Phys. Rev. D23, 1070 (1980), A. Bodek and J. L. Ritchie, Phys. Rev. D24, 1400 (1981)*
- ❖ **Local Fermi Gas (LFG)** has a position-dependent momentum distribution. *AK. S. Kuzmin, V. V. Lyubushkin, and V. A. Naumov, Eur.Phys.J. C54, 517 (2008)*

Meson Exchange Current models (MEC)



Example meson exchange current interaction, from a more detailed list (J Morfín). This illustrates a correlation.

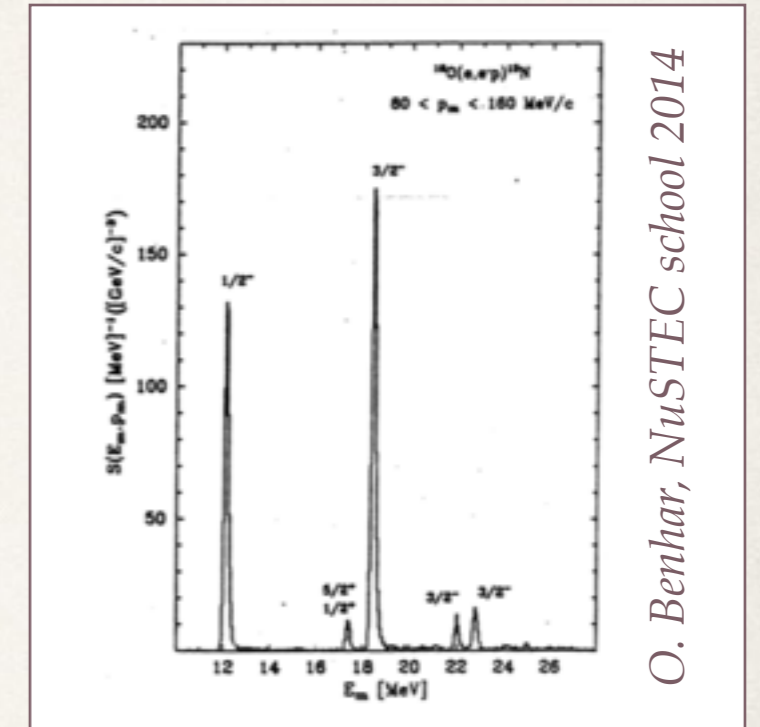
- ❖ Cross sections for meson-exchange current diagrams, including correlations, have been calculated *J. Nieves, I. Ruiz Simo and M. J. Vicente Vacas, Phys. Rev. C 83 (2011) 045501*
- ❖ These can address both short- and medium-range correlations and interactions between nucleons



More nuclear models

Spectral functions (SF)

- ❖ The shell model of the nucleus gives spectral lines, which can be seen in electron-nucleus scattering experiments
- ❖ For a more accurate model of the nucleus, a contribution for correlated pairs is added to the spectral function *O. Benhar, A. Fabrocini, S. Fantoni, and I. Sick, Nucl.Phys. A579, 493 (1994)*

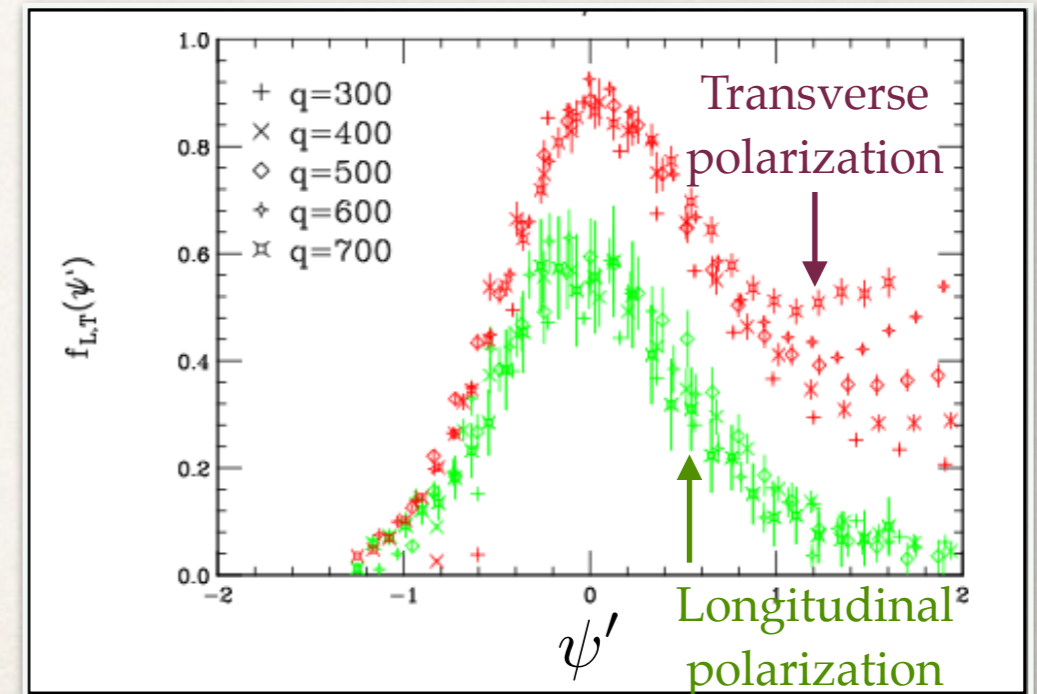


O. Benhar, NuSTEC school 2014

Transverse Enhancement Model (TEM)

$$F_1(Q^2) = \frac{G_E + \tau G_M}{1 + \tau} \quad \xi F_2(Q^2) = \frac{G_M - G_E}{1 + \tau}$$

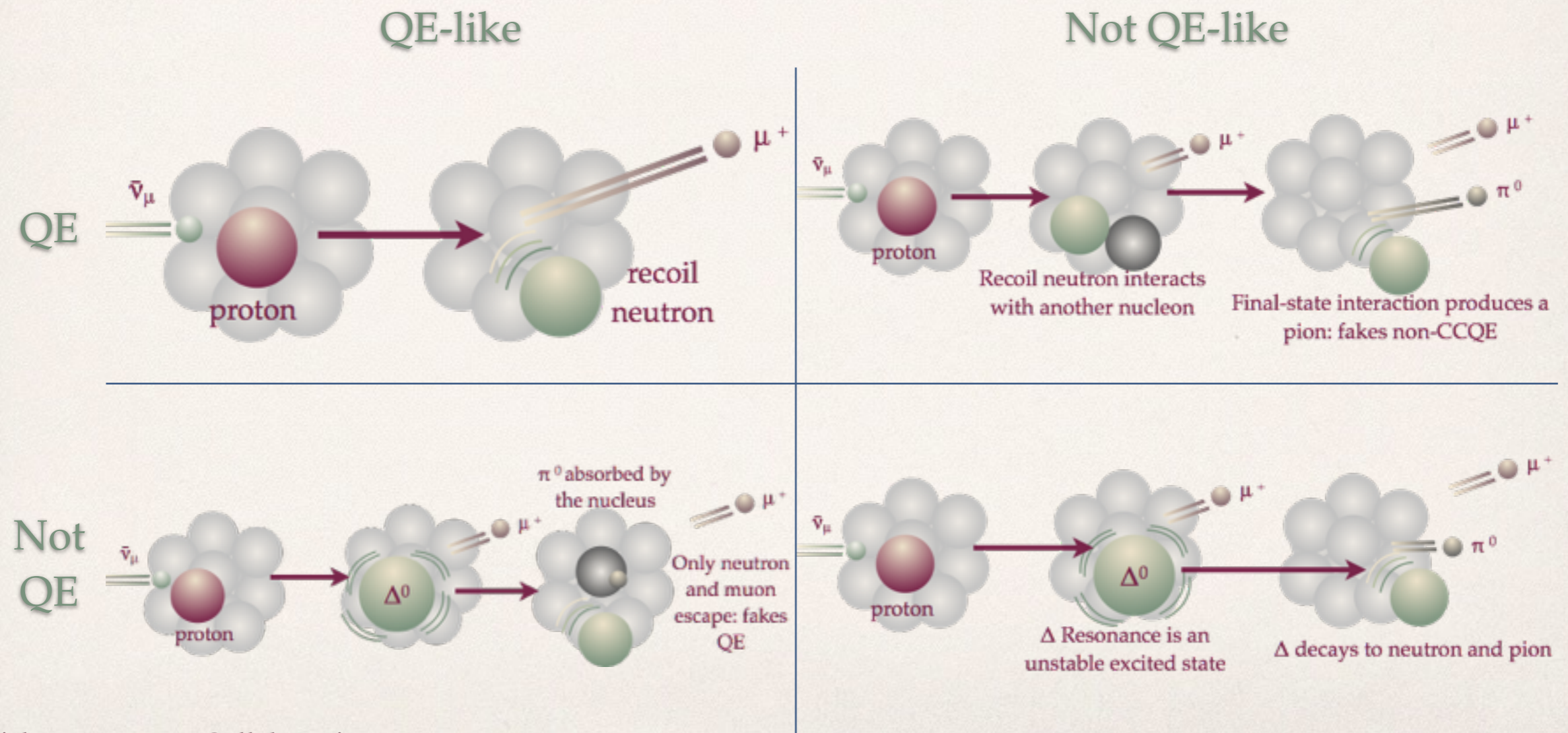
- ❖ Parameterizes correlation effect seen in electromagnetic electron scattering by modifying nucleon magnetic form factor *A. Bodek, H. Budd, and M. Christy, Eur.Phys.J. C71, 1726 (2011)*
- ❖ This was seen in pure vector scattering - how does it extend to weak (V-A) interactions?



Transverse & longitudinal cross sections
J. Carlson et al, PRC 65, 024002 (2002)

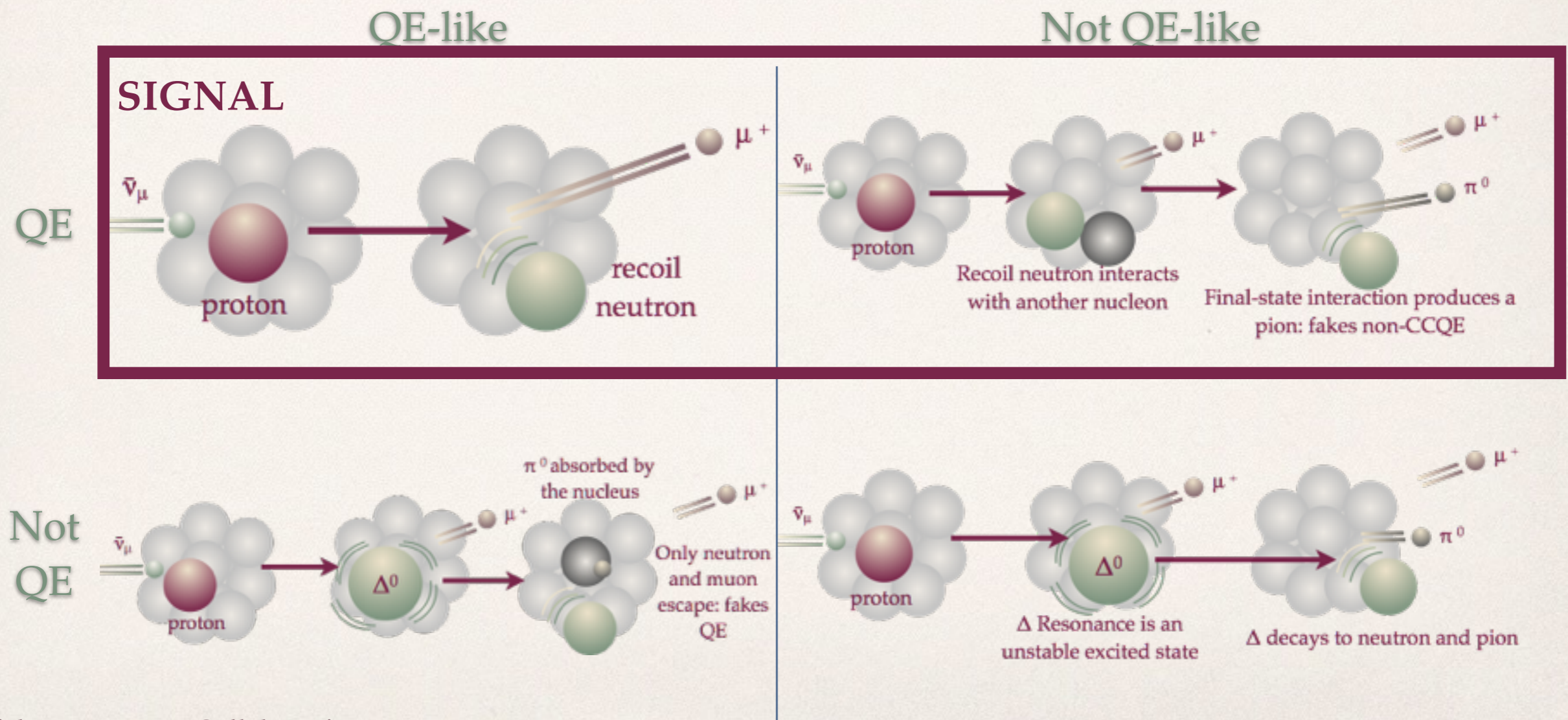
Final-state interactions

- ❖ Hadrons produced in a scattering interaction may re-interact with other nucleons before they escape the nucleus: we call these final-state interactions
- ❖ Thus the particles that exit the nucleus may be different, both in type and in energy, from those generated in the initial interaction



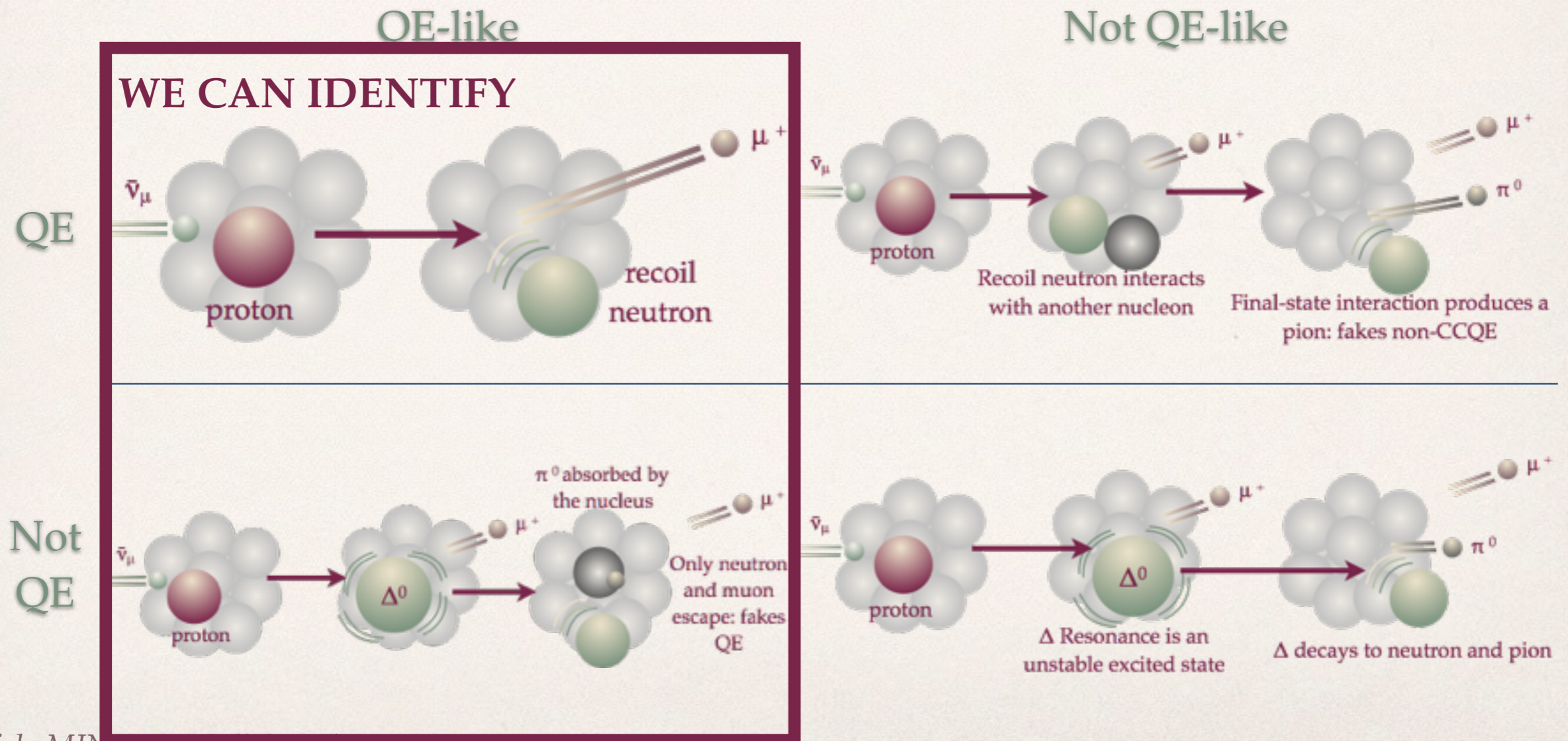
Final-state interactions

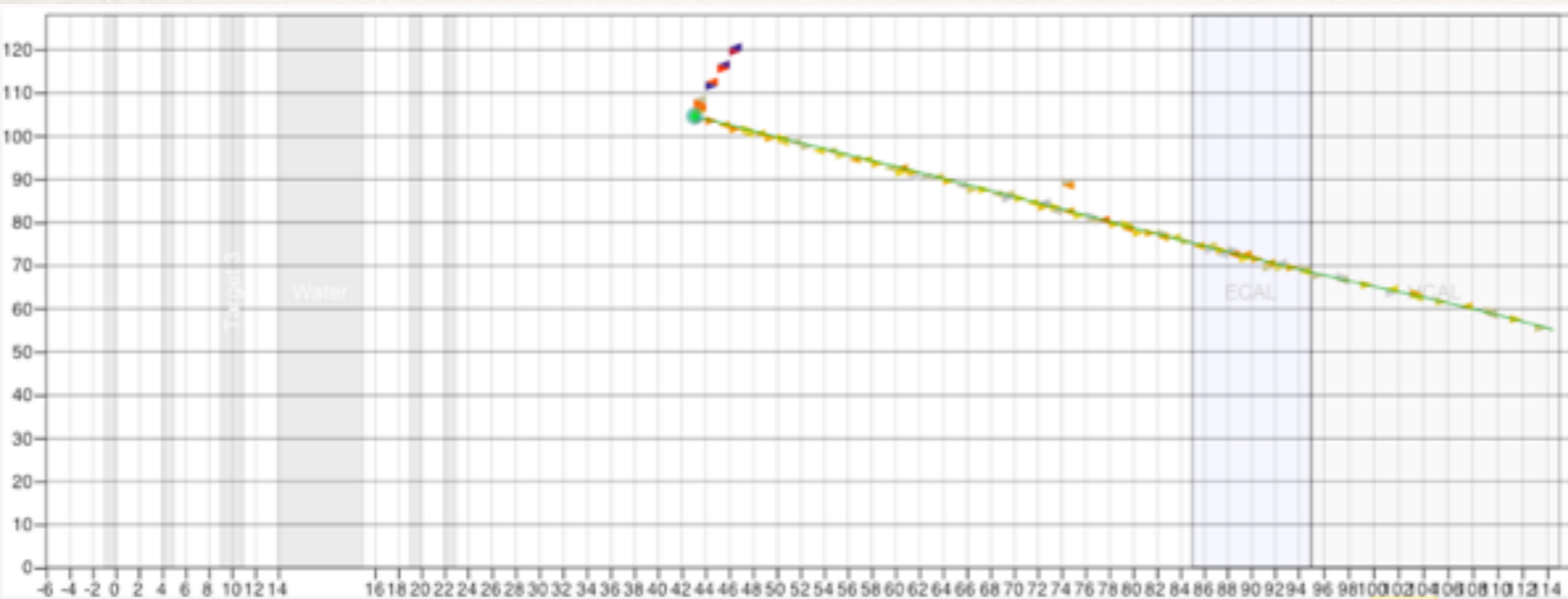
- ❖ Hadrons produced in a scattering interaction may re-interact with other nucleons before they escape the nucleus: we call these final-state interactions
- ❖ Thus the particles that exit the nucleus may be different, both in type and in energy, from those generated in the initial interaction



Final-state interactions

- ❖ Hadrons produced in a scattering interaction may re-interact with other nucleons before they escape the nucleus: we call these final-state interactions
- ❖ Thus the particles that exit the nucleus may be different, both in type and in energy, from those generated in the initial interaction



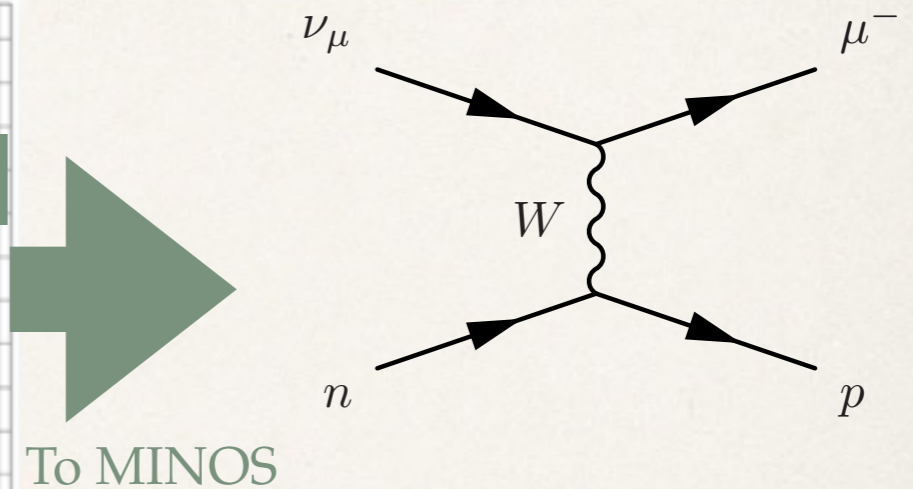
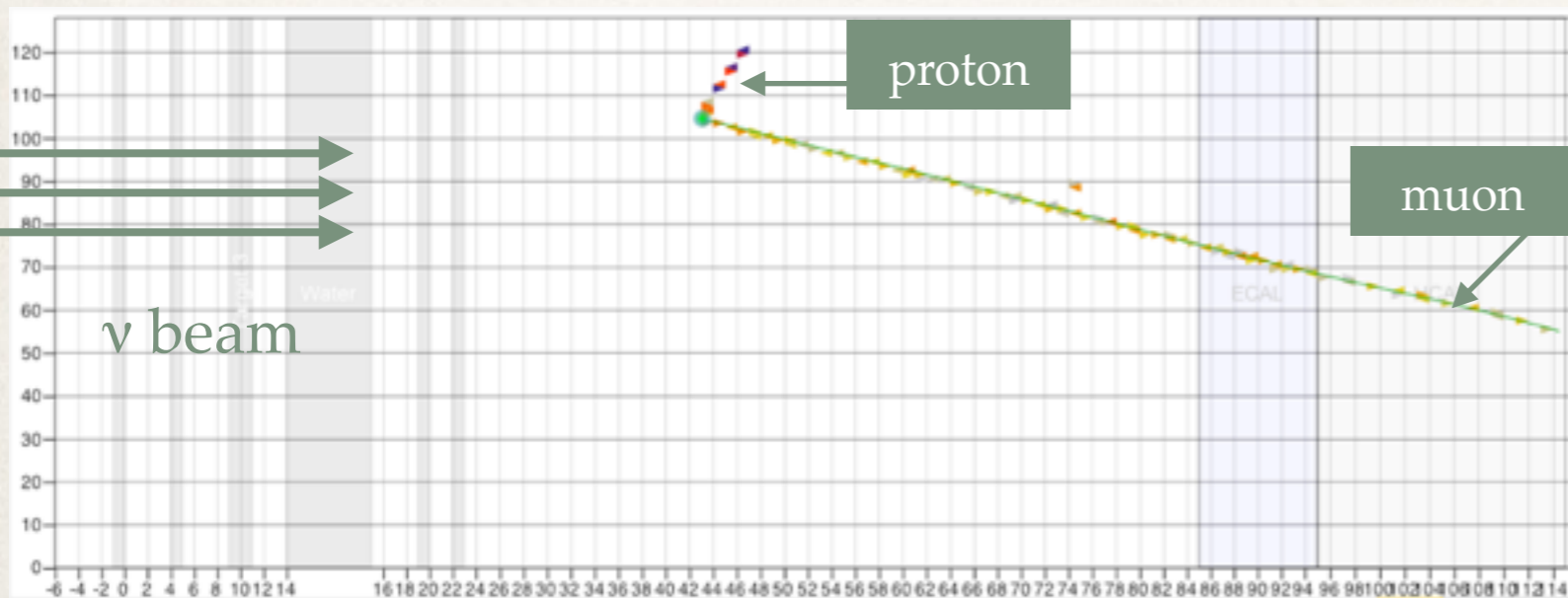


Measuring the quasi-elastic cross section

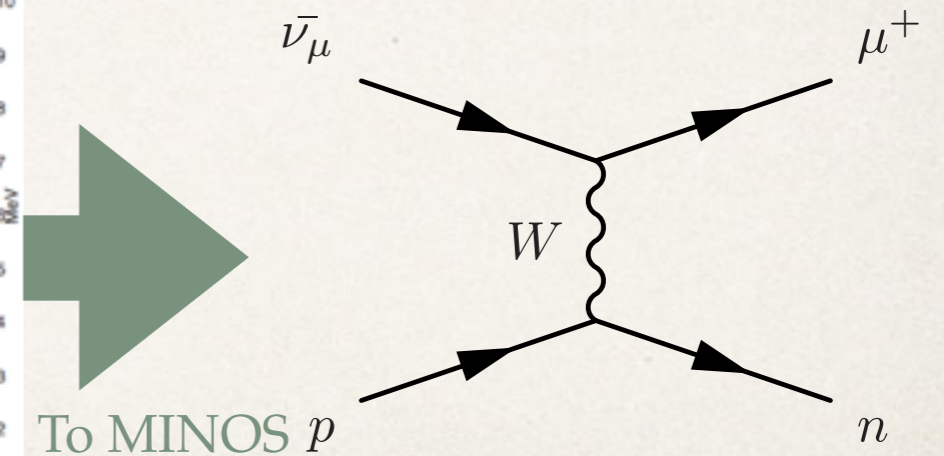
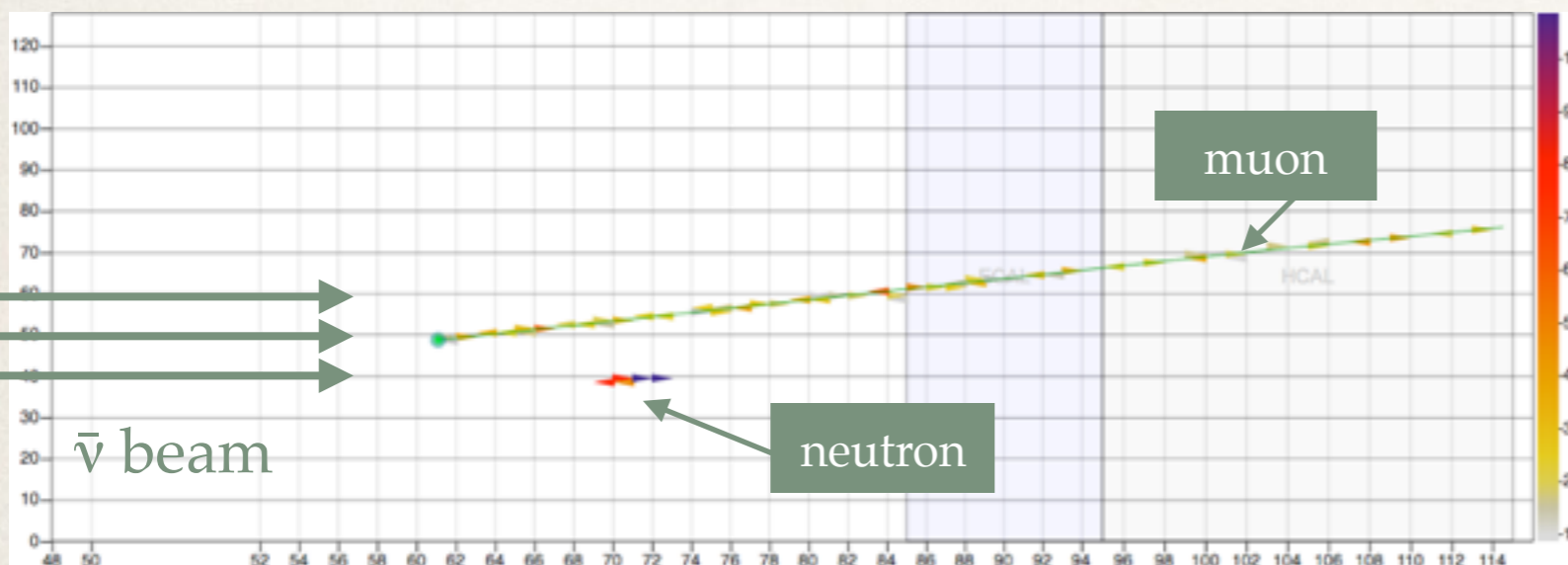
An example MINERvA analysis

Quasi-elastic events in MINERvA

Neutrino mode

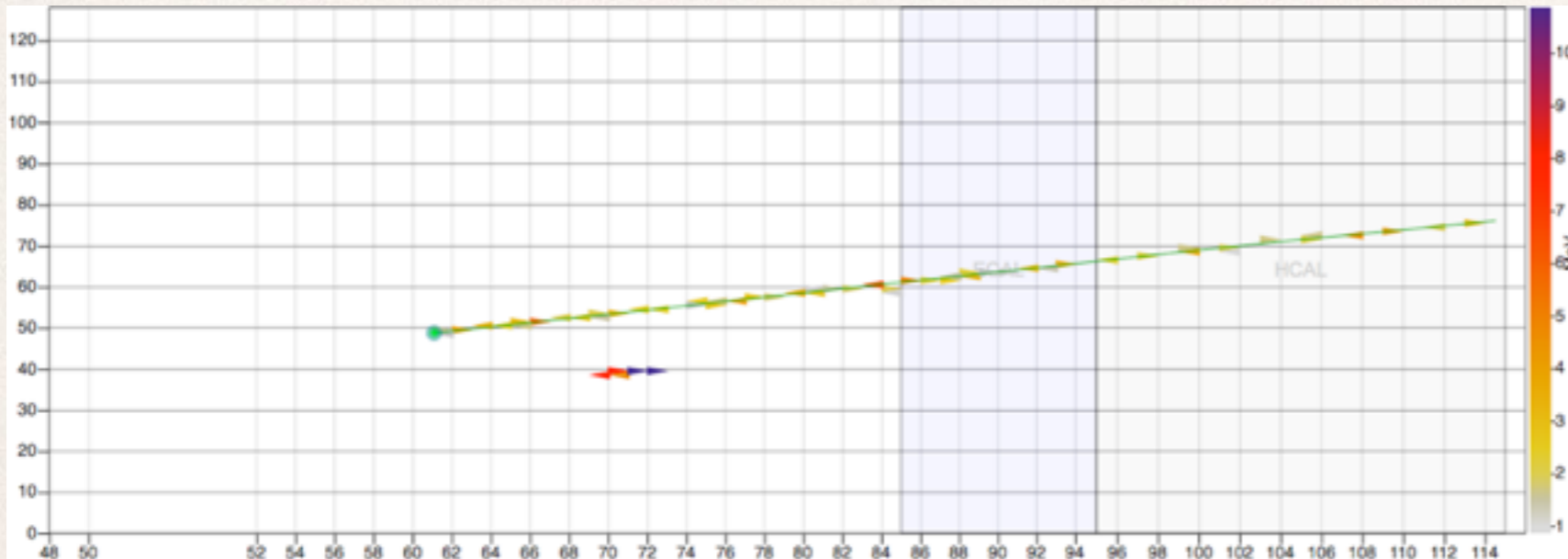


Antineutrino mode

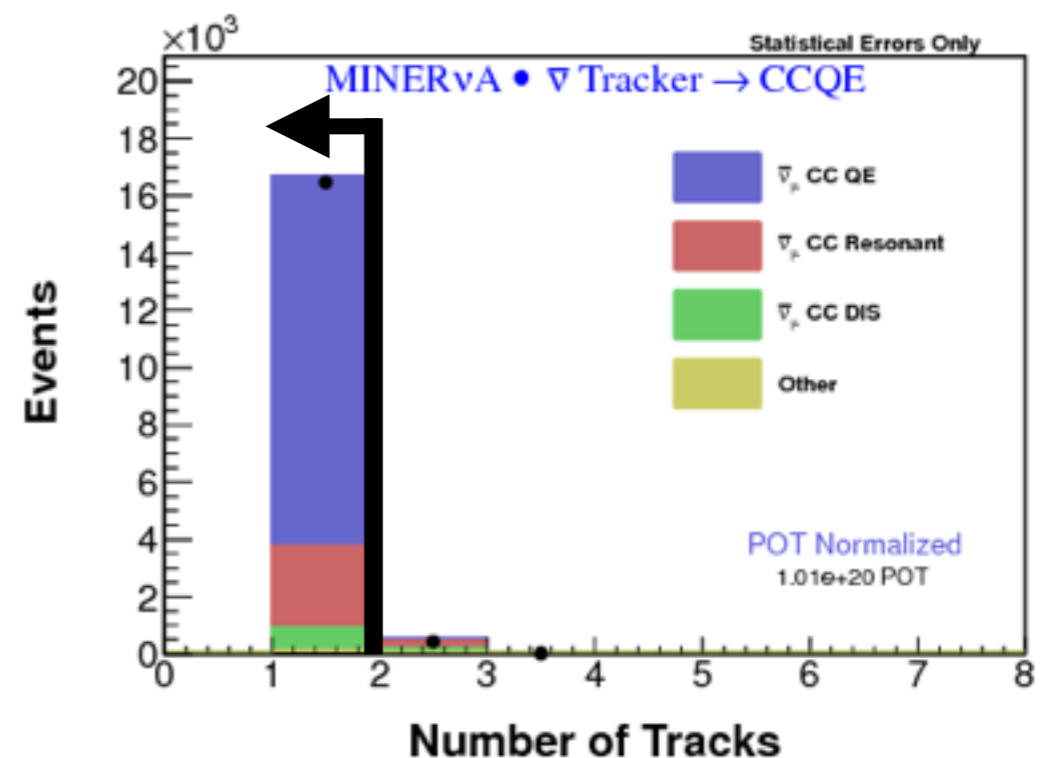


Event selection: tracks: $\bar{\nu}$

Antineutrino mode

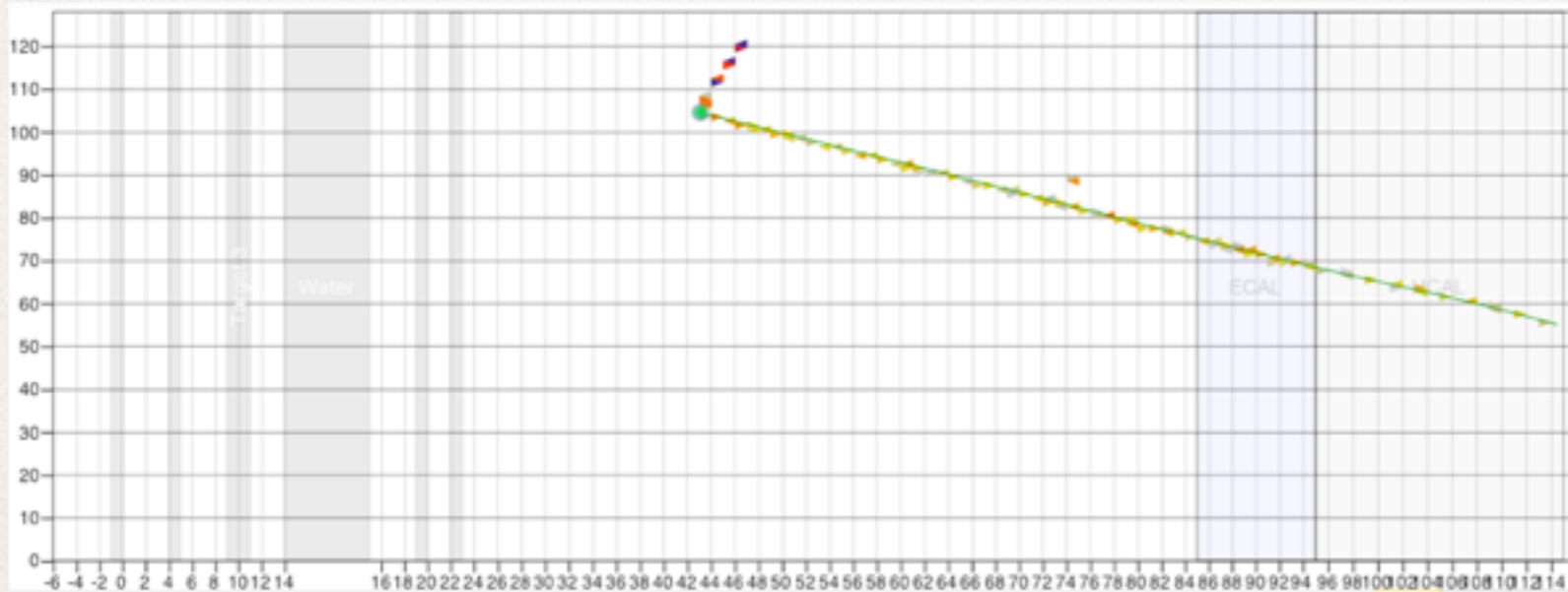


- ❖ Muon track charge matched in MINOS as a μ^{+}
- ❖ **No additional tracks from the vertex**
- ❖ The ejected neutron may scatter, leaving an energy deposit, but it does not make a track from the vertex

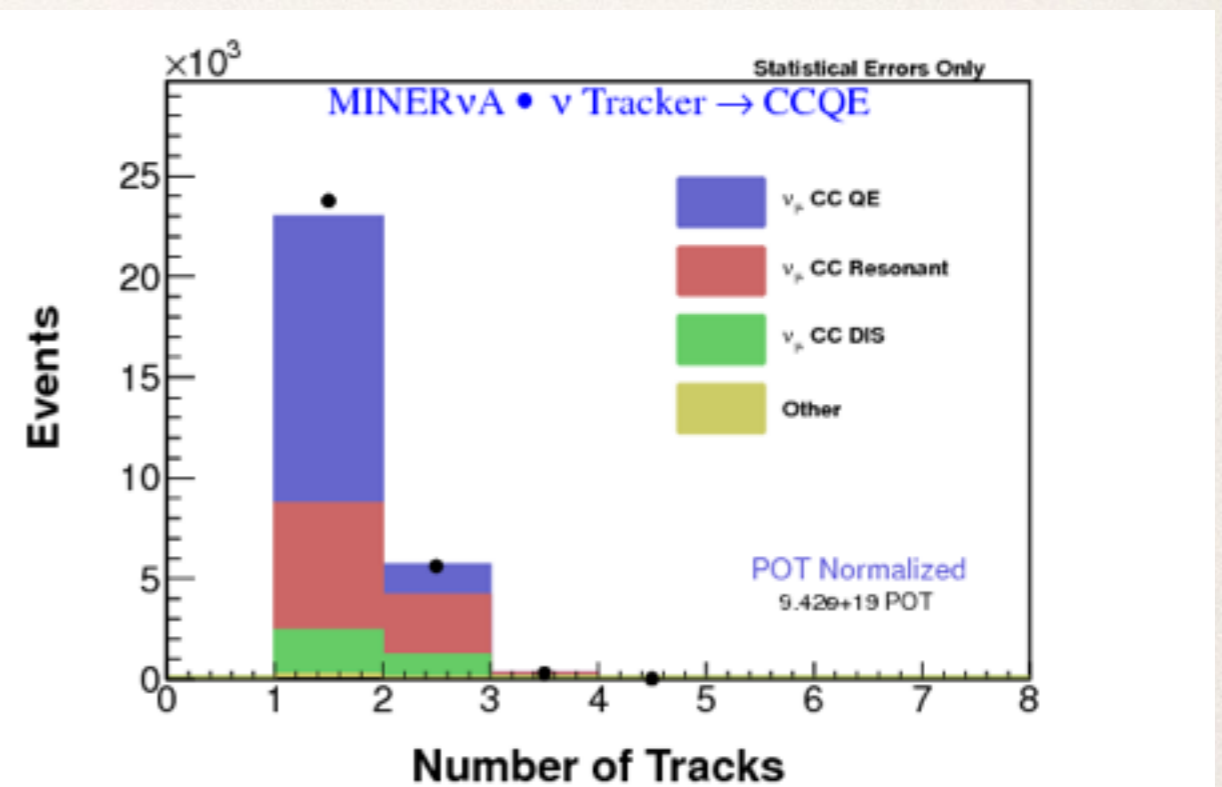


Event selection: tracks: ν

Neutrino mode



- * Muon track charge matched in MINOS as a μ^{-}
- * **No requirement on the number of additional tracks from the vertex**
- * The ejected proton may make a track, as in the example
- * But we can't track low-energy protons... we'll come back to this later

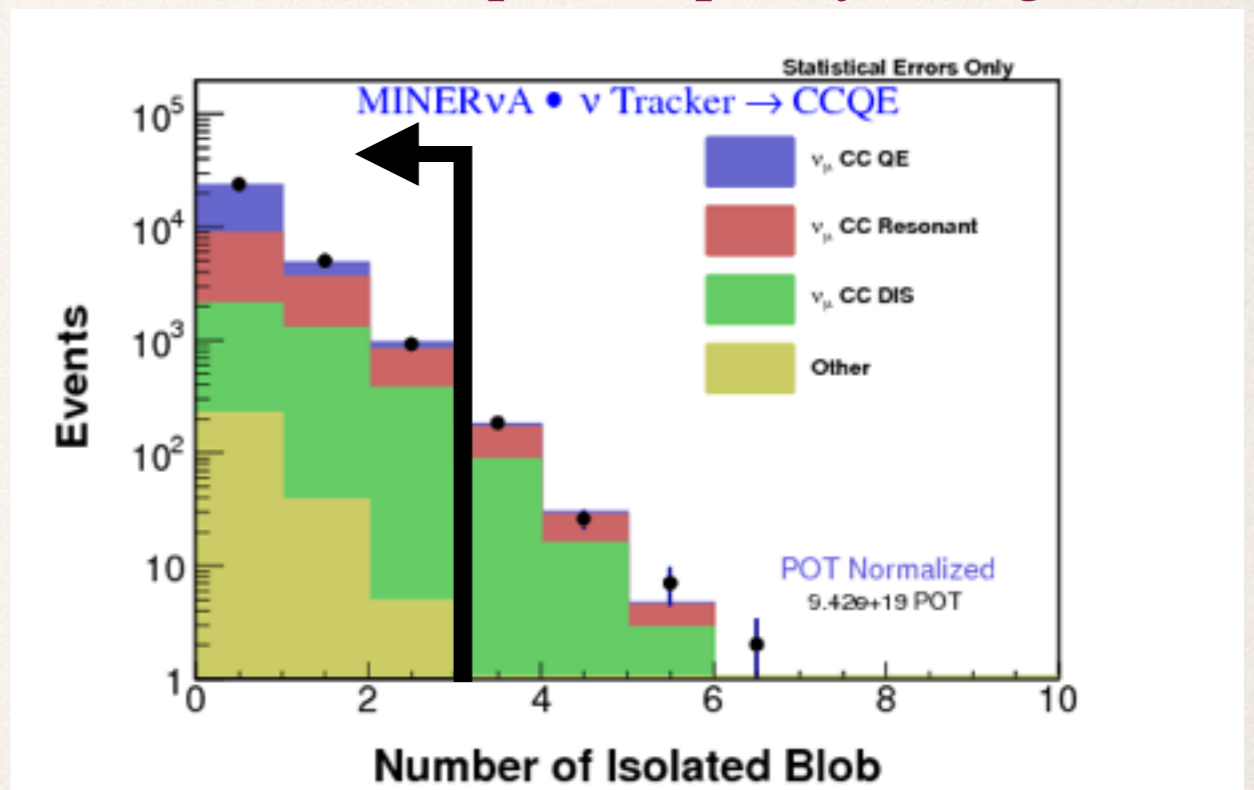
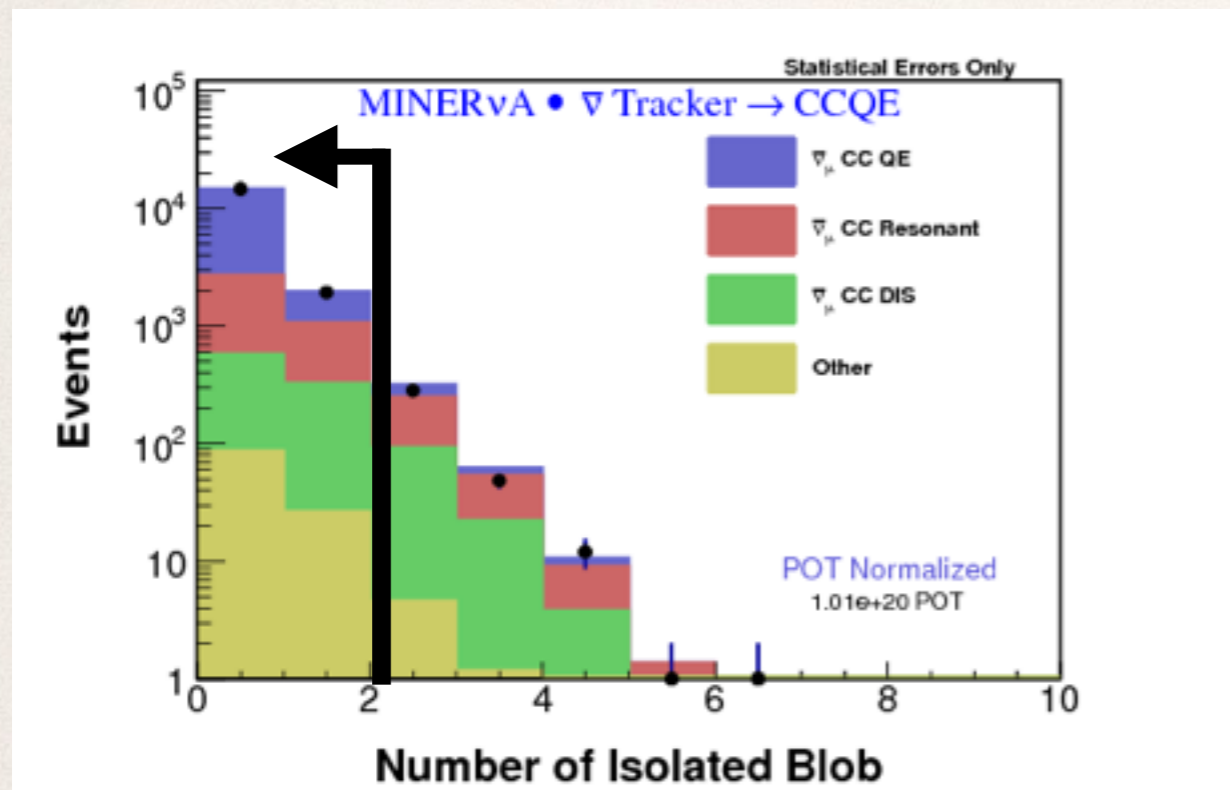
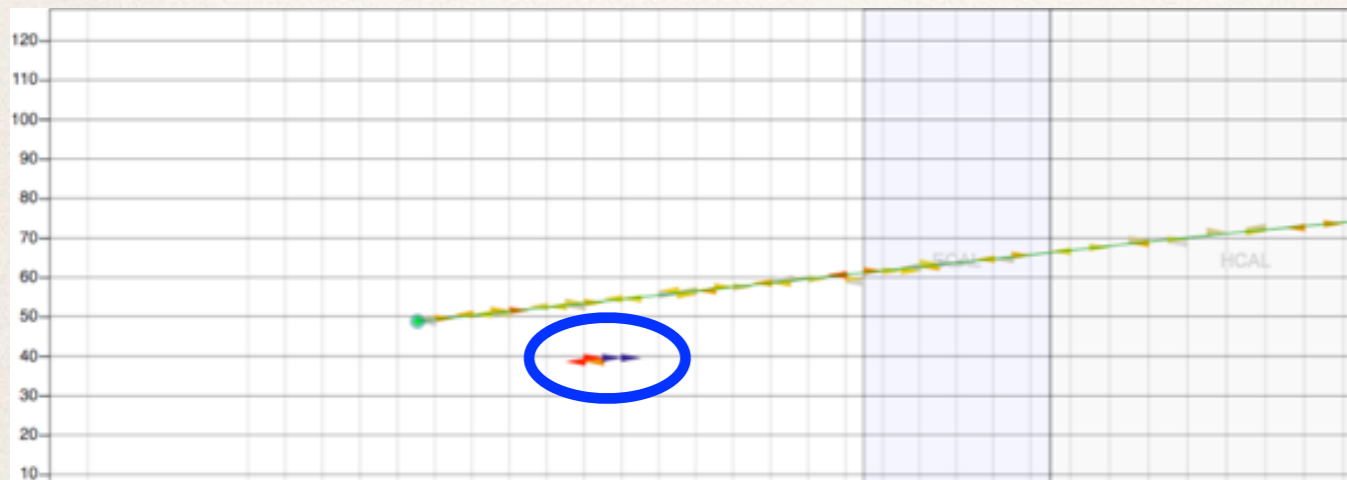


Event selection: isolated energy

Antineutrino mode



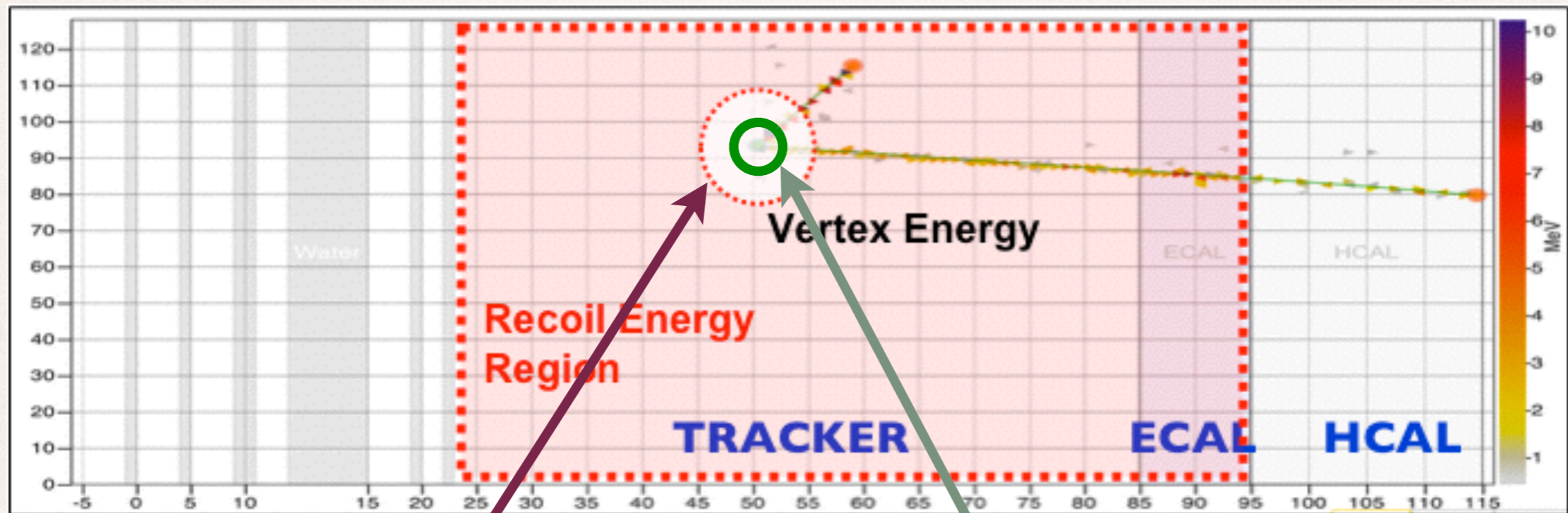
- * Energy deposits outside of the muon track, excluding cross-talk
- * Neutron scattering may deposit energy
- * Frequently, only the muon track is visible; no isolated deposits
- * This cut makes little difference at low Q^2 , but improves purity at high Q^2



Antineutrino - maximum 1 isolated deposit

Neutrino - maximum 2 isolated deposits

Event selection: recoil energy

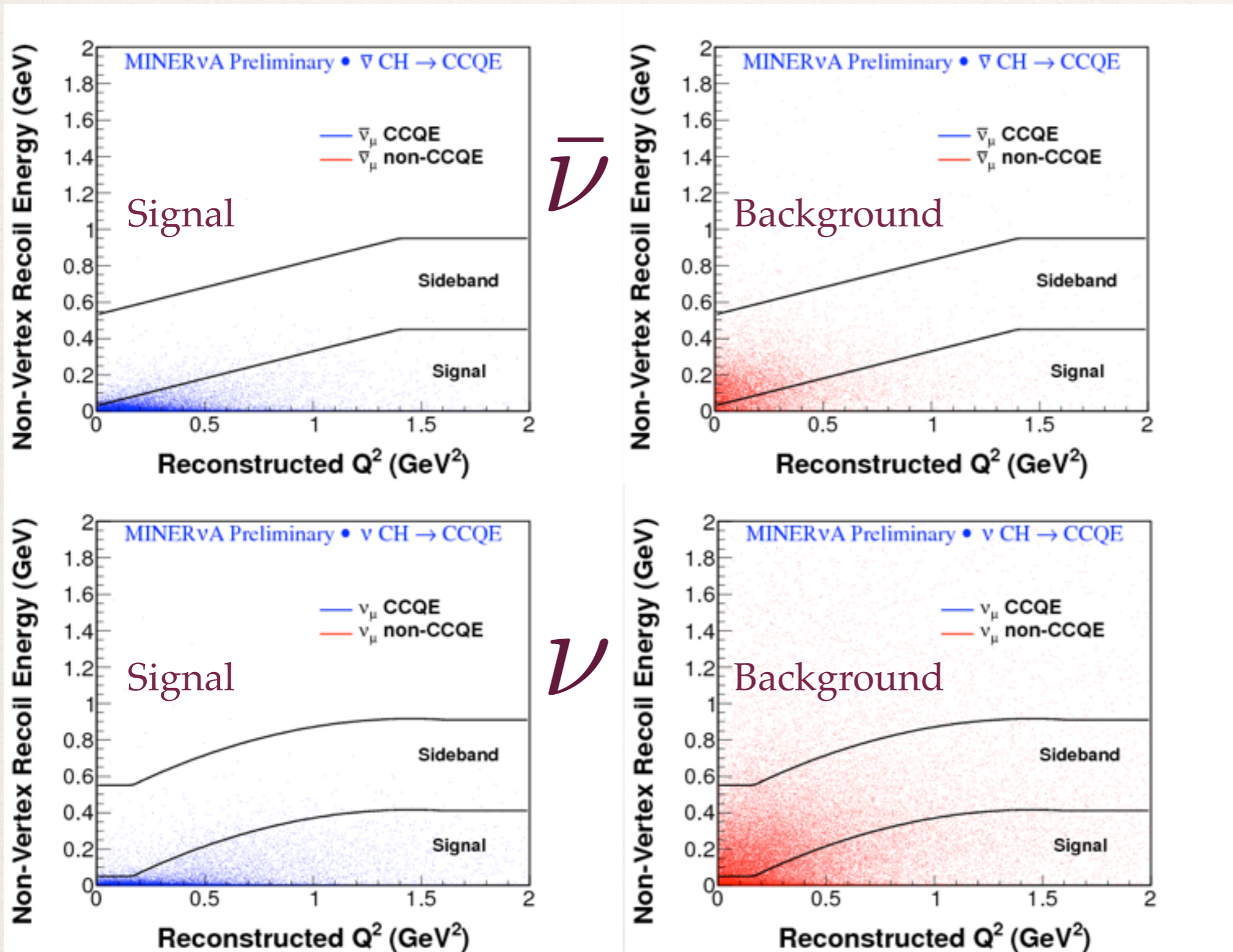


Exclude vertex region:
30 g/cm² for neutrino mode
Contains < 225 MeV protons

Antineutrino mode
exclude 10 g/cm²
Contains < 120 MeV protons

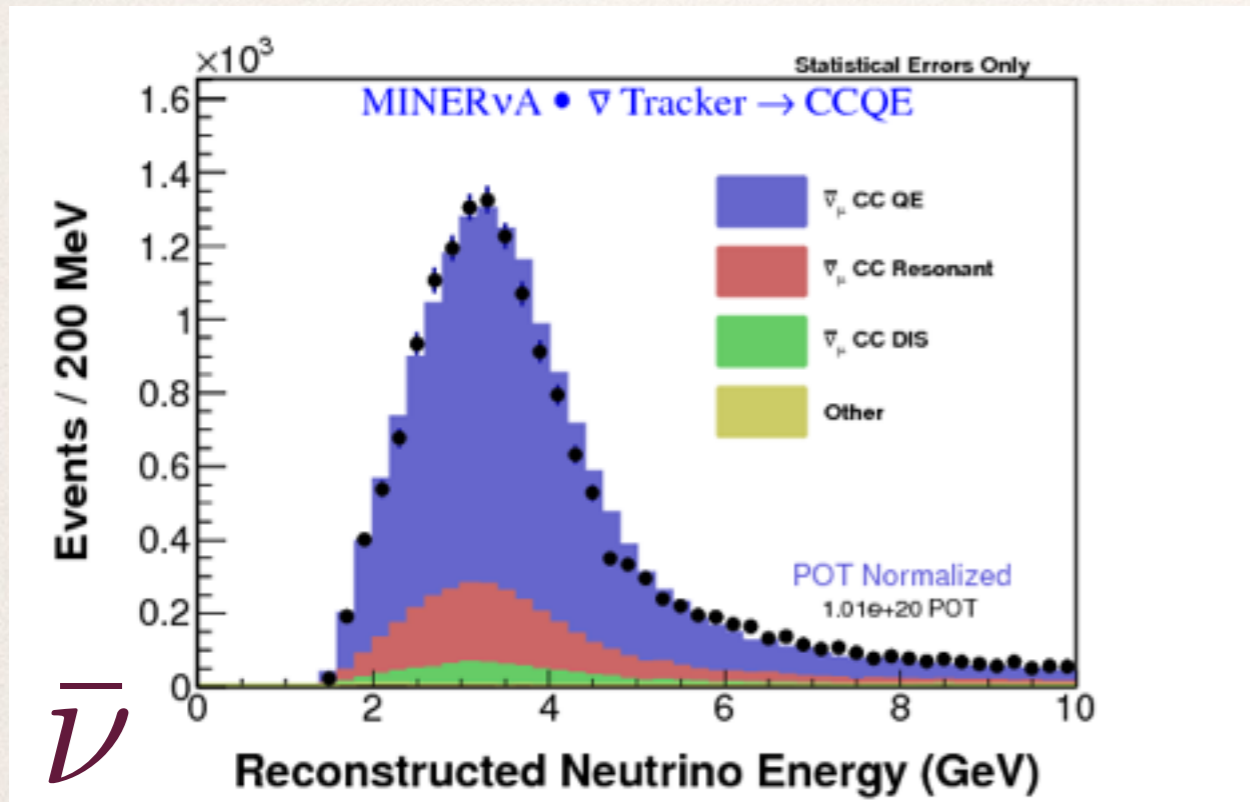
- * Sum the energy deposited in the recoil region (typically from pions)
- * Exclude the **vertex region** where **extra low-energy nucleons** could result from correlated pairs

Event selection: recoil

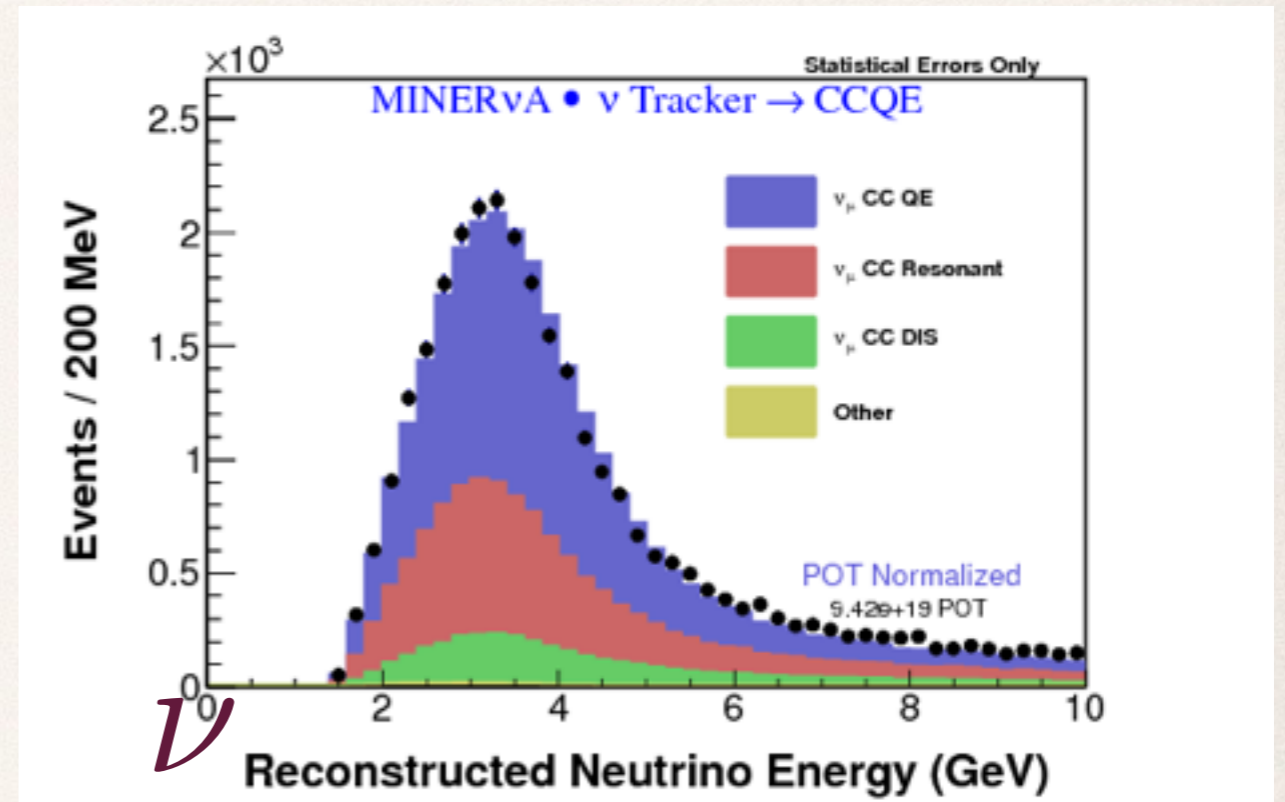


- Additional cuts:**
- ❖ Event in fiducial volume
 - ❖ Reconstructed energy 1.5-10 GeV

Backgrounds



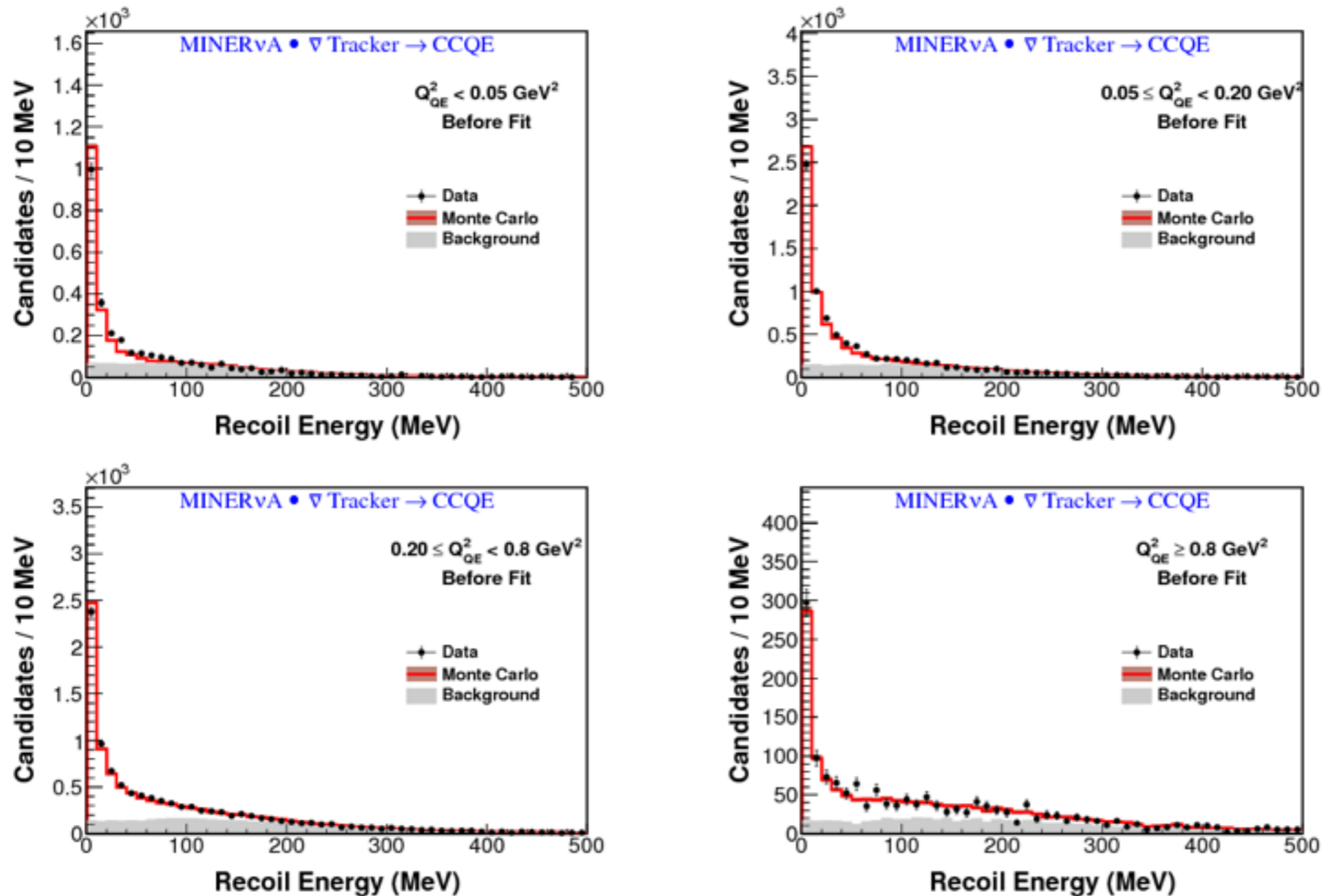
$\bar{\nu}$: 54% efficiency, 77% purity



ν : 47% efficiency, 49% purity

- * Backgrounds include events such as
 - * **Quasi-elastic-like resonant events**, where the pion is absorbed
 - * **QE-like deep-inelastic scattering events**
 - * Other DIS or resonant events which are not removed by our cuts

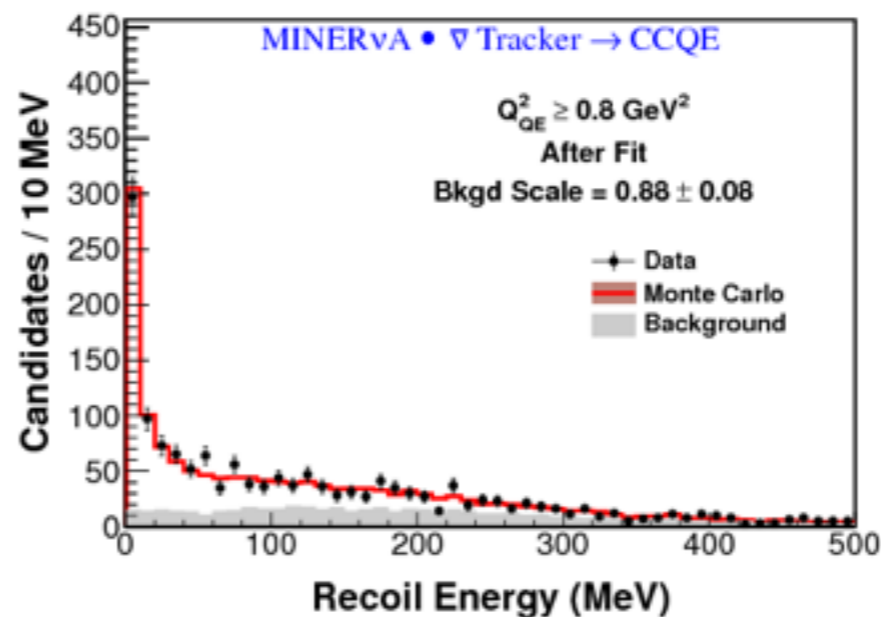
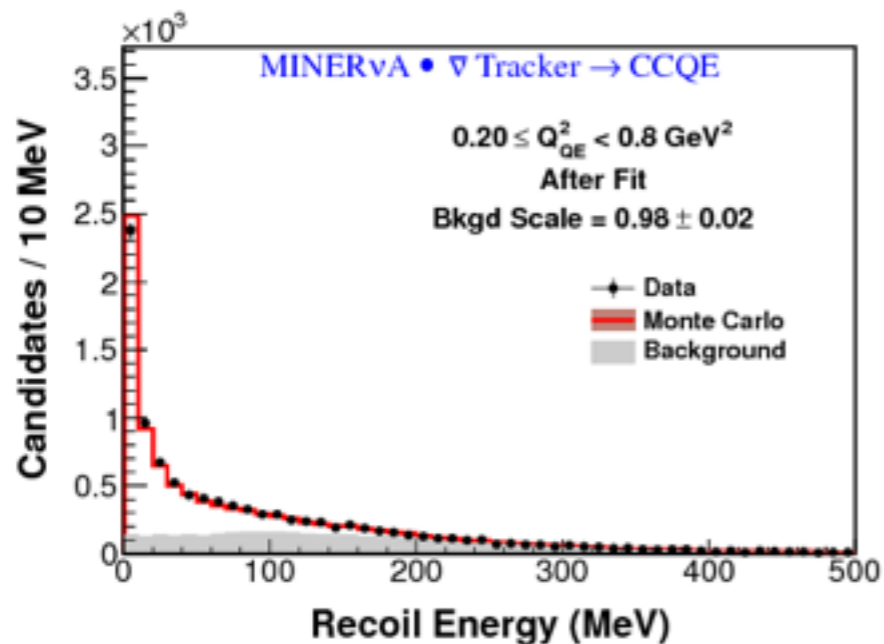
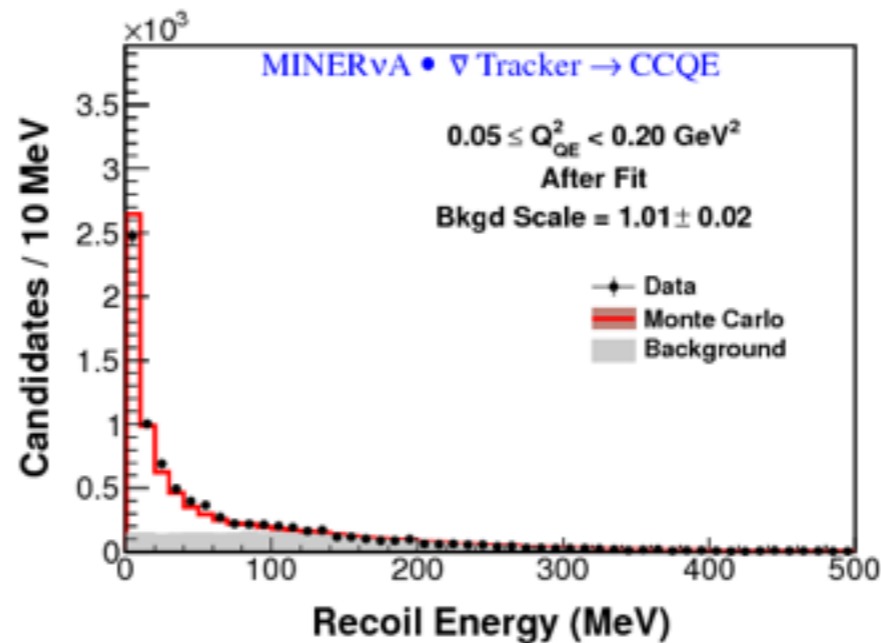
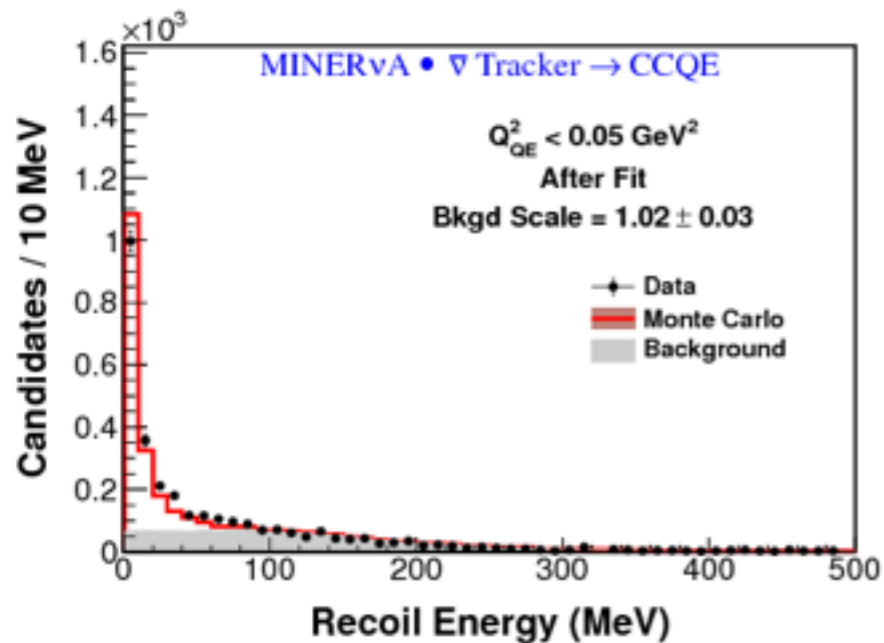
Background subtraction: before



These plots show data for antineutrinos, before the background fit

We use data to estimate our backgrounds by performing a fraction fit of simulated signal and background recoil energy distribution shapes from our Monte Carlo, in each of 4 Q^2 bins

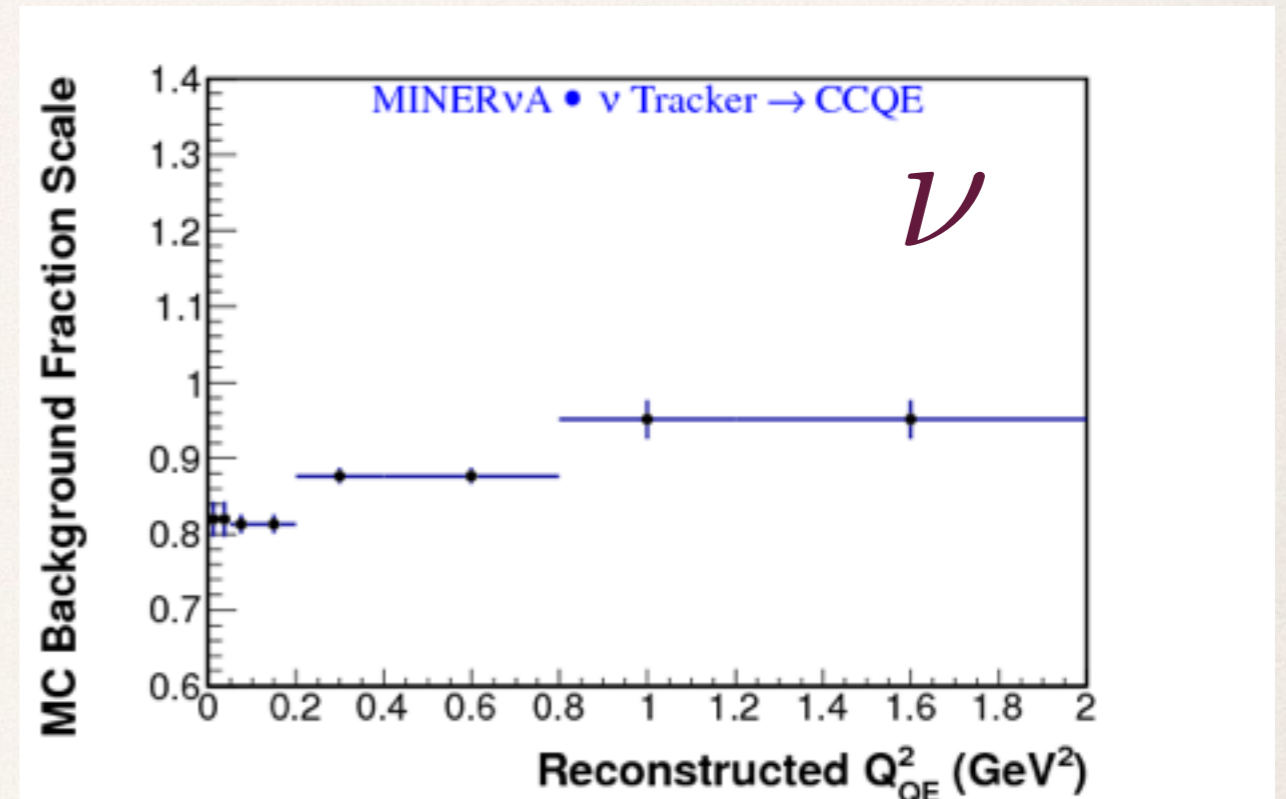
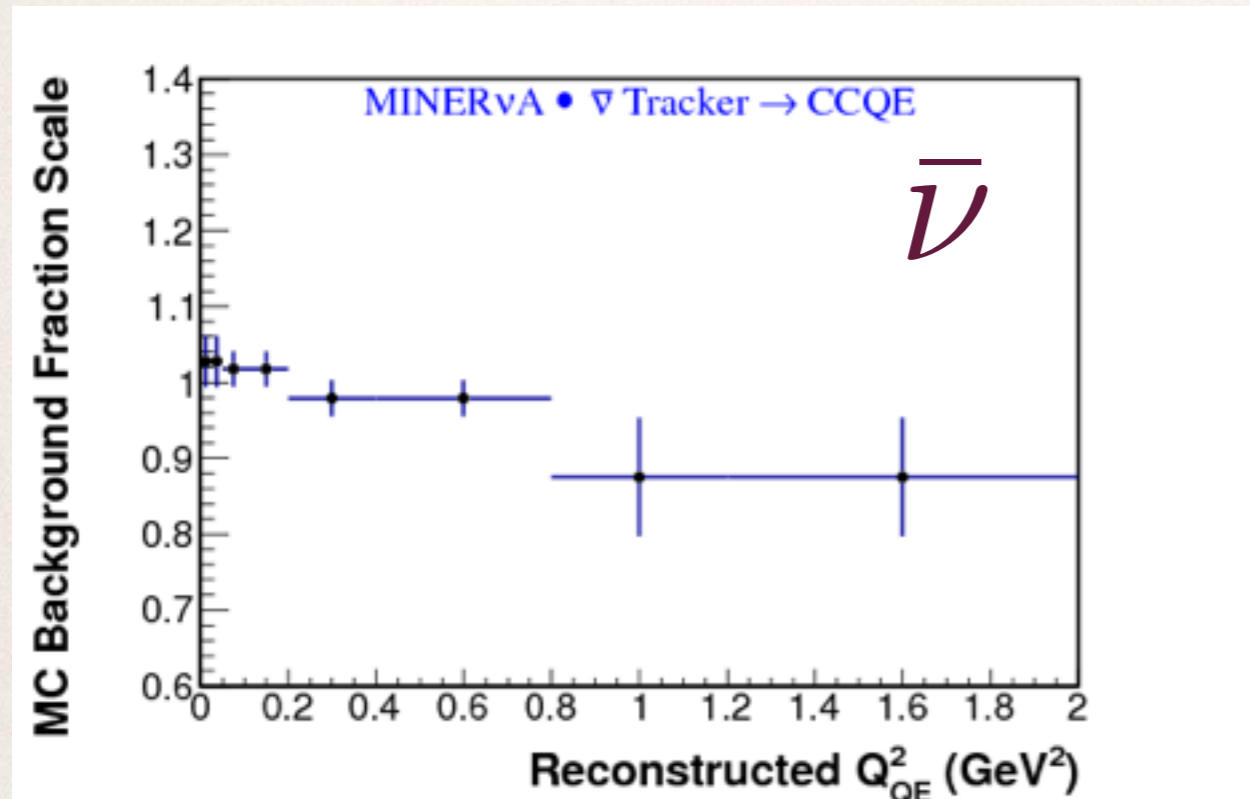
Background subtraction: after



These plots show data for antineutrinos, after the background fit

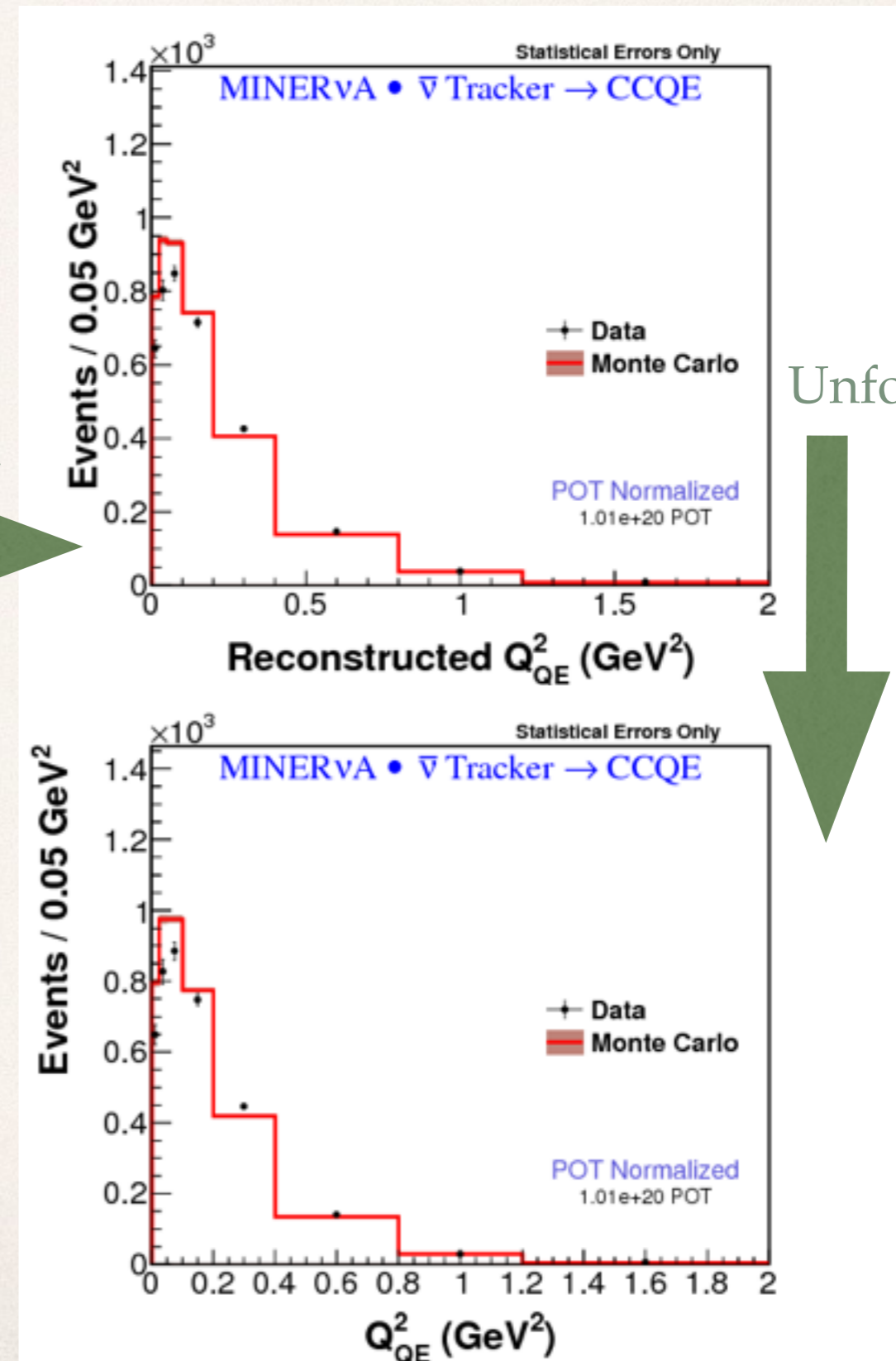
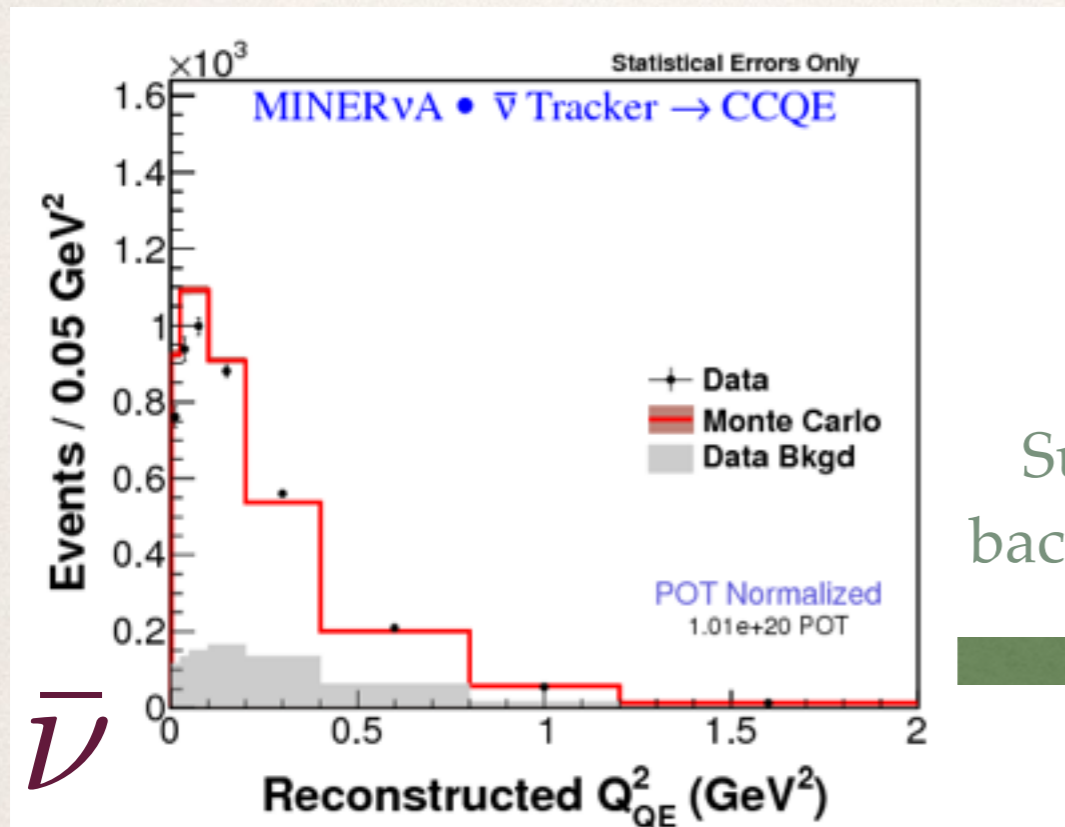
We use data to estimate our backgrounds by performing a fraction fit of simulated signal and background recoil energy distribution shapes from our Monte Carlo, in each of 4 Q^2 bins

Background scales



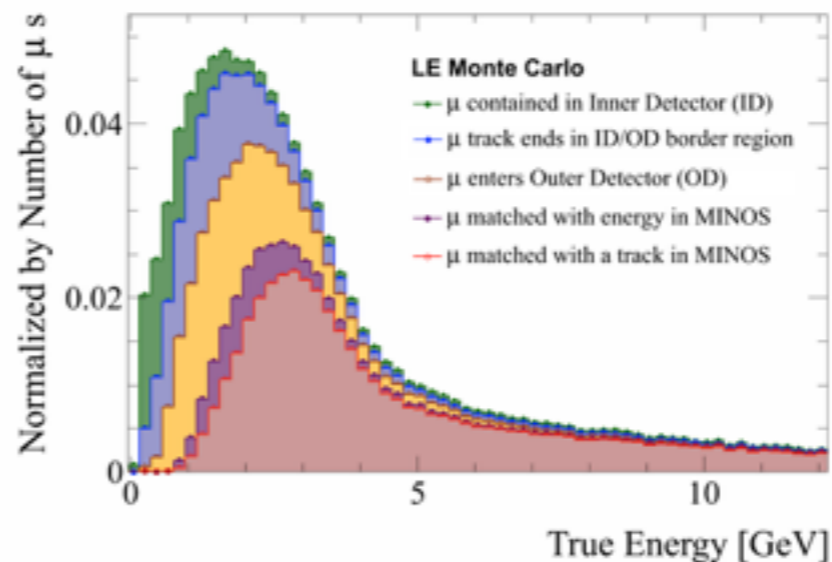
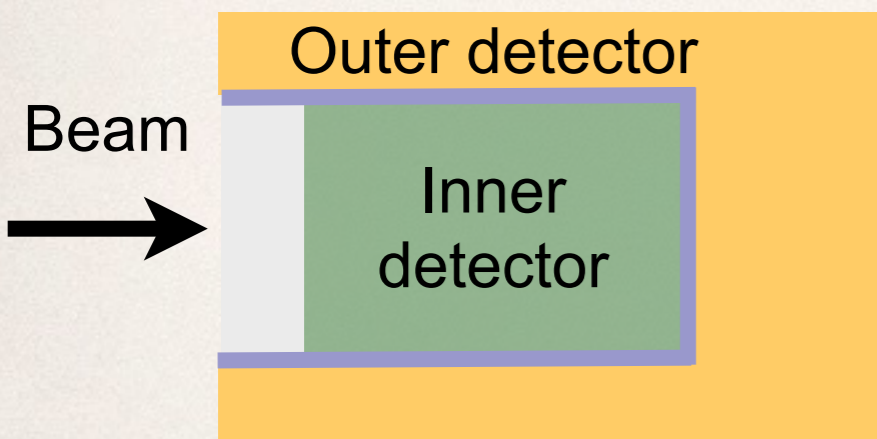
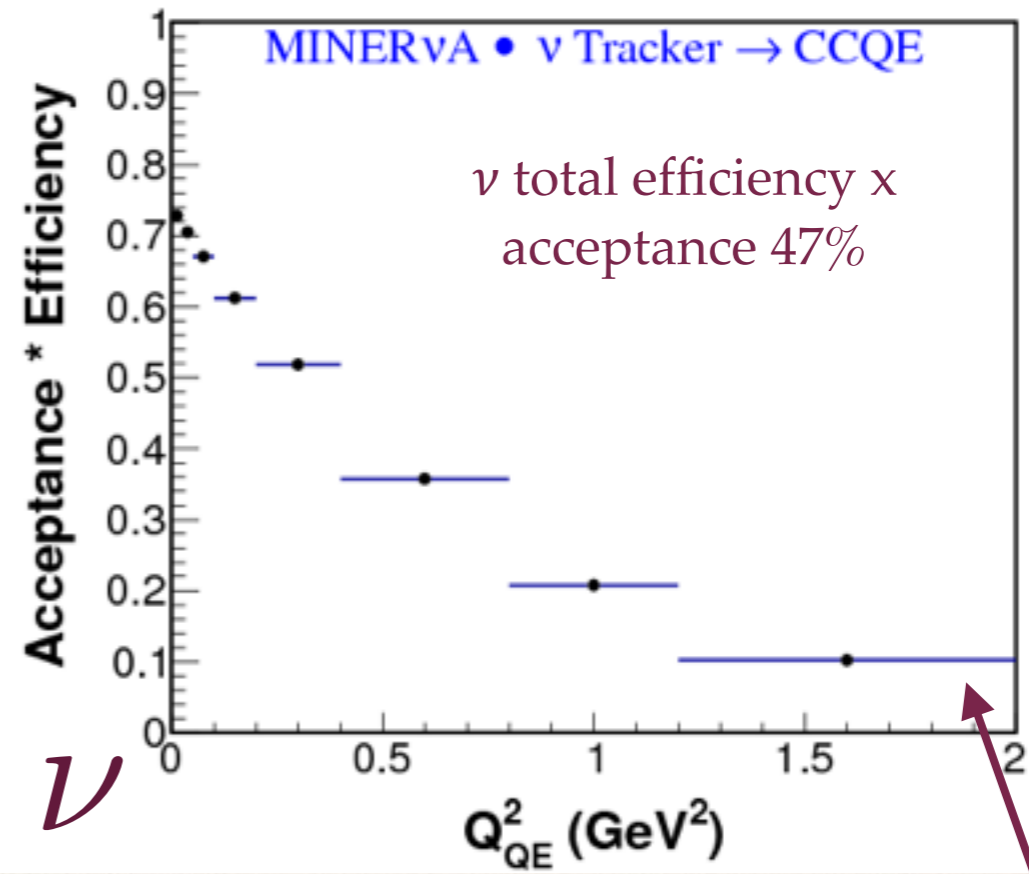
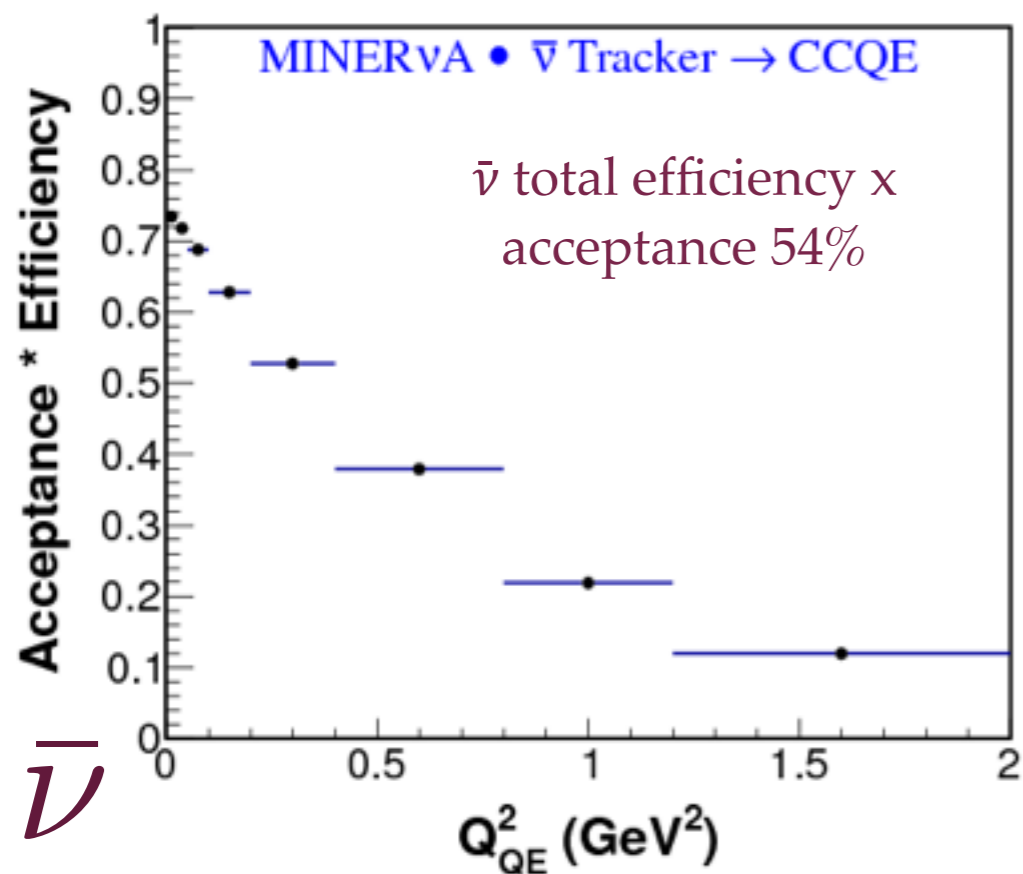
For each data bin, we subtract the Monte Carlo **background fraction** times the **scale**

Unfolding



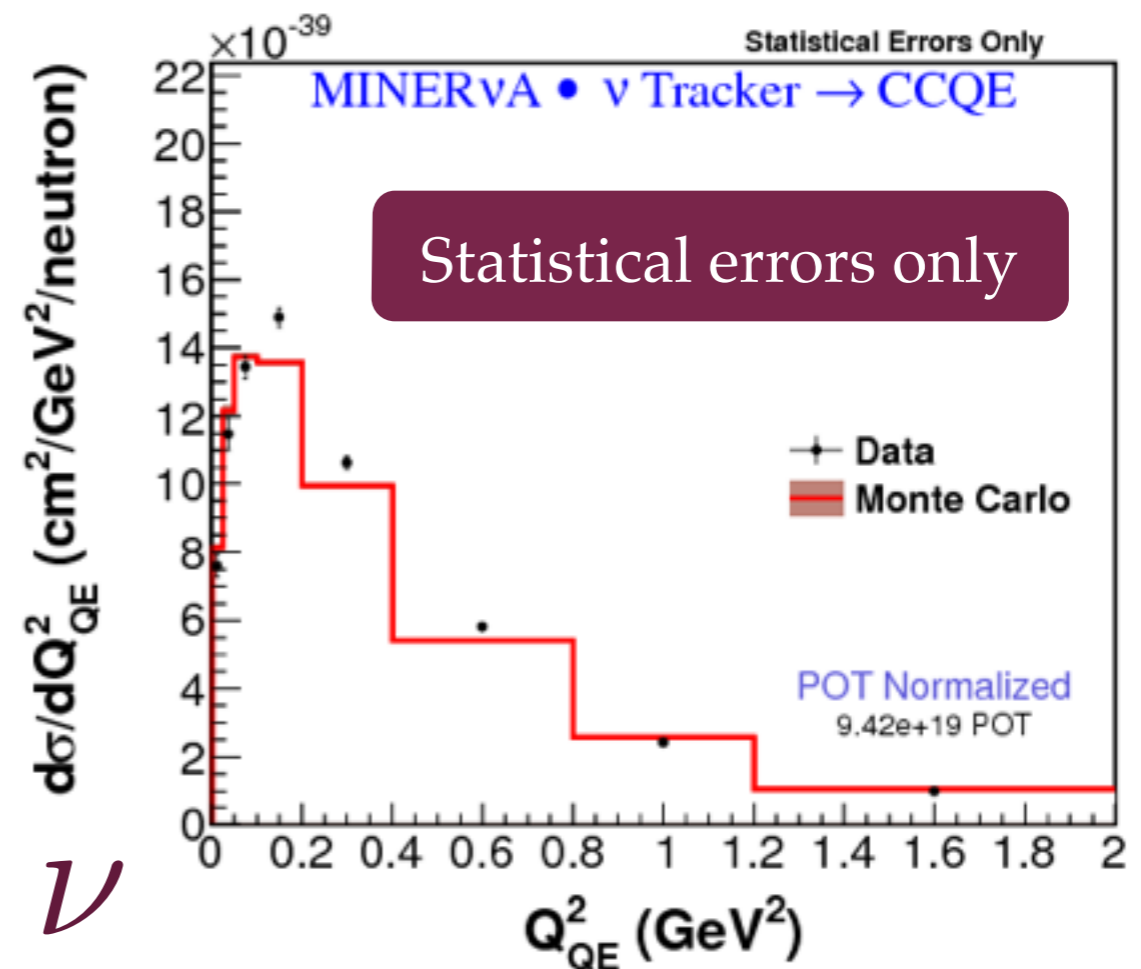
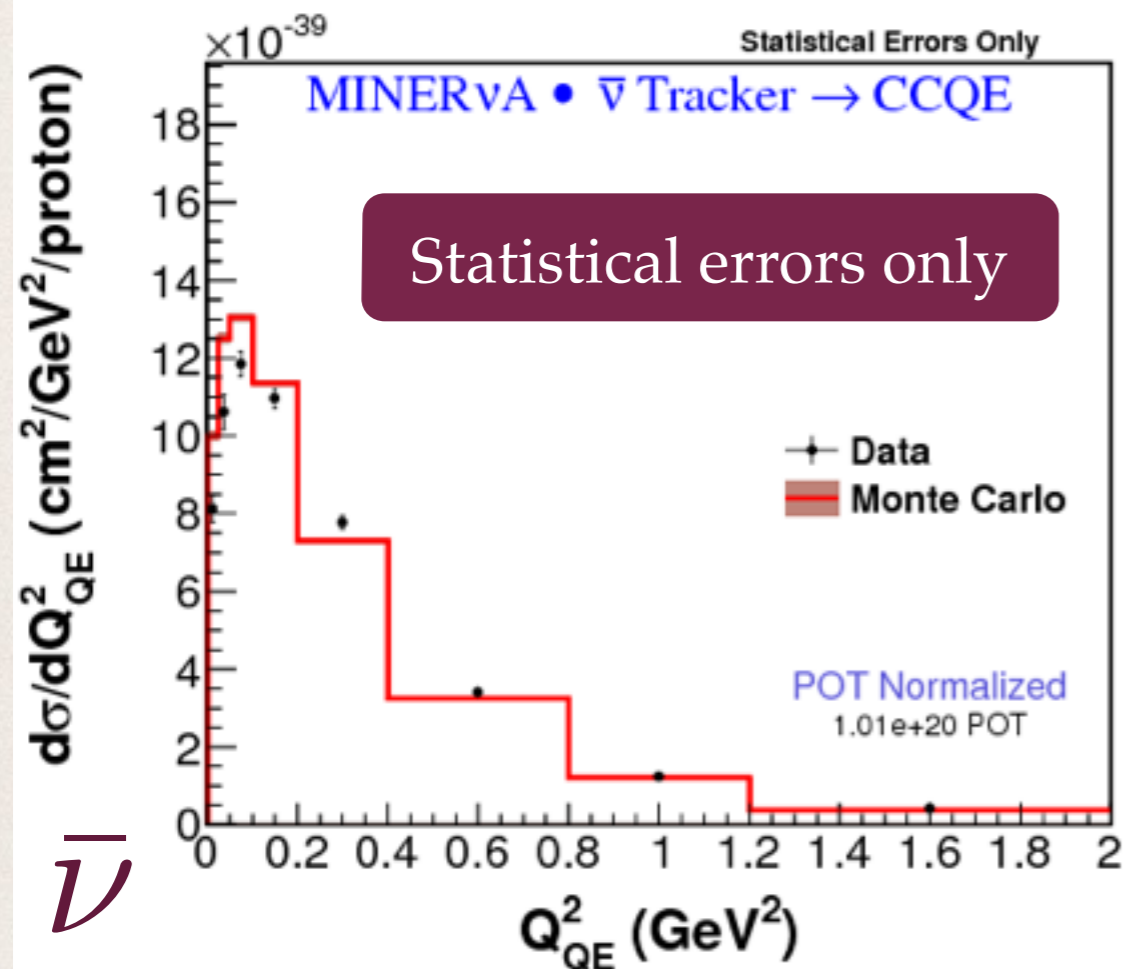
- * We use four iterations of a Bayesian unfolding method
- * The unfolding maps **reconstructed Q^2_{QE} to generated Q^2_{QE}**
- * Note: True Q^2_{QE} refers to Q^2 as constructed from true muon kinematics in the CCQE hypothesis, NOT to the actual 4-momentum transfer squared

Efficiency and acceptance



MINOS match requirement limits acceptance at high angles

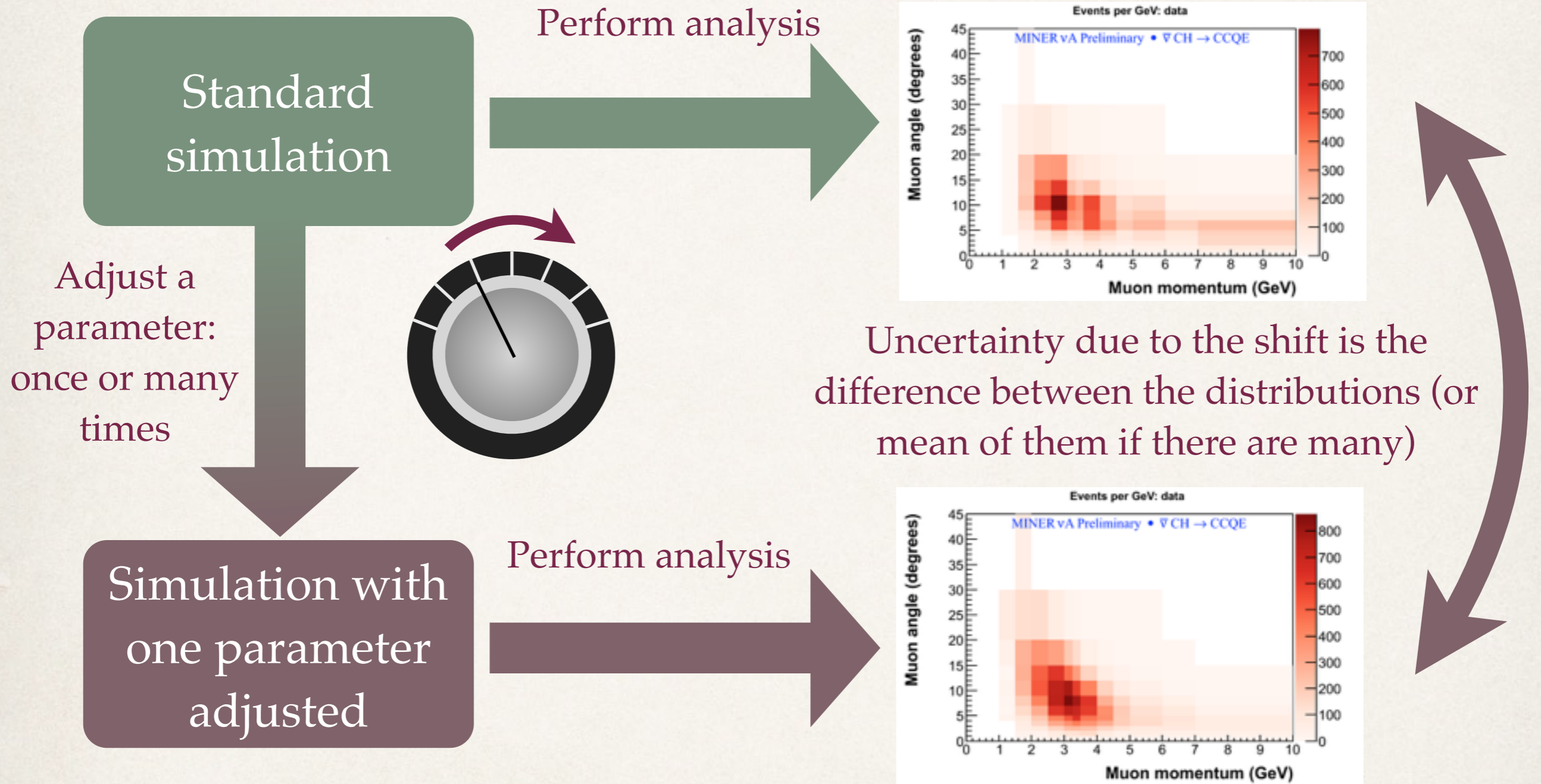
Cross-sections



- * To get a final cross-section, we normalize by number of **target nucleons**, number of **protons on target** and integrated (anti)neutrino **1.5-10 GeV flux** per proton on target

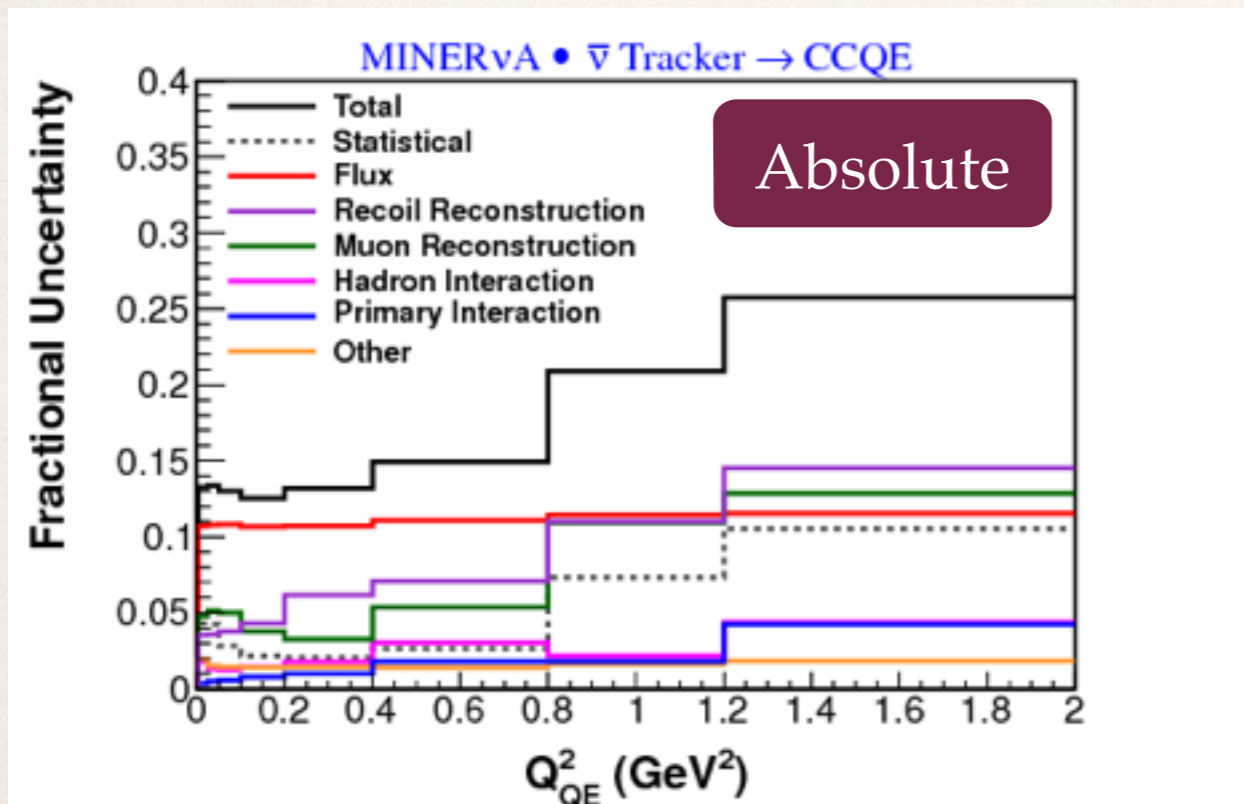
	Antineutrino	Neutrino
Protons on target	1.01 e20	9.42 e19
Integrated flux (1.5-10 GeV)	2.43 e-8 /cm ² /POT	2.91 e-8 /cm ² /POT
Target nucleons	1.91 e30 protons	1.65 e30 neutrons

Systematic uncertainties



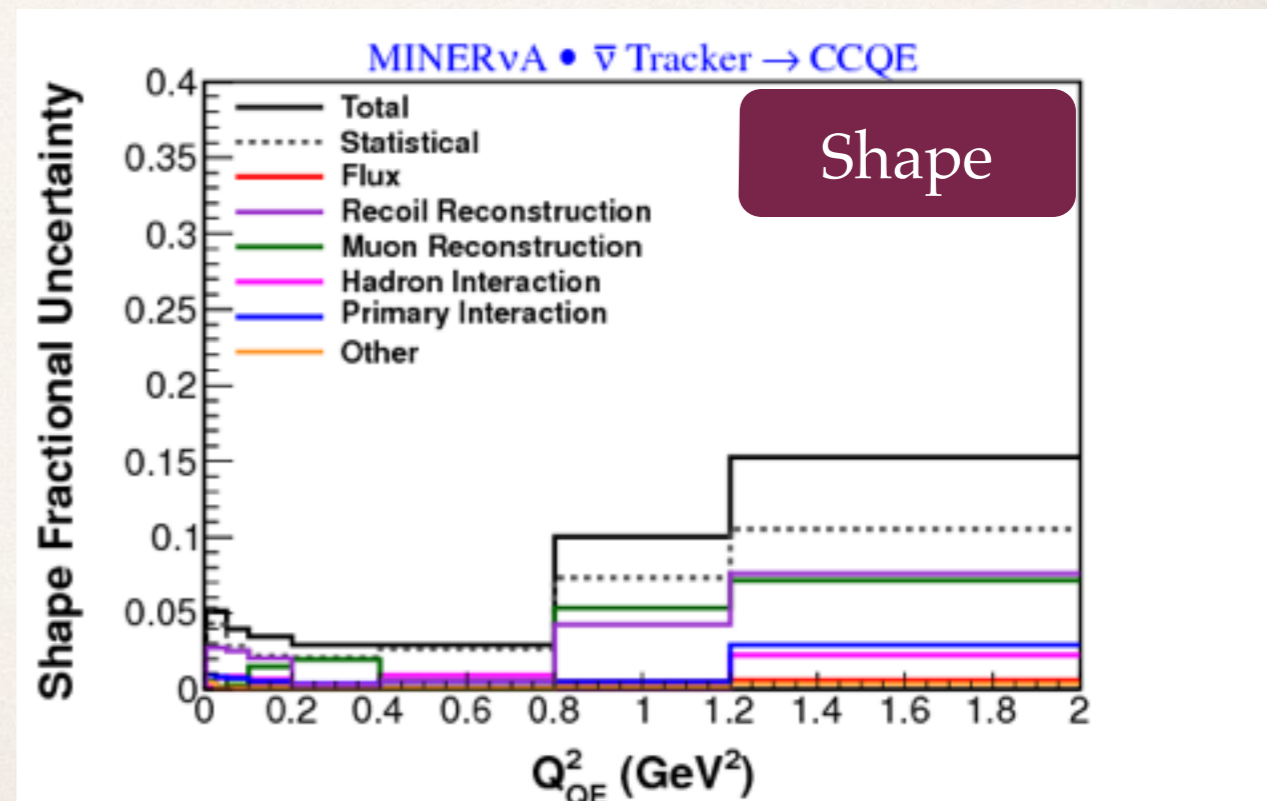
Examples: tracking efficiency, GENIE interaction rates, 100 “universes” of flux changes

Systematic uncertainties ($\bar{\nu}$)



- * Flux uncertainty
- - - * Statistical uncertainty
- * Recoil reconstruction uncertainty
- * Muon reconstruction uncertainty
- * Total uncertainty

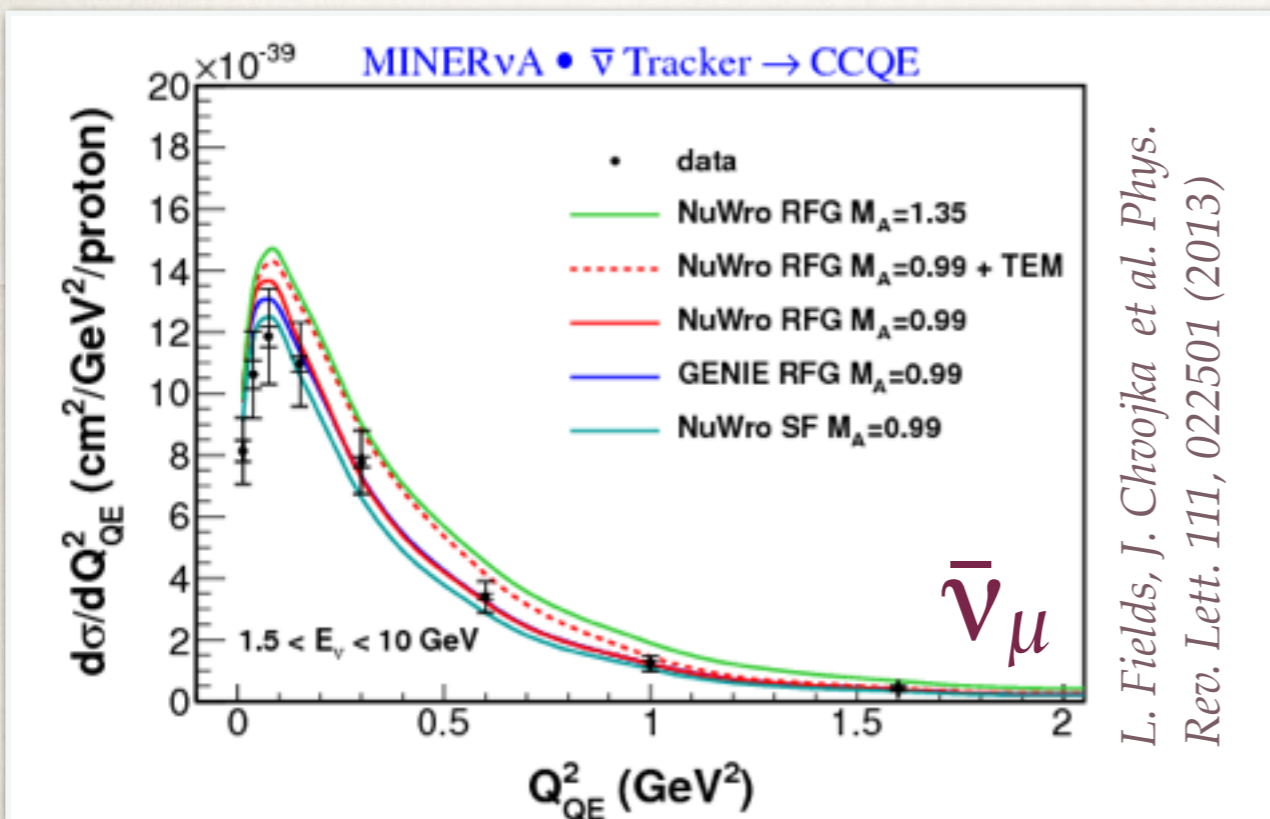
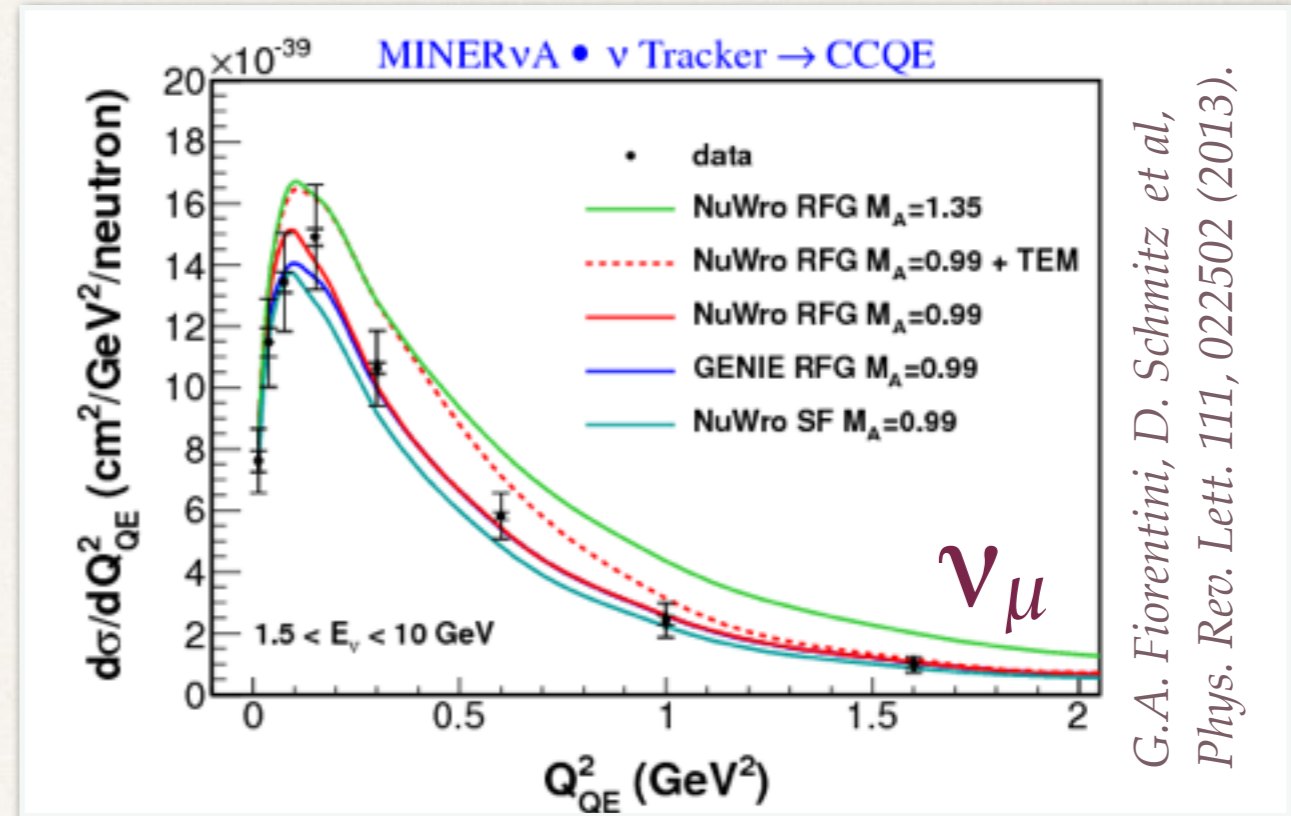
- * Plot above shows absolute uncertainties
- * Plot to right shows shape-only uncertainties
- * Flux dominates the **absolute** uncertainty
- * **Uncertainty in flux mostly affects normalization, not shape**
- * Statistical uncertainties dominate the shape distribution, and total uncertainty is reduced



Quasi-elastic results: muon kinematics

- ❖ Compare data to **GENIE RFG** *C. Andreopoulos, et al., NIM 288A, 614, 87 (2010)* and **NuWro** *K. M. Graczyk and J. T. Sobczyk, Eur.Phys.J. C31, 177 (2003)* nuclear models

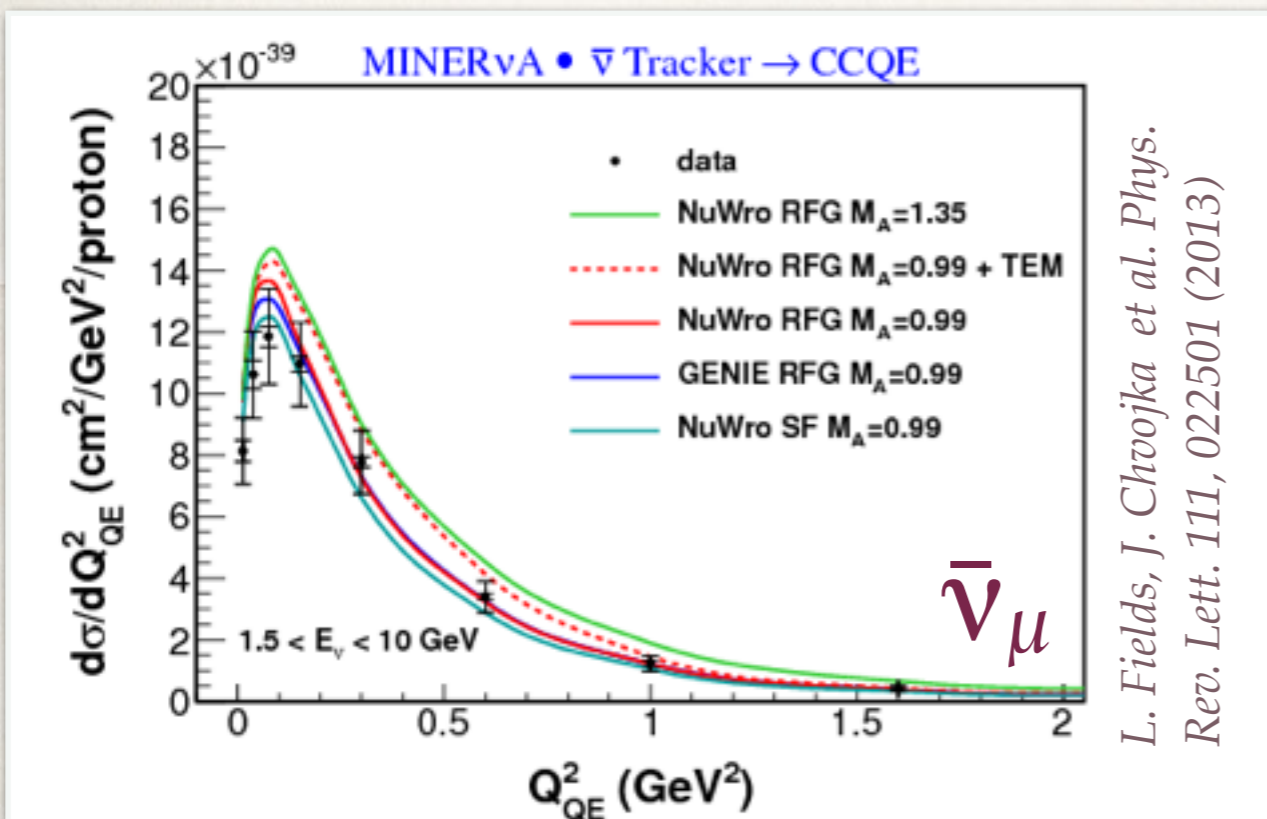
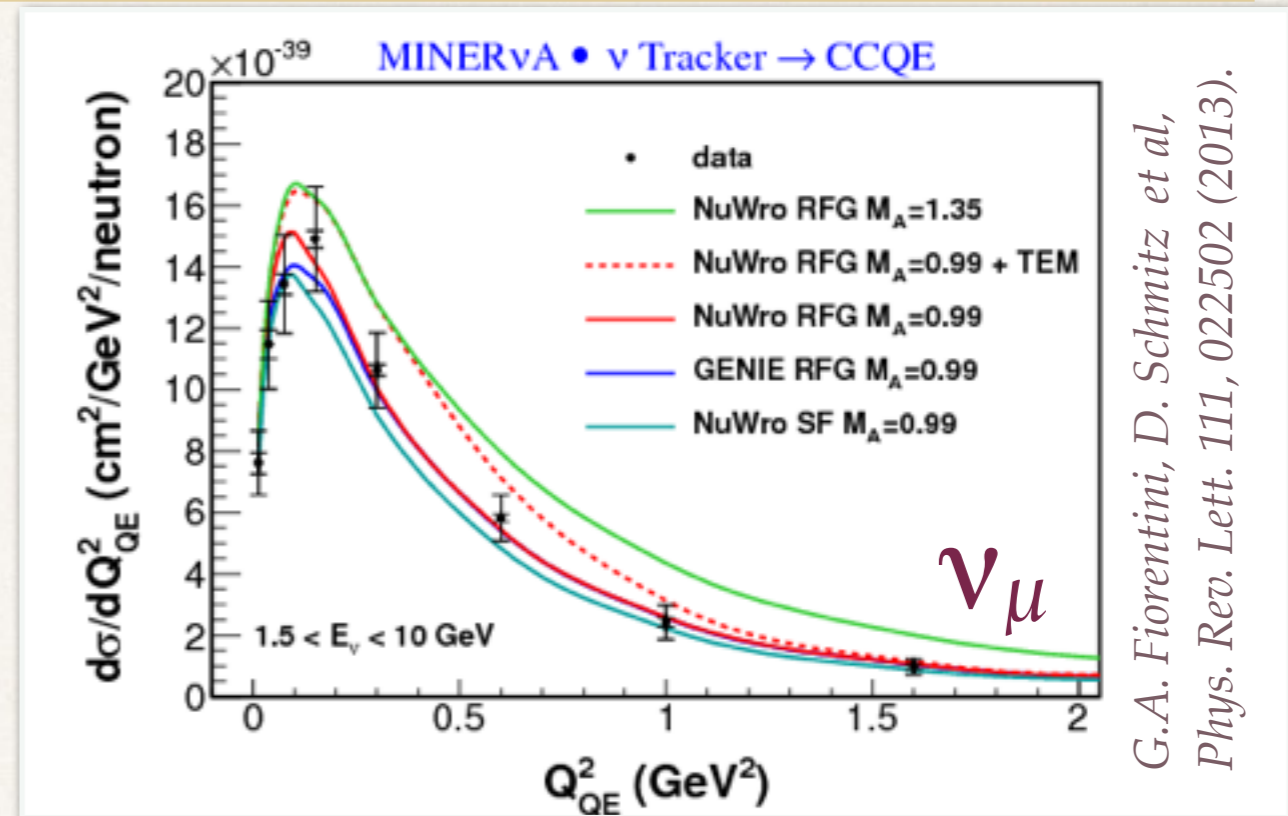
- GENIE RFG $M_A=0.99$
- NuWro RFG $M_A=0.99$
- NuWro RFG $M_A=1.35$
- ⋯ NuWro RFG+TEM $M_A=0.99$
- NuWro SF $M_A=0.99$



Quasi-elastic results: muon kinematics

- ❖ Compare data to **GENIE RFG** *C. Andreopoulos, et al., NIM 288A, 614, 87 (2010)* and **NuWro** *K. M. Graczyk and J. T. Sobczyk, Eur.Phys.J. C31, 177 (2003)* nuclear models

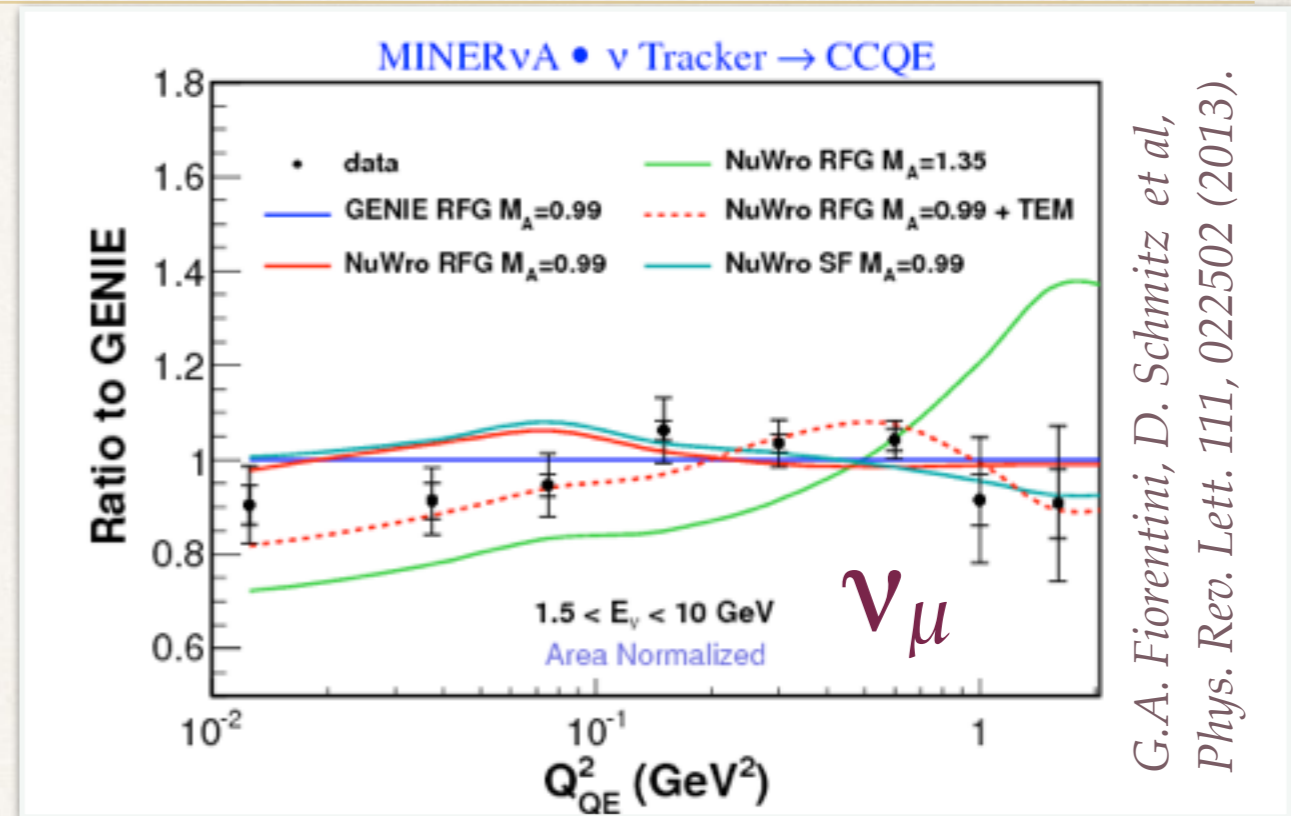
- GENIE RFG $M_A=0.99$
- NuWro RFG $M_A=0.99$
- NuWro RFG $M_A=1.35$
- ⋯ NuWro RFG+TEM $M_A=0.99$
- NuWro SF $M_A=0.99$



- ❖ To make it easier to distinguish:
 - ❖ Take **ratios** to GENIE (the MC we used for acceptance correction etc)
 - ❖ Use **log scale** to see differences at low Q^2
 - ❖ Look at distribution **shapes** to reduce systematic uncertainty, particularly due to flux

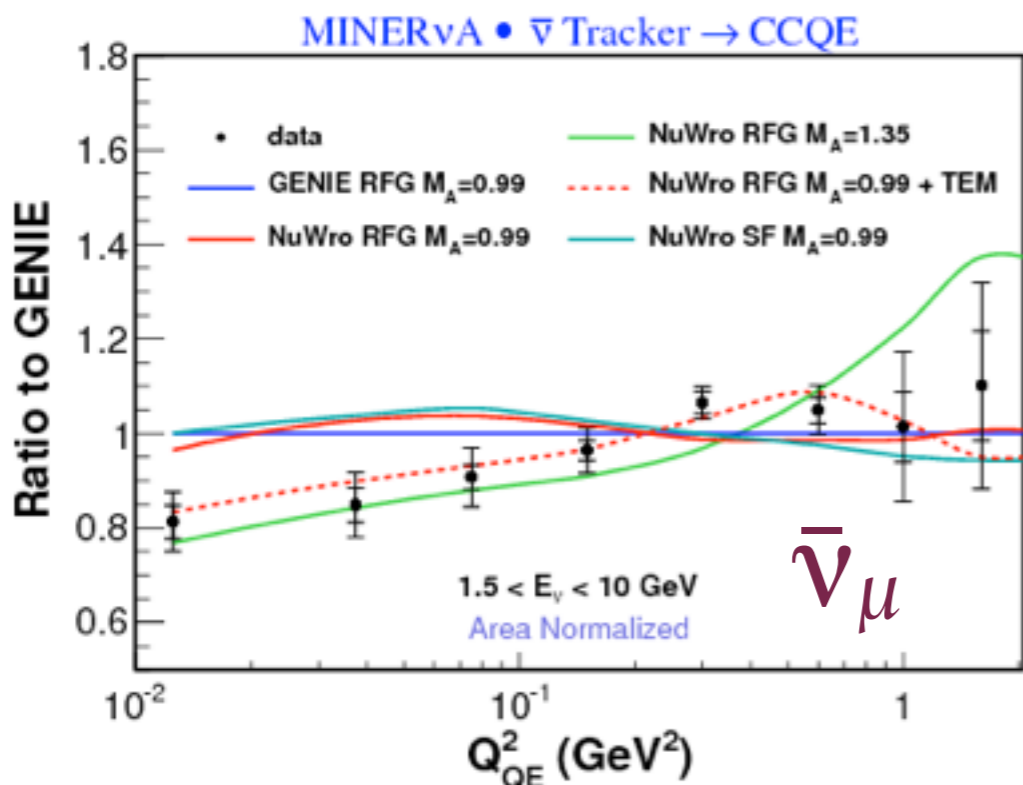
Quasi-elastic results: muon kinematics

- GENIE RFG $M_A=0.99$
- NuWro RFG $M_A=0.99$
- NuWro RFG $M_A=1.35$
- - - NuWro RFG+TEM $M_A=0.99$
- NuWro Spectral functions $M_A=0.99$

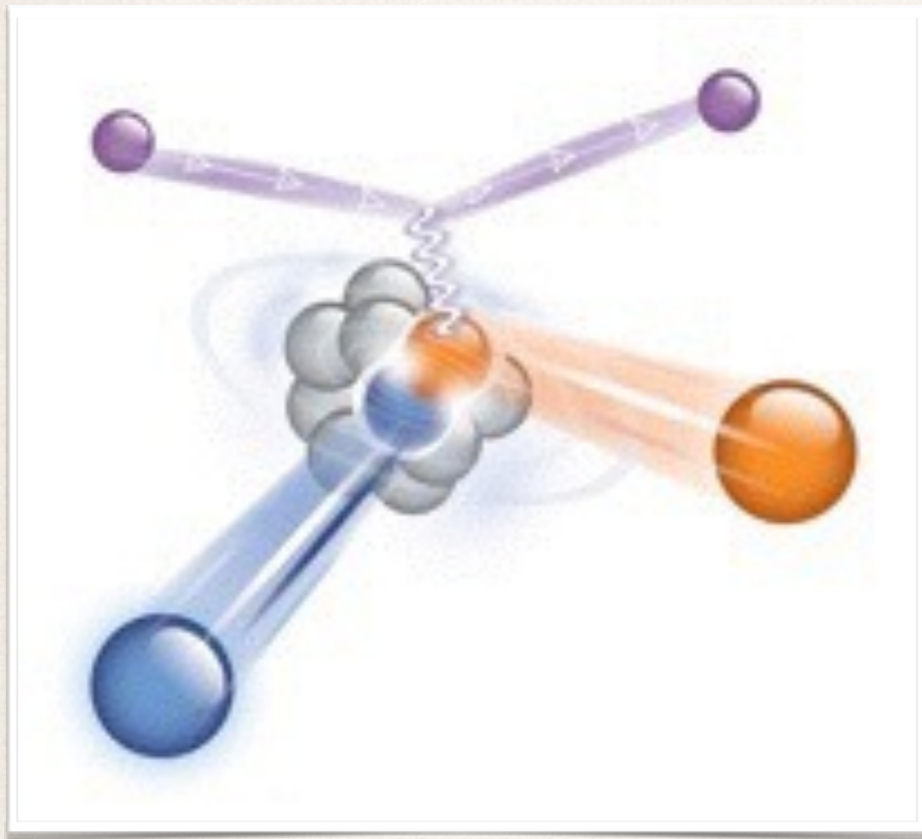


χ^2 per degree of freedom:

	$\bar{\nu}_\mu$	ν_μ
■ RFG ($M_A = 1.35$):	1.73	2.1
■ RFG ($M_A=0.99$):	2.90	4.1
▨ RFG ($M_A=0.99$, TEM):	0.66	1.7
■ SF ($M_A=0.99$):	2.99	3.8



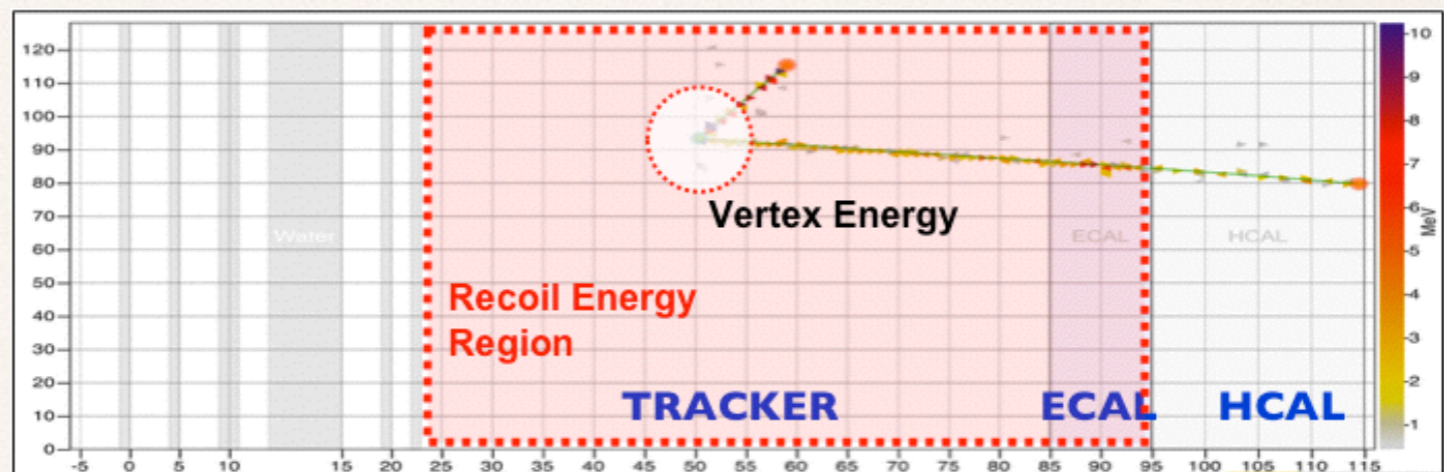
Energy around the vertex



R. Subedi et al. 2008 Science 320 1476

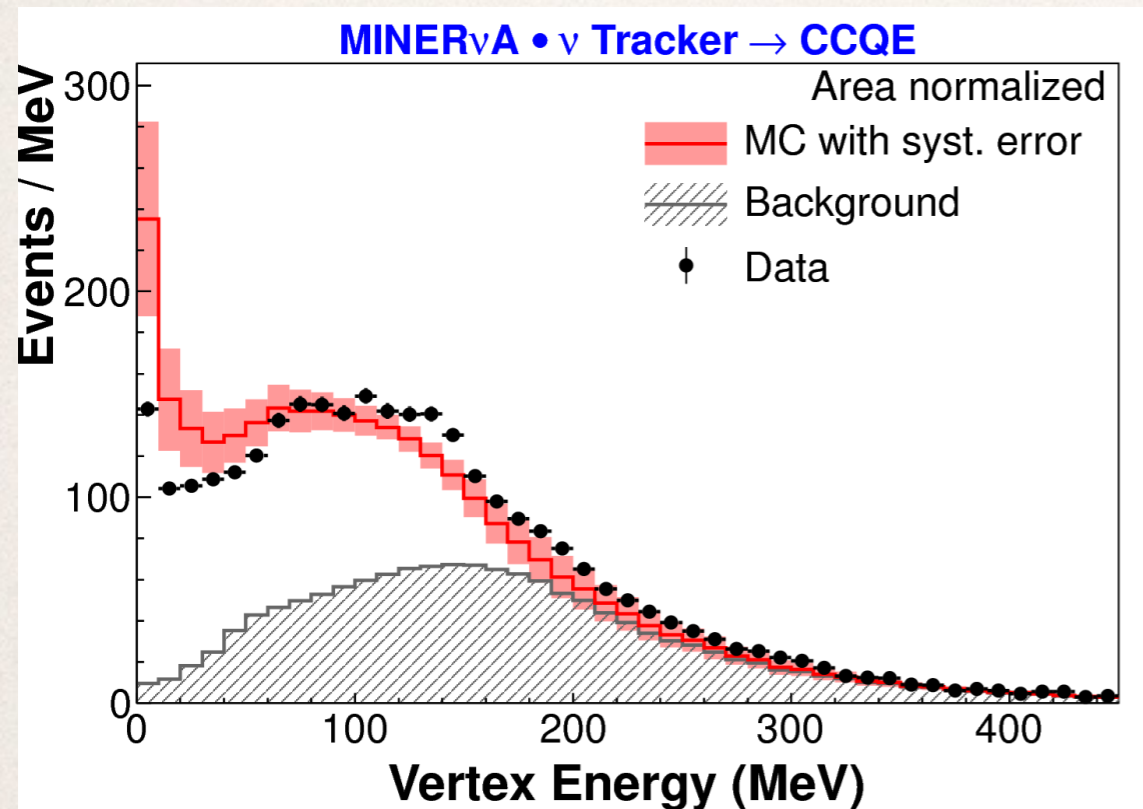
Transverse enhancement parameterizes a model with **correlated pairs** of nucleons

If a neutrino interacts with a paired nucleon, its partner may also be ejected



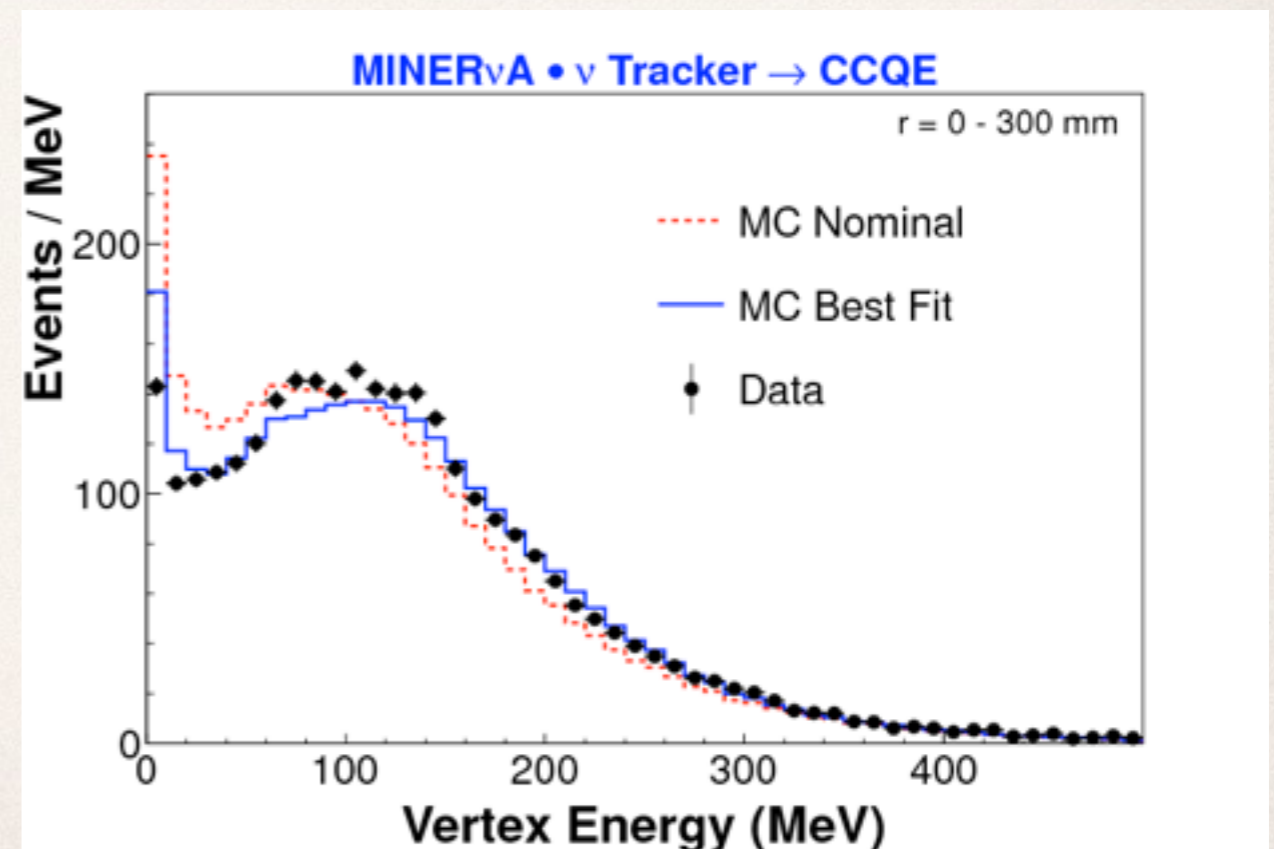
- ❖ Recall that we neglected an **area around the vertex** when we counted the total recoil energy
- ❖ We now compare the non-track energy deposited within that region to our Monte Carlo, to look for evidence of **additional nucleons**
- ❖ Our “vertex region” would contain nucleons with an energy up to 225 MeV (neutrino mode) or 120 MeV (antineutrino mode)

Vertex energy - extra protons

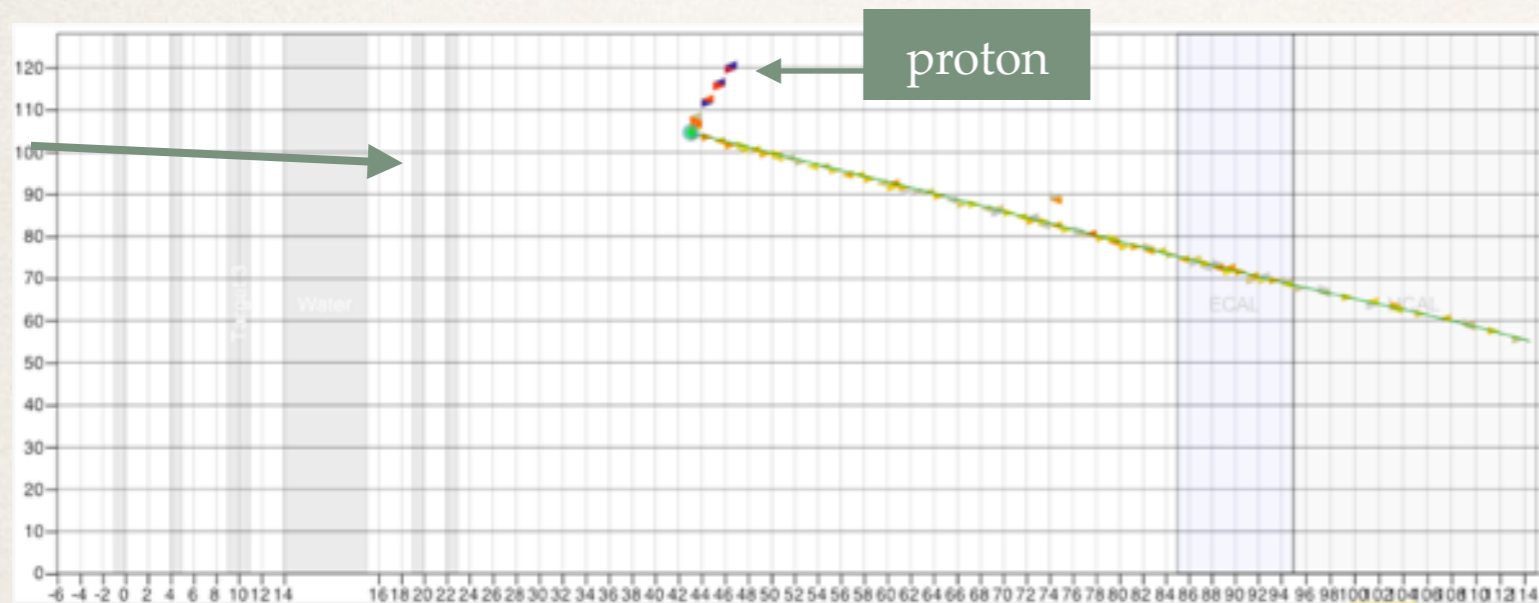


- ❖ Modeling an **additional proton $25 \pm 9\%$** of the time gave the best fit to the data
- ❖ Final state protons suggests initial state **proton-neutron correlations**
- ❖ This would explain why no such effect was seen for **antineutrino mode**; we would expect **low-energy neutrons**, to which we have low sensitivity

- ❖ A **harder neutrino-mode energy spectrum** is seen in data than Monte Carlo
- ❖ It is not seen in antineutrino mode
- ❖ We simulated extra protons with kinetic energies up to 225 MeV to see how this would change the Monte Carlo distribution



Quasi-elasticics from proton kinematics

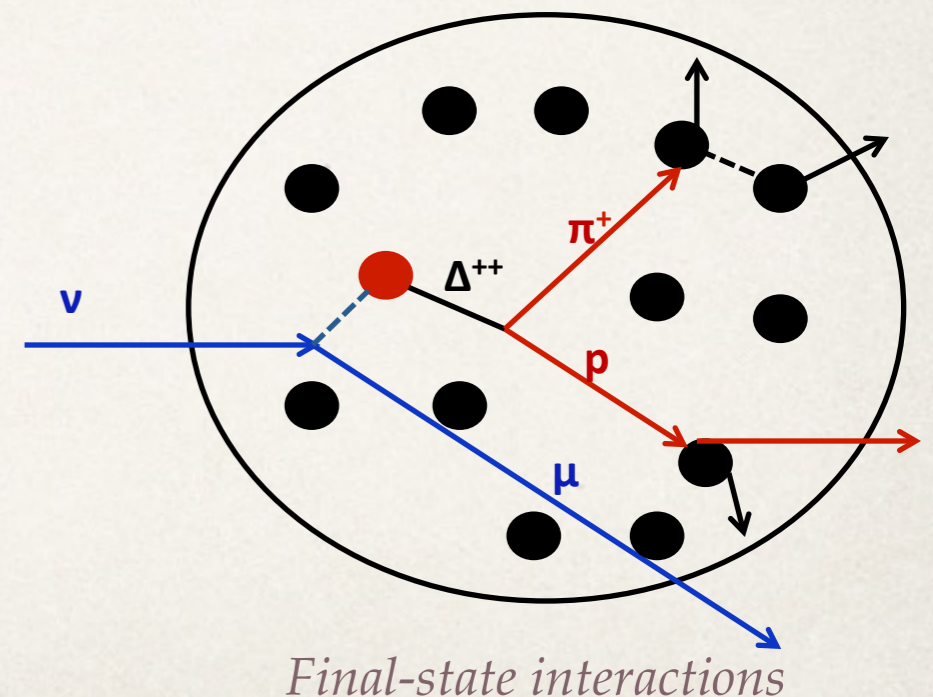


- ❖ Instead of using the muon, we can instead reconstruct Q^2 from the kinematics of a **stopping proton**
- ❖ Protons can undergo **final-state interactions**, so this is particularly **sensitive to FSI modeling**

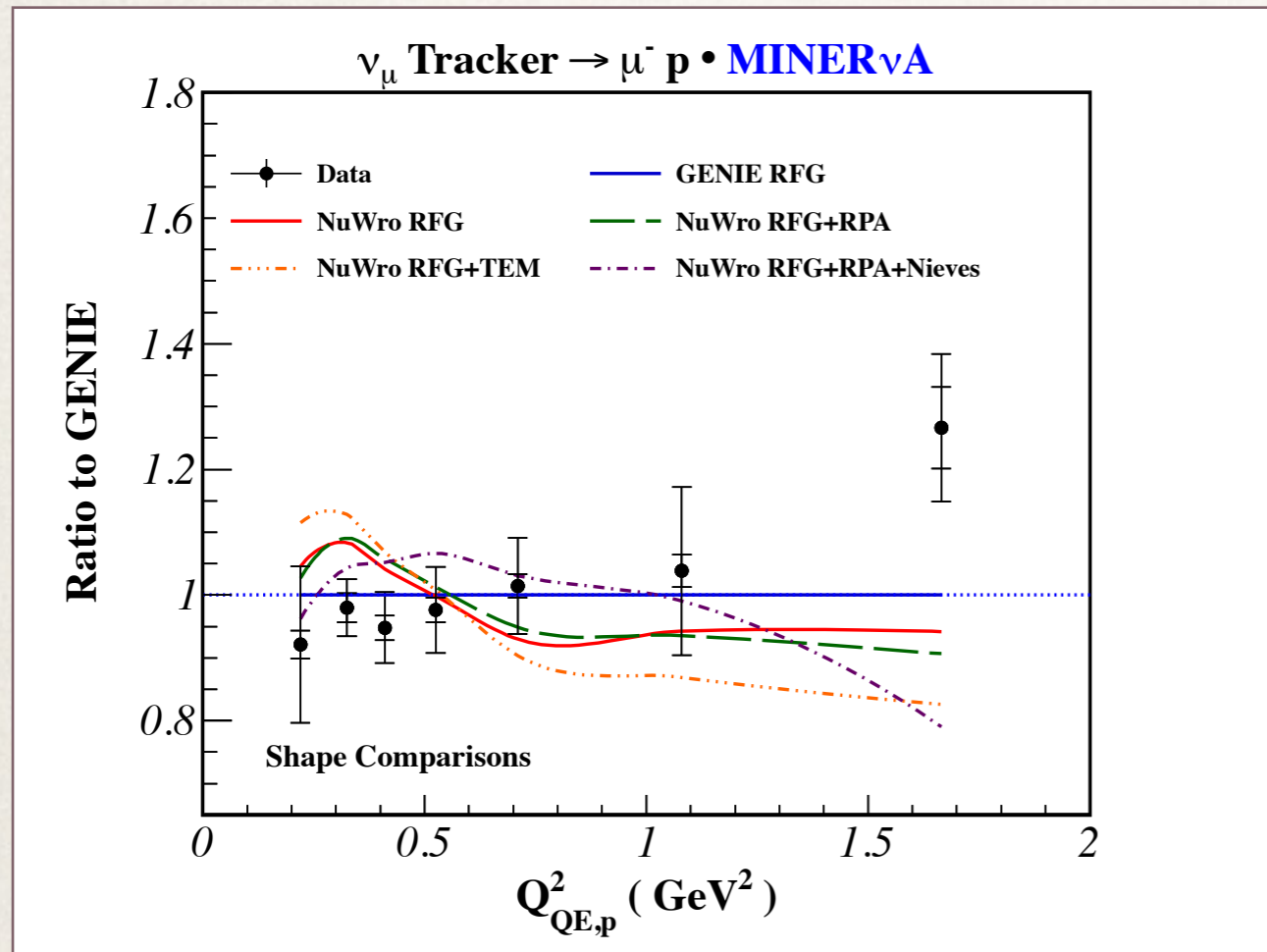
$$Q_{QE,p}^2 = (M_n - E_B)^2 - M_p^2 + 2(M_n - E_B)(T_p + M_p - M_n + E_B)$$

$M_{n,p}$ = neutron, proton mass, T_p =proton KE, E_B =binding energy

- ❖ In this study, our signal definition is QE-like, based on final-state particles
- ❖ Thus our signal includes some resonant and DIS interactions



Quasi-elasticics from proton kinematics



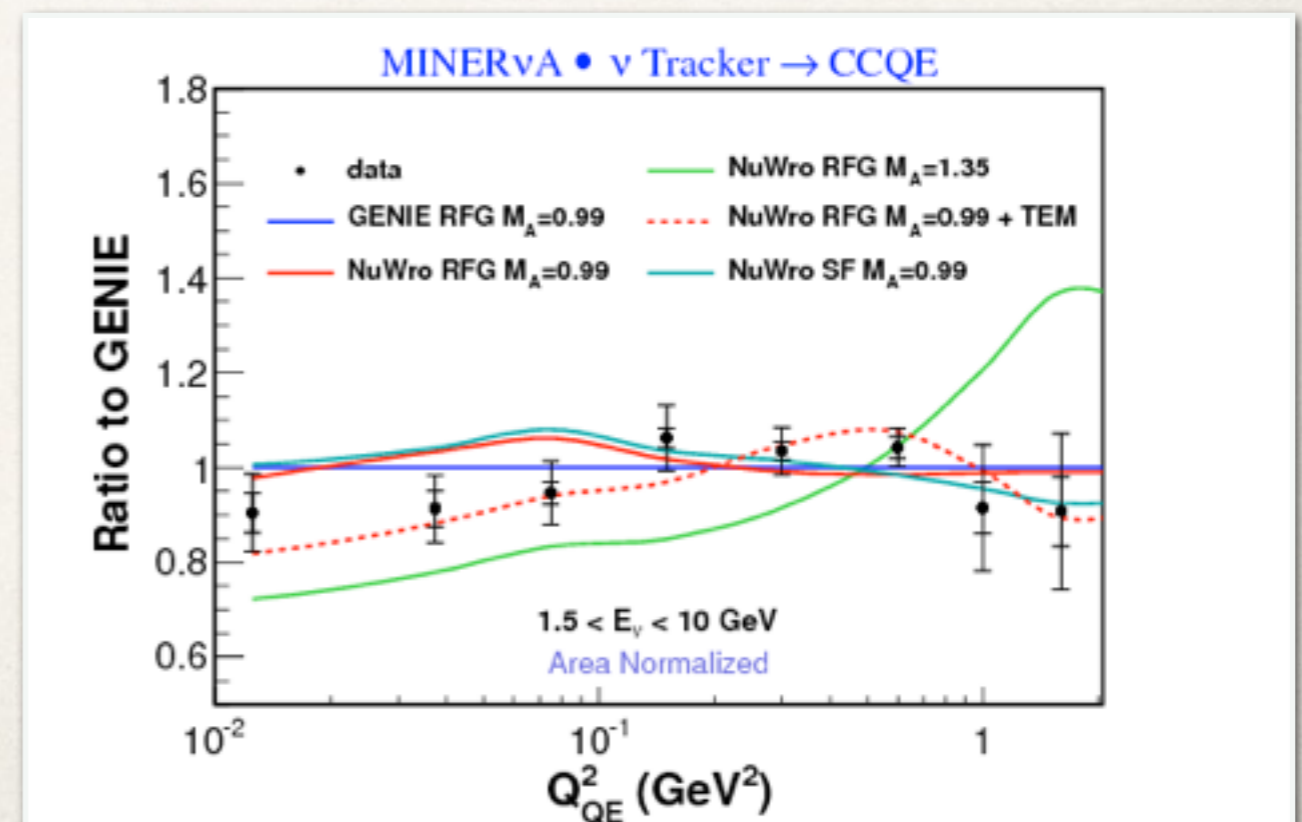
T Walton et al, Phys. Rev. D 91, 071301(R)

- ❖ No one model is able to simulate both our muon- and proton-kinematics data sets

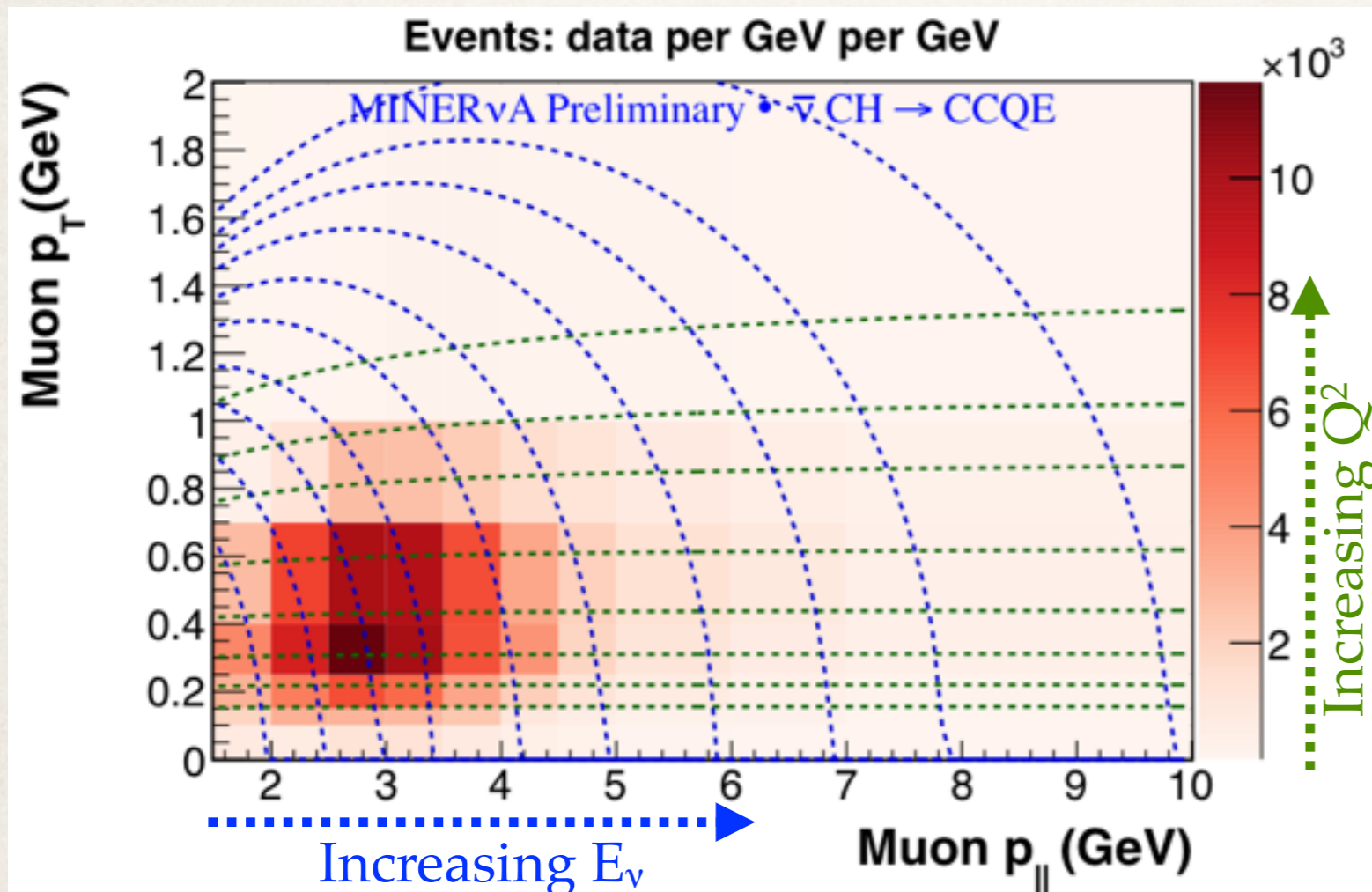
We need a model that gets everything right!

C. Patrick, MINERvA Collaboration

- ❖ The proton-kinematics study favors GENIE's **Relativistic Fermi Gas model**, with no additional nuclear effects
- ❖ Contrast to muon-kinematics study
- ❖ Note that the proton-based study has a greater **acceptance** (no MINOS match)
- ❖ However, it is **unable to examine the low Q^2 region** due to tracking limitations



Next - double-differential cross section

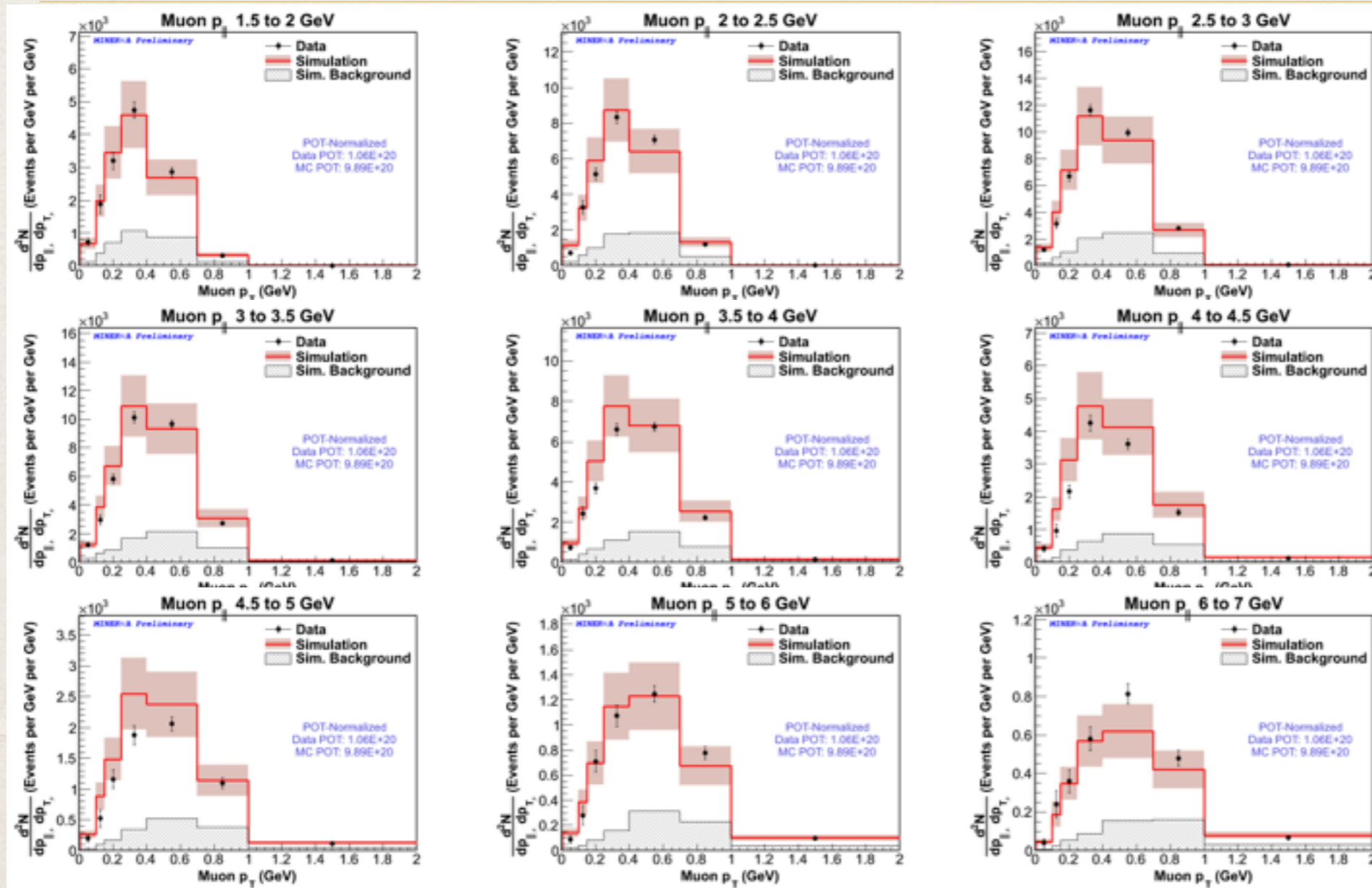


- * Requested by NuSTEC group for use in global fits
- * Muon longitudinal and transverse momentum are measurable quantities
- * This dual parameter space should give additional power to distinguish between models
- * QE and QE-like signals
- * Updated reconstruction

Challenges:

- * More bins means fewer events per bin, and acceptance can change rapidly
- * Distinguishing QE-like (but not QE) events from background is tricky
- * A flexible framework enables calculations vs other parameters

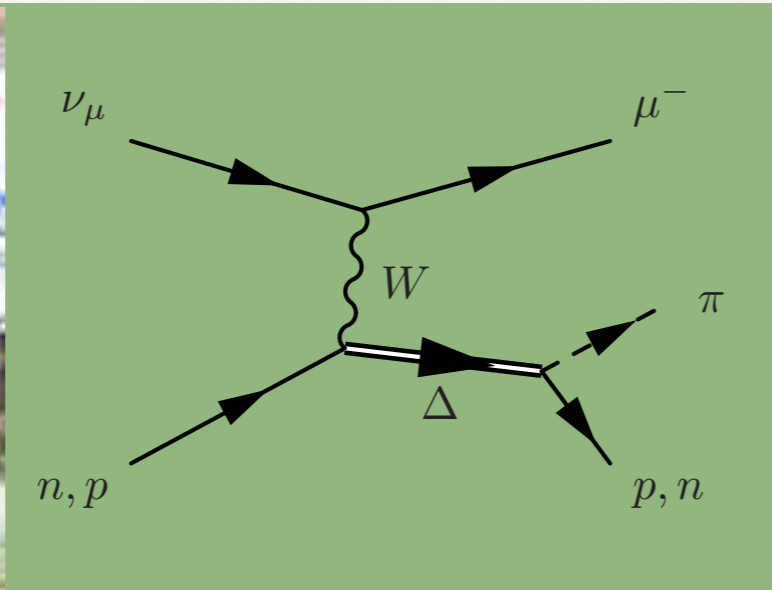
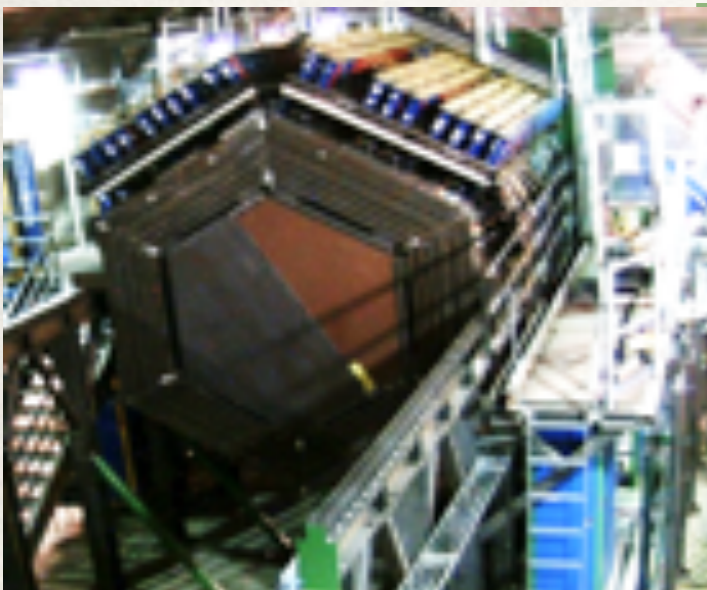
Double-differential cross sections



The plots to the left are data and MC distributions for the antineutrino CCQE sample

Neutrino and antineutrino results coming soon!

- ❖ Uncertainties on reconstruction and interaction model are shown on the simulation
- ❖ The GENIE model carries the largest uncertainty in many bins
- ❖ Reducing the uncertainty on the interaction model is a key goal of this analysis



Other recent results

Charged-current π^\pm production from ν

$$\nu_\mu A \rightarrow \mu^- \pi^\pm X$$

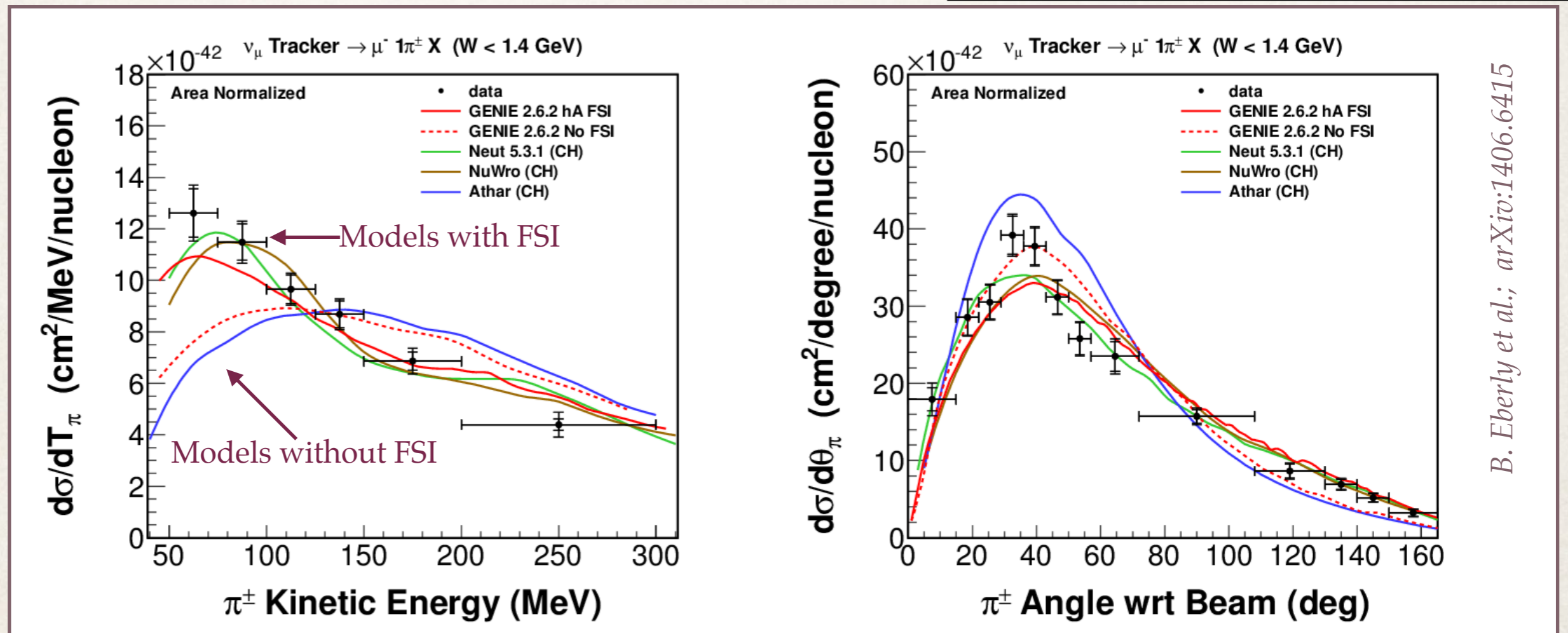
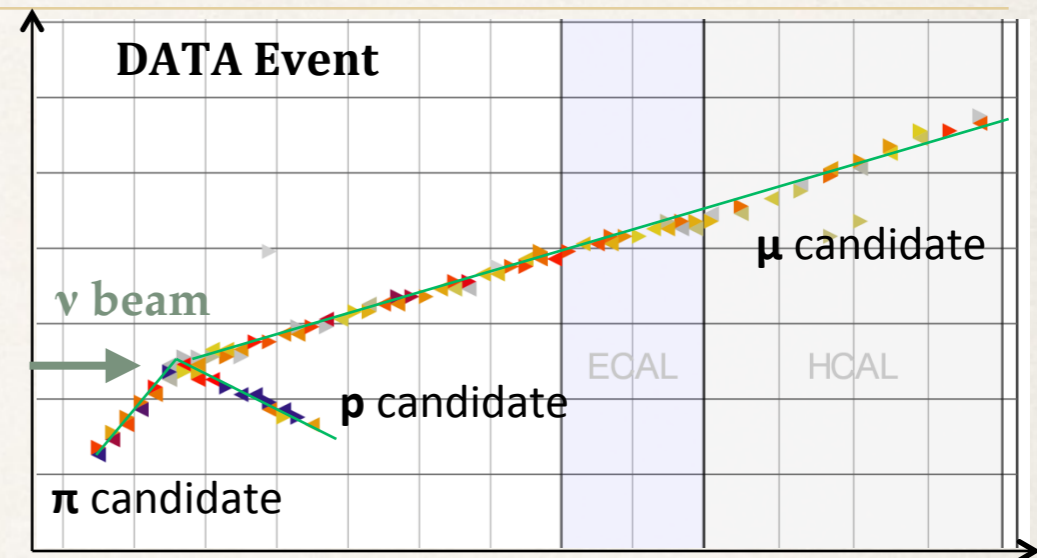
A is the initial nucleus

X is a recoil nucleus plus any other particles that are not pions

$$\nu_\mu A \rightarrow \mu^- \pi^+ A$$

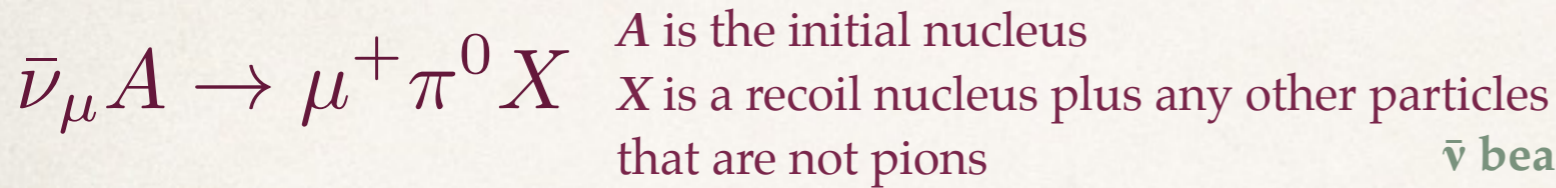
GENIE 2.6.2 and NuWro use Rein-Sehgal model for resonant pion production
Athar, M., Chauhan, S., and Singh, S. K., *Eur. Phys. J. A*43, 209–227 (2010).

Neut (Rein-Sehgal+FSI): Y. Hayato, *Acta Phys.Polon. B*40 (2009) 2477-2489



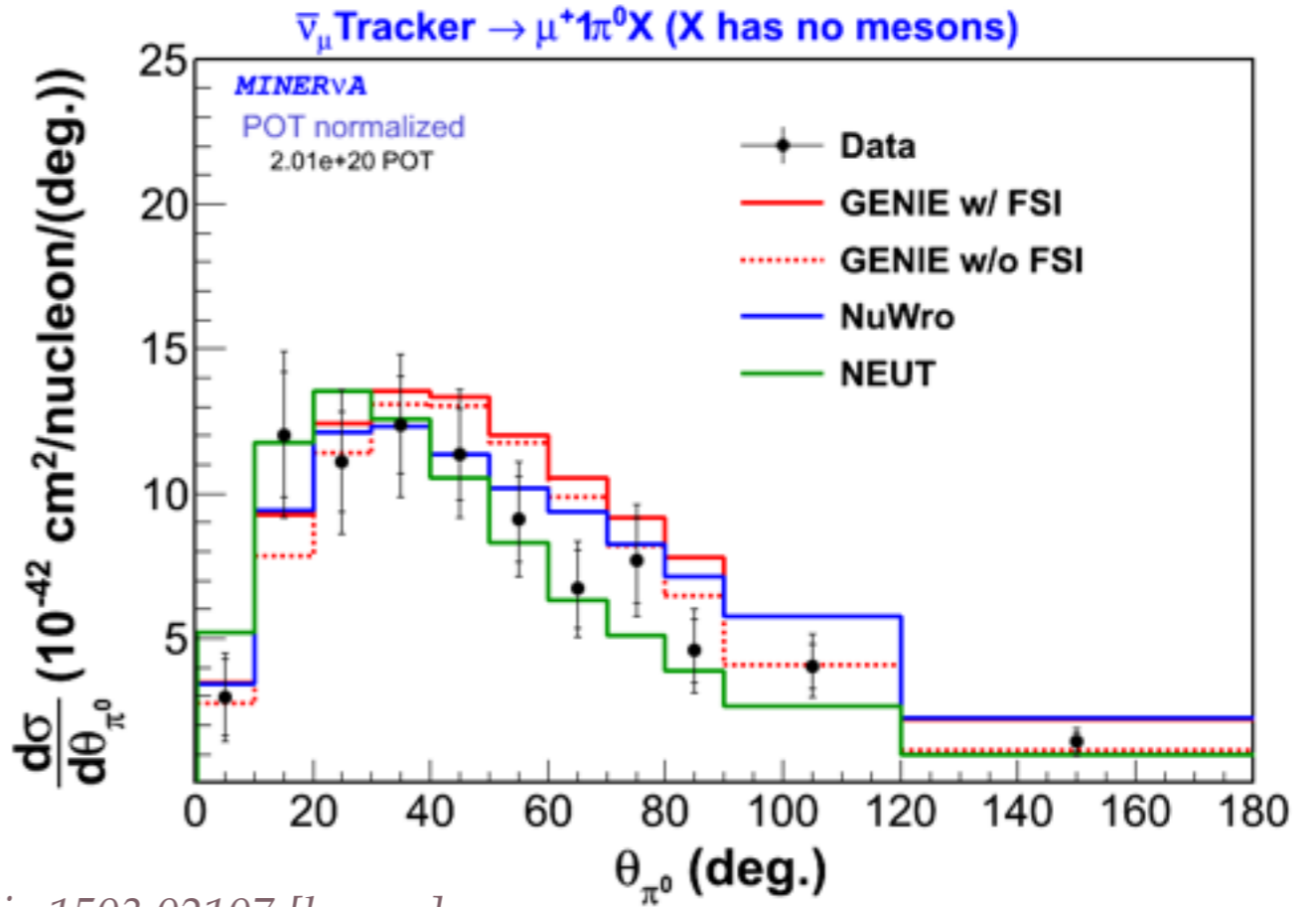
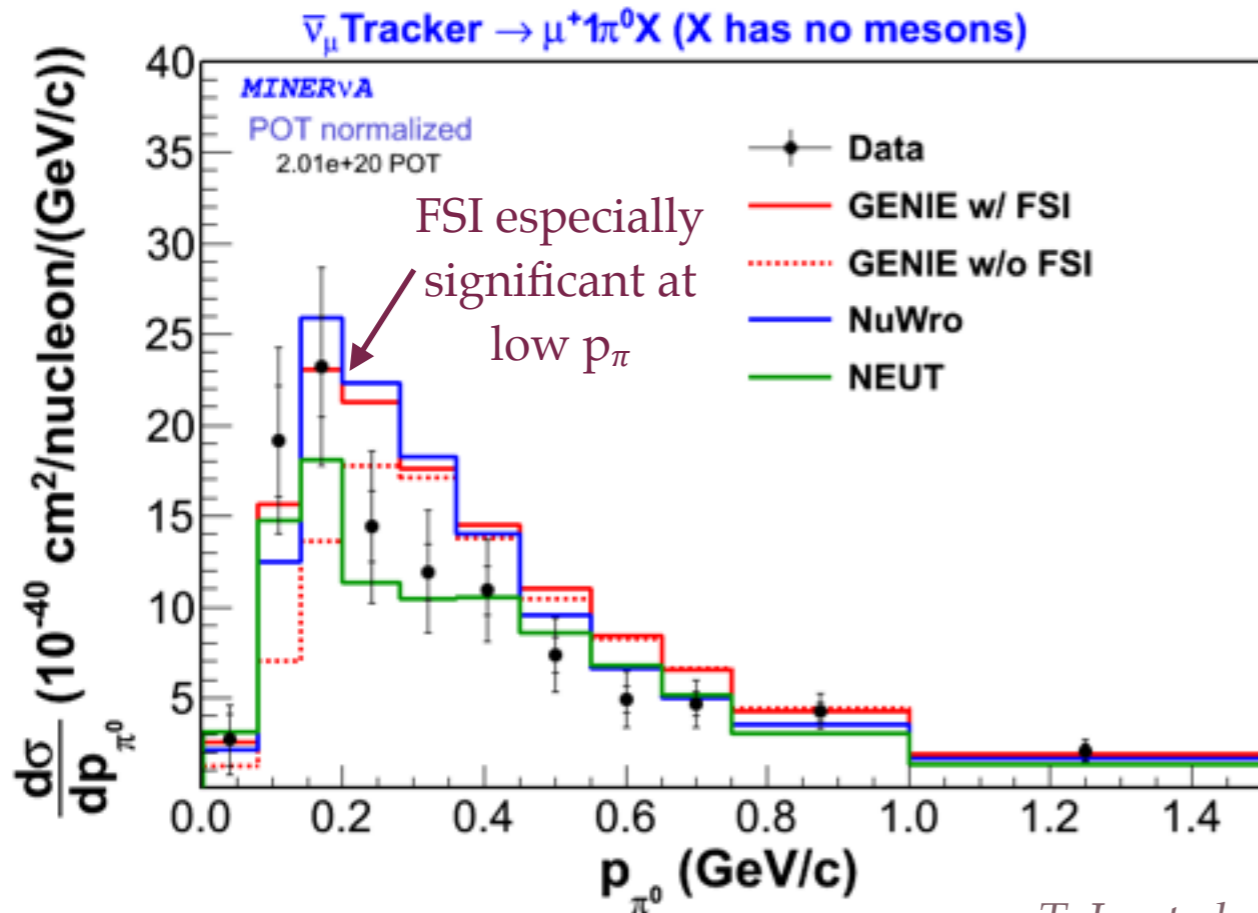
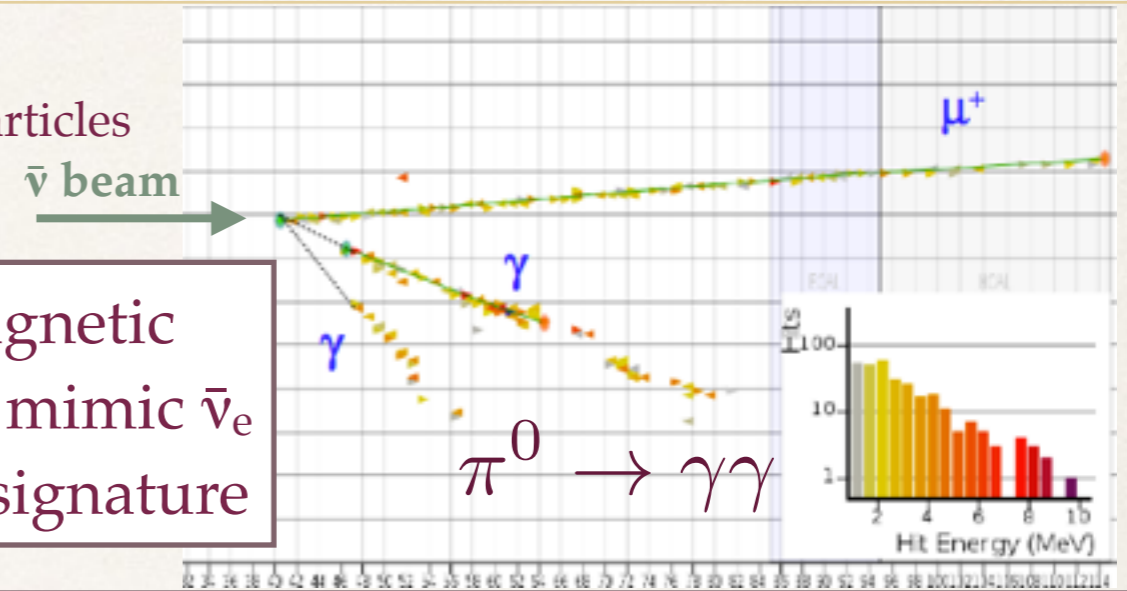
B. Eberly et al.; arXiv:1406.6415

π^0 production from antineutrinos



This can help evaluate the approximations made in different generators' FSI models

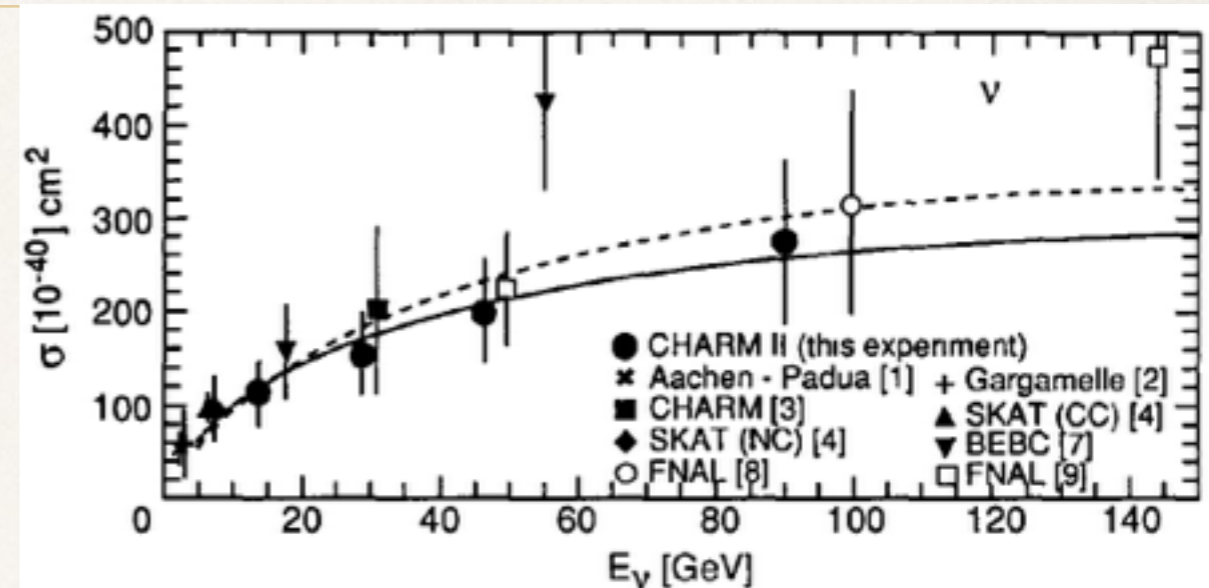
Electromagnetic showers can mimic $\bar{\nu}_e$ appearance signature



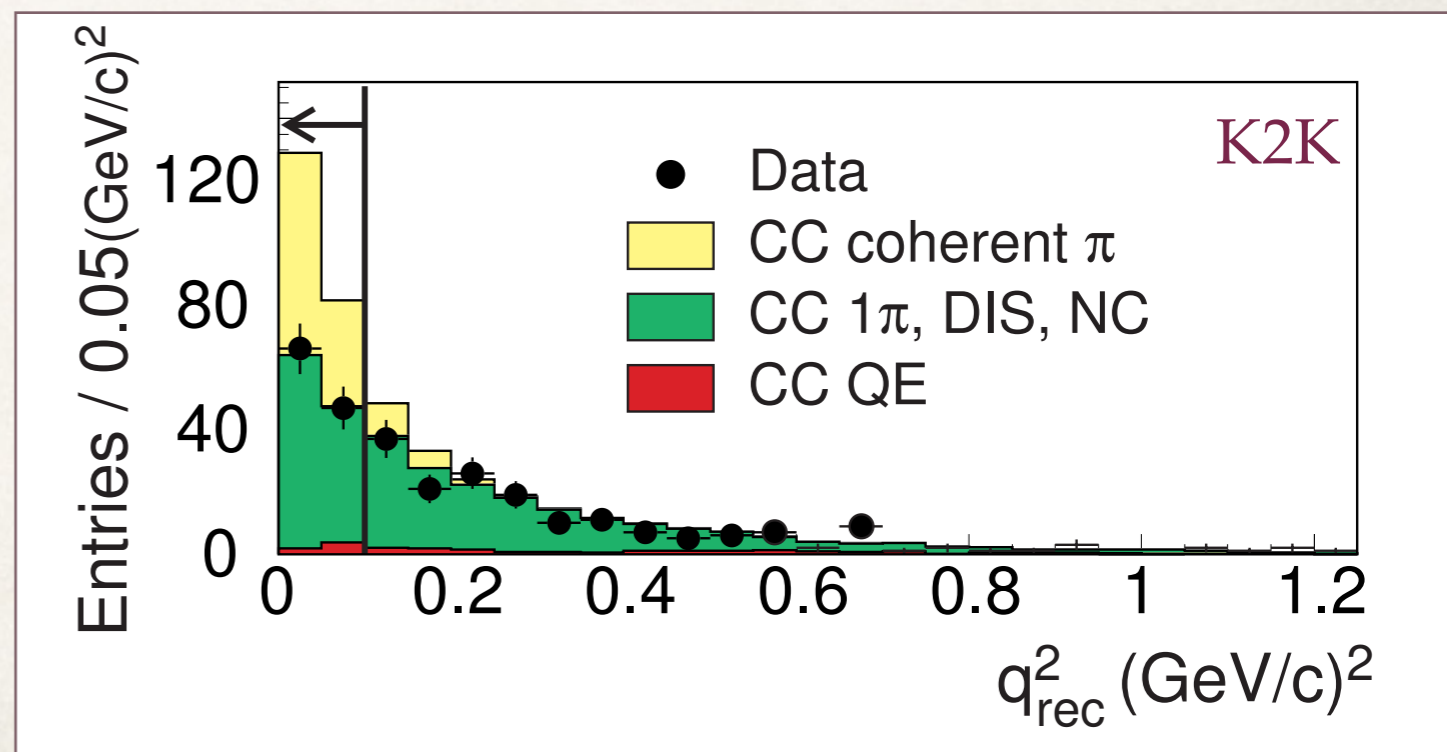
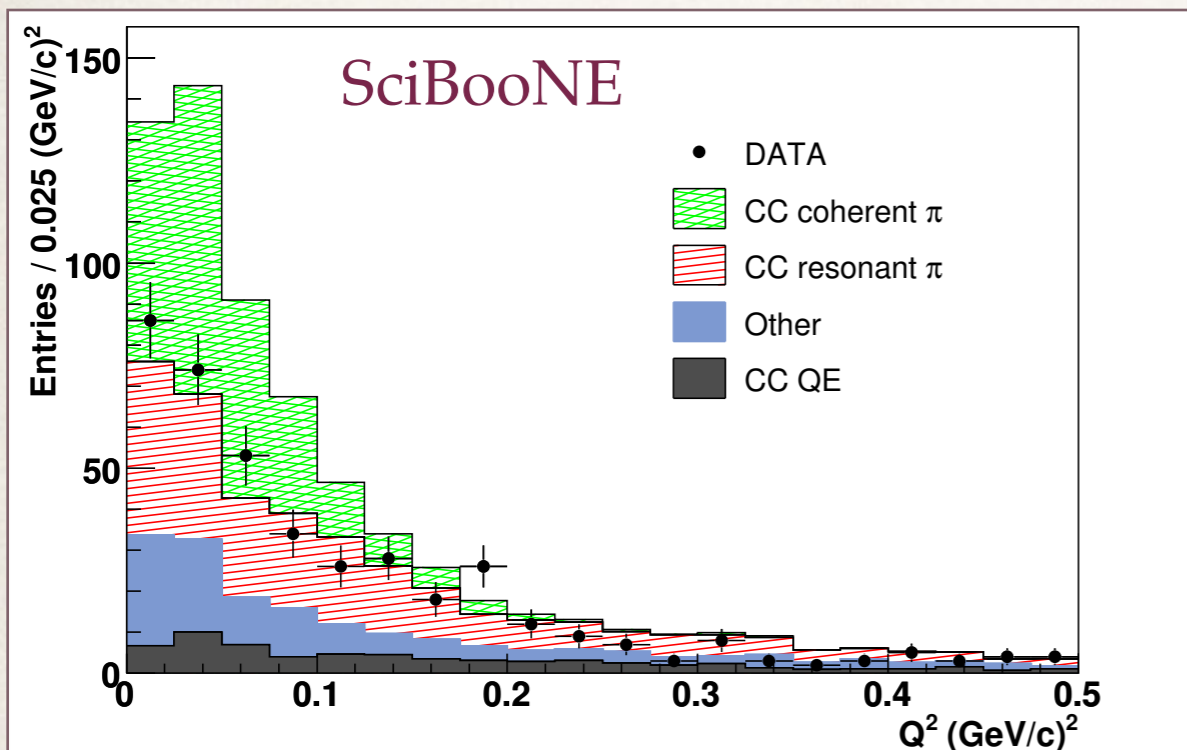
T. Le et al., arXiv:1503.02107 [hep-ex]

Coherent pion production: I

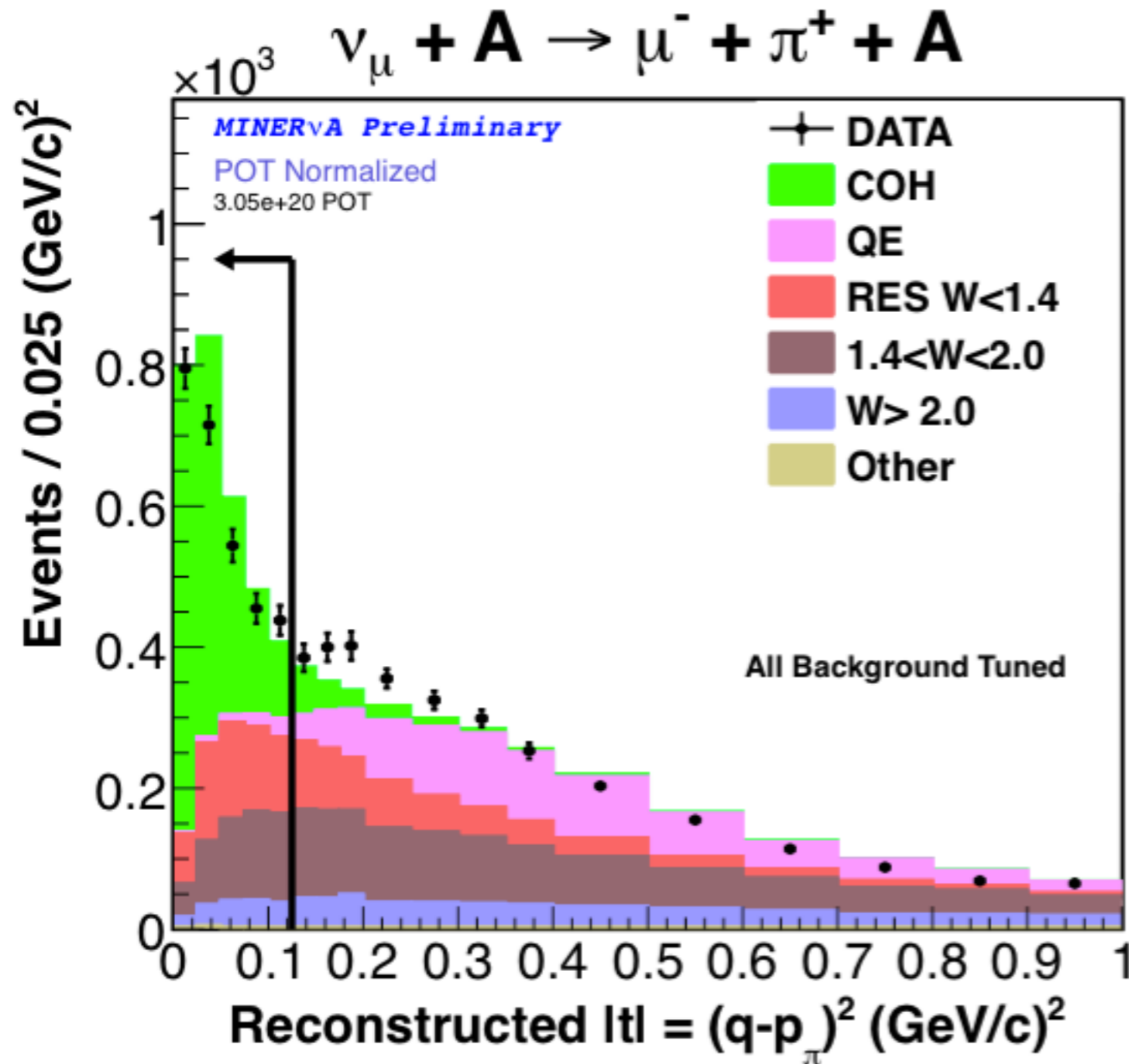
- Early experiments at high energies see clear evidence of coherent pion production (scattering without breaking up the nucleus)



- Lower energy experiments saw results consistent with NEUT's background predictions



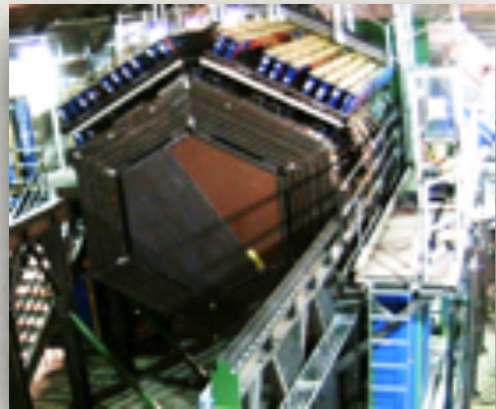
Coherent pion production: II



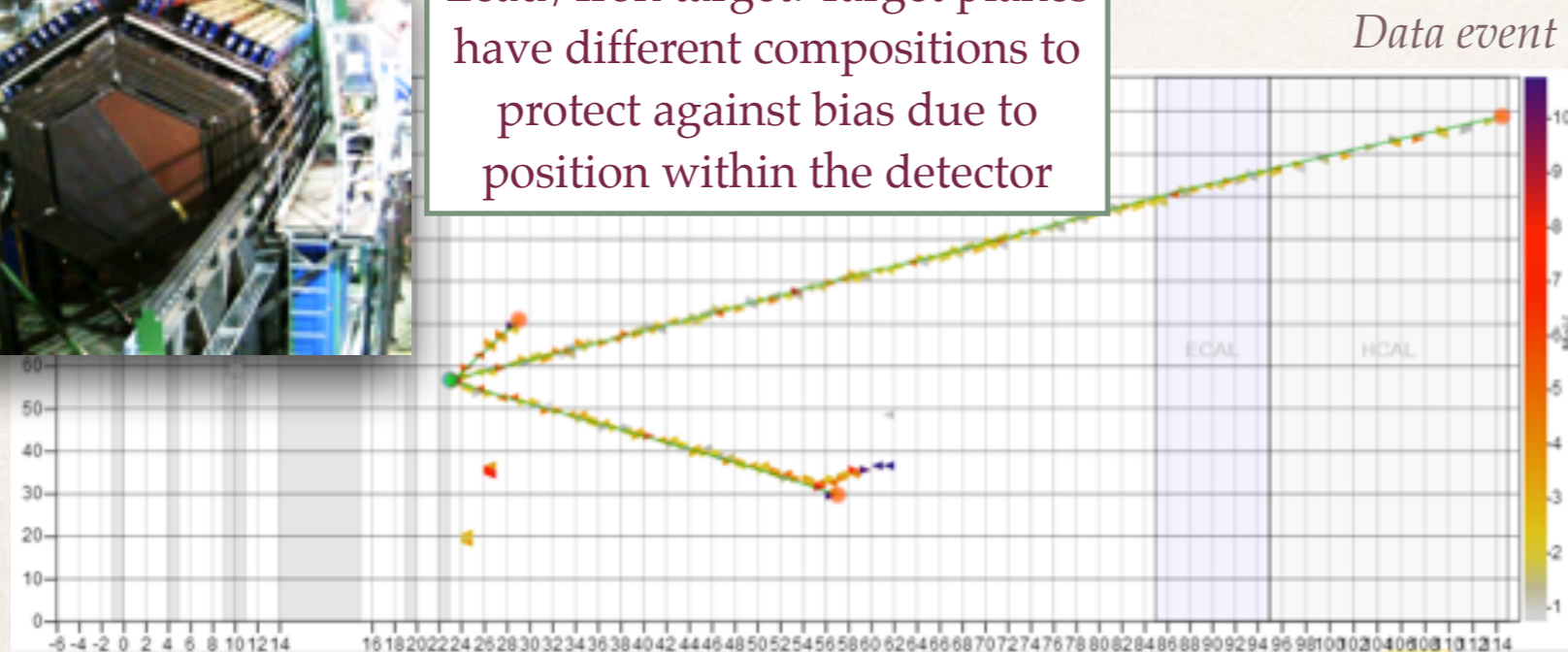
A Higuera, A Mislevic et al., Phys. Rev. Lett. 113, 261802 (2014)

- ❖ MINERvA sees clear evidence of coherent scattering in the few-GeV energy region
- ❖ Our ability to measure the quantity $|t|$ enables us to identify coherent candidates in a model-independent way
- ❖ The slope of the $|t|$ distribution is related to the size of the target, so it is easy to distinguish scattering off a nucleus from a nucleon

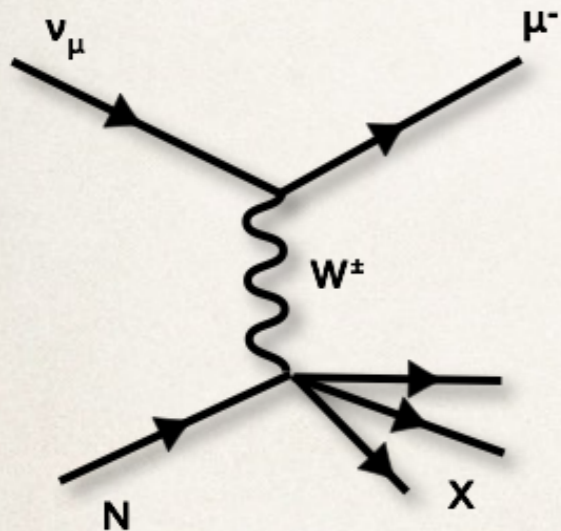
Cross-sections on other materials



Lead/Iron target. Target planes have different compositions to protect against bias due to position within the detector



MINERvA's nuclear target region allows us to look at scattering on different materials, to see how the the composition of the nucleus affects cross section

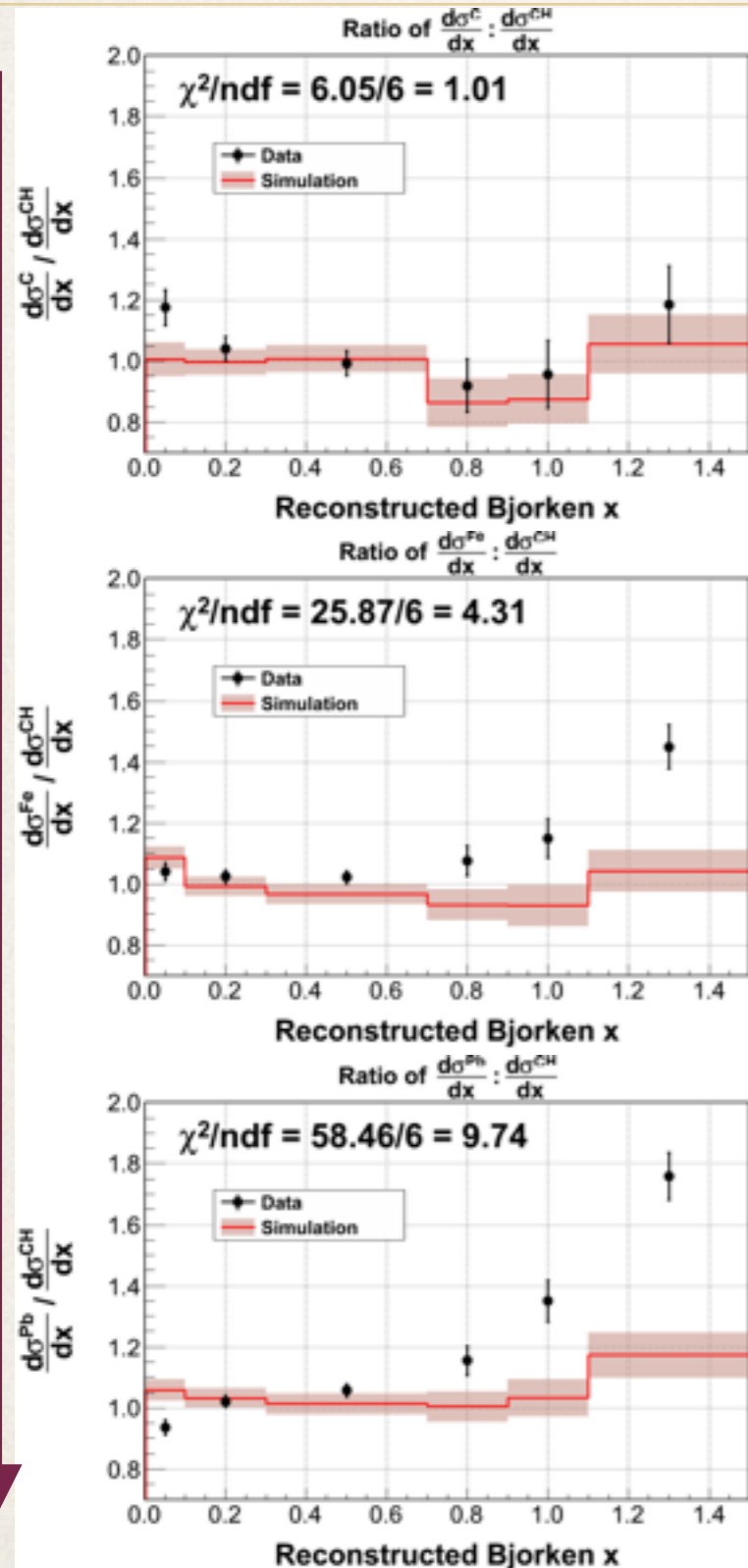


We look at the **charged-current inclusive** cross sections: **all** interactions that produce a negative muon.

Oscillation experiments need to understand cross sections on the materials their detectors are made of, especially if they can't take near/far detector ratios

CC-inclusive cross sections on nuclei

Heavier nuclei



C

Fe

Pb

- * Bjorken x characterizes the type of interaction

$$x = \frac{Q^2}{2M\nu}$$

- * Our simulation
 - * overestimates at low x (*shadowing region*)
 - * underestimates at high x (*more elastic*)
- * ...with an effect more pronounced for heavier nuclei

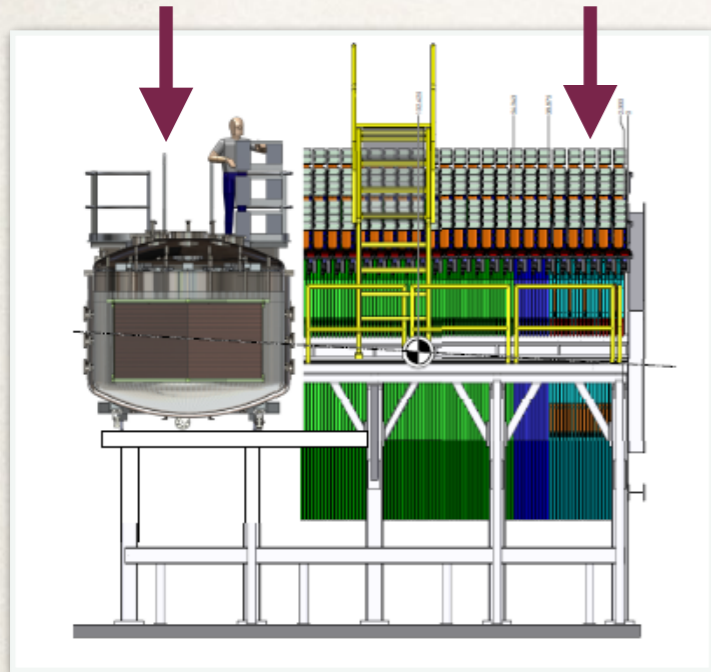
There are no current models that explain these nucleus-dependent behaviors

- * But it's vital we understand cross sections on these materials
- * MINERvA's **medium-energy dataset** will provide a large, DIS-rich sample to test this further and look at individual interaction channels

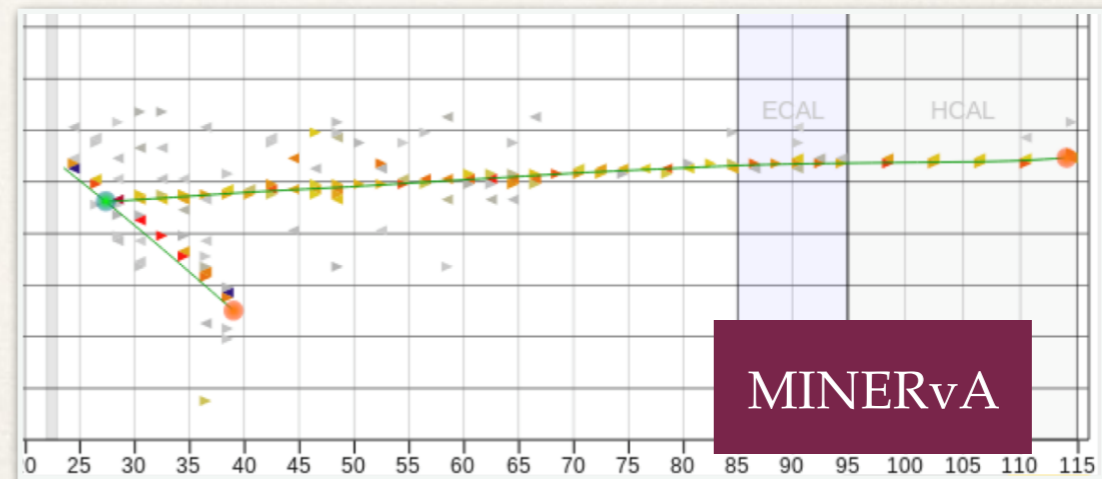
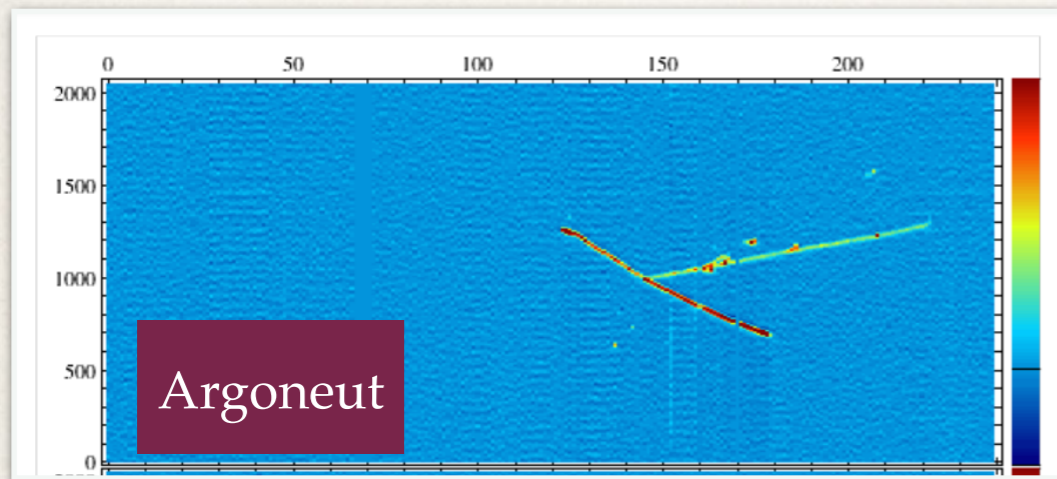
CAPTAIN-MINER ν A



CAPTAIN MINER ν A



- * Oscillation experiments (T2K) are already using MINER ν A's cross section measurements
- * But DUNE will have a liquid argon detector, and we don't have an argon target... how can we help?
- * **PROPOSAL:** insert **CAPTAIN** detector upstream of MINER ν A!
 - * CAPTAIN is a 5-ton liquid argon time-projection chamber
 - * Study nuclear effects around the event vertex
 - * Complements MicroBooNE's studies by looking at first DUNE oscillation maximum



Comparison of similar event displays in LAr TPC (Argoneut) and MINER ν A tracker

In summary

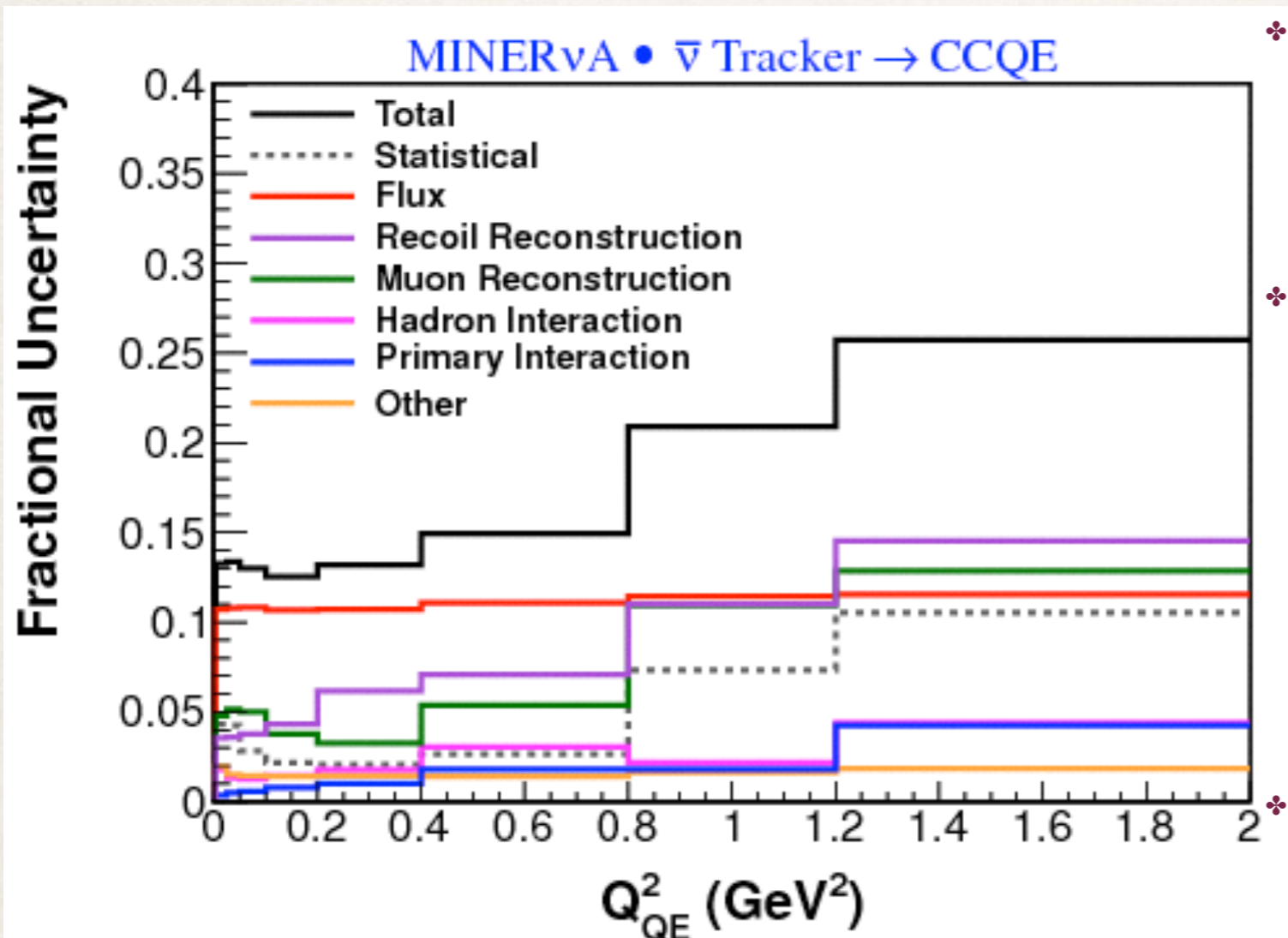
- ❖ MINERvA has been measuring cross sections for various neutrino-nucleus interactions
- ❖ We're investigating nuclear effects and helping generators refine their nuclear models
- ❖ We've observed effects that vary depending on the size of the nucleus
- ❖ We're already starting to provide cross section data for oscillation experiments, and our distributions will reduce important uncertainties
- ❖ ... and there is lots more to come!



Thank you!

Backup slides

Sources of systematic uncertainty



* Recoil

- * recoil energy due to particle
- * neutron response model

* Muon reconstruction

- * energy scale (MINOS range and curvature, MINERvA dE/dx)
- * tracking reconstruction
- * overlapping MINOS tracks
- * vertex resolution

* Hadron interaction

- * final state interaction model

* Primary interaction

- * quasi-elastic interaction model
- * resonant background model
- * nuclear model

- * This indicates systematics evaluated for the CCQE antineutrino analysis
- * Different effects are important for different analyses (for example some are especially sensitive to FSI)

* Flux

List of GENIE model uncertainties

Uncertainty	GENIE Knob name	1 σ
M_A (Elastic Scattering)	MaNCEL	$\pm 25\%$
Eta (Elastic scattering)	EtaNCEL	$\pm 30\%$
M_A (CCQE Scattering)	MaCCQE	+25% -15%
CCQE Normalization	NormCCQE	+20% -15%
M_A (CCQE Scattering, shape only)	MaCCQEshape	$\pm 10\%$
CCQE Vector Form factor model	VecFFCCQEshape	
CC Resonance Normalization	NormCCRES	$\pm 20\%$
M_A (Resonance Production)	MaRES	$\pm 20\%$
M_V (Resonance Production)	MvRES	$\pm 10\%$
1pi production from $\nu p / \bar{\nu} n$ non-resonant interactions	Rvp1pi	$\pm 50\%$
1pi production from $\nu n / \bar{\nu} p$ non-resonant interactions	Rvn1pi	$\pm 50\%$
2pi production from $\nu p / \bar{\nu} n$ non-resonant interactions	Rvp2pi	$\pm 50\%$
2pi production from $\nu n / \bar{\nu} p$ non-resonant interactions	Rvn2pi	$\pm 50\%$
DIS CC Normalization	NormDISCC	??
Modify Pauli blocking (CCQE) at low Q^2	CCQEPauliSupViaKF	$\pm 30\%$

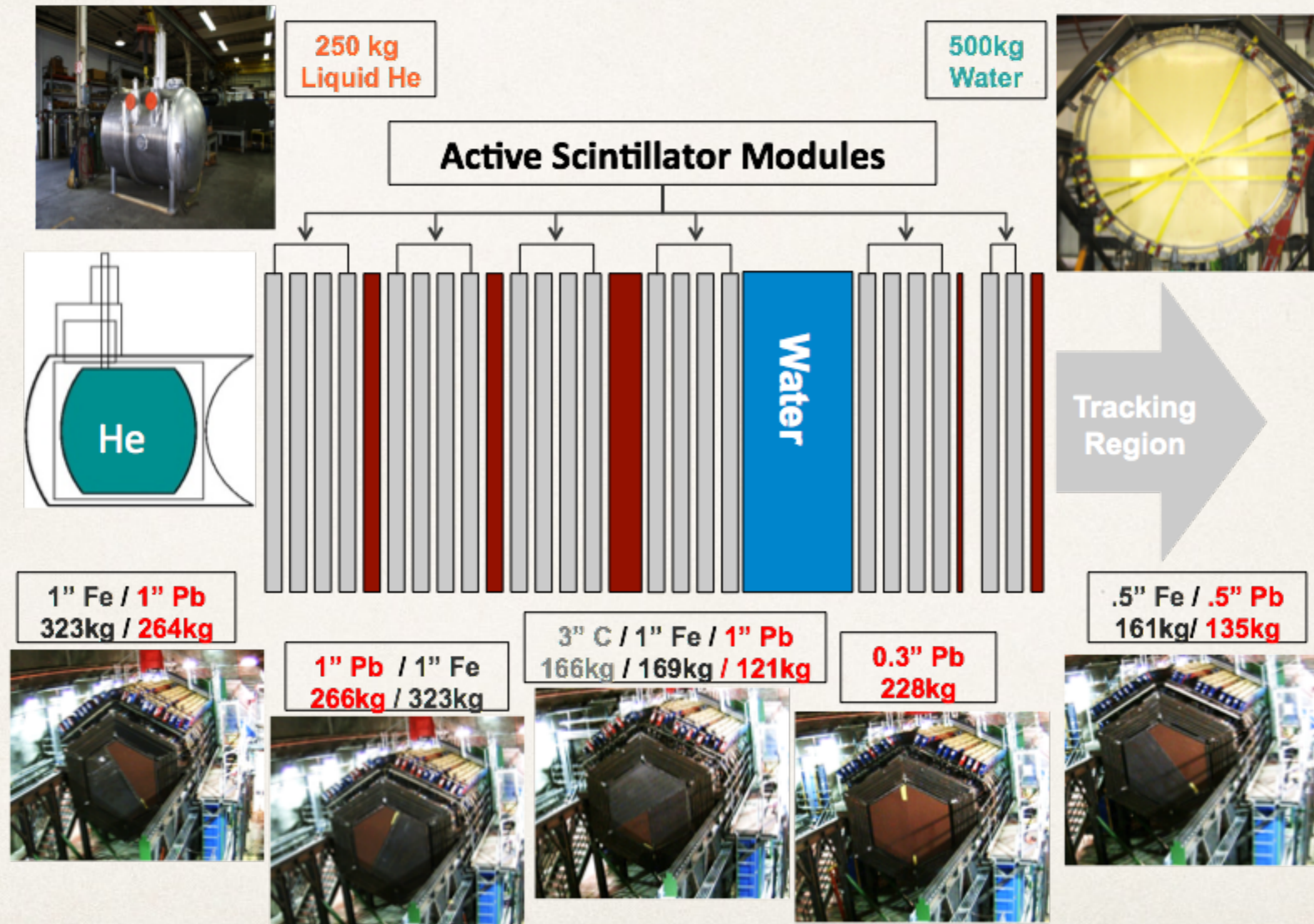
Uncertainty	GENIE Knob name	1 σ
CCQE Normalization (maintaining energy dependence)	NormCCQEenu	
NC Resonance Normalization	NormNCRES	$\pm 20\%$
M_A – shape only (CC Resonance Production)	MaCCRESshape	$\pm 10\%$
M_V – shape only (CC Resonance Production)	MvCCRESshape	$\pm 5\%$
M_A – shape only (NC Resonance Production)	MaNCRESshape	$\pm 10\%$
M_V – shape only (NC Resonance Production)	MvNCRESshape	$\pm 5\%$
Bodek-Yang parameter A_{HT}	AhtBY	$\pm 25\%$
Bodek-Yang parameter B_{HT}	BhtBY	$\pm 25\%$
Bodek-Yang parameter C_{V1u}	CV1uBY	$\pm 30\%$
Bodek-Yang parameter C_{V2u}	CV2uBY	$\pm 40\%$
Bodek-Yang parameter A_{HT} – shape only	AhtBYshape	$\pm 25\%$
Bodek-Yang parameter B_{HT} – shape only	BhtBYshape	$\pm 25\%$
Bodek-Yang parameter C_{V1u} – shape only	CV1uBYshape	$\pm 30\%$
Bodek-Yang parameter C_{V2u} – shape only	CV2uBYshape	$\pm 40\%$
Nu/Nubar CC cross section ration	RnubarCC	??
Coherent model M_A	MaCOHpi	$\pm 40\%$
Coherent model R_0	R0COHpi	$\pm 10\%$
Nuclear modifications to DIS	DISNuclMod	On/off
Fermi gas -> spectral function	CCQEMomDistroFGtoSF	On/off

GENIE model uncertainties (cont.)

Uncertainty	GENIE Knob name	1 σ
Pion mean free path	MFP_pi	$\pm 20\%$
Nucleon mean free path	MFP_N	$\pm 20\%$
Pion fates – absorption	FrAbs_pi	$\pm 30\%$
Pion fates – charge exchange	FrCEX_pi	$\pm 50\%$
Pion fates – Elastic	FrElas_pi	$\pm 10\%$
Pion fates – Inelastic	FrInel_pi	$\pm 40\%$
Pion fates – pion production	FrPiProd_pi	$\pm 20\%$
Nucleon fates – charge exchange	FrCEX_N	$\pm 50\%$
Nucleon fates – Elastic	FrElas_N	$\pm 30\%$
Nucleon fates – Inelastic	FrInel_N	$\pm 40\%$
Nucleon fates – absorption	FrAbs_N	$\pm 20\%$
Nucleon fates – pion production	FrPiProd_N	$\pm 20\%$
AGKY hadronization model – x_F distribution	AGKYxF1pi	$\pm 20\%$
Delta decay angular distribution	Theta_Delta2Npi	On/off
Resonance decay branching ratio to photon	RDecBR1gamma	$\pm 50\%$

Uncertainty	GENIE Knob name	1 σ
AGKY hadronization model – pion p_T distribution	AGKYpT1pi	$\pm 3\%$
Formation Zone	FormZone	$\pm 50\%$
Resonance decay branching ratio to eta	RDecBR1eta	$\pm 50\%$

MINERvA Nuclear targets

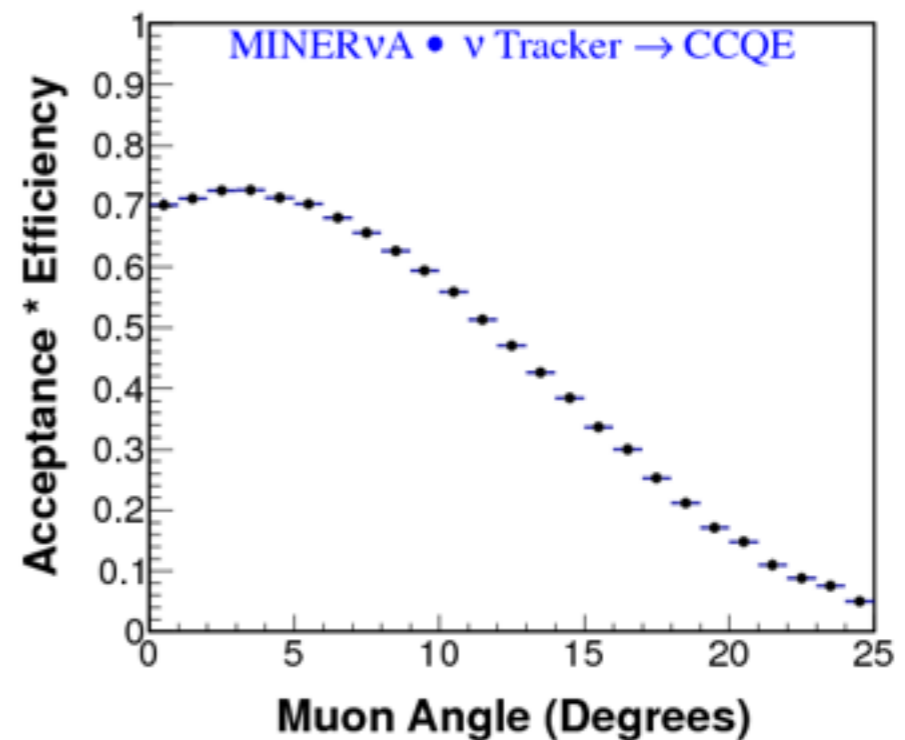
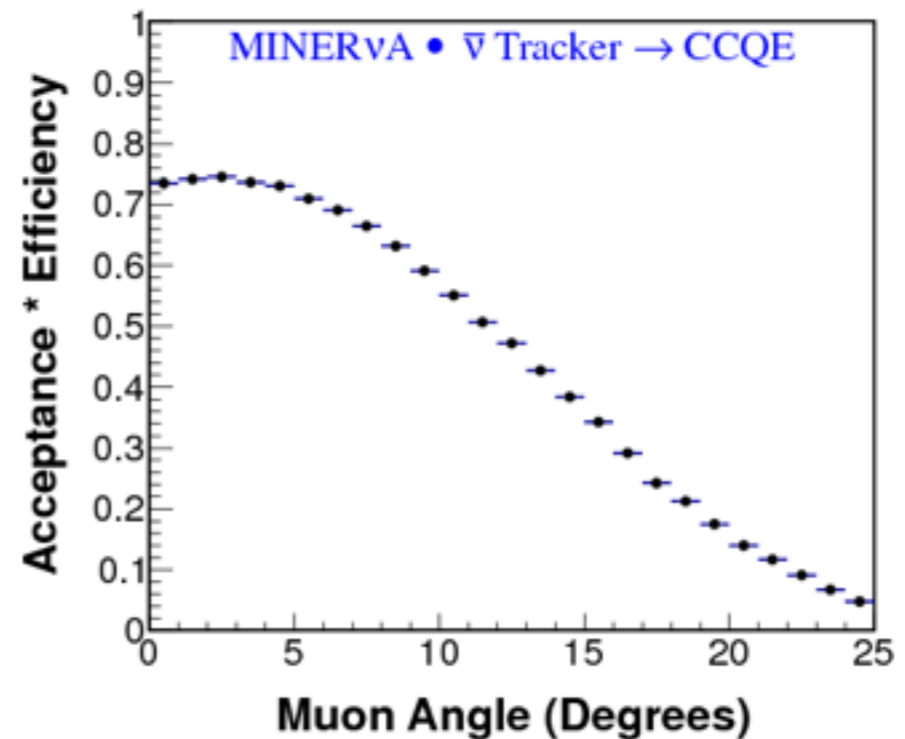
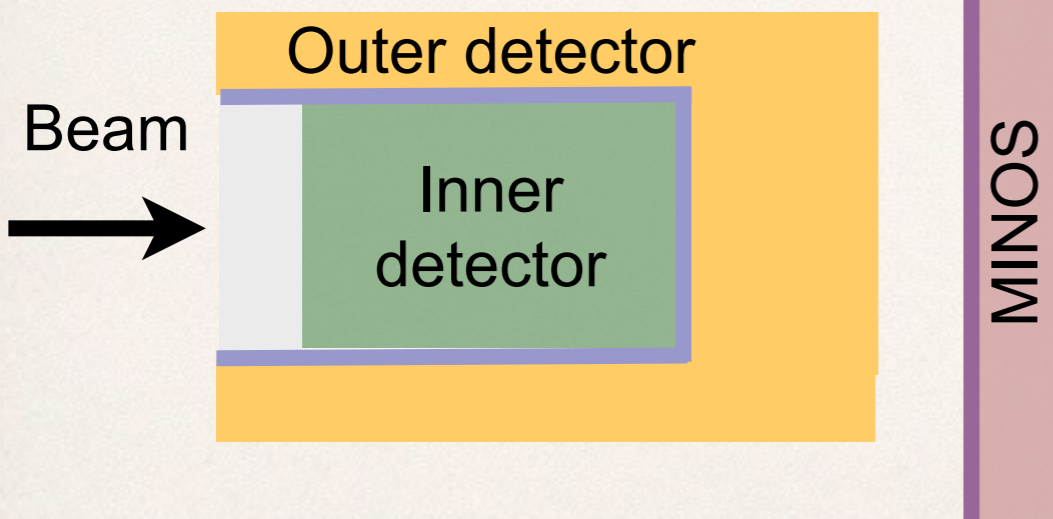
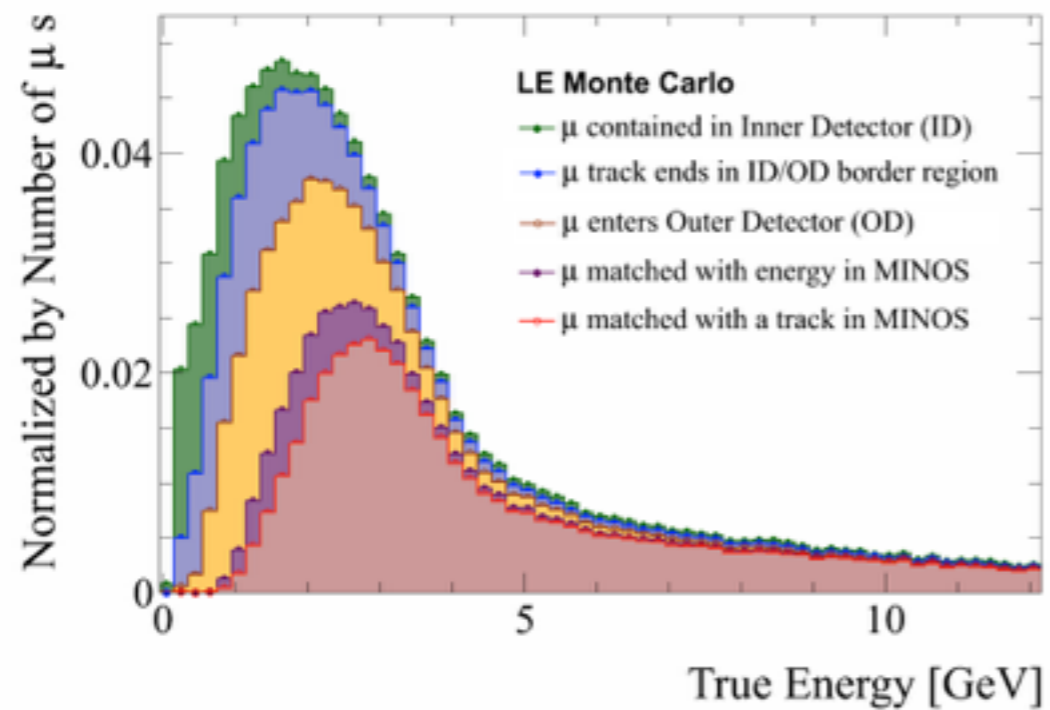


Our Monte Carlo: GENIE 2.6.2

Interaction models	CCQE: axial form-factor	Dipole with axial mass 0.99 GeV
	CCQE: Vector form-factors	BBBA05
	CCQE: Pseudoscalar form-factors	PCAC / Goldberger-Treiman
	Resonance and coherent	Rein-Seghal
	DIS	GRV94 / GRV98 with Bodek-Yang
	DIS and QEL charm	<i>Kovalenko, Sov.J.Nucl.Phys.52:934 (1990)</i>
	Nuclear effects	Nuclear model
FSI modeling		INTRANUKE-hA <i>(S. Dytman, AIP Conf Proc, 896, pp. 178-184 (2007))</i>
Hadronization model		AGKY – transitions between KNO-based and JETSET <i>T. Yang, AIP Conf. Proc.967:269-275 (2007)</i>
Formation zone		SKAT

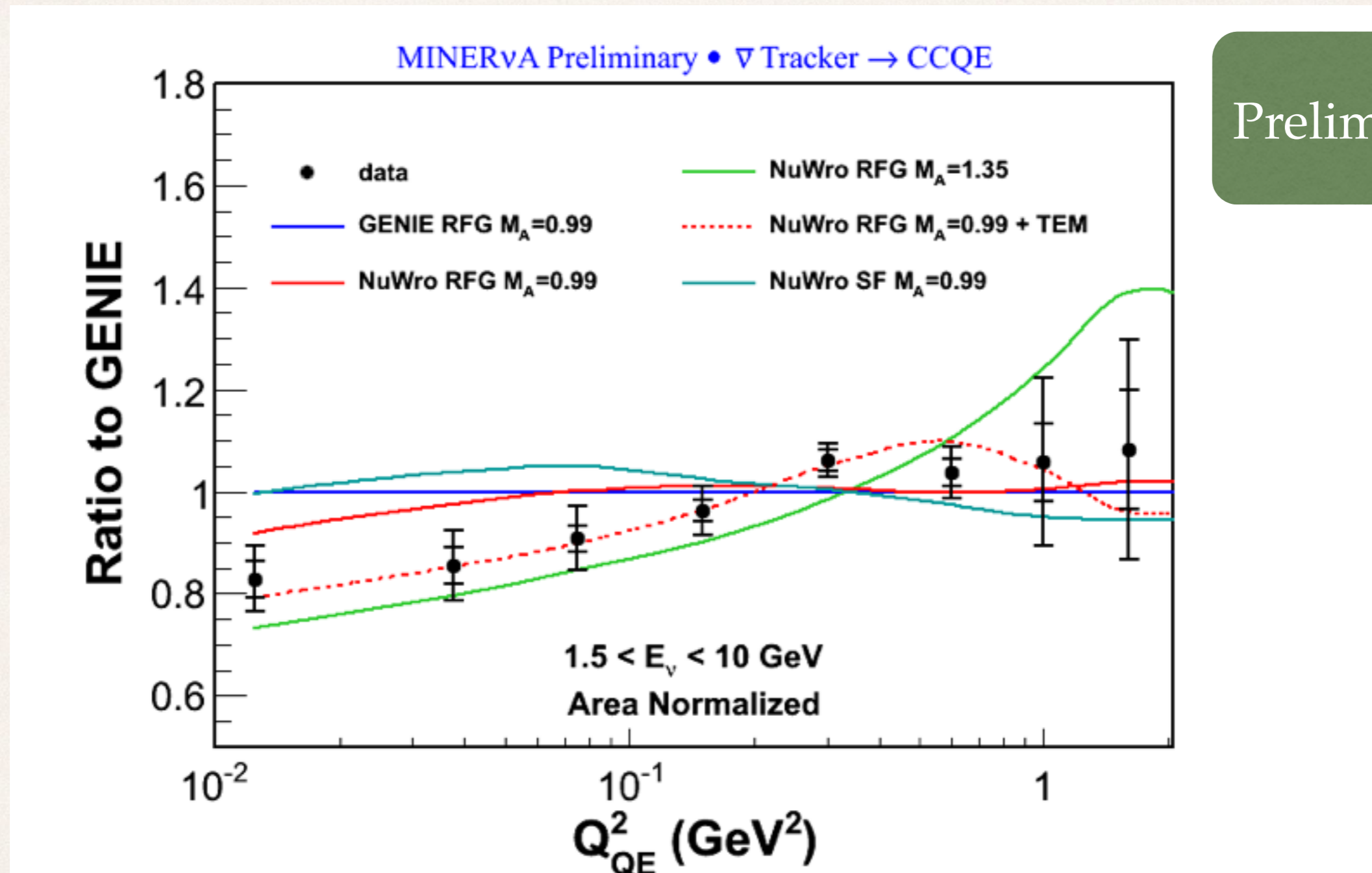
C. Andreopoulos, et al., NIM 288A, 614, 87 (2010)

MINOS-match requirement



- * MINOS-match requirement limits angular acceptance

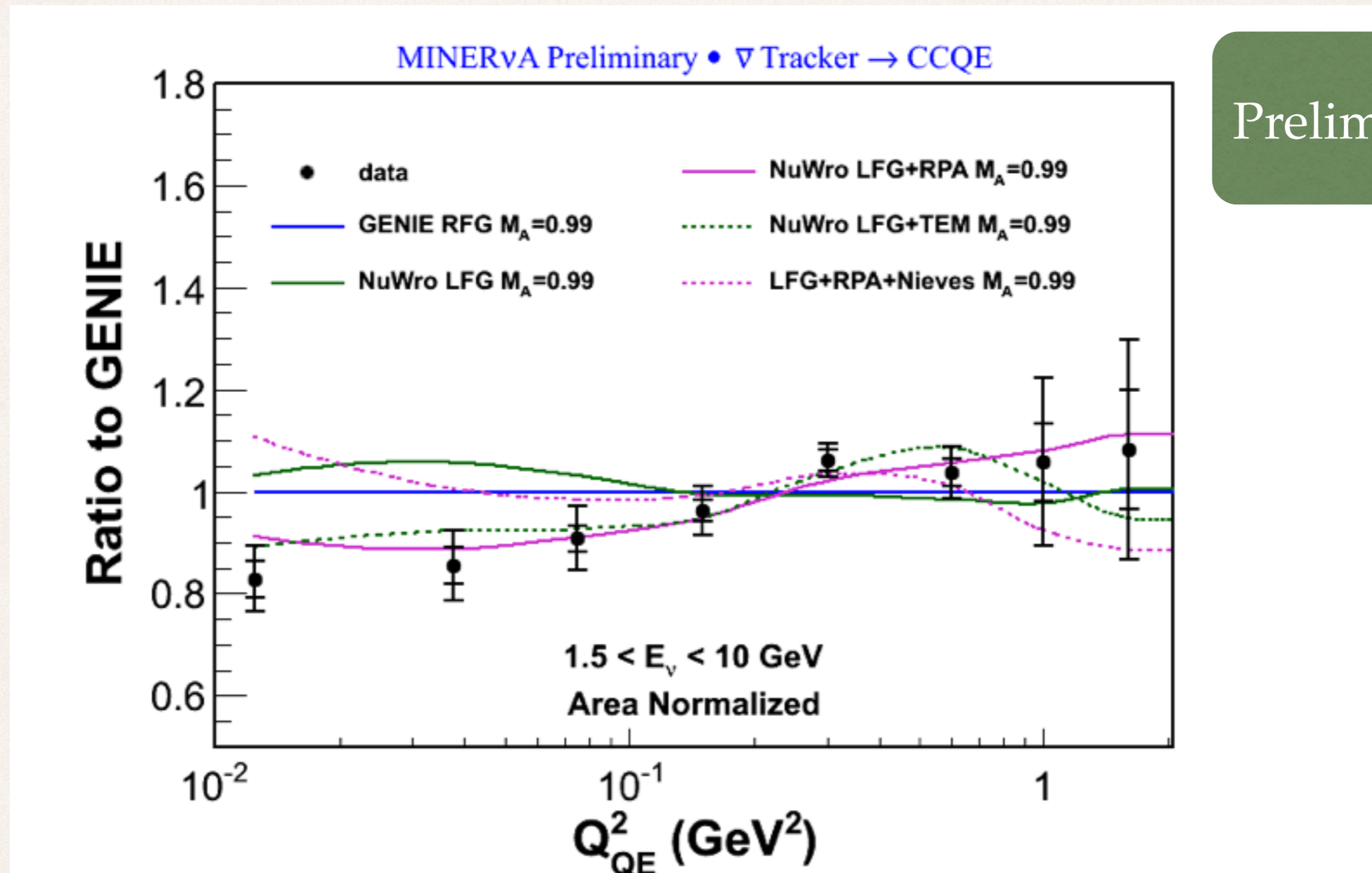
Antineutrino: shape-only ratio (RFG)



Preliminary

Data appears to favor **TEM**, suggesting initial-state nucleon-nucleon correlations

Antineutrino: shape-only ratio (LFG)



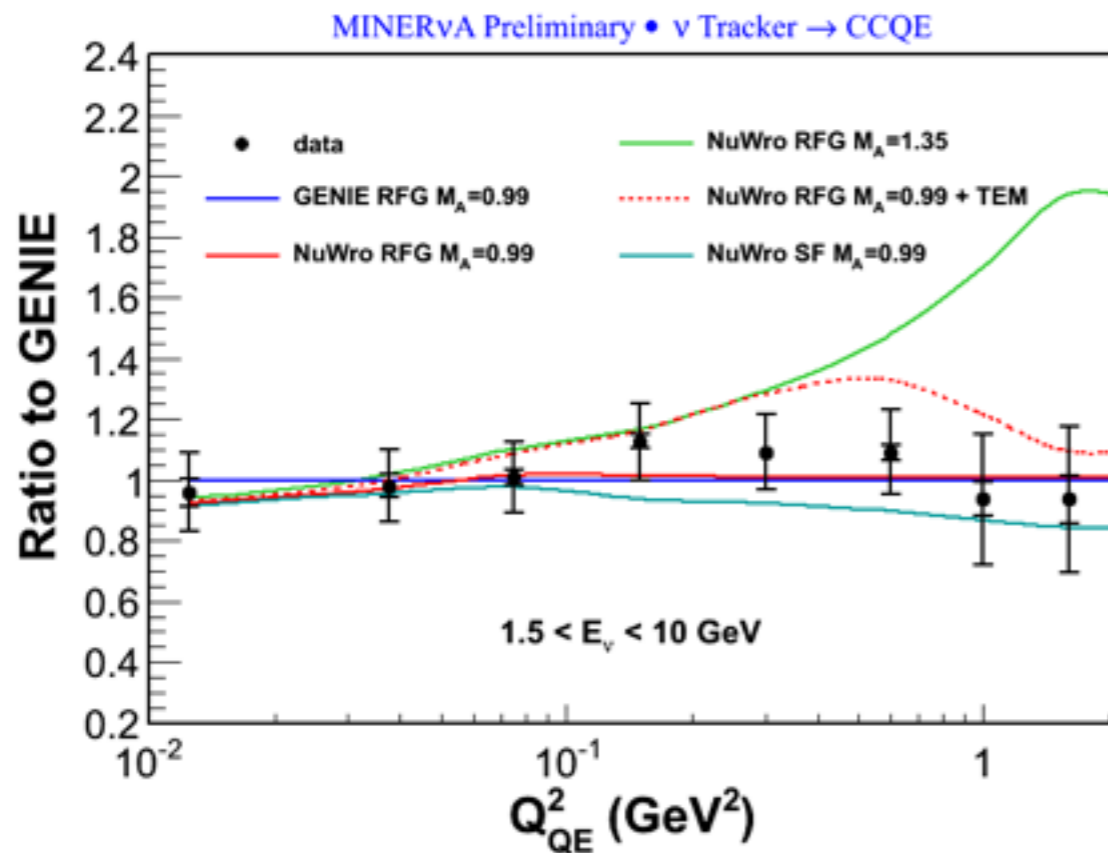
Again, the TEM model appears promising, as does RPA. However, we must also consider correlations between bins when evaluating the models

χ^2 for fits to antineutrino data

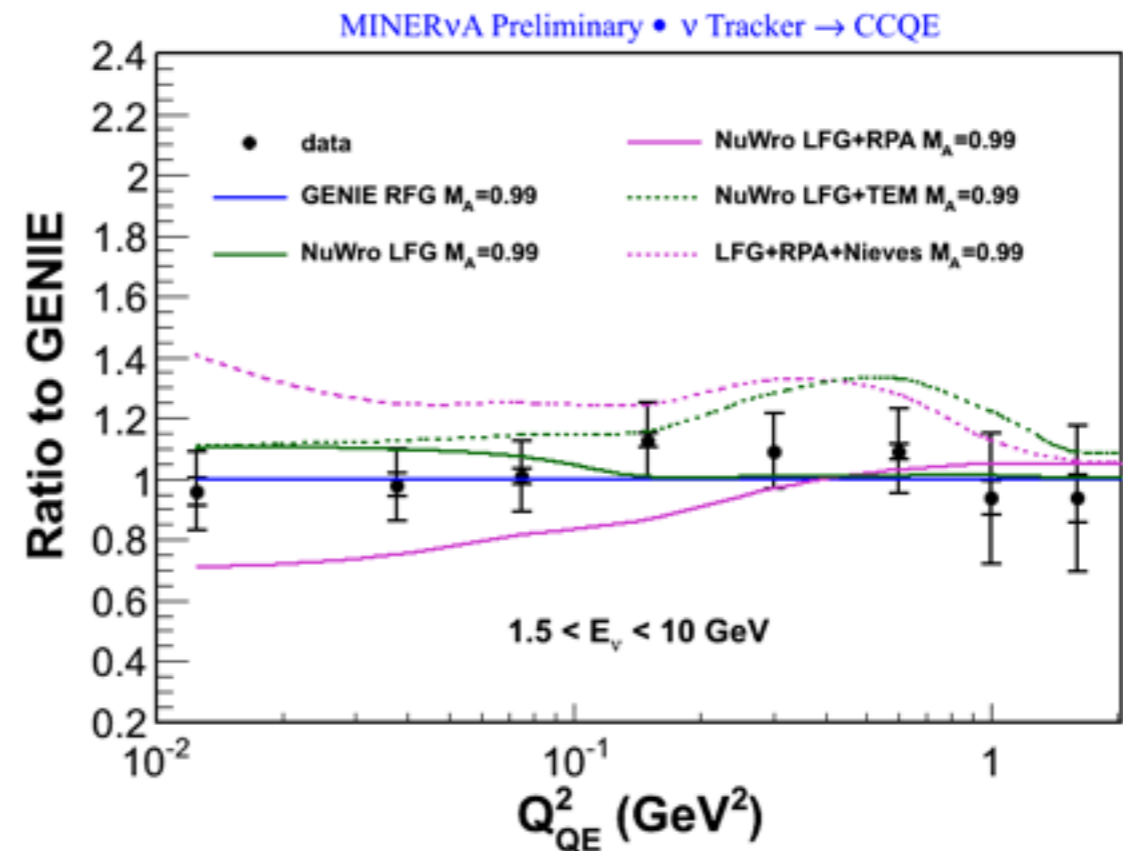
Preliminary

	Model	Rate $\chi^2/\text{d.o.f}$ (8 degrees of freedom)	Shape $\chi^2/\text{d.o.f}$ (7 degrees of freedom)
—	GENIE RFG $M_A=0.99$	2.2	2.44
—	NuWro RFG $M_A=0.99$	1.19	1.37
—	NuWro RFG $M_A=1.35$	1.98	1.27
⋯	NuWro RFG $M_A=0.99$ + TEM	0.667	0.447
—	NuWro SF $M_A=0.99$	1.89	2.61
—	NuWro LFG $M_A=0.99$	3.61	3.97
—	NuWro LFG + RPA $M_A=0.99$	0.771	0.953
⋯	NuWro LFG + TEM $M_A=0.99$	1.54	1.09
⋯	NuWro LFG + RPA + Nieves $M_A=0.99$	7.06	4.63

Rate model comparisons (ν)

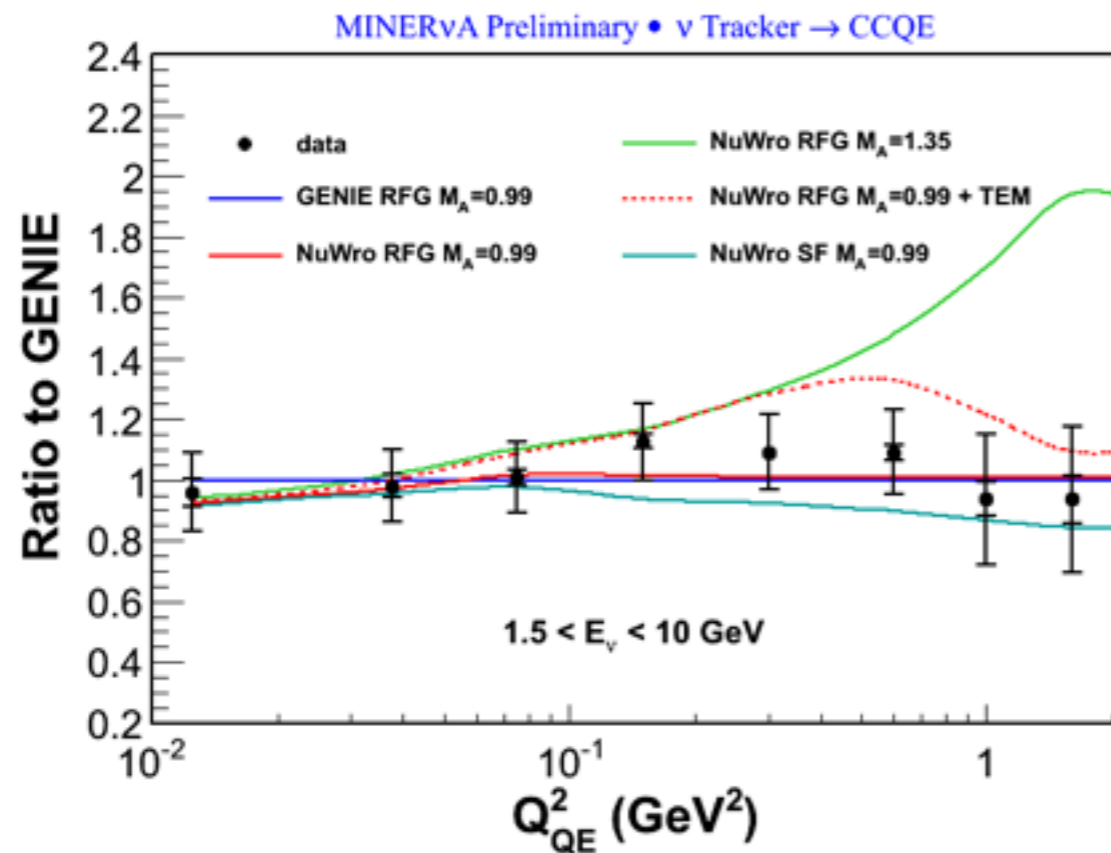


Preliminary



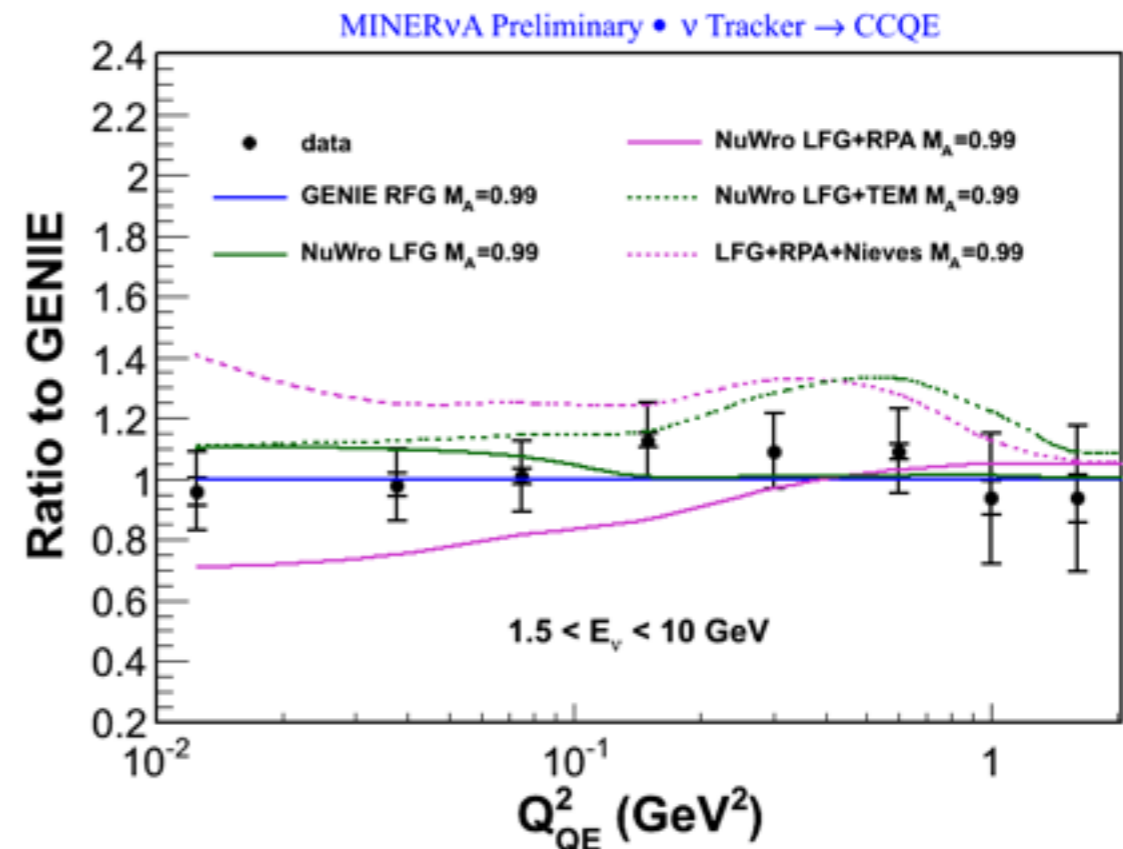
- GENIE RFG $M_A=0.99$
- NuWro RFG $M_A=0.99$
- NuWro RFG $M_A=1.35$
- ⋯ NuWro RFG $M_A=0.99+TEM$
- NuWro SF $M_A=0.99$
- NuWro LFG $M_A=0.99$
- NuWro LFG+RPA $M_A=0.99$
- ⋯ NuWro LFG+TEM $M_A=0.99$
- ⋯ NuWro LFG+RPA+Nieves $M_A=0.99$

Rate model comparisons (ν)



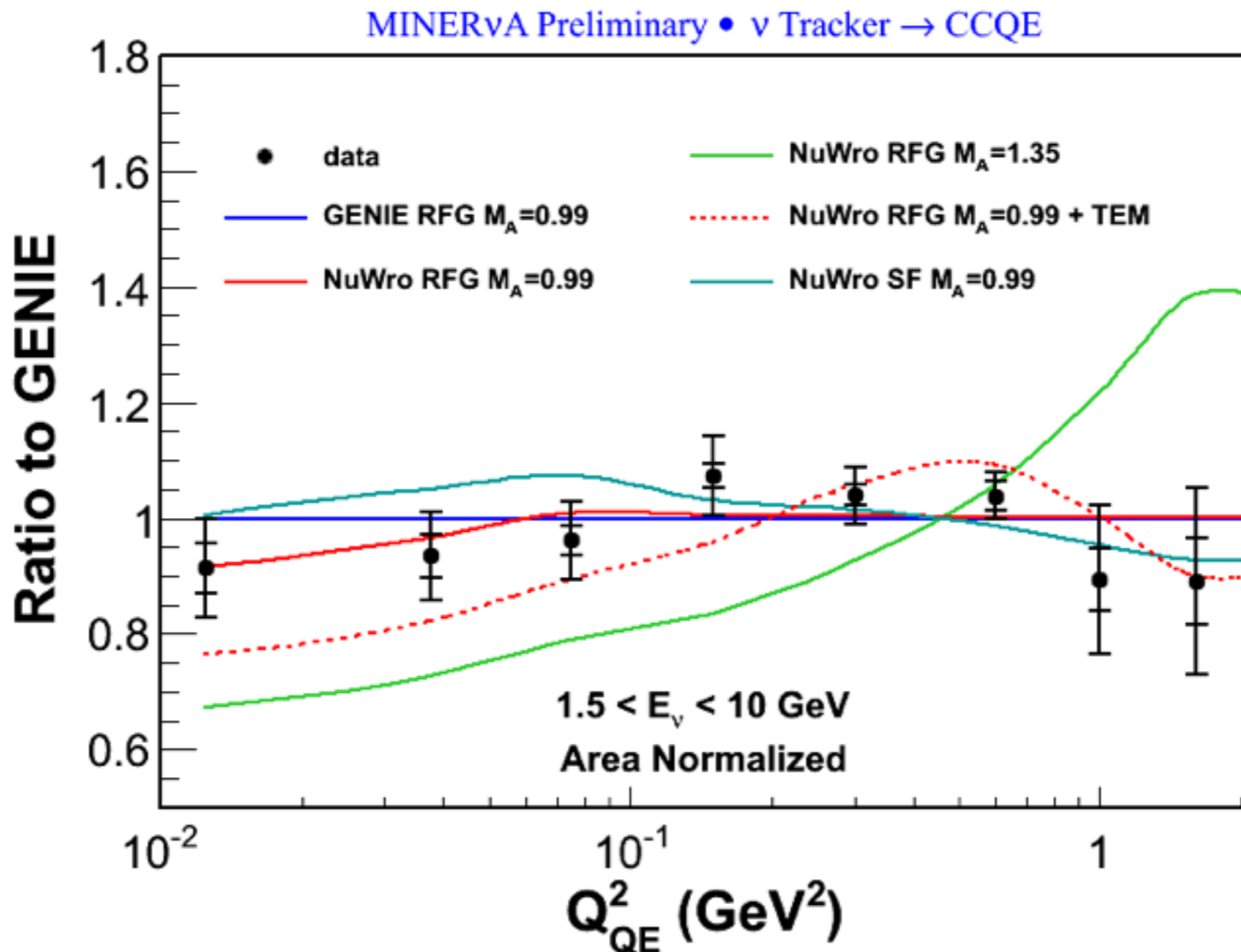
- ✦ Again, a **shape-only** comparison with models would avoid misleading results due to flux uncertainty

Preliminary



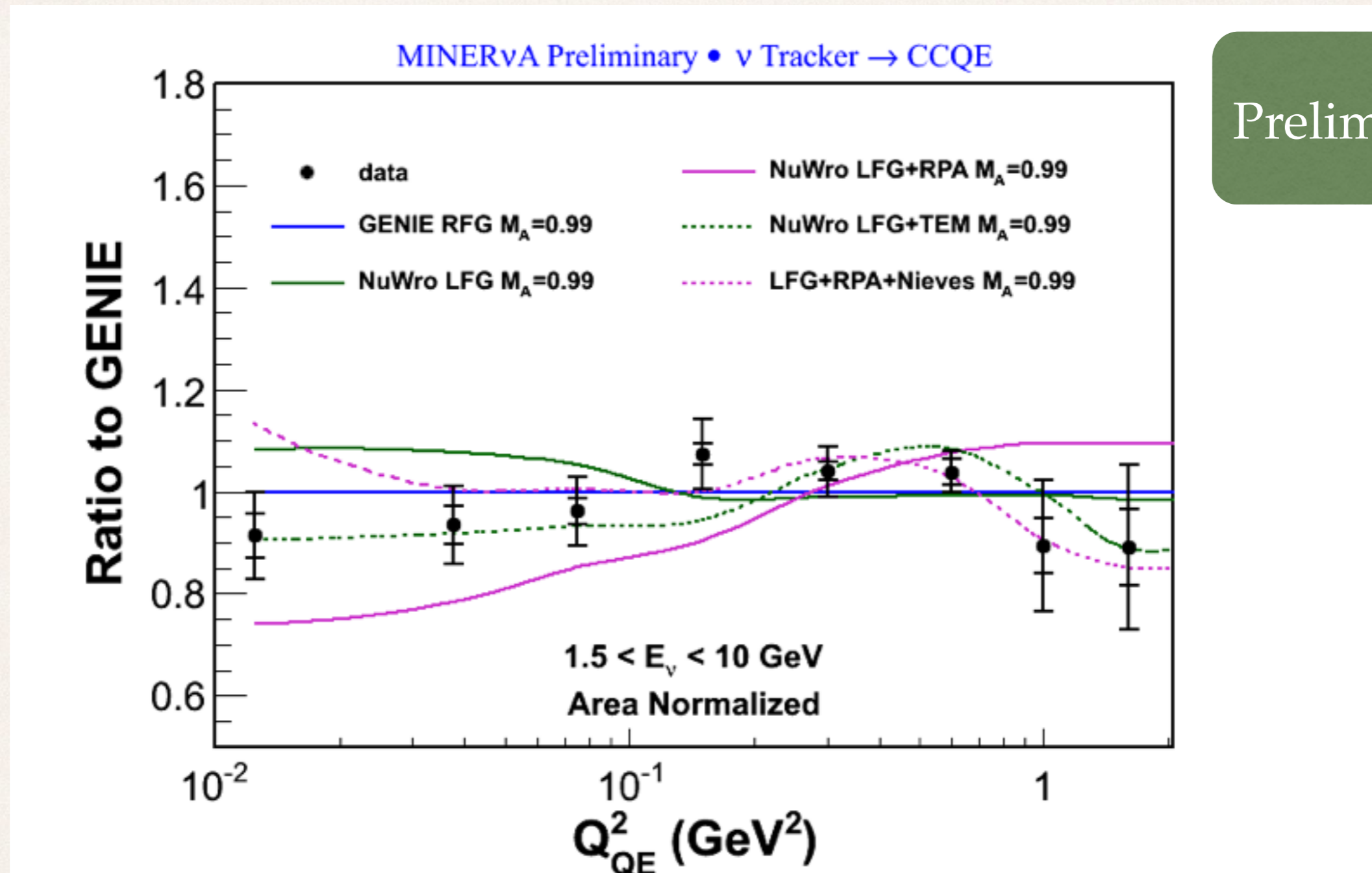
- GENIE RFG $M_A=0.99$
- NuWro RFG $M_A=0.99$
- NuWro RFG $M_A=1.35$
- ⋯ NuWro RFG $M_A=0.99 + \text{TEM}$
- NuWro SF $M_A=0.99$
- NuWro LFG $M_A=0.99$
- NuWro LFG+RPA $M_A=0.99$
- ⋯ NuWro LFG+TEM $M_A=0.99$
- ⋯ NuWro LFG+RPA+Nieves $M_A=0.99$

Neutrino: shape-only ratio (RFG)



Preliminary

Neutrino: shape-only ratio (LFG)



Again, the TEM model appears promising, but the χ^2 will be able to tell us about how the models compare when we take correlations into account

χ^2 for fits to neutrino data

Preliminary

	Model	Rate χ^2 /d.o.f (8 degrees of freedom)	Shape χ^2 /d.o.f (7 degrees of freedom)
—	GENIE RFG $M_A=0.99$	1.86	2.06
—	NuWro RFG $M_A=0.99$	1.47	1.66
—	NuWro RFG $M_A=1.35$	3.38	1.99
⋯	NuWro RFG $M_A=0.99$ + TEM	2.92	2.26
—	NuWro SF $M_A=0.99$	2.64	3.43
—	NuWro LFG $M_A=0.99$	4.77	5.3
—	NuWro LFG + RPA $M_A=0.99$	1.73	1.83
⋯	NuWro LFG + TEM $M_A=0.99$	3.53	2.75
⋯	NuWro LFG + RPA + Nieves $M_A=0.99$	5.49	4.1

χ^2 for $\bar{\nu}$ and ν rates, combined

Preliminary

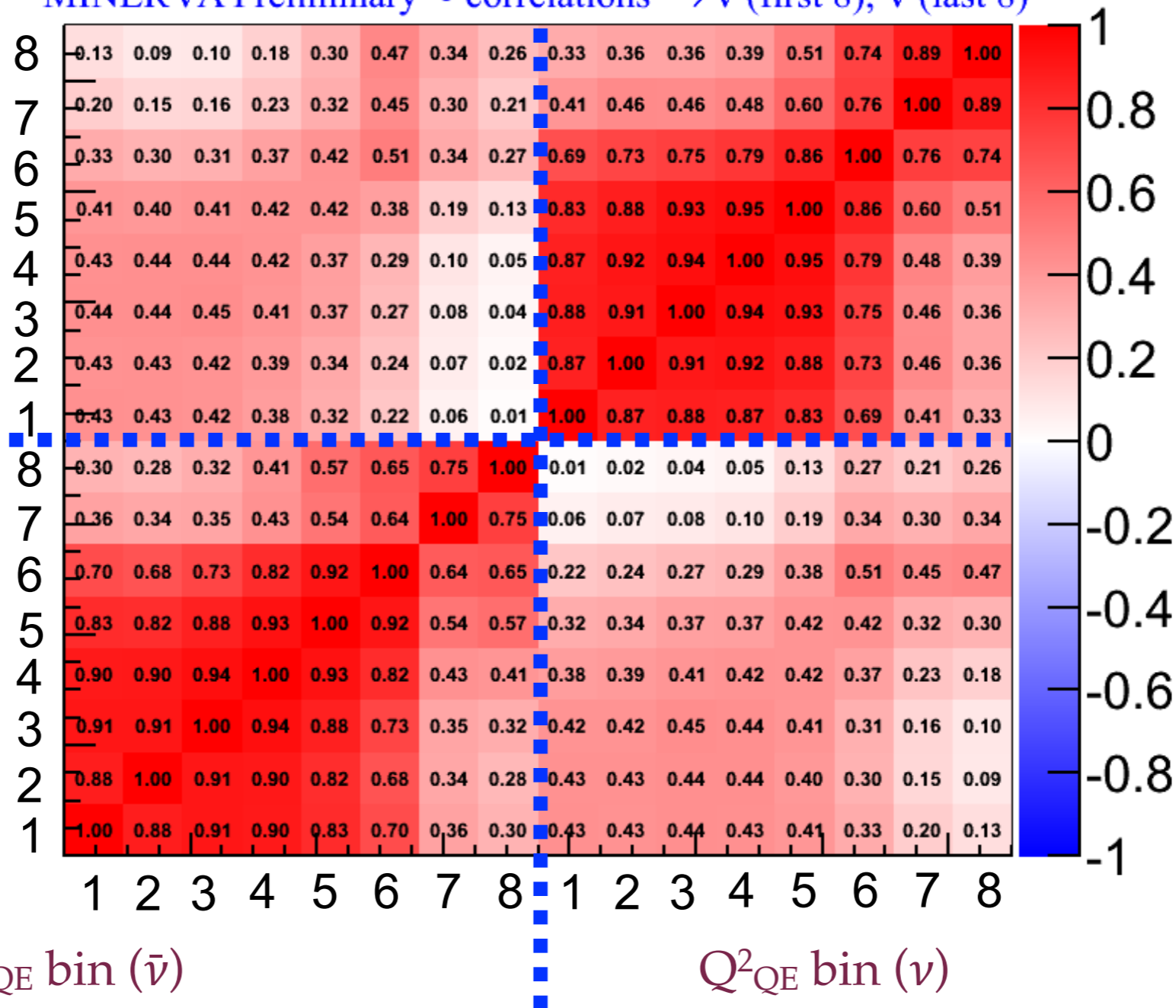
	Model	Combined rate $\chi^2/\text{d.o.f}$ (16 degrees of freedom)
—	GENIE RFG $M_A=0.99$	2.04
—	NuWro RFG $M_A=0.99$	1.53
—	NuWro RFG $M_A=1.35$	3.14
⋯	NuWro RFG $M_A=0.99$ + TEM	1.92
—	NuWro SF $M_A=0.99$	2.22
—	NuWro LFG $M_A=0.99$	3.88
—	NuWro LFG + RPA $M_A=0.99$	1.93
⋯	NuWro LFG + TEM $M_A=0.99$	2.59
⋯	NuWro LFG + RPA + Nieves $M_A=0.99$	5.79

Correlation matrix - absolute

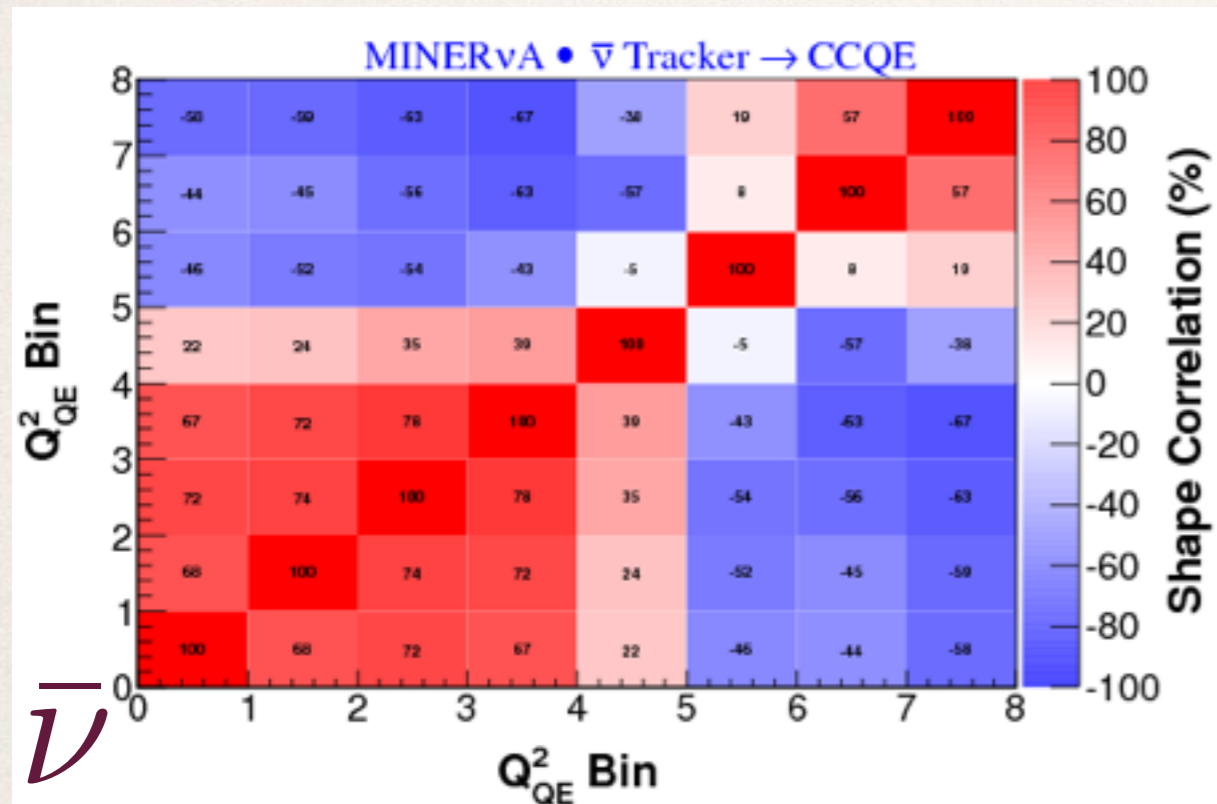
Q^2_{QE} bin (ν)

Q^2_{QE} bin ($\bar{\nu}$)

MINER νA Preliminary • correlations $\rightarrow \bar{\nu}$ (first 8), ν (last 8)

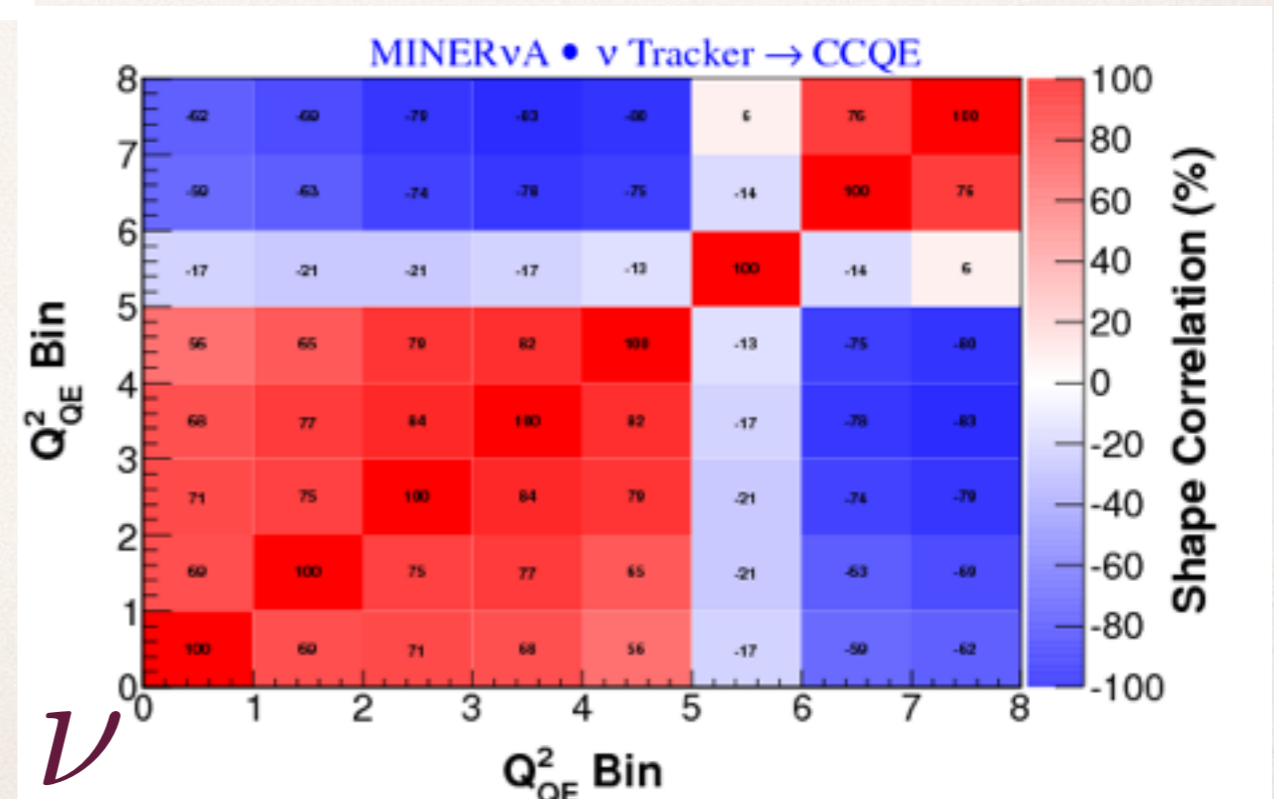


Correlation matrices: shape-only

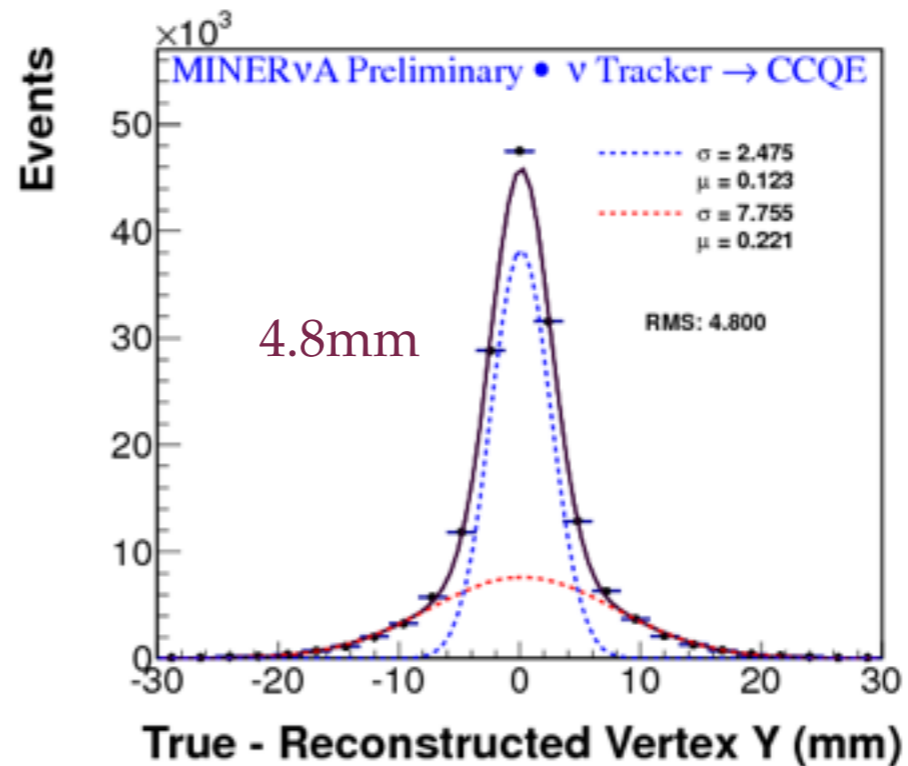
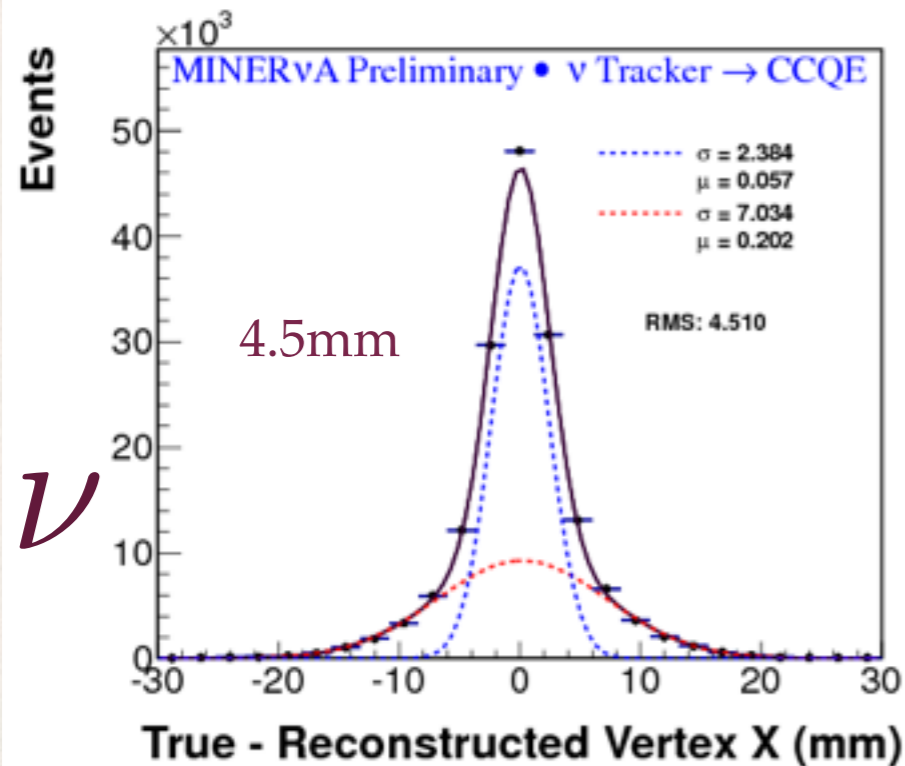
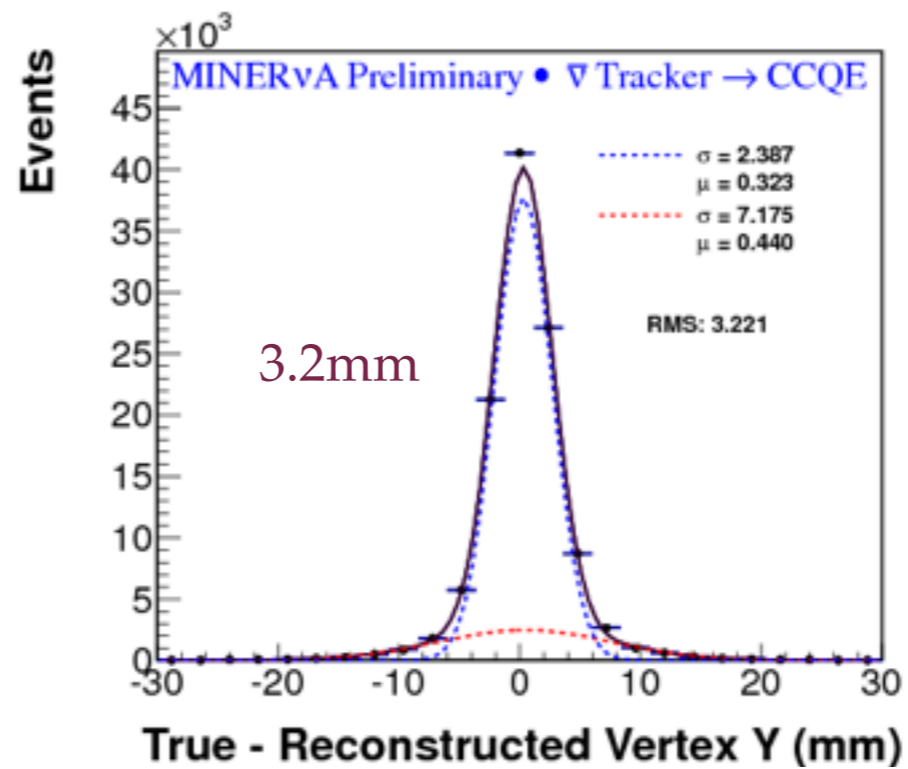
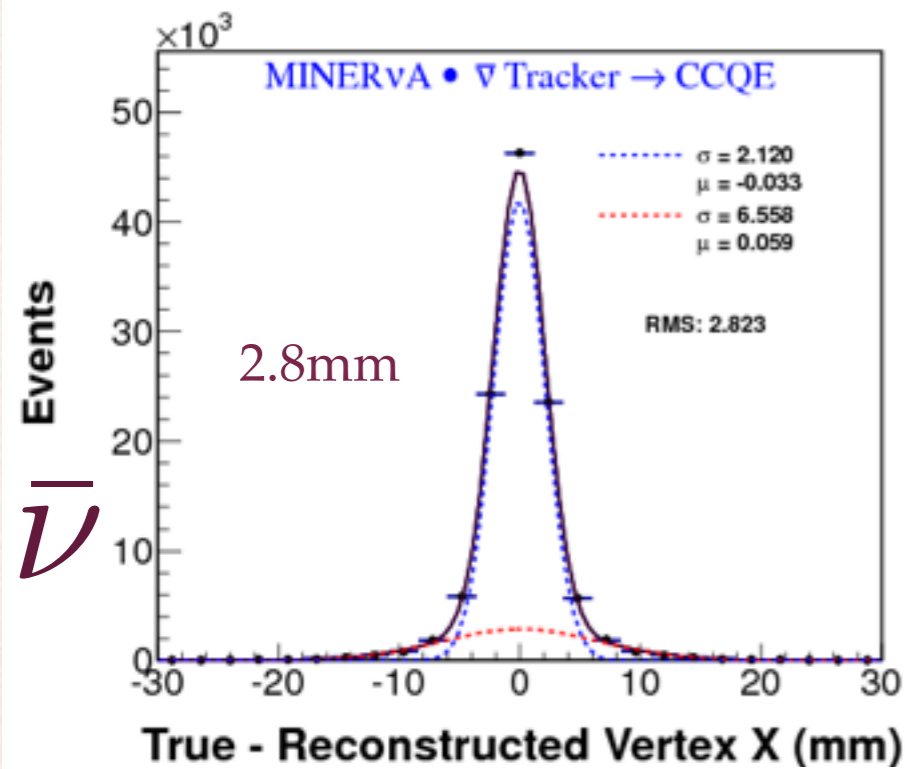


- * Red indicates positive correlation
- * Blue indicates negative correlation

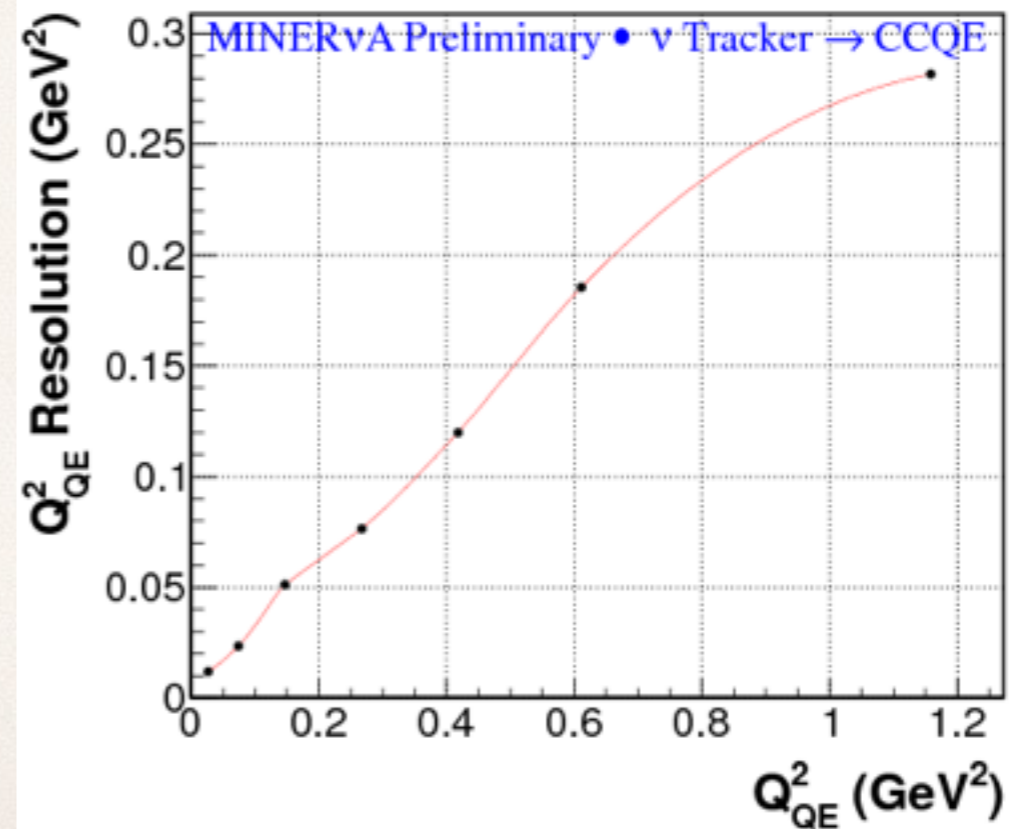
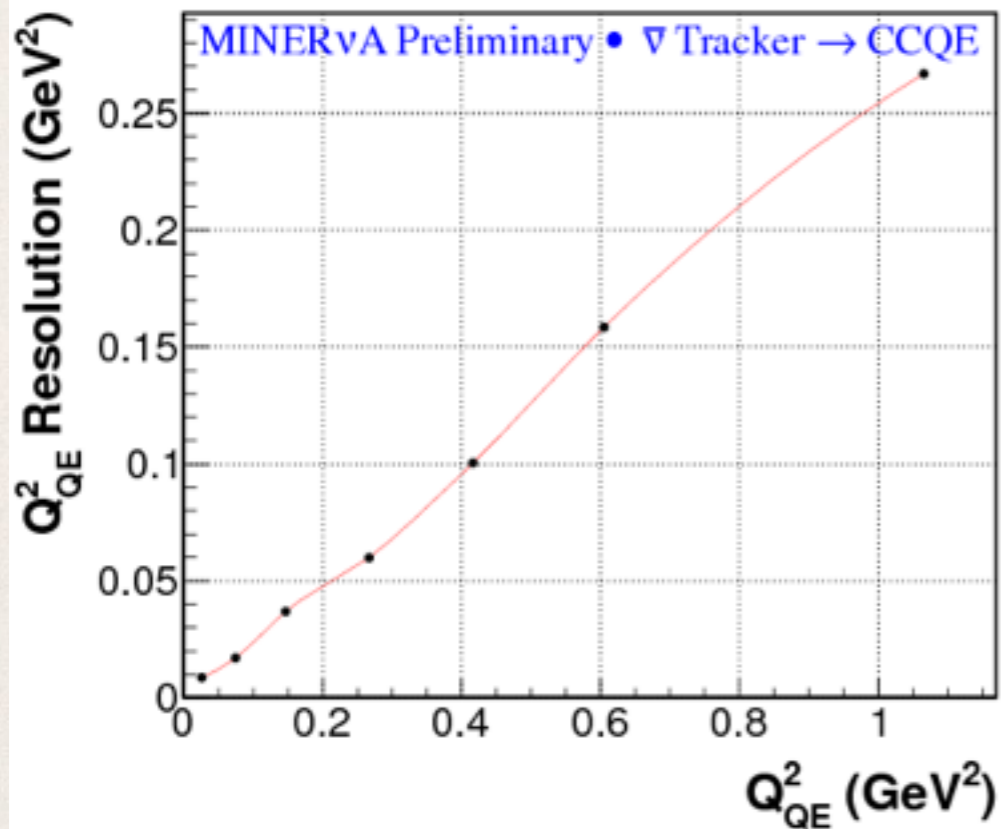
- * The strong positive and negative correlations between bins can lead to surprisingly low χ^2/NDF when data is compared to models that at first glance seem poor fits
- * Conversely, a model that appears to be a good fit can have a poor χ^2/NDF



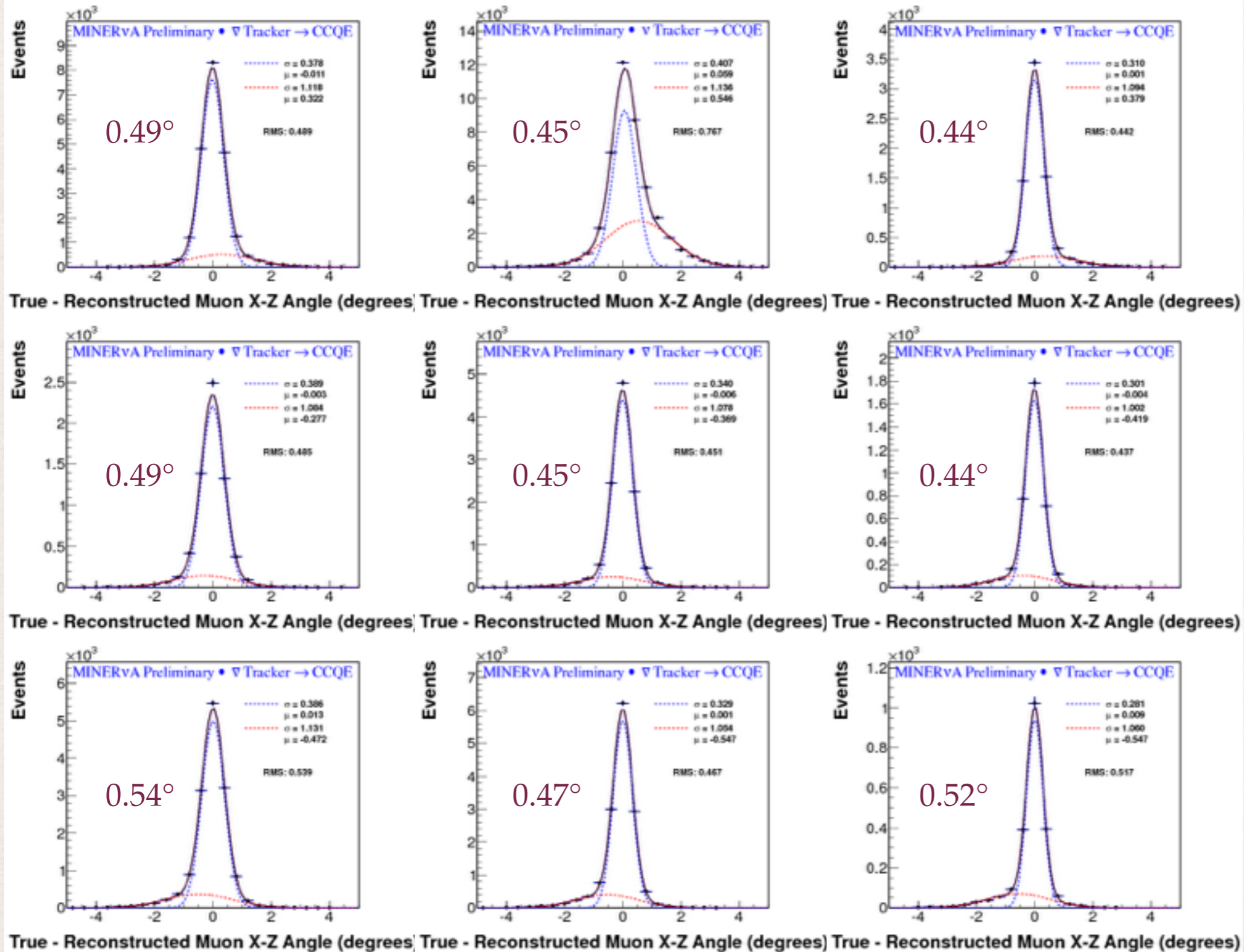
Vertex resolution < 5mm



$$Q^2_{QE} \text{ resolution} \sim Q^2_{QE}/4$$



Angular resolution: x-z plane, $\bar{\nu}$

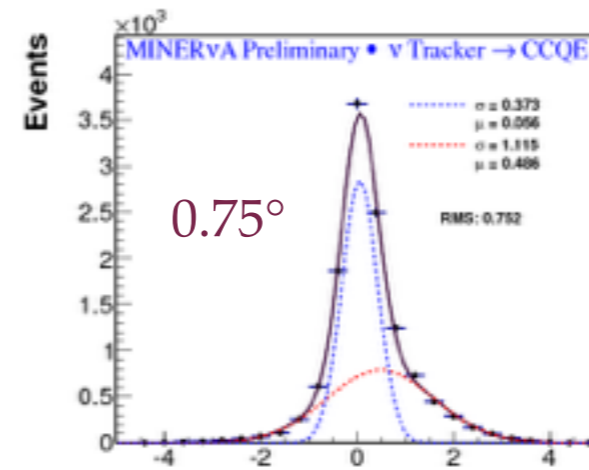
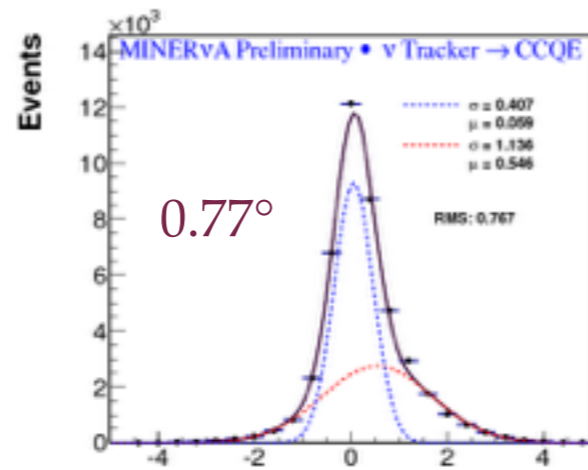
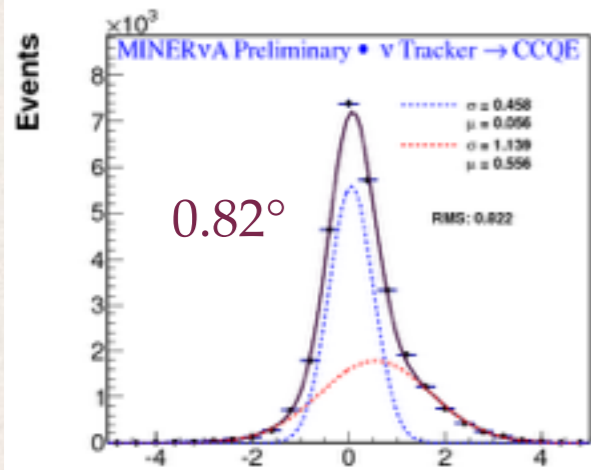


$E_\mu < 3\text{ GeV}$,
 $3 - 5\text{ GeV}$,
 $> 5\text{ GeV}$

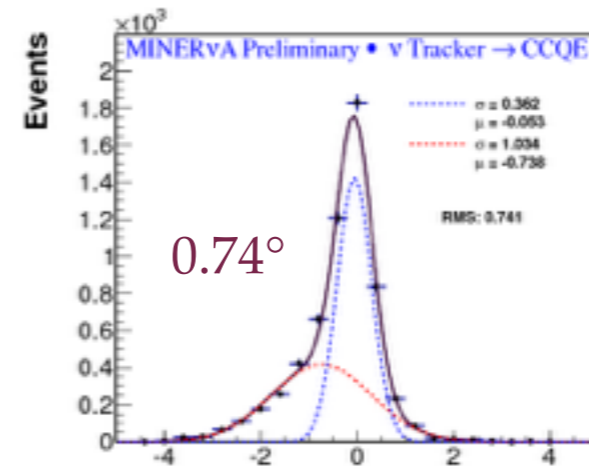
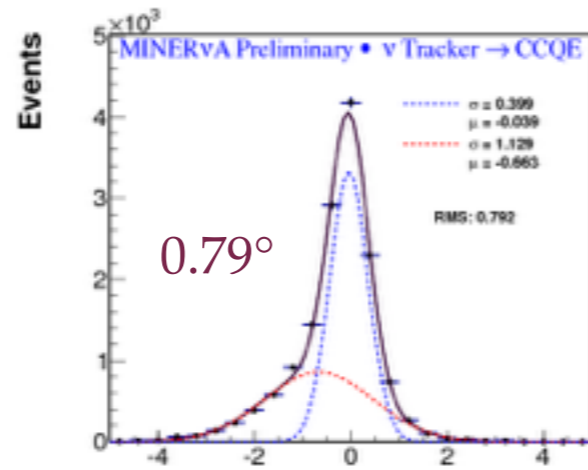
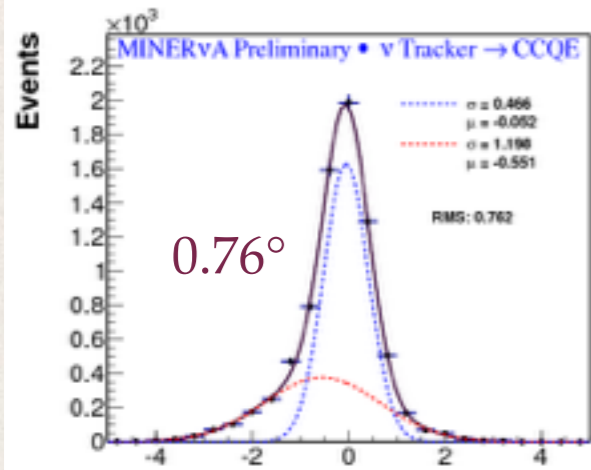


$\theta_{\mu,x} < 1^\circ$,
 $1 - 4^\circ$,
 $> 4^\circ$

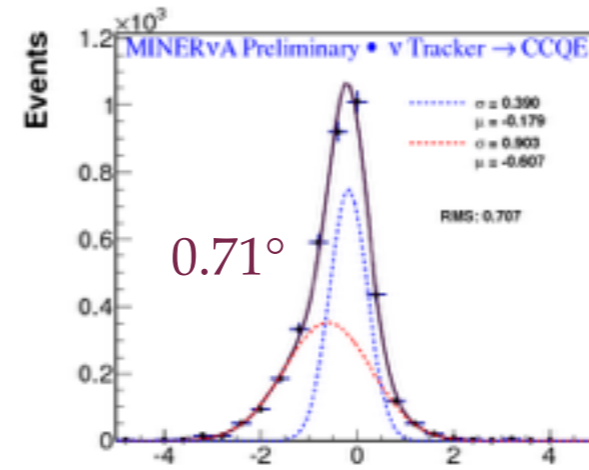
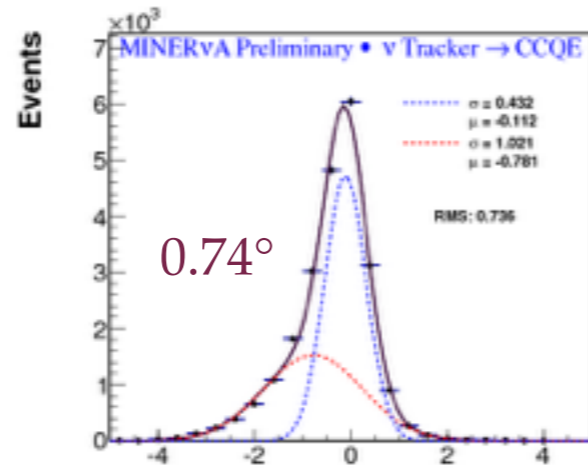
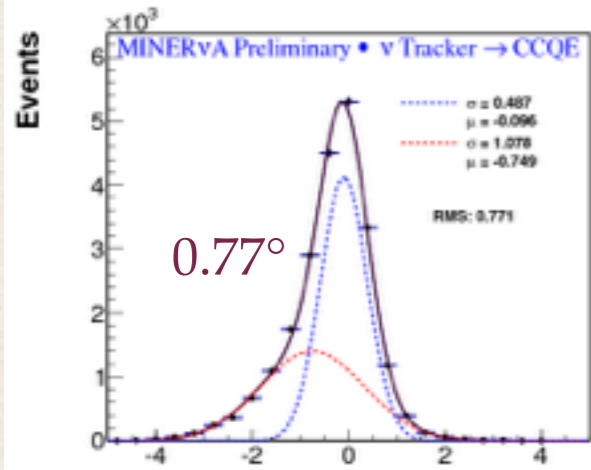
Angular resolution: x-z plane, ν



True - Reconstructed Muon X-Z Angle (degrees) True - Reconstructed Muon X-Z Angle (degrees) True - Reconstructed Muon X-Z Angle (degrees)



True - Reconstructed Muon X-Z Angle (degrees) True - Reconstructed Muon X-Z Angle (degrees) True - Reconstructed Muon X-Z Angle (degrees)



True - Reconstructed Muon X-Z Angle (degrees) True - Reconstructed Muon X-Z Angle (degrees) True - Reconstructed Muon X-Z Angle (degrees)

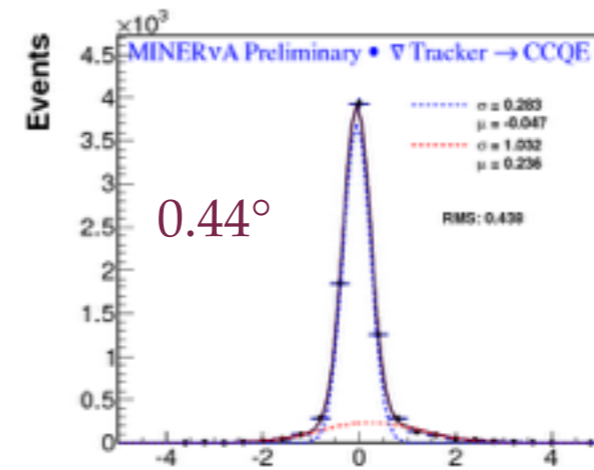
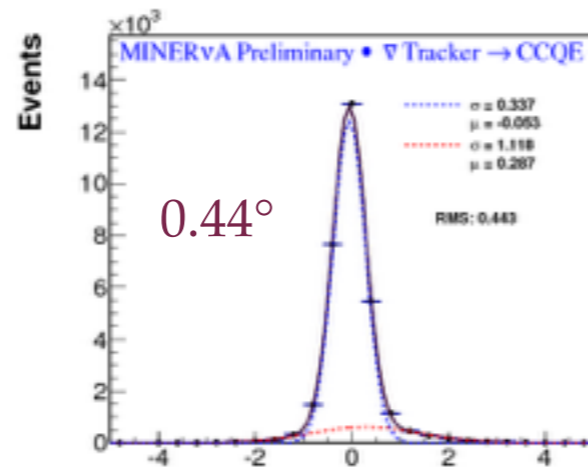
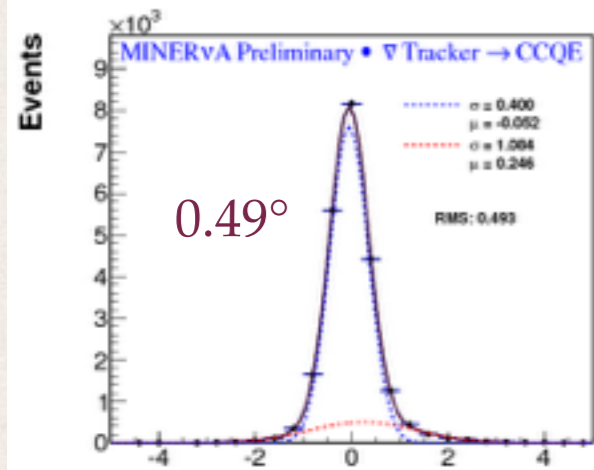


$E_\mu < 3\text{ GeV}$,
 $3 - 5\text{ GeV}$,
 $> 5\text{ GeV}$

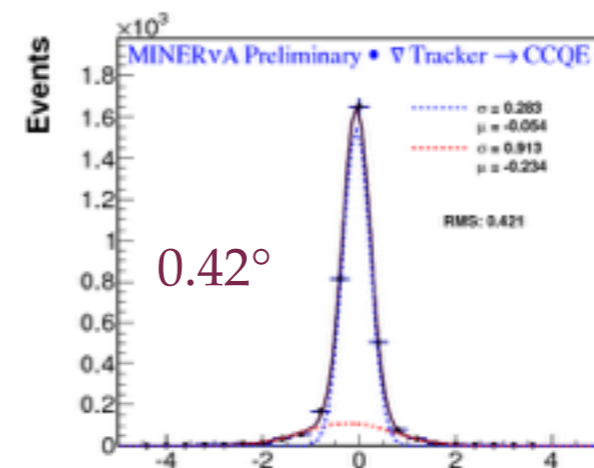
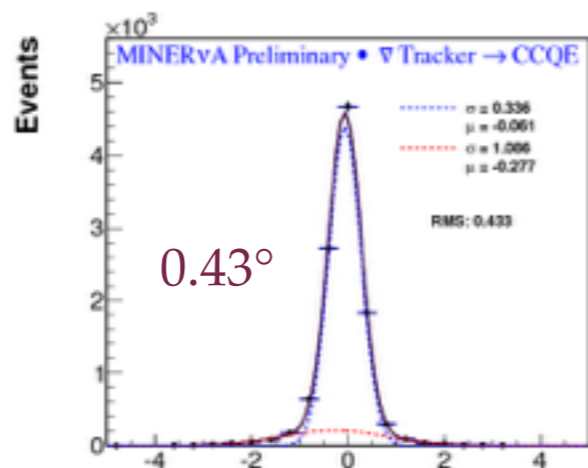
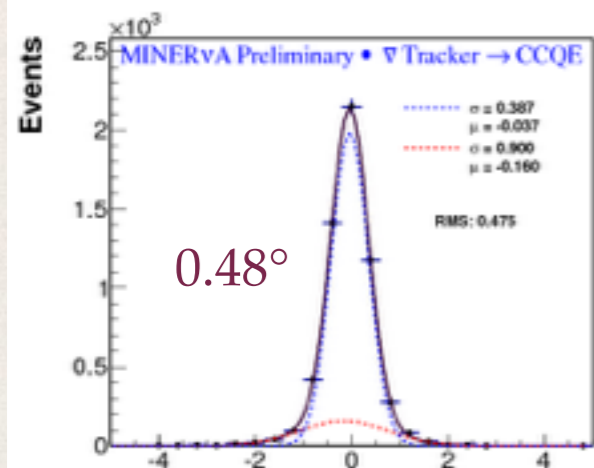


$\theta_{\mu,x} < 1^\circ$,
 $1 - 4^\circ$,
 $> 4^\circ$

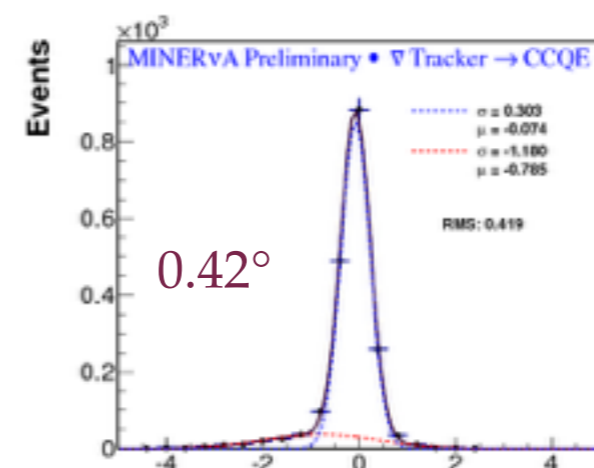
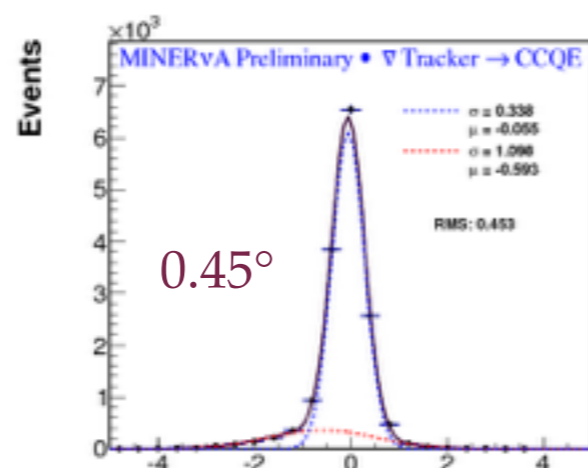
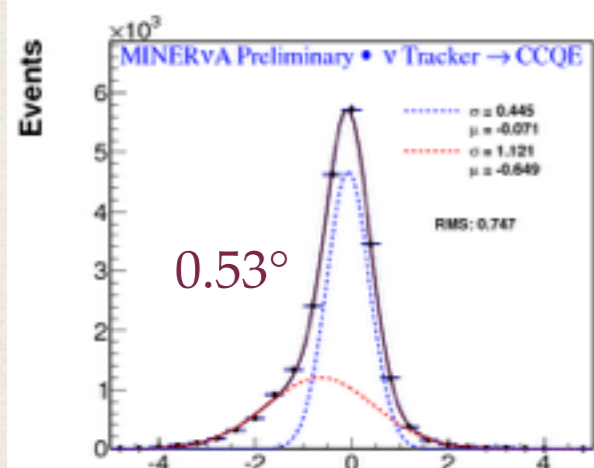
Angular resolution: y - z plane, $\bar{\nu}$



True - Reconstructed Muon Y-Z Angle (degrees) True - Reconstructed Muon Y-Z Angle (degrees) True - Reconstructed Muon Y-Z Angle (degrees)



True - Reconstructed Muon Y-Z Angle (degrees) True - Reconstructed Muon Y-Z Angle (degrees) True - Reconstructed Muon Y-Z Angle (degrees)



True - Reconstructed Muon Y-Z Angle (degrees) True - Reconstructed Muon Y-Z Angle (degrees) True - Reconstructed Muon Y-Z Angle (degrees)



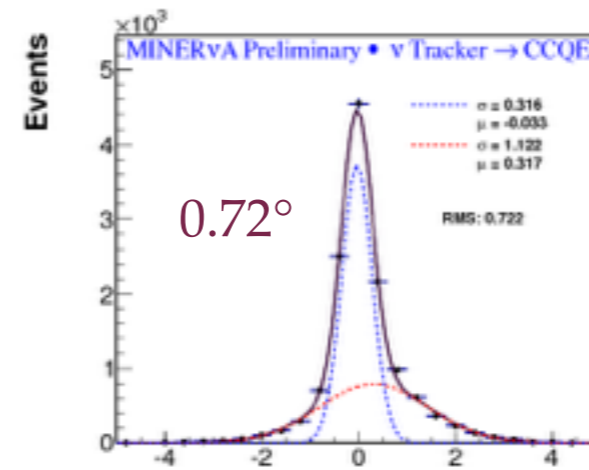
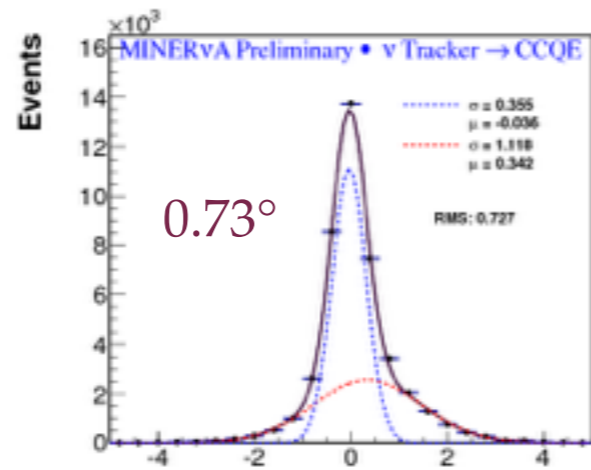
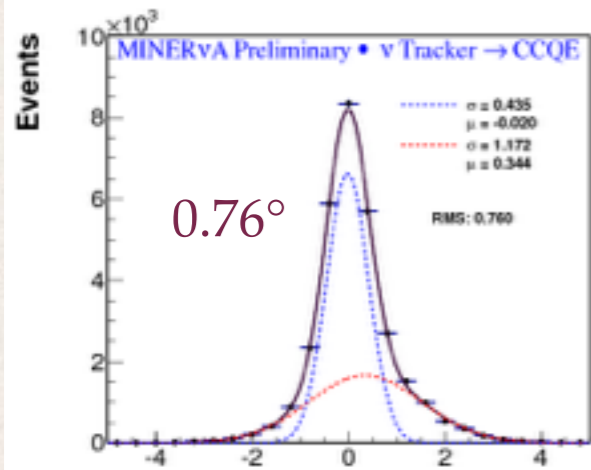
$E_\mu < 3\text{GeV}$,
 $3 - 5 \text{ GeV}$,
 $> 5\text{GeV}$



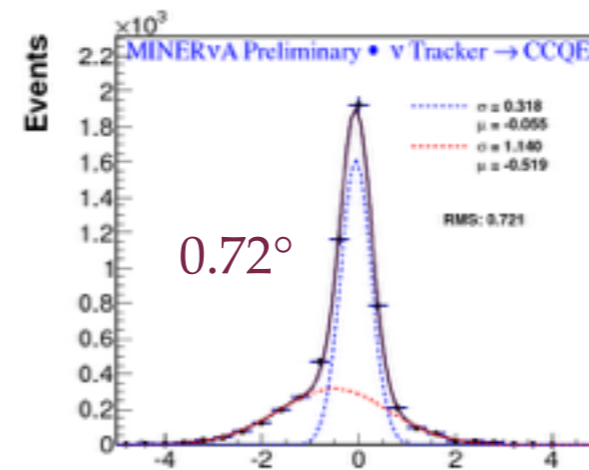
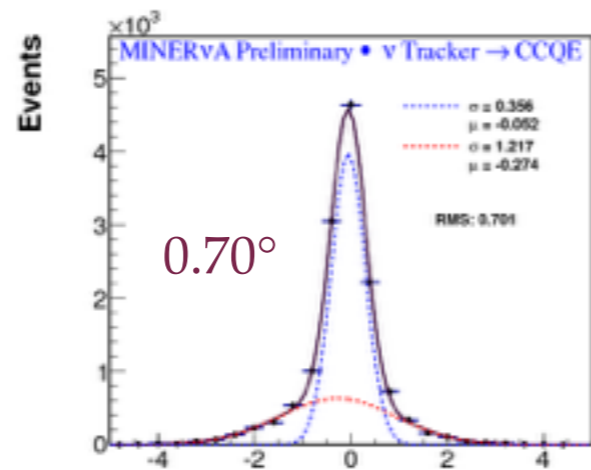
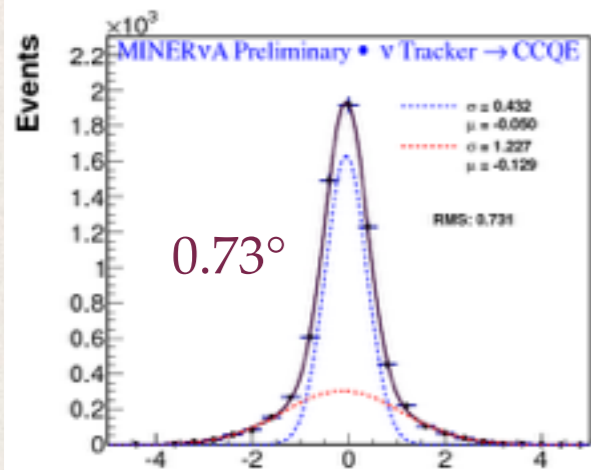
$\theta_{\mu,y} < 1^\circ$,
 $1 - 4^\circ$,
 $> 4^\circ$

Note: the beam is
in the y - z plane,
slightly
misaligned
from the z axis

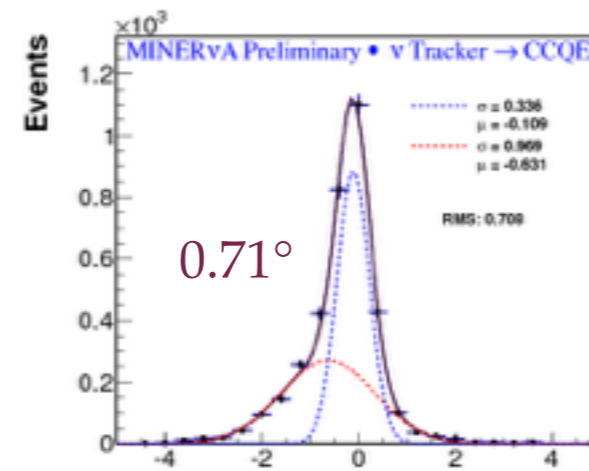
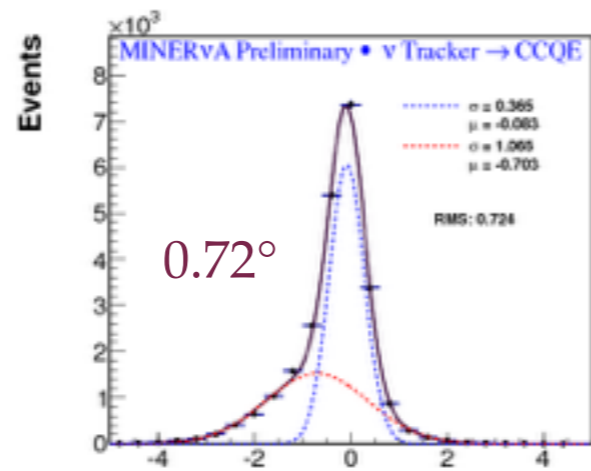
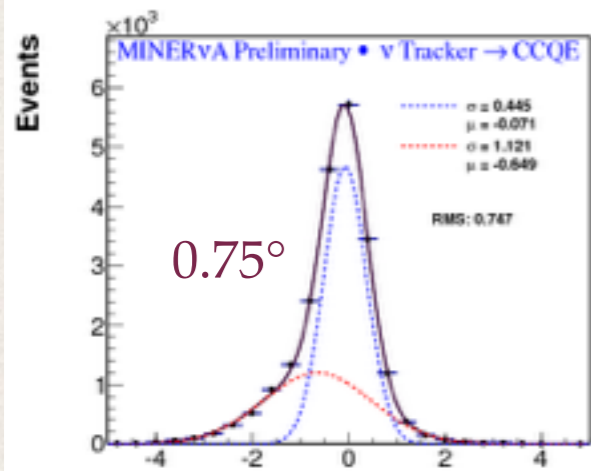
Angular resolution: y-z plane, ν



True - Reconstructed Muon Y-Z Angle (degrees) True - Reconstructed Muon Y-Z Angle (degree: True - Reconstructed Muon Y-Z Angle (degrees)



True - Reconstructed Muon Y-Z Angle (degrees) True - Reconstructed Muon Y-Z Angle (degree: True - Reconstructed Muon Y-Z Angle (degrees)



True - Reconstructed Muon Y-Z Angle (degrees) True - Reconstructed Muon Y-Z Angle (degree: True - Reconstructed Muon Y-Z Angle (degrees)



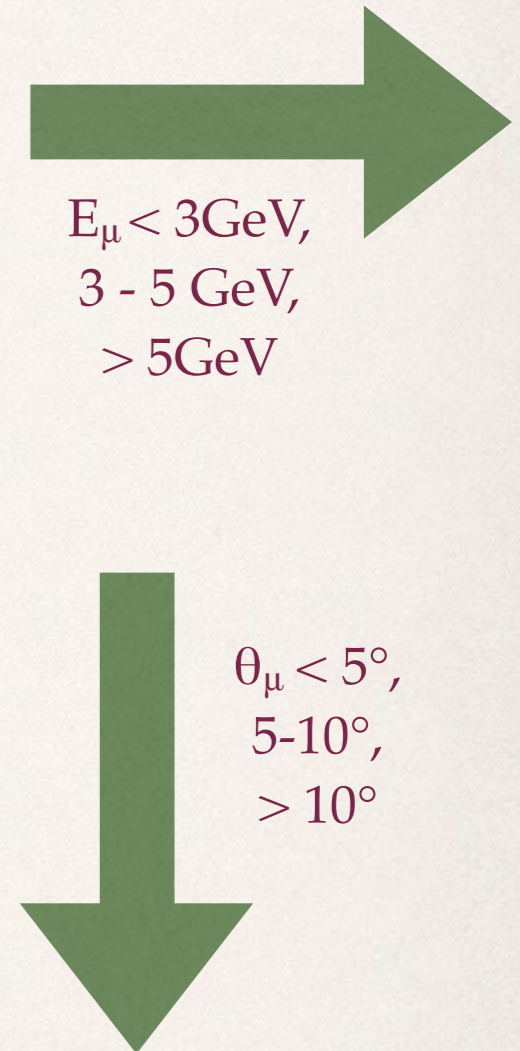
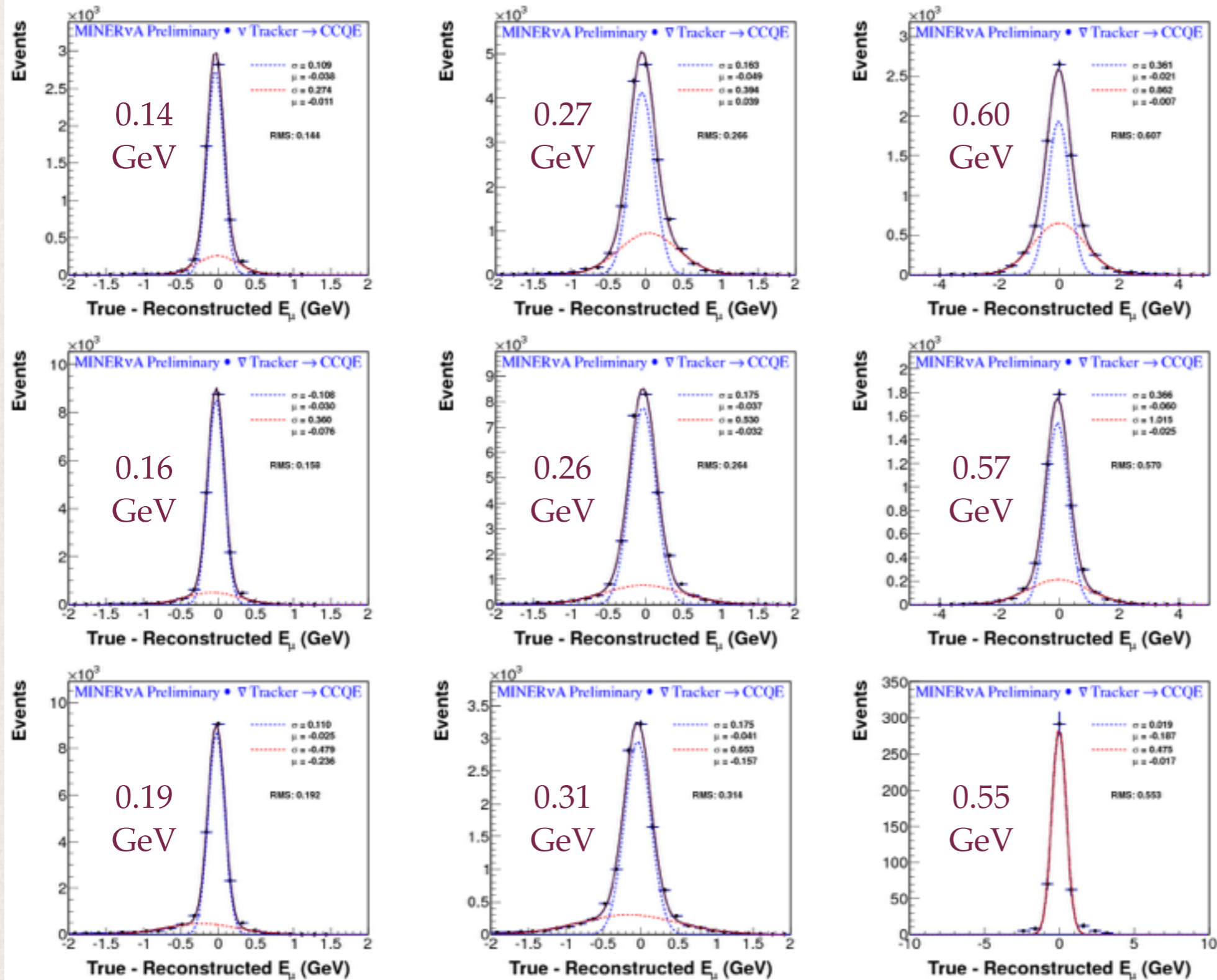
$E_\mu < 3\text{GeV}$,
3 - 5 GeV,
> 5GeV



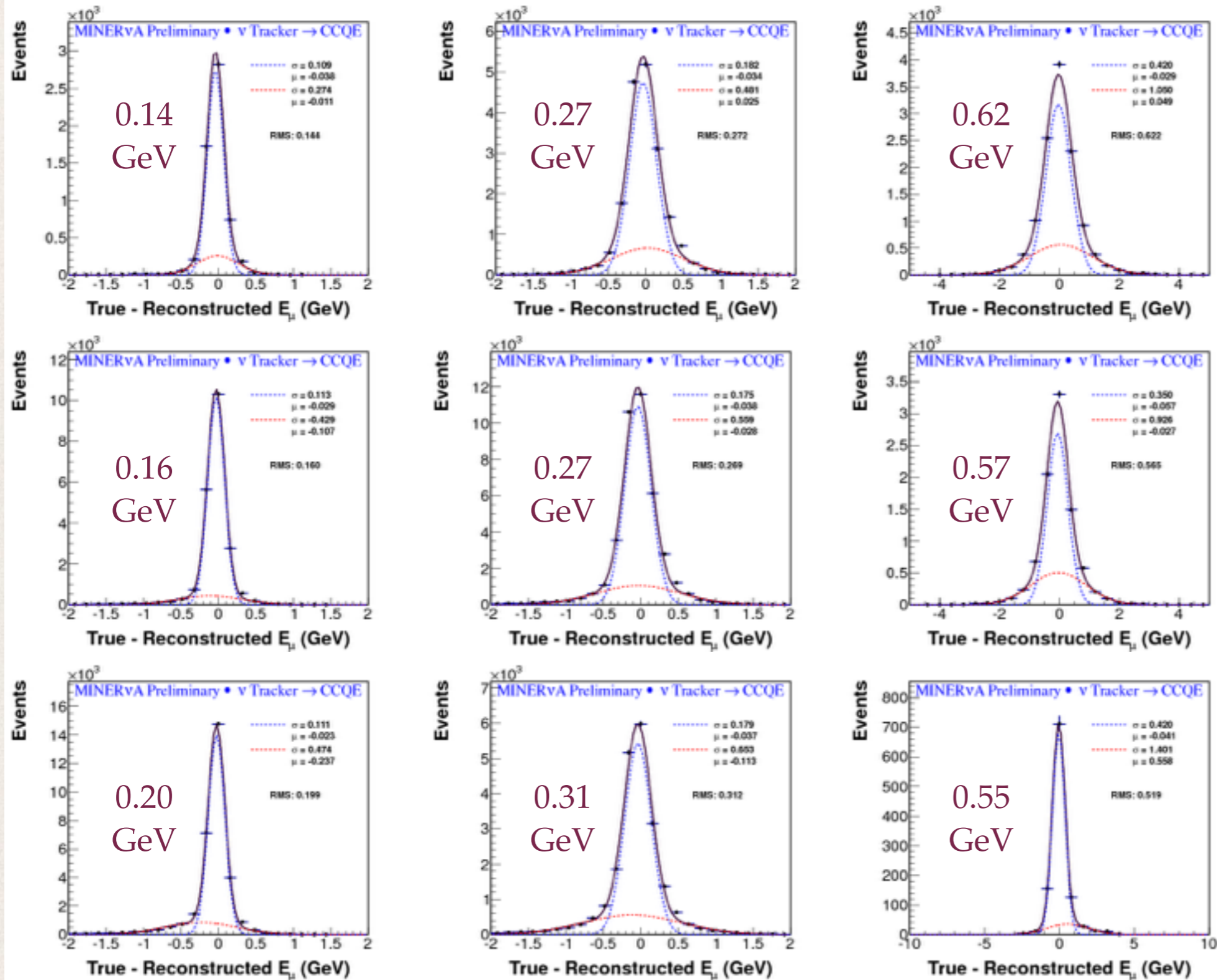
$\theta_{\mu,y} < 1^\circ$,
1 - 4°,
> 4°

Note: the beam is
in the y-z plane,
slightly
misaligned
from the z axis

Muon energy resolution, $\bar{\nu}$



Muon energy resolution, ν



$E_\mu < 3\text{GeV}$,
 $3 - 5\text{ GeV}$,
 $> 5\text{GeV}$



$\theta_\mu < 5^\circ$,
 $5-10^\circ$,
 $> 10^\circ$